PRESTRESSED CONCRETE STRUCTURES

PASALA DAYARATNAM
Department of Civil Engineering
Indian Institute of Technology
Kanpur

OXFORD & IBH PUBLISHING CO.
CALCUTTA · BOMBAY · NEW DELHI

© 1970 PASALA DAYARATNAM

Published by Mohan Primlani, Oxford & IBH Publishing Co., Oxford Bldg.,
N-88 Cannaught Circus, New Delhi-1 and printed at Prem Printing Press,
257 Golaganj, Lucknow-1.

To my parents
Kamalakshmi and Solomon, Pasala

PREFACE

This book is the natural growth of my several years of teaching and consulting in structural engineering with a particular emphasis on prestressed concrete structures. Economic criteria and a rational approach to design need not necessarily depend on intuition and experience but can be based on sound scientific principles coupled with practical constraints. The book is developed with detailed examples and illustrations to give basic concepts and a feeling for the variety of prestressed concrete structures. It is meant as a complete course in prestressed concrete structures useful for teaching advanced undergraduate and postgraduate students. Considerable literature supplied by various prestressed concrete manufacturers and consultants has been incorporated which gives the book a practical orientation.

The first chapter develops concepts of prestressing and the second chapter presents introductory material for prestressed concrete. These two chapters together form an introduction to the subject. Chapters three to seven discuss the service load design of various discrete structural systems such as simple composite and non-composite beams, tie bars, columns and piers, pipes and ring beams, and continuous beams. There is a greater emphasis on economic criteria of design and the cross sectional responses of various elements to different parameters. Chapters eight and nine present ultimate flexure and shear-moment failure criteria of design. Rigorous and approximate methods of computation of ultimate capacity of the beams are presented. The ultimate load design of prestressed concrete beams is also illustrated.

Chapters ten and eleven discuss the design of continuum structures such as two way and flat slabs, folded plates, water tanks, domes and ring beams, as well as cylindrical shell roofs. These two chapters are written especially for a student or designer who does not have a basic background in the classical plate and shell theories, and still wants to design such structures.

Chapters twelve and thirteen present design of end zones of pretensioned and post-tensioned prestressed concrete structural elements.

A set of tables useful for the design of beams and shells is presented in appendix A. Relevant references to the subject are given in appendix B. The references given are not meant as an exhaustive set.

I take this opportunity to express my thanks to Mr. S. C. Goel, Indian Institute of Technology, Kanpur, for his constant help at various stages of development of the book. I am grateful to Mrs. Jane G. Merriam, for her kind help in editing the book; the Indian Institute of Technology, Kanpur, for providing encouraging facilities for preparing the manuscript; and the students who have made significant comments for the presentation of the book.

Kanpur
1970

Pasala Dayaratnam

LIST OF SYMBOLS

Greek Letters:

α = change in slope of cable/tendon; angle of plane of principal stress; angle of deviation in folded plate
β = compatibility factor; bending moment coefficients in slab
γ = unit weight (density) of concrete or water
Λ = shape factor $(=y_b/y_t)$
ϵ = eccentricity ratio $(=e/h)$; strain
ϵ_0 = ultimate strain
ϵ_s = strain due to shrinkage
ϵ_b = strain in bottom fibre
ϵ_c = mean elastic strain, strain in concrete
ϵ_{ce} = strain in concrete at working
ϵ_s = strain in prestressed steel
ϵ_{se} = effective strain in prestressed steel
ϵ_t = strain in top fibre; tension strain in concrete
ϵ_u = limiting compressive strain of concrete
η = P_e/P_1
θ = slope of the tendon; rotation of beams etc.
λ = A_{cs}/A
μ = coefficient of friction
ν = Poisson's ratio
ρ = efficiency factor $(=r^2/h^2)$
Σ_0 = total parameter of the steel
σ_1 = maximum principal stress
σ_2 = minimum principal stress
σ_x = normal stress on x plane
σ_y = normal stress on y plane
τ = shear stress
τ_b = bond stress
ϕ = ratio of prestressing force at mid-section to that at the end section of the beam; rotation of joints
ω = depth factor $(=hf'_c/\gamma L^2)$

English Letters:

Capital Letters:

A = area of cross section
A_c = area of composite section, area of concrete column

A_{cs} = area of concrete slab in composite beams ($b_s t_s$)
A_{cse} = effective area of slab ($= b_{se} t_s = n_c A_{cs}$)
A_{sv} = area of shear reinforcement
B = breadth of column
C = compression
C_c = creep coefficient
C.G.C. = centre of gravity of gross section
C.G.S. = centre of gravity of prestressing steel
D = diameter of steel wires ; total depth of (column) sections
E_c = Young's modulus of concrete
E_s = Young's modulus of steel
E_{cs} = Young's modulus of material of the slab in composite construction
F = axial force; (direct tension or compression)
F_b = bursting force
F_c = axial load at cracking
F_{ult} = ultimate axial load
GJ = torsional rigidity of section
H = horizontal force in edge of shells
I = moment of inertia
I_c = moment of inertia of the gross composite section about its centroidal axis
I_h = moment of inertia about horizontal axis
I_v = moment of inertia about vertical axis
L = length of span
M = bending moment
M_a = moment due to external loads ($M_l + M_s$)
M_{be} = bending moment at working load due to unbalanced load
M_{bt} = bending moment at transfer due to unbalanced load
M_g = bending moment due to self weight
M_{gs} = bending moment due to self weight of slab
M_l = bending moment due to live load
M_{pb} = bending moment due to prestressing balancing force
Ms = bending moment due to superimposed load
M_t = bending moment due to total load ($= M_a + M_s$)
M_u = ultimate bending moment
N = normal force
N_g = load factor for dead load
N_l = load factor for live load
P = prestressing force, line load at folds in folded plates
P_a = axial force due to shrinkage
P_E = Euler's buckling load
P_e = effective prestressing force after loss of prestress

P_0 = prestressing force at anchorage (force indicated by jack)
P_t = prestressing force at transfer
P_{ta} = prestressing force in long span of slabs
P_{tb} = prestressing force in short span of slabs
P_x = prestressing force at distance x
Q = transverse shear in slabs ; $M_u/bd^2 f'_c$
Q_y = first moment of area
R = moment ratio ($=M_a/M_g$) ; M_1/M_2 ; reactions of supports; radius of curvature
R_1 = M_a/M_{gs}
R_2 = M_{s1}/M_{gs}
T = age of concrete (in days) at transfer, self balancing shear force at folds in folded plates
V = shear force, vertical force
V_p = shear force due to prestressing force ($=P_e\frac{dy}{dx}$)
Z = modulus of section

Small Letters :

a = distance of neutral axis from top fibre ; radius of sphere ; depth of anchor plate ; span of slab in x direction, lever arm
b = width, span of slab in y-direction (short span length)
b_s = width of slab
c_a = $A/b_t h$
c_b = t_b/h
c_{ce} = compression stress coefficient at effective load
c_{ct} = compression stress coefficient at transfer
c_f = b_b/b_t
c_I = I/bh^3
c_t = t_t/h
c_{te} = tension stress coefficient at effective load
c_{tt} = tension stress coefficient at transfer
c_w = b_w/b_t
c_{yb} = y_b/h
c_{yt} = y_t/h
c'_{ce}, c'_{ct},
c'_{te}, c'_{tt} = limiting stress coefficients
d = distance from C. G. S. to top fibre
d′ = distance from C. G. S. to bottom fibre
e = eccentricity
e_a = maximum eccentricity of cable in long span of slab
e_b = maximum eccentricity of cable in short span of slab

e_x = *eccentricity at distance x*
f = *stress*
f_a = average stress ($=P/A$)
f_{ct} = compressive stress in concrete at transfer
f_s = stress in steel
f_{se} = effective stress in steel
f_{so} = stress in steel at anchorage
f_{st} = stress in steel at transfer
f_{su} = allowable ultimate stress of prestress steel
f_{sv} = allowable stress in vertical stirrup steel
f_{sy} = yield stress of prestress steel
f_t = stress in the folded plate due to shear force T
f_{tc} = tensile stress in concrete at working loads
f_{tt} = stress at tension fibre at transfer
f_y = stress in y direction (i.e. transverse stress in beam) ; bursting stress
$f_{y\,max}$ = maximum tensile stress ordinate (bursting stress)
f'_c = ultimate cube stress of concrete
f'_{cb} = ultimate compressive stress of concrete in pure bending
f'_{cp} = ultimate concrete prism stress in compression ($=k_p\, f'_c$)
f'_{cs} = ultimate compressive stress of concrete subjected to combined bending and shear
f'_s = ultimate tensile stress of prestressing steel
f'_{sv} = ultimate stress in vertical stirrup steel
g = maximum sag of cable
h = overall depth the beam ; rise of shell
k = wobble correction coefficient
k_1 to k_7 = concrete strength coefficients
k_b = bottom kern distance
k_t = top kern distance
l_b = bond length
l_t = transmission length
l_u = total bond length
m = reinforcement ratio ; bending moment in transverse direction in folded plates
m_c = Poisson's ratio for concrete
m_s = Possion's ratio for steel
n = modular ratio
n_c = modular ratio of composite section
p = percentage of reinforcement
p_s = ratio shear steel ($=A_{sv}/sb$)
q = intensity of load; $A_s/b_t d$
r = radius of gyration
r_c = radius of gyration of composite section

s = spacing of stirrups
t = *thickness*
t_b = thickness of bottom flange
t_s = thickness of slab/plate
t_t = thickness of top flange
u's = composite section coefficients
v = displacement (lateral or horizontal direction)
w = vertical deflection; load per unit length
y = profile of cable; distance from C.G.C.
y_b = distance of bottom fibre from C.G.C.
y_{bc} = distance of bottom fibre of the beam to the centroidal axis of the composite section
y_t = distance of top fibre from C.G.C.
y_{tc} = distance of top fibre of the beam from the centroidal axis of the composite section
z = discrete function defining the cable profile both in x & y directions

Subscripts:

a = shrinkage; a span direction in slabs
b = bottom flange; bond; beam; balancing: of b span direction in slabs
be = balancing at working
bt = balancing at transfer
c = concrete; compression; composite section
d = dome
e = effective prestressing stage (working load condition)
g = self weight
h = horizontal
l = live load; line load
m = moment
o = external load; anchorage
s = steel; slab; shell
t = top flange; transfer condition; total, tension
u = ultimate
v = vertical
w = web
ϕ = moment; rotation

Superscripts :

prime (′) = ultimate; secondary; maximum
c = column strip
m = middle strip

distribution procedure; Continuous beams with variable section; Load balancing method

CHAPTER VI.—MISCELLANEOUS STRUCTURAL MEMBERS 100
Introduction; Compression members (prestressed concrete piles, poles, towers, piers and abutments); Tension members (tie member, prestressed concrete ring beams and circular tanks, prestressed concrete pipes); Prestressed concrete pavements (roads, runways, and concrete sleepers)

CHAPTER VII.—DEFLECTION OF PRESTRESSED CONCRETE BEAMS 114
Introduction; Deflections based on load balancing method; Effect of camber

CHAPTER VIII.—FLEXURAL ULTIMATE STRENGTH AND ULTIMATE LOAD DESIGN OF PRESTRESSED CONCRETE BEAMS 119
Introduction; Flexural failure; Ultimate moment; Simplified method for determination of ultimate moment; Ultimate design of prestressed concrete beams; Ultimate load design procedure; Ultimate moment by I. S. Code of Practice

CHAPTER IX.—ANALYSIS AND DESIGN OF PRESTRESSED CONCRETE BEAMS FOR SHEAR .. 132
Introduction; Shear stress; Principal stresses: Stirrups for working loads; Failure due to shear; Moment shear failure; Ultimate moment under combined bending and shear of I—girder; Location of failure section; Suggestions from experimental investigations

CHAPTER X.—PRESTRESSED CONCRETE FLOORS AND SLABS 147
Introduction; One-way slab; Two-way slab; Prestressed concrete beam and slab construction; Prestressed concrete flat slabs

CHAPTER XI.—FOLDED PLATE AND SHELL STRUCTURES 166
Introduction; Analysis of folded plates; Design of folded plates; Introduction to prestressed concrete shells; Design

of cylindrical tanks; Dome-ring construction; Introduction to prestressed concrete cylindrical shell; Method of analysis of cylindrical shell

CHAPTER XII.—BOND IN PRESTRESSED CONCRETE 221
Introduction; Bond in pre-tensioned construction; Bond in post-tensioned construction

CHAPTER XIII.—ANCHORAGE OF PRESTRESSING CABLES 228
Post-tensioned construction: Prestressing cable at the centroidal axis; Symmetric multiple cables causing axial thrust; Cable with eccentricity; Inclined prestressing cable; Spalling stresses

APPENDIX—A : Tables. 238
Table 1: Values of Δ_0
Table 2: Sectional properties
Table 3: Fixed end moments due to prestressing force
Tables 4 to 9: Tables for design of cylindrical shells

APPENDIX—B : References. 320

INDEX 325

CHAPTER I

CONCEPTS OF PRESTRESSING

1.1. DEFINITION: Prestressed concrete may be defined as the concrete in which effective internal stresses are induced artificially with tensioned steel before loading the structure. An illustration of prestressing could be seen in the tightened waist belt of a middle aged lady who is about to go to a formal dinner. If the belt is tightened before dinner the waist is restricted to stay within reasonable limits even after a heavy dinner. A simple engineering example which has used the principle of prestressing since several centuries is that of the formation of a wooden barrel. As steel ropes or bands are wound around wooden staves and tightened, compressive stresses are produced in the barrel. Under working load conditions, the liquid in the barrel will cause tensile stresses which are counter balanced by the previously induced compressives tresses. This type of operation of tightening the steel bands before working operations is called prestressing.

Concrete is poor in tension, so at sections of concrete where tension is expected, compressive stresses are introduced before working loads. There are several methods of tensioning the steel and transferring the steel force to the concrete. The prestressing steel, when used in concrete members, is usually called tendon. The systems and operations of prestressing are discussed later.

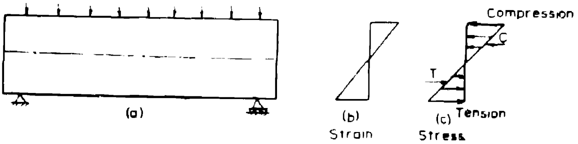

Fig. 1.2.1 : Simply supported beam

1.2. STRESS DISTRIBUTION: The distribution of stress and strain in a simply supported beam is shown in fig. 1.2.1 assuming that the plane section remains plane even after bending. Certain amount of tension is produced in the bottom fibre by the external loads and, because concrete is poor in tension, some kind of tension bearing capacity has to be induced at the tensile zone. The tension capacity is provided in two ways: (i) sufficient steel can be embedded in the beam at the tension zone which will take the tension directly. This method is defined as reinforced concrete construction; (ii) a compressive stress can be induced at the tension fibre through tensioned steel. This system is called prestressed concrete construction and it is illustrated in fig. 1.2.2.

If a simply supported beam is first subjected to prestressing force of P_t alone, then the stresses in the beam are given by

$$f_{t1} = \frac{P_t}{A}\left(1 - \frac{ey_t}{r^2}\right) \qquad .. \qquad (1.2.1)$$

$$f_{b1} = \frac{P_t}{A}\left(1 + \frac{ey_b}{r^2}\right) \qquad .. \qquad (1.2.2)$$

Where

P_t = prestressing force introduced through the tendon
A = area of cross section
r = radius of gyration
e = eccentricity
y_t = distance of the extreme top fibre from C. G. C
y_b = distance of the extreme bottom fibre from C. G. C
f_{t1} = stress at top fibre in stage 1
f_{b1} = stress at bottom fibre in stage 1

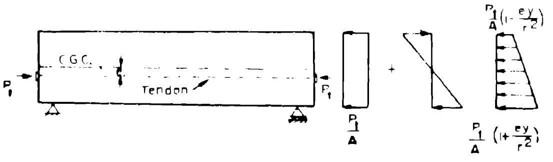
C.G.C.
Tendon
P_t
P_t
$\frac{P_t}{A}$
+
$\frac{P_t}{A}(1-\frac{ey}{r^2})$
$\frac{P_t}{A}(1+\frac{ey}{r^2})$

Stage 1 at transfer without any external load

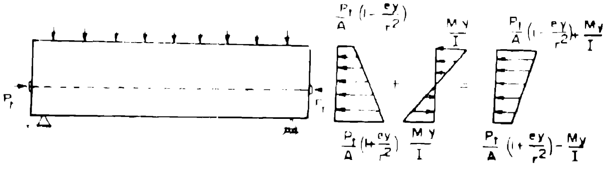
P_t
P_t
$\frac{P_t}{A}(1-\frac{ey}{r^2})$
$\frac{My}{I}$
$\frac{P_t}{A}(1-\frac{ey}{r^2})+\frac{My}{I}$
+
=
$\frac{P_t}{A}(1+\frac{ey}{r^2})$
$\frac{My}{I}$
$\frac{P_t}{A}(1+\frac{ey}{r^2})-\frac{My}{I}$

Stage 2 at working load

Fig. 1.2.2 : Simply supported beam with prestress

The self weight of the beam is neglected in this case. In the second stage when working load acts, the stresses are given by

$$f_{t2} = \frac{P_t}{A}\left(1 - \frac{ey_t}{r^2}\right) + \frac{My_t}{I} \qquad .. \qquad (1.2.3)$$

$$f_{b2} = \frac{P_t}{A}\left(1 + \frac{ey_b}{r^2}\right) - \frac{My_b}{I} \qquad .. \qquad (1.2.4)$$

where a subscript 2 indicates stage 2 (working load) and M the bending moment at the section. From eq. 1.2.4, it can be seen that tensile stress at working load is compensated by prestressing compressive stress. The amount of prestressing force 'P_t' and the eccentricity 'e' are fixed by the allowable stresses. P_t cannot arbitrarily be increased just to compensate the negative stresses. As P_t increases, f_{t2} also increases so the allowable compressive stress of concrete governs. Compensation of tensile force can also be achieved by increasing the eccentricity 'e'; but as the eccentricity increases, f_{t1} in eq. 1.2.1 might turn out to be a tensile stress beyond allowable limits. The values of P_t and e have to be carefully selected. The advantage of providing thrust P_t at the bottom is illustrated in example 1.2.1.

Example 1.2.1 : A simply supported beam of span 8 m is loaded with a uniformly distributed load of 5000 kg/m. The cross section of the beam is 80 by 30 cm. Determine the stresses with and without a horizontal thrust of 240,000 kg acting at 20 cm below the centroidal axis. The self weight of the beam is included in the load.

$$f=\frac{P}{A}\pm\frac{Pey}{I}\pm\frac{My}{I},\ (y_t=y_b=y)$$

$$=\frac{240{,}000}{80\times30}\pm\frac{240{,}000\times20\times40}{1{,}280{,}000}\mp\frac{4{,}000{,}000\times40}{1{,}280{,}000}$$

$$=\ 100\pm150\mp125\ \text{Kg/sq cm.}$$

Stresses without horizontal thrust $= \pm125$ kg/sq cm

Stresses with horizontal thrust $= +75$ or $+125$ kg/sq cm

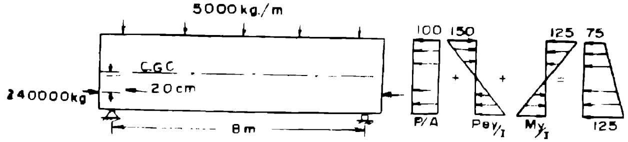

Fig. 1.2.3 : Stress distribution at mid section

It can be seen from fig. 1.2.3 that a tensile stress of 125 kg/cm² exists without horizontal thrust, but with the introduction of horizontal thrust, there is compressive stress throughout the cross section.

1.3. PROFILE OF TENDONS : It may be seen from example 1.2.1 that there are two critical sections, one at mid span and another at end span. The stress distributions of these two sections are shown in fig. 1.3.1.

From fig. 1.3.1 it can be seen that the stress distribution at the end section is more dominant than that at middle of the beam mainly because of zero external bending moment at the end section. The

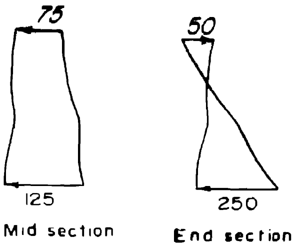

Fig. 1.3.1 : Stress distribution—Example 1.2.1

stress distribution due to external bending moment starts with zero values at the end and reaches maximum at the centre of the beam, whereas the stress distribution provided by the horizontal thrust stays constant throughout the beam. The critical stress distribution at the end section can easily be avoided by providing zero eccentricity at the end while keeping the 20 cm eccentricity at the middle of the beam. Now it is necessary to discuss the transition of the eccentricity along the span. The stress variation along the span due to the uniformly distributed load is parabolic; so a tendon of parabolic profile will be effective to compensate the tensile stresses due to the external loads. Sometimes the prófile is also taken as two straight lines with a bend at the middle of the section. These profiles are shown in fig. 1.3.2. The eccentricity of the tendon at the end of the beam need not necessarily be zero. To provide for a steep curvature, a negative eccentricity can also be given. The variation of vertical component of the tendon force will compensate the external load as illustrated in fig. 1.3.3. The following two examples illustrate the stress behaviour due to inclined profiles of the tendons.

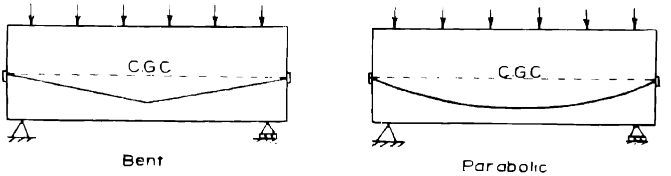

Fig. 1.3.2 : Possible profiles of tendons

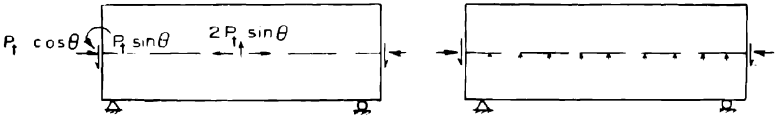

Fig. 1.3.3 : Vertical component of tendon force

Example 1.3.1 : (same as example 1.2.1 with a modification in the profile of the tendon) : The eccentricity at the end is — 10 cm and at the mid section is 20 cm with a straight line variation. Determination of the stresses at the end and mid section (-ve sign of e indicates eccentricity above C. G. C.).

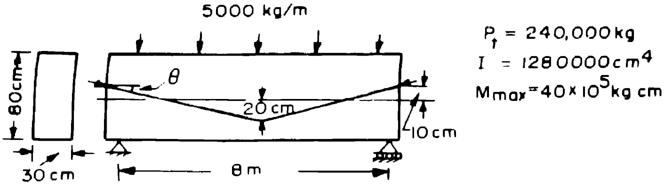

Fig. 1.3.4 : Example 1.3.1

The slope of the tendon is small so

$$\text{Sin } \theta \simeq \tan \theta \simeq \frac{30}{400}$$

The vertical component of the tendon force at the middle of the section

$$= 2 \text{ P}_t \text{ Sin } \theta = 2 \times 240{,}000 \times \frac{3}{40} = 36000$$

The horizontal component (H) $= \text{P}_t$ Cos $\theta \simeq \text{P}_t$

Stresses at end section of the beam:

$$f = \frac{\text{P}_t}{\text{A}} \pm \frac{\text{P}_t \text{ ey}}{\text{I}}$$

$$= 100 \pm \left(- \frac{240{,}000 \times 10 \times 40}{1280{,}000} \right)$$

$$= (100 \pm 75)$$

Stresses at mid section of the beam: In addition to the bending moment caused by the external load, the vertical component of the tendon force will also cause bending moment but in opposite direction (fig. 1.3.5).

$$\text{M}_l = \frac{\text{wL}^2}{8} = \frac{5000 \times 8 \times 800}{8} = 40 \times 10^5 \text{ kg cm}$$

$$\text{M}_{pb} = -\frac{36000\text{L}}{4} = -\frac{36000 \times 800}{4} = -72 \times 10^5 \text{ kg cm}$$

where : M_l = bending moment due to live load
M_{pb} = bending moment due to prestressing balancing force
$\text{M} = \text{M}_l + \text{M}_{pb} = -32 \times 10^5$ kg cm
$f = 100 \pm 75 \pm (-32/40)\ 125$
$= (100 \pm 75 \mp 100)$ kg/sq cm

Fig. 1.3.5 shows the stress distribution at the end and middle sections of the beam. It may be seen from the two previous examples that the profile of the cable has considerable effect on the distribution of stress at different sections of the beam. Another two examples are given to illustrate the effect of the cable profile on the stresses in the beam.

(Note : The stress pointing towards the beam is assumed to be compression as given in the figures.)

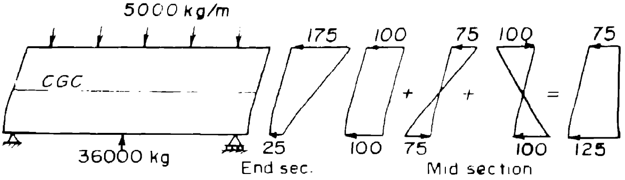

Fig. 1.3.5 : Stress distribution—Example 1.3.1

Example 1.3.2 : (same as example 1.3.1 except that the eccentricity at the ends is 10 cm instead of −10 cm) : The stresses distribution due to the external load and prestressing force are computed as done in example 1.3.1 and shown in figure 1.3.6.

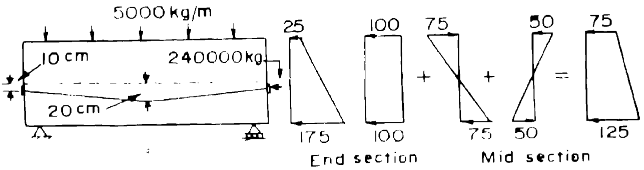

Fig. 1.3.6 : Stress distribution—Example 1.3.2

Example 1.3.3 : Same as example 1.3.2 except that the profile of the cable is parabolic.

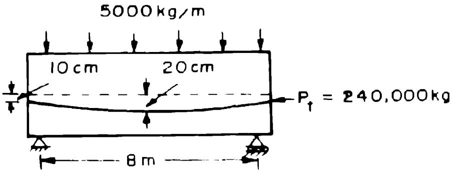

Fig. 1.3.7 : Example 1.3:3

Equation of parabola with origin at the end of the beam is

$$y = \frac{x}{16000}(L-x) = \frac{Lx-x^2}{16000}$$

$$\frac{d^2y}{dx^2} = \frac{-2}{16000} = \frac{-1}{8000}$$

Vertical component of force

$$= P_t\left(\frac{d^2y}{dx^2}\right) = \frac{-240{,}000}{8{,}000}$$

$$= -30 \text{ kg/cm}$$

$$= -3000 \text{ kg/m}$$

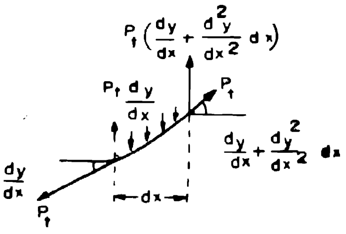
$P_t\left(\frac{dy}{dx}+\frac{d^2y}{dx^2}dx\right)$
$P_t\frac{dy}{dx}$
P_t
$\frac{dy}{dx}+\frac{d^2y}{dx^2}dx$
$\frac{dy}{dx}$
dx
P_t

Fig. 1.3.8

The vertical component of the tendon force is uniformly distributed, acting upwards and is equal to 3000 kg/m.

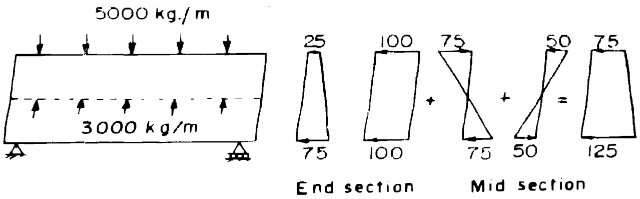

Fig. 1.3.9 : Stress distribution—Example 1.3.3

The effective vertical load on the beam is (5000 − 3000) = 2000 kg/m and is acting downwards. The stresses are calculated for this load and the stress distribution is shown in fig. 1.3.9.

A comparative study of stress distribution of the four examples is given in table 1.3.1. Beams 2 to 5 have used the same amount of mate-

TABLE 1.3.1 : STRESS DISTRIBUTION ON BEAM WITH TENDON

S.NO	EXAMPLE	END SECTION	MID SECTION
1	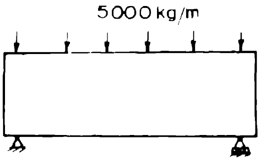	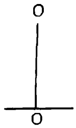	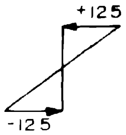
2	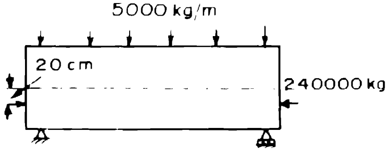	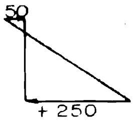	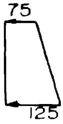
3	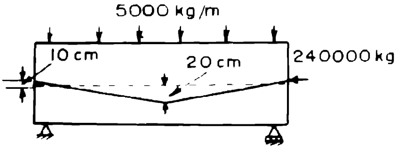	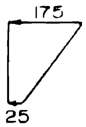	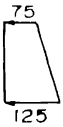
4	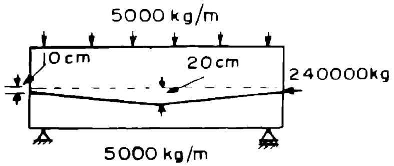	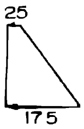	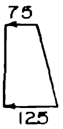
5	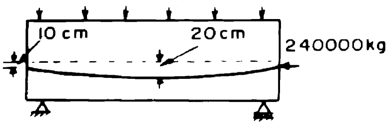	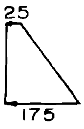	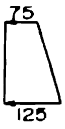

rial under same external load conditions except for the profile of the tendon. It can be seen from the stress block that the profile and the eccentricity of the tendon has considerable effect on the stresses.

1.4. LOAD BALANCING METHOD : From the previous examples, it can be seen that the external load could be balanced by the transverse component of the cable force. A design method in which the external load is balanced by the transverse component of the cable is called 'load balancing method' (1.1). Fig. 1.4.1 illustrates the selection of cable force and profile for load balancing method.

Example 1.4.1 : Provide a load balancing cable for a given cable force (P=160000 kg) for the beam shown in fig. 1.4.1.

Two alternative solutions exist for this type of problem. If the cable force is specified, the eccentricity could be adjusted or vice versa. In this example, cable force is fixed so the eccentricity is adjusted.

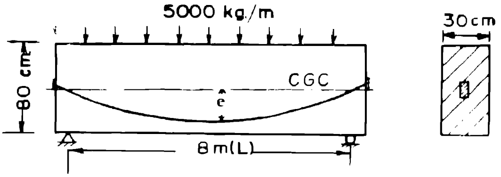

Fig. 1.4.1 : Example 1.4.1

(Given P—calculate cable profile)

$$y = \frac{4e}{L^2}\left(Lx - x^2 \right)$$

$$\frac{d^2y}{dx^2} = -8e/L^2$$

$8eP/L^2 = 5000 =$ balancing force

$$\therefore \quad e = \frac{5000L^2}{8P} = 25$$

$$f_a = \frac{P}{A} = \frac{160000}{2400} = 66.7 \text{ kg/sq cm}$$

Where : f_a = average stress

Example 1.4.2 : Determine necessary cable force to balance the external load of the beam shown in fig. 1.4.2 with 20 cm eccentricity at mid span.

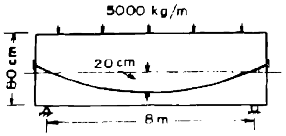

Fig. 1.4.2 : **Example 1.4.2**

Balancing force due to cable $= \dfrac{8Pe}{L^2}$

Load to be balanced $= 5000$ kg/m

$$\frac{8Pe}{L^2} = 5000$$

$\therefore$ $P = 200000$ kg

$f_a = P/A = 83.33$ kg/sq cm

Typical examples of load balancing cable profiles are shown in figures 1.4.3. (a) and (b).

$$2P \sin \theta = w_b$$

$$\text{or } 2P\,(e/\frac{L}{2}) = w_b$$

$$\therefore\ Pe = \frac{(w_b L)}{4}$$

where: w_b = balancing force
If P is fixed, e could be selected, or
if e is fixed, P could be selected.

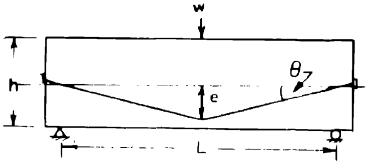

Fig. 1.4.3(a)

$$(Pe/\frac{L}{3}) = w$$

$$\therefore\ Pe = \frac{(wL)}{3}$$

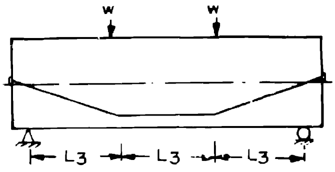

Fig. 1.4.3 (b)

In some beams, the external load could be partially balanced by the cable component and the unbalanced load could be treated as effective external load. Examples given in section 1.3 illustrate the partially balancing technique.

1.5. BASIC PHASES OF LOADING IN PRESTRESSED CONSTRUCTION : There are about six stages in the load conditions of a prestressed concrete structure. Some stages of loading override some other stages so the effective loading conditions need not necessarily be six. However for the sake of clarity, all the important phases of loading on the structure are recorded below :

(i) Transfer of prestressing force : Transfer condition may be defined as the condition at which prestressing force is transferred to the beam. The loads acting on the member in this stage, are the prestressing force and the self weight.

(ii) Prestressing force, self weight and the superimposed loads (slab load etc.).

(iii) Prestressing load, self weight, live load : The first three stages are more or less the stages that occur in the first few weeks of casting of the beam. During these few weeks, the concrete and steel undergo the time dependent strain variations such as shrinkage and creep of concrete and creep of steel. Because of these deformations, the original elongation provided for the initial prestressing force decreases and the amount of prestressing force available also decreases. A steady state might result after a long period. The amount of prestressing available after a steady state, is called effective prestressing force.

(iv, v & vi) Conditions (i), (ii) and (iii) of loading are repeated with effective prestressing force instead of initial prestressing force. Conditions (i) and (vi) are the critical load conditions which govern the allowable stresses. The two conditions may be called as governing conditions which are discussed in detail in chapter III.

1.6. MATERIALS : This section is devoted to materials mainly used in the prestressed concrete construction. Because of variety of reasons seen later, it is necessary to have some concept about the material properties used in the construction. Basically there are two materials used in the prestressed concrete construction and they are (i) steel, and (ii) concrete.

(i) **Steel :** Mild and hard steels used in reinforced concrete construction have a yield limit of 2000 kg/cm^2 to 3000 kg/cm^2. If this steel is used in prestressed concrete and tensioned to about 2000 kg/cm^2 at the initial stage, the effective prestressing force available after shrinkage and creep of concrete and creep of steel will be negligible. The approximate loss of prestressing due to shrinkage of concrete, creep of concrete and steel is estimated to be of the order of 1750 kg/sq cm to 2500 kg/sq cm. Obviously no prestressing force will be left in the mild steel after the losses. The high tensile steels have ultimate strength capacity as high as 21,000 kg/sq cm and the use of such steels will provide considerable amount of effective prestressing force even after losses in prestress.

Prestressing steel available is mainly in the form of wires which are cold-drawn from high tensile steel bars. The process of cold drawing tends to realign the crystals and the strength of the wire is increased by each drawing so that the strength of the wire increases as the diameter decreases. The cold drawing process decreases the ductility of the material which is a disadvantage. High tensile steel wires are also obtained as 'as-drawn' wires. These wires have low proportional limit and to increase the proportional limit, the wires are subjected to some type of stress relieving processes. Variation of ultimate stress with respect to the diameter of the wire is shown in fig. 1.6.1.

The prestressing steel is also available in form of strands which are obtained by twisting wires together. By using strands, the number of units to be handled decreases. Small diameter wires of very high tensile strength can be used for strands. Approximate chemical composition of the high tensile steel wires is:

> carbon = 0.60 to 0.85%, manganese = 0.7 to 1.0%, phosphorus = 0.05%, sulphur = 0.055% and a small amount of silicon.

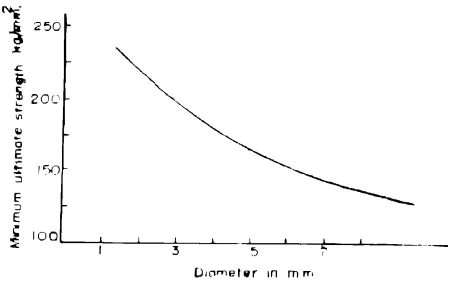

Fig. 1.6.1 : Typical variation of ultimate strength w.r.t. diameter

Physical properties: The proportional limit or yield point of high tensile steel is rather hard to find. Because of the absence of low carbon steel in the high tensile steel, the yield point does not exist. A typical stress strain curve of a high tensile steel is shown in fig. 1.6.2.

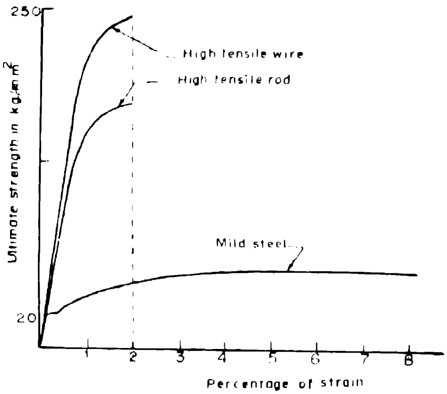

Fig. 1.6.2 : Stress strain curve of steels

From fig. 1.6.2 it can be observed that the proportional limit or yield point of high tensile steel is not very clearly seen. The yield point of high tensile steel is generally defined at 0.2% set, i.e., at 0.2% of permanent inelastic deformation. The approximate yield points are given in table 1.6.1.

TABLE 1.6.1: APPROXIMATE YIELD AND PROPORTIONAL LIMITS

Wire	Yield point	Proportional limit
Wires as drawn	$0.75\ f'_s$	$0.35\ f'_s$
Prestretched	$0.85\ f'_s$	$0.55\ f'_s$
Temp. treated wires	$0.87\ f'_s$	$0.70\ f'_s$
Strands—stress relieved	$0.90\ f'_s$	$0.75\ f'_s$

The modulus of elasticity of high tensile steel may be taken as shown in table 1.6.2.

TABLE 1.6.2: MODULUS OF ELASTICITY OF STEEL

Description	E_s
Cold drawn wires	2.1×10^6 kg/cm²
Heat treated wires	2.0×10^6 kg/cm²

As it is rather hard to establish any positive limits for high tensile steels, it is desirable that sufficient tests be conducted on the specimens to be used in any particular job.

The creep characteristics of high tensile wires are given in fig. 1.6.3.

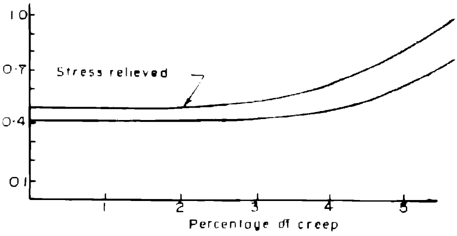

Fig. 1.6.3 : Creep in steel

In most of the high tensile wires, the creep is negligible upto $0.45\ f'_s$ and it is about 3% at 0.5 and $0.55\ f'_s$ stress level. The steel is subjected to high tension during the first stages of construction, so most of the creep occurs in the early stage of construction. The wires and strands are generally supplied in coils of sufficient big diameter as not to cause any inelastic deformation.

(ii) Concrete: Consequent to the use of high tensile steel in prestressed concrete construction, the concrete has to be of high strength character. The Indian code of practice suggests a minimum cube strength of 420 kg/sq cm for pre-tensioned system and 350 kg/sq cm for post-tensioned system. A typical concrete strength vs. water-cement ratio is shown in fig. 1.6.4.

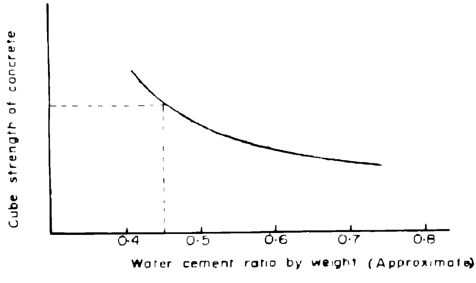

Fig. 1.6.4 : Cube strength vs. water-cement ratio

As the water cement ratio increases, the strength of concrete decreases. For most prestressed concrete constructions, a water-cement ratio of about 0.45 is used. For water-cement ratio less than 0.4, the workability of concrete decreases, with the result that compact and high density concrete is difficult to obtain. High workability with less water-cement ratio requires a higher percentage of cement and well graded aggregate. 12 mm to 25 mm slumps are sometimes used with controlled vibration.

The strength of the concrete referred in this book is always to be that of a 15 cm cube at 28 days unless otherwise stated. The actual concrete strength after several months of casting will be higher than that of 28 days strength. A typical relation between strength of concrete with age is shown in fig. 1.6.5.

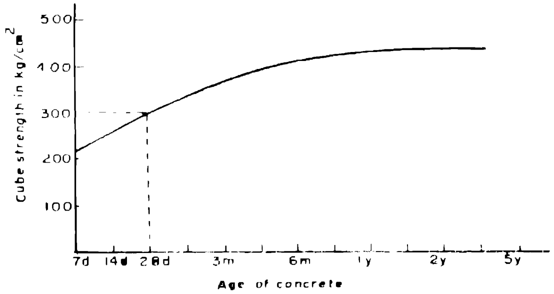

Fig. 1.6.5 : Strength of concrete with age

A typical stress strain curve of a good graded concrete is shown in fig. 1.6.6 and the stress strain relation (1.2) may be expressed as

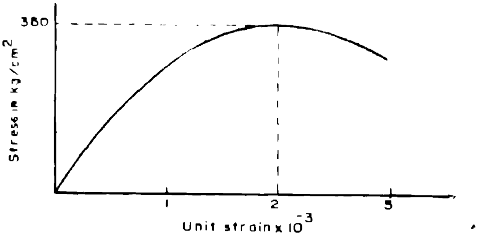

Fig. 1.6.6 : Typical stress strain curve of concrete

$$f_c = E_c \epsilon \left(1 - \frac{\epsilon}{2\epsilon_0}\right) \qquad \ldots \qquad (1.6.1)$$

Where ϵ_0 = ultimate strain (about 0.003). The stress-strain curve of concrete is desirable for determination of ultimate load capacity of the beams and also for understanding Young's modulus of the concrete itself. Determination of Young's modulus for concrete is not as specific as it is for steel. This can be easily observed from the curve. There have been many formulae developed to determine Young's modulus of concrete; they are given below:

(a) As per Indian code of practice:

$E_c = 18{,}000\sqrt{f'_c}$ (kg/sq cm)

or $E_c = 68{,}000\sqrt{f'_c}$ (psi)

Where f'_c is the 28 days 15 cm cube strength for a portland cement and 7 days cube strength for a rapid hardening cement.

(b) As per American concrete institute:

$E_c = 33\gamma^{3/2}\sqrt{f'_c}$ (psi)

Where γ = weight of concrete per cft and

f'_c = 6″ cylinder strength (psi)

(c) Hognestad has proposed:

$E_c = 1{,}800{,}000 + 460\ f'_c$ (psi)

Where f'_c = 28 days cylinder strength.

(d) As per German code:

Cube strength (kg/cm²)	Corresponding cylinder strength (psi)	E_c (psi)
300	3400	4.8×10^6
450	5100	5.7×10^6
600	6800	6.2×10^6

(e) British coae specifies as:

Cube strength (psi)	E_c (psi)
3000	3×10^6
4000	4×10^6
5000	4.5×10^6
6000	5.0×10^6
8000	6.0×10^6
10,000	6.5×10^6

It can be seen from the various specifications that there is no absolute basis on which Young's modulus could be determined. Young's modulus is a function of the ultimate strength of the concrete. The modulus of elasticity plays an important part on the deformation and loss of prestress characteristics. A certain amount of tolerance has to be assumed in the use of Young's modulus. The Poissons' ratio for prestressed concrete varies from 0.15 to 0.22and an average of 0.17 may be adopted in the calculations.

Time dependent character of concrete shrinkage: As concrete is cast, cured and exposed to weather conditions, some drying and chemical changes take place. Consequently the concrete undergoes change in volume depending upon time, moisture content, water-cement ratio and weather conditions. The change of deformation independent of stress is called shrinkage. The amount of shrinkage varies from 0 to .001. Some amount of the shrinkage is recoverable upon restoring the moisture content of the concrete. (In some extreme wet conditions with certain aggregates, the concrete is likely to expand.) The amount of shrinkage is proportional to the water-cement ratio. It is desirable to use a low water-cement ratio to reduce the effect of shrinkage. The aggregate properties also affect the shrinkage. Aggregate with low percentage absorption will give less shrinkage. The chemical decomposition of cement or even the chemical reactions in the cement will have some influence on the shrinkage. It is always possible to make an approximate estimate of shrinkage of concrete while designing a concrete mix (1.3). For purposes of design, the shrinkage may be assumed as 0.0002 to 0.0004.

Creep in concrete: The creep strain is defined as the time dependent deformation resulting from the presence of stress. The creep deformation is a complex phenomenon especially in concrete. Most materials subjected to a particular stress level will continue to deform for a certain period even without any change in the stress level. Normally there is no creep at low stress levels, but as the stress level increases the creep also increases. The creep of concrete is a function of several quantities such as (i) stress level, (ii) the duration of stress, (iii) age of concrete, (iv) previous history of stress, (v) water-cement ratio, (vi) strength of concrete, (vii) aggregate, (viii) cement, and (ix) weather conditions to which the concrete is exposed. The creep of concrete assumes an asymitotic behaviour tending to stabilise the strain in a longer period. However most of the creep occurs in the first year. The ratio of the final strain in time to the initial strain of concrete is called the creep coefficient. A typical creep curve is shown in fig. 1.6.7. The creep of concrete decreases with moisture and weather conditions. For the purposes of design the creep coefficient of concrete is taken as 2.5 to 3.0.

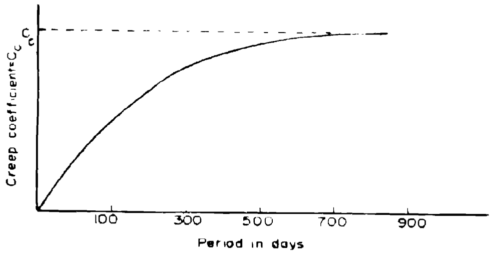

Fig. 1.6.7 : Creep of concrete

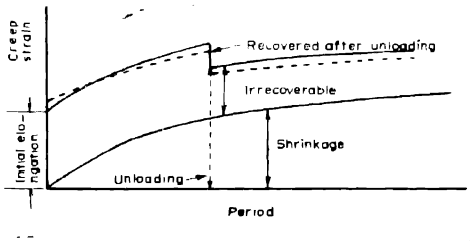

Fig. 1.6.8 : Creep of concrete

Problems

1.1 A simply supported beam of span L and depth h is subjected to self weight W_g and a live load of W_e. Both the loads are distributed uniformly over the span. Find a cable force and profile so that a load of $W_g + W_e/2$ is balanced by the cable.

1.2 A simply supported beam of span L and depth h is subjected to self weight W_g uniformly distributed and four concentrated loads of each F, spaced at equal interval. Find load balancing cables for these loads. Adopt two different cables for the two load systems.

1.3 A double overhang beam has the middle span as L and the overhang span on either side as L/4. Determine a prestressing cable for balancing a uniformly distributed load on the entire beam.

CHAPTER II

PRESTRESSING SYSTEM AND LOSSES OF PRESTRESS

2.1. CLASSIFICATION: Prestressed concrete construction may be classified into a number of groups based on design, construction, method of applying prestressing and purpose of the structure. Some of them are discussed here.

2.2. EXTERNAL OR INTERNAL PRESTRESSING SYSTEM: Introduction of a horizontal thrust through the ends of a beam can be achieved either through an external force or through a built up internal thrust. The external prestressing can be obtained by external reactions introduced through different support conditions. For a simply supported beam, the external reaction can be obtained by jacking against abutments as shown in fig. 2.2.1 ; a continuous beam can be prestressed externally by jacking the appropriate supports to get the desired effect (fig. 2.2.2). Economical external prestressing of statically indeterminate structures is not simple and is often impossible. External prestressing is not common even though theoretically possible. It requires greater degree of accuracy in planning, maintenance and execution. Shrinkage of the beam releases certain thrust of the external jack thus reducing the prestressing force on the beam. Similarly a small expansion of the beam will create very high thrust in the beam due to the restraint of the jacks.

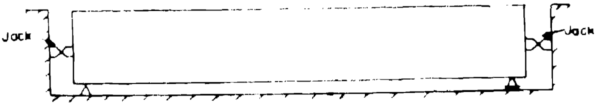

Fig. 2.2.1 : Externally prestressed concrete simply supported beam

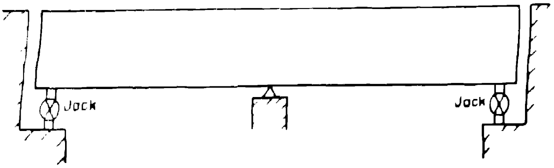

Fig. 2.2.2 : Externally prestressed concrete—continuous beam

2.3. LINEAR OR CIRCULAR PRESTRESSING: Linear prestressing is done in straight members such as beams, piles and slabs whereas circular prestressing is applied to circular structures such as tanks, pipes, silos in which the tendons or wires are put in curve going around the structure.

2.4. PRE-TENSIONING: Pre-tensioning is obtained by stressing the tendons in position to a predetermined amount and placing the concrete in position while maintaining the stress in the tendons through an external force system. As the concrete hardens, the tensioned tendons are bonded; when the tendons are released from external jacks, the tendons will try to regain the original length. The concrete, as a result, is stressed. The tendons are strained (stressed) through hydraulic jacks and the strain is maintained during curing. A typical pre-tensioning bed is illustrated in fig. 2.4.1. Methods of prestressing, anchoring and other items of construction vary with patent. Since tendon force is transferred from steel to the concrete through bond, it is desirable to use small diameter wires. If the profile of the tendon is curved, then necessary profile fixing arrangements have to be provided.

The tendon is stretched between two bulk heads or rigid supports and then anchored to supports till its force is transferred to the proper members. Some type of anchorage arrangements have to be provided for holding the tendons to the supports.

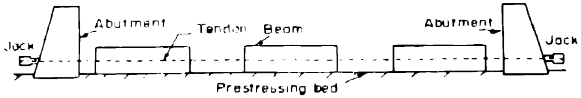

Fig. 2.4.1 : Typical pre-tensioning bed

2.5. POST-TENSIONING SYSTEM: Concrete is cast while there is no stress in the tendon. When the concrete is hardened, the tendons are stretched through hydraulic jacks bearing against the concrete. The tendon force is transferred to the member through necessary anchorage wedges or similar blocks at the end of the member. A flexible hose or rubber tube may be used to house the tendons so that bond is not developed between the wires and concrete while casting or curing the concrete. The hose gets bonded to the concrete as the concrete sets. Sometimes the void between the hose and the wire is filled with a grouting mixture in which case the wire develops a bond with the concrete. This method is called bonded construction in post-tensioning system. In some construction, an inflated water-filled rubber hose is placed in position. As the concrete hardens, the pressure in the hose is released and the hose is pulled out leaving a duct in the concrete. The tendon is inserted in the duct and stressed with the help of jacks. Then the tendon force is transferred to the concrete through anchorages which are usually fixed at the ends of the member. In some cases of construction, the cable is coated with grease or bituminous material and then wrapped in paper so that no bond is developed between the concrete and the tendon. This type of construction is called unbonded construction.

Post-tensioning system can be used for either in situ or pre-cast construction. In most cases, the tensioning of the tendons is done in stages either at site or in factory. Post-tensioning construction does not require rigid abutments, so it is more versatile for large spans. The anchorage is obtained through several patent methods using wedges or cones and bearing plates etc. Some typical anchorage arrangements are shown in fig. 2.5.1.

2.6. PARTIAL PRESTRESSED CONCRETE: A construction where some amount of tensile stresses are allowed to be taken by mild steel bars provided as reinforcement is called a partial prestressed concrete construction. Ordinary reinforcement is also provided to take some of the stresses caused due to handling (2.1—2.10).

2.7. CLASSIFICATION BASED ON METHODS OF PRESTRESSING: The basic principle of prestressing and the behaviour of prestressed beam is more or less the same in all prestressed construction. However the methods of application of prestressing force or the anchorage devices used in different constructions are likely to vary. Based on the methods of application and construction, prestressed concrete is divided into several systems. There are hundreds of patents covering a number of prestressing systems. Every patent has its own method of prestressing force and its own details of anchorages.

(a) Pre-tensioning systems: As described previously, the pre-tensioning system is very adaptable for factory manufacturing of prestressed concrete members. There are several patents for pre-tensioned systems; one of the systems, the Hoyer system has been used in various countries. It consists of stretching the wires between bulk heads placed several metres apart on prestressing bed. The prestressing bed itself is capable of adjusting the bulk heads and span and also of positioning the tendons in profile. To keep the vertical profile of tendons, some kind of tie downs are provided from the roof. The wires are tensioned with hydraulic jacks of long strokes. The anchorage arrangement is simple and can be based on the wedge friction principle. There are several other popular patents in practice which are not discussed in this book.

(b) Post-tensioning systems: In post-tensioning systems, the tensioning is normally done with hydraulic jacks developed particularly to suit the patented system. The anchoring of the wires to the concrete itself needs more care than the anchoring to bulk heads done in a pre-tensioning system. Some popular post-tensioning systems are: (i) Freyssinet, (ii) Magnel, (iii) Hobling, (iv) Leondhardts, (v) Lee-McCall, and (vi) Ryerson BBRV system.

The Freyssinet double acting jack pulls a number of wires at a time using a main ram which reacts against the embedded anchorage. As the required tension of the wire is reached, the inner piston pushes the plug into the anchorage thus causing an anchorage of the wires without much loss of tension from anchorage take up. Similarly other systems use a specific type of jacking to achieve the required tension.

The principles of anchorages can broadly be listed in three groups: (i) wedge action producing frictional grip on wires, (ii) direct bearing from rivet or bolt heads formed at the end of the wires, and (iii) looping of the wires around the concrete. The Freyssinet system uses a concrete cylinder with a conical interior opening and cones reinforced with steel wires. The conical plug has longitudinal grooves to receive the wires. The cylinder is placed flush with the face of the concrete and serves to transmit the reaction of the jack and the prestressing force to the member (fig. 2.5.1). The Magnel system uses tapered sandwich plate with wedges as shown in fig 2.5.1. The Lee-McCall system uses steel rod with nut arrangement. Strescon and Prescon systems use rivet heads bearing against end steel plates. Ryerson BBRV posttensioning system does not use the friction or

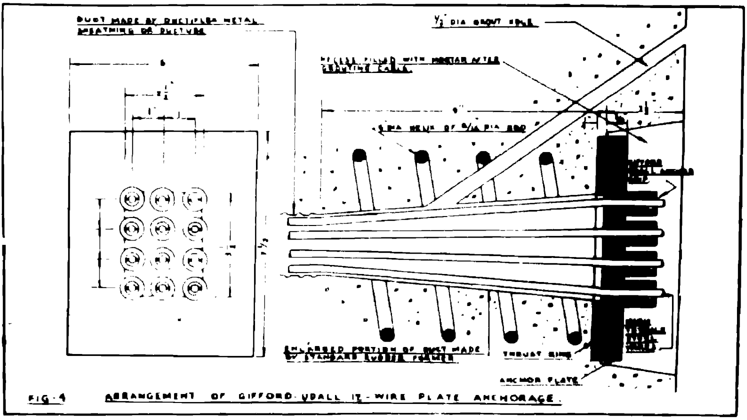
DUCT MADE BY DUCTIFLEX METAL SHEATHING OR DUCTUBE
1/2" DIA GROUT HOLE
RECESS FILLED WITH MORTAR AFTER TENSIONING CABLE
6"
6 DIA HELIX OF 5/16 DIA ROD
ENLARGED PORTION OF DUCT MADE BY STANDARD RUBBER FORMER
THRUST RING
ANCHOR PLATE
FIG-4 ARRANGEMENT OF GIFFORD-UDALL 12-WIRE PLATE ANCHORAGE.

Gifford-Udall-CCL Anchor Grip for 4, 5 & 7 mm wires used in pre-tensioning and in plate anchorages for post-tensioning
(*Courtesy of Killick, Nixon & Co., Ltd., Bombay*)

wedge type of grips but inserts flat plate shims after the necessary extension of the wires. There is variety of stressing and anchors used to suit different situations; one typical example is shown in fig. 2.5.1.

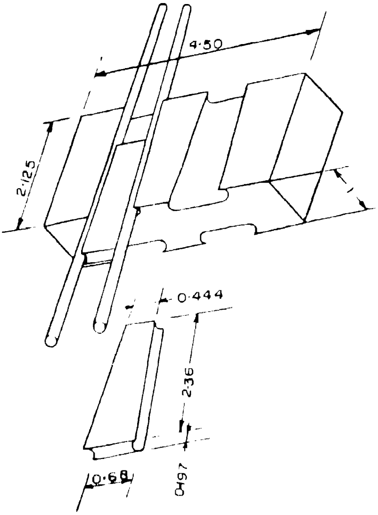

(a) Anchorage of Magnel system
(*Courtesy of Stressed Concrete Construction Ltd., Madras*)

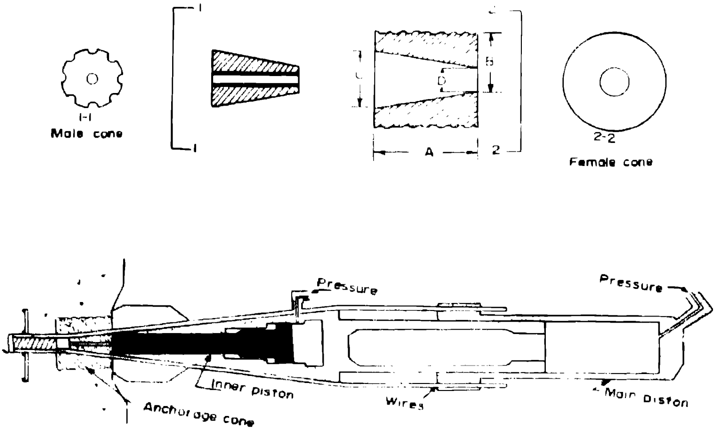

(b) Freyssinet jack and other cone system
(*Courtesy of Freyssinet Prestressed Concrete Co. Ltd., India*)

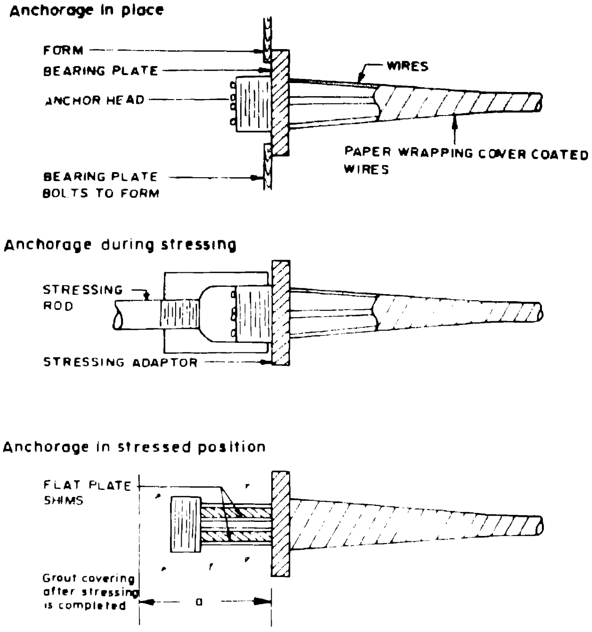
Anchorage in place
FORM
BEARING PLATE
ANCHOR HEAD
WIRES
PAPER WRAPPING COVER COATED WIRES
BEARING PLATE BOLTS TO FORM
Anchorage during stressing
STRESSING ROD
STRESSING ADAPTOR
Anchorage in stressed position
FLAT PLATE SHIMS
Grout covering after stressing is completed
a

(c) Type M stressing anchorage Ryerson BBRV System
(*Courtesy of Joseph T. Ryerson & Son, Inc. U. S. A.*)
Fig. 2.5.1 : Typical stressing end anchorage

2.8. LOSS OF PRESTRESS : Prestressing force is measured either through the extension of the prestressed wire or by a pressure gauge reading of hydraulic jack at the time of jacking. The force recorded at the time of jacking at the jack position is not necessarily the amount of force available at all sections of the beam and at various working stages of the beam. In addition to the analytical calculations based on reasonable assumptions, a large amount of experimental data based on material behaviour has also been used to predict the loss of prestress. The various losses of prestressing may be due to (i) creep in steel, (ii) shrinkage of concrete, (iii) creep in concrete, (iv) steam curing, (v) elastic shortening of the member, (vi) anchorage take up, (vii) bending of the member, (viii) friction.

2.9. LOSS OF PRESTRESS DUE TO CREEP IN STEEL : The amount of creep in steel varies from 2 % to 6 % depending on the steel and also on its stress level. As the stress level increases, the creep of steel too increases. An average of 2 % to 3 % creep strain may be taken where the stress level of steel is about 0.6 times the ultimate strength. Most of the creep in steel occurs in the first 1000 hours of its stress. The stress on steel or concrete is not constant in the history of the structure. As the concrete relieves some prestress, the stress in steel drops; therefore the creep in steel could be assumed as relatively low.

2.10. LOSS OF PRESTRESS DUE TO SHRINKAGE OF CONCRETE : The loss of prestress due to shrinkage is to be calculated based on shrinkage of concrete. The following shrinkages are adopted for design by Indian code of practice.

For pre-tensioning concrete, total shrinkage $= 0.0003$

For post-tensioning concrete, total shrinkage $= (0.0003)/\log_{10}(T+2)$

where $T =$ age of concrete in days at transfer

2.11. LOSS OF PRESTRESS DUE TO CREEP IN CONCRETE : As explained in chapter I, creep in concrete is a complex phenomenon. For the purpose of the design, the following creep coefficients are adopted by Indian code of practice.

TABLE 2.11.1 : CREEP COEFFICIENTS

Conditions of exposure	Creep coefficient
In water	$0.5\ C_{c1}$ to $1.0\ C_{c1}$
In humid air	$1.5\ C_{c1}$ to $2.0\ C_{c1}$
In average humid air	$2.0\ C_{c1}$ to $3.0\ C_{c1}$
In dry atmosphere	$2.5\ C_{c1}$ to $4.0\ C_{c1}$

Where the value of C_{c1} is taken as given in table 2.11.2.

TABLE 2.11.2

Ratio of strength of concrete at transfer to that 28 days	C_{c1}
0.50	2.2
0.84	1.5
1.00	1.0

2.12. LOSS OF PRESTRESS DUE TO STEAM CURING : Steam curing is often used with a pre-tensioning system. The curing period has to be accelerated so as to release the pre-tensioning bed and the equipment for further fabrication. Raising the temperature of concrete with steam before hardening heats the prestressed steel and thus relaxes some of the prestressing force. On cooling, the concrete contracts and offsets the strain recovery in the steel. Creep characteristics of steel changes at 100°C temperature; consequently there will be a considerable loss of prestress in the member.

2.13. LOSS OF PRESTRESS DUE TO ELASTIC SHORTENING OF THE MEMBER : Elastic shortening depends upon the modulus of elasticity of concrete, steel and the initial prestressing force. In pre-tensioned construction, the prestressing force is measured while jacking against bulk heads. As soon as the transfer of the prestressing force takes place, the member undergoes an elastic deformation. While computing prestress losses, all the transfer force should be considered towards elastic shortening.

In post-tensioned construction, wires are stretched with reaction against the member itself, so the elastic deformation takes place simultaneously and the jacking or the initial stresses are independent of the elastic shortening. If the tensioning of wires is done in stages, the wires that were anchored will undergo elastic shortening while the jacking is done for the next stage of prestressing. The wires anchored at the very first time will loose a maximum of prestressing force whereas the wires stretched later will not undergo any loss of prestress from elastic shortening. If the prestressing is done at equal intervals, an average prestressing force could be taken for computing the elastic shortening.

2.14. LOSS OF PRESTRESS DUE TO ANCHORAGE TAKE UP : In a post-tensioned system, an allowance should be made for slipping of steel at the time of transferring the tendon force from the jacks to the member. In most of the systems, there is likely to be a small amount of adjustment of anchorage cones resulting in a small amount of relaxation of prestress. An average of about 0.25 cm is estimated as anchorage slip in wedge type of grips ; for heavy strands the slip may be 0.5 cm.

2.15. LOSS OF PRESTRESS DUE TO BENDING OF THE MEMBER : Loss of prestress due to bending depends on the bonding character of the construction. In an unbonded construction when the beam bends due to external load, there is bound to be some change in the length of the prestressed steel, and the loss of prestress due to bending is illustrated in fig. 2.15.1. In bonded construction, even though there will be a change in the length of the tendon as the live load comes, it would cause only a local effect and no effect on the prestressing force. As soon as the live load is taken away, the loss due to bending will be recovered. For design calculations while working with live loads, the loss due to bending has to be considered for all unbonded construction.

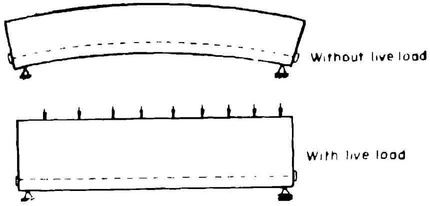

Fig. 2.15.1 : Effect of bending on loss of prestress

2.16. LOSS OF PRESTRESS DUE TO FRICTION :

There will be considerable movement of sliding of tendon relative to the surrounding duct during the tensioning operation. Because the tendon is in direct contact with the duct or with spacers provided, the friction will cause a reduction in prestressing force as the distance from the jack increases. There will also be some amount of friction in the jack and in the anchorage system. The loss of prestress due to friction is discussed below :

(a) *Friction in jack and anchorage :* This friction is directly proportional to the jack pressure and will considerably depend upon the system of stressing. The loss of prestress due to this friction has to be specified by the patent.

(b) *Friction due to alignment variations :* Whether a duct is straight or curved, there will be a certain amount of variation caused by vibrations or constructional methods in the actual alignment. The variation in the alignment will cause some points of contact of the wire with the duct and also with other wires or spacers ; this will cause friction. The prestressing force at any distance x from jack may be expressed as

$$P_x = P_0 e^{-kx} \qquad .. \quad (2.16.1)$$

Where

P_0 = prestressing force at jacking end

e = the base of Napierian logarithm (2.718)

k = constant depending upon the type of duct (wobble correction factor).

$\cong$0.0015 per metre for metal sheating with good supports for sheating

$\cong$0.003 per metre for metal sheating without rigid supports for sheating

The various values of k are shown in table 2.16.1 (derivation of this expression is given in the next section).

(c) *Friction in duct due to curvature* : For curved tendons, the friction depends on the curvature. The derivation is given below with reference to a small element of the tendon. The normal component of P in the radial direction is given by

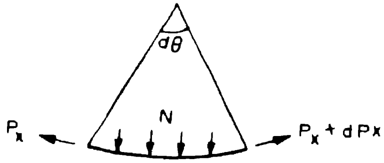

Fig. 2.16.1 : Radial component of cable

$N = (P_x + dP_x)(\theta + d\theta) - P_x\theta = P_x d\theta$ (neglecting second order terms)
$= P_x (d\theta/dx)\, dx$

Frictional loss $= dP_x = \mu N = \mu P_x (d\theta)$

Where μ = coefficient of friction
N = normal component of force

$$\frac{dP_x}{P_x} = \mu d\theta$$

On integration from x to o gives

$$\text{Log } \frac{P_0}{P_x} = \mu(\theta_0 - \theta_x)$$

Or

$$P_0 = P_x e^{\mu(\theta_0 - \theta_x)} \quad \ldots (2.16.2)$$

Let $(\theta_0 - \theta_x) = \alpha$ (change in slope between jacking point and the point under consideration)

Loss of prestress $= P_0 - P_x = P_x(e^{\mu\alpha} - 1)$

$$\text{Frictional loss} = \frac{P_0 - P_x}{P_x} \left(e^{\mu\alpha} - 1 \right) \quad \ldots (2.16.3)$$

The values of frictional coefficient μ varies from 0.25 to 0.55 depending upon the duct surface. Approximate values are tabulated in table 2.16.1.

TABLE 2.16.1 : FRICTIONAL COEFFICIENT

	Duct	μ	k
1.	Steel moving on smooth concrete	0.30 to 0.45	0.0015
2.	Duct formed by withdrawing tubing	0.35 to 0.55	0.0015 to 0.003
3.	Rubber core	0.40 to 0.55	0.0015 to 0.003

The total effect of friction due to alignment and curvature may be written as (adding the frictional force due to alignment variations to the curvature) :

$$\frac{dP_x}{P_x} = (\mu d\theta + kdx)$$

on integration $P_0 = P_x e^{(\mu\alpha + kx)}$ .. (2.16.4)

$$P_0 - P_x = [e^{(\mu\alpha + kx)} - 1] P_x \simeq [\mu\alpha + kx] P_x \quad .. \ (2.16.5)$$

The various losses in prestress due to different causes are shown in table 2.16.2.

If P_t is the transfer prestress then jacking stress P_0 is given as :

$P_0 = P_t$ + (loss of prestress due to frictional effects)

TABLE 2.16.2 : ABSTRACT OF LOSS OF PRESTRESS
(Average values for normal conditions)

Nature of loss due to		Post-tensioning system		Pre-tensioning system	Remarks
		unbonded	bonded		
1		2	3	4	5
1.	Creep in steel	2 to 3% of initial prestress	2 to 3%	1.5 to 2%	
2.	Shrinkage in concrete	0.0002	0.0002	0.0003	
3.	Creep in concrete	2.0 to 3.0%	2.0 to 3.0%	2.0 to 3.0%	
4.	Elastic shortening (Strain)	$P_t/2AE$ If prestressing is done in stages at equal intervals.	$P_t/2AE$	P_t/AE	
5.	Anchorage take up	0.25 cm to 0.50 cm	0.25 cm to 0.50 cm	Very little	for wires to strand
6.	Bending	As per moment curvature		0	
7.	Steam curing			As per calculation	
9.	Frictional effect	$(e^{\mu\alpha + kx} - 1)$		0	Values of μ & k are given in table 2.16.1

Example 2.16.1 : Determination of loss of prestress in a pre-tensioned prestressed concrete beam of 8 m span to carry a load of 5000 kg/m. The beam is prestressed with 180000 kg at transfer and the cable has a parabolic profile with maximum eccentricity of 10 cm at the middle of the span.

Given data :

Cross section $= 30 \times 80$ cm

$A_s = 18$ sq cm, $P_t = 180000$ kg

$E_s = 2 \times 10^6$ kg/sq cm, $E_c = 3 \times 10^5$ kg/sq cm

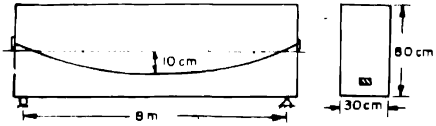

Fig. 2.16.2 : Example 2.16.1

Solution :

Prestress at transfer $= f_s = \dfrac{180000}{18} = 10000$ kg/sq cm

ϵ_s (strain in steel) $= \dfrac{f_s}{E_s} = 5 \times 10^{-3}$

Losses of prestress due to various causes are computed one after another and finally tabulated at the end.

(i) Elastic shortening : Elastic shortening of beam which will affect the prestressing force is the cumulative compressive strain of the concrete fibre at the steel profile level. It is rather hard to calculate exact shortening of the fibres at steel level if the cables do not have smooth profiles. Calculations could become very tedious if the cables have some complicated profiles. Approximate and fairly accurate methods of determination of loss due to elastic shortening are illustrated in this example. Profile of the cable which is of a parabolic form, can be given by

$$e_x = \frac{4ex\,(L-x)}{L^2} \qquad \ldots \quad (2.16.6)$$

Where

e_x = eccentricity of the cable at distance **x** from the end of the span

Then compressive strain at steel level due to prestressing force $\Big\} = \dfrac{1}{E_c}\left(\dfrac{P_t}{A} + \dfrac{P_t\,e^2_x}{I}\right)$

If ϵ_c is the mean elastic strain due to prestressing force, then

$$\epsilon_c = \frac{1}{LE_c}\int^{L}\left(\frac{P_t}{A} + \frac{P_t\,e^2_x}{I}\right)dx$$

On substitution of the respective quantities in the above expression ϵ_c works out to be

$$\epsilon_c = \frac{82.5}{E_c}$$

An approximate mean strain could be obtained by taking a mean value of strain at maximum and minimum strain points. In this problem, minimum compressive strain occurs at support and maximum strain occurs at mid-span.

$$\text{Strain at end section} = \frac{P_t}{AE_c} = \frac{75}{E_c}$$

$$\text{Strain at mid section} = \frac{1}{E_c}\left(\frac{P_t}{A} + \frac{P_t\, e^2_x}{I}\right) = \frac{89}{E_c}$$

$$\text{Approximate mean strain } \epsilon_c = \frac{89+75}{2E_c} = \frac{82}{E_c}$$

As seen from the above calculations the difference between the approximate mean strain and the mean strain is not very much. The difference is negligible in this particular problem.

$$\text{Loss of strain due to elastic shortening} = \frac{82.5}{E_c} = 2.75 \times 10^{-4}$$

(ii) Shrinkage strain : As per Indian code of practice the shrinkage strain may be taken as 0.0003.

(iii) Creep strain in concrete : Creep coefficient in average humid weather conditions may be taken as 2.5 for transfer of prestress at 28 days of curing of concrete.

$$\text{Creep strain} = (C_c - 1)\ \epsilon_c = 4.12 \times 10^{-4}$$

(iv) Creep in steel : Let creep in steel be about 2% then

$$\text{Creep strain in steel} = 0.02\ \epsilon_s$$

(v) Other losses : Loss of prestress due to anchorage take up and friction of spacers and end block is small in pre-tensioned system. About 2% of strain loss may be counted due to anchorage take up and friction of the spacers. The loss of prestress and the corresponding percentage is shown in table 2.16.1.

The example gives an approximate idea of losses of prestress due to various reasons. Percentage loss of prestress in this example is 23.7.

TABLE 2.16.1 : LOSS OF PRESTRESS

Loss due to	Loss of strain	Percentage loss
(i) Elastic shortening	2.75×10^{-4}	5.5
(ii) Shrinkage	3.0×10^{-4}	6.0
(iii) Creep in concrete	4.12×10^{-4}	8.2
(iv) Creep in steel	1×10^{-4}	2.0
(v) Anchorage etc	1×10^{-4}	2.0
Total	11.87×10^{-4}	23.7

Effective prestress force P_e is 76.3%

$$\eta = \frac{\epsilon_s - \text{loss}}{\epsilon_s} = \frac{Pe}{P_t} = (1 - 0.237) = 0.763$$

$$P_e = \eta P_t = 0.763 \times 180000 = 137340 \text{ kg}$$

Example 2.16.2 : A post-tensioned prestress concrete beam of 50 m span is subjected to a transfer prestress force of 93.8×10^4 kg. Transfer of force is at 28 day strength. Profile of the cable is parabolic with maximum eccentricity at mid section as 110 cm. Determine the loss of prestress and find the jacking force required. The beam is subjected to a live load of 2400 kg/m and jacking is done from both ends of the beam.

Given data:

$P_t = 93.8 \times 10^4$ kg, $A = 9471$ sq cm,

$A_s = 89.3$ sq cm, $I = 6224 \times 10^4 \text{ cm}^4$,

$f_s = 10500$ kg/sq cm,

$E_s = 2.1 \times 10^6$ kg/sq cm,

$E_c = 3.82 \times 10^5$ kg/sq cm

Solution :

Elastic strain in steel at transfer condition is given by

$$\epsilon_s = \frac{f_s}{E_s} = \frac{10500}{2.1 \times 10^6} = 50 \times 10^{-4}$$

(i) Loss due to elastic shortening :

$$\text{Elastic strain at end section} = \frac{P_t}{AE_c} = 2.60 \times 10^{-4}$$

$$\text{Elastic strain at mid section} = \left(\frac{P_t}{AE_c} + \frac{Me}{IE_c}\right) = 3.66 \times 10^{-4}$$

Where

M = bending moment due to prestressing force and self weight of the beam

$$\text{Mean elastic strain} = \left(\frac{3.66+2.6}{2}\right)\times 10^{-4} = 3.13\times 10^{-4}$$

The strands are strained at intervals so half the mean strain is the effective loss in the shortening.

$$\text{Loss of strain} = \frac{3.13\times 10^{-4}}{2} = 1.56\times 10^{-4}$$

(ii) Shrinkage in concrete :

$$\text{Shrinkage} = \frac{3\times 10^{-4}}{\log(T+2)} = 2\times 10^{-4}$$

(iii) Creep in concrete :

Assuming a creep coefficient of 2.5,
creep strain $= 1.5\times 3.13\times 10^{-4} = 4.69\times 10^{-4}$

(iv) Creep in steel :

Assuming a creep strain in steel as about 2.0 %
creep strain in steel $= 0.02\ \epsilon_s = 1.0\times 10^{-4}$

(v) Anchorage take up :

Let 0.25 cm be the anchorage take up at each jacking end,

$$\text{so loss of strain} = \frac{0.25}{L/2} = 1.0\times 10^{-4}$$

(vi) Strain due to external force :

Strain in concrete at the steel level at mid span due to external load is given by

$$\frac{M_1 c}{IE_c} = -3.47\times 10^{-4}$$

Where M_1 is bending moment at mid span due to ext. loads.

The negative sign is given to indicate that there is a gain in strain instead of loss (local strain at mid span).

(vii) Frictional loss :

Assuming a metallic sheathing, the frictional coefficients may be taken as

$$\mu = 0.25$$
$$k = 0.0015$$

As the jacking is done from both ends, effective length of 25 m span is taken for calculations. The profile of the cable is given by

$$e_x = \frac{4e}{L^2}(Lx-x^2)$$

$$\left[\frac{de_x}{dx}\right]_{x=0} = 0.088$$

The slope change α = (0.088) radians

$$\frac{P_0-P_t}{P_t} = \left(\mu\alpha + \frac{kL}{2}\right) = 0.0595$$

$$\text{Strain loss} = \frac{P_0-P_t}{E_s\,A_s} = 0.0003$$

The loss of prestress due to various causes are tabulated in table 2.16.2.

TABLE 2.16.2 : LOSS OF PRESTRESS

Loss due to	Loss of strain	Percentage loss
(i) Shortening	1.56×10^{-4}	3.13
(ii) Shrinkage	2.00×10^{-4}	4.00
(iii) Creep in concrete	4.69×10^{-4}	9.38
(iv) Creep in steel	1.00×10^{-4}	2.00
(v) Anchorage take up	1.00×10^{-4}	2.00
(vi) Bending	-3.47×10^{-4}	-6.94
Total	6.78×10^{-4}	13.57

$$\eta = 1-0.1357 = 0.8643$$

$$P_e = 0.8643\,P_t = 80.9\times10^4\ \text{kg}$$

$$P_0 = P_t + \text{frictional loss} = (1+0.0595)\,P_t = 99.4\times10^4\ \text{kg}$$

Problems

2.1 A simply supported beam of 16 m span is provided with a straight cable profile with a kink at the mid span. The cable has zero eccentricities at both end sections and e at mid section. If P_t is the prestressing force required at the mid section, determine the prestressing forces at both the end sections of the beam. Wobble and frictional coefficients may be taken as k and μ respectively.

2.2 A simply supported pre-tensioned concrete beam of 8 m span is rectangular in cross section of 30 by 80 cm size. It is provided with a parabolic cable with 20000 kg prestressing force and a sag of 20 cm. Determine the loss of prestress and find the jacking force. Use the following coefficients :

$k=0.0015$ per metre, $\mu=0.45$, $C_c=2.0$, $E_s=2.1\times10^6$ kg/sq cm, $E_c=3.2\times10^5$ kg/sq cm.

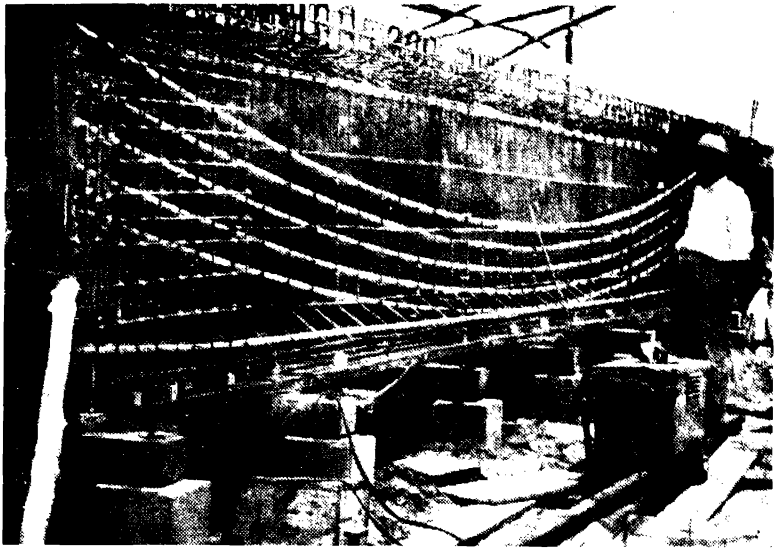

Bridge beam showing cables, ready for casting
(*Courtesy of Killick, Nixon & Co., Ltd., Bombay*)

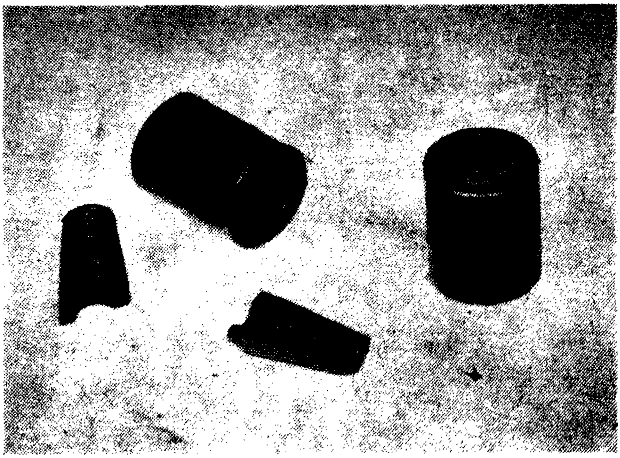

Gifford-Udall-CCL 12/7 mm anchorage used for post-tensioning
(*Courtesy of Killick, Nixon & Co., Ltd., Bombay*)

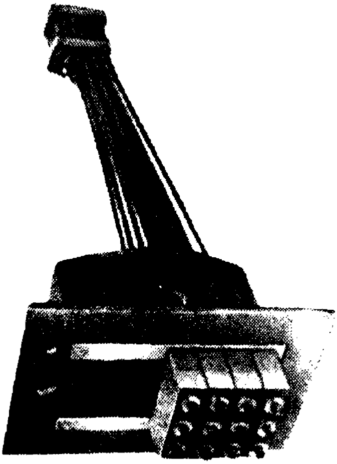

21 Strand Anchorage Assembly

(Courtesy of Stressed Concrete Constructions Pvt. Ltd., Bombay-1)

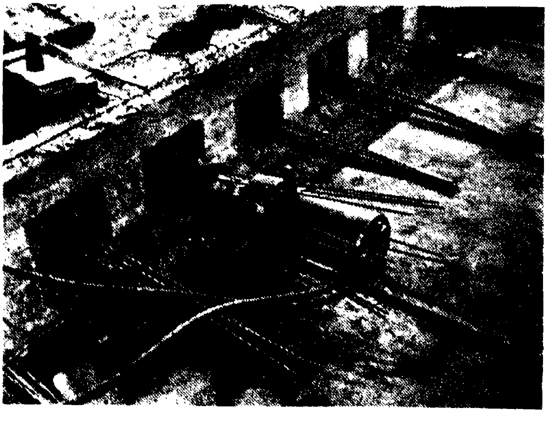

Prestressing operation in progress

(Courtesy of Freyssinet Prestressed Concrete Co., Ltd., Bombay)

CHAPTER III

WORKING LOAD DESIGN OF SIMPLY SUPPORTED PRESTRESSED CONCRETE BEAMS

3.1. INTRODUCTION : In working load design, the stresses in member due to various working loads are calculated assuming elastic behaviour of the material. These stresses are adopted based on safety and economy of the material. The following basic assumptions are used in service load design :

(i) Elastic and linear behaviour of the material.
(ii) Homogeneous property of the material.
(iii) Plane section remains plane even after bending.
(iv) No cracking at any section.
(v) Principal stresses not used as criteria of design.

3.2. LOAD CONDITIONS : Prestressed concerte beams are subjected to two limiting conditions of loading, (i) transfer of prestress, and (ii) working load. Prestressing bed and the equipment may be released for continuous operation by transferring the prestress before the concrete attains its full strength. Prestressing force decreases with time (because of various losses of prestress) and reaches a steady state after long period and by this time the concrete attains its full strength. A qualitative behaviour of concrete strength and the prestressing force with age is shown in fig. 3.2.1. Hence at transfer condition, prestressing force is maximum and concrete strength is minimum.

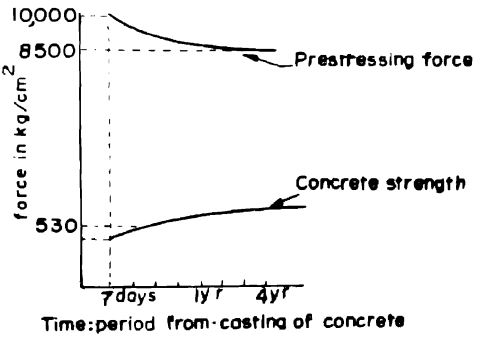

Fig. 3.2.1 : Typical stress variation

The second design criteria occurs when the concrete and steel reach a steady state with critical working loads. In this condition, concrete strength is maximum and prestressing force is minimum while superimposed and live loads are at maximum. All possible load conditions that are likely to occur in prestress concrete construction are tabulated in table 3.2.1.

TABLE 3.2.1 : CONDITIONS OF LOADING

Load condition	Loads acting*	Prestressing force	Concrete strength	Remarks
(i)	$P+G$	Max $(=P_t)$	$\leqslant f'_c$	critical post tensioning transfer condition.
(ii)	$P+G+S$	Max $(\leqslant P_t)$	$\leqslant f'_c$	
(iii)	$P+G+S+L+I$	Max $(\leqslant P_t)$	$\leqslant f'_c$	possible only if the L.L. acts immediately after casting.
(iv)	$P+G$	Min $(\geq P_e)$	$\geqslant f'_c$	
(v)	$P+G+S$	Min $(\geq P_e)$	$\geqslant f'_c$	
(vi)	$P+G+S+L+I$	Min $(\geq P_e)$	$\geqslant f'_c$	critical

*where the letters P, G etc. indicate

P = prestressing force ; G = self weight of beam

S = superimposed load ; L = live load, and I = impact load.

Load condition (ii) or (v) comes if a superimposed load such as false work or some slabs are imposed immediately during transfer conditions.

3.3. ALLOWABLE STRESSES : Having determined the critical load conditions, it is essential to fix some limitations on the allowable stresses at various load conditions. A set of nondimensionalised allowable stress coefficients are generally used and the limitations of these stress coefficients are given in table 3.3.1.

TABLE 3.3.1 : STRESS COEFFICIENTS

Critical condition	Types of stresses	Stress coefficients	
		working	I.S.* code limits
Transfer	compression	$c_{ct} \leqslant c'_{ct}$	$c'_{ct} = 0.43$ to 0.50
	tension	$c_{tt} \leqslant c'_{tt}$	$c'_{tt} = 0.1$ or $10/f'_c$
Working load	compression	$c_{ce} \leqslant c'_{ce}$	$c'_{ce} = 0.31$ to 0.40
	tension	$c_{te} \leqslant c'_{te}$	$c'_{te} = 0.1$ or $10/f'_c$

*I.S. refers to Indian standards code of practice

$c'_{ct}\,f'_c$ =allowable compressive stress at transfer

$c'_{tt}\,f'_c$ =allowable tensile stress at transfer

$c'_{ce}\,f'_c$ =allowable compressive stress at working load

$c'_{te}\,f'_c$ =allowable tensile stress at working load.

3.4. CRITICAL STRESS CONDITIONS :

Extreme stresses occur at bottom and top fibres of a beam at given cross-section for each of the load conditions. Hence the working load design is governed by the extreme fibre stresses in the two load conditions. The expressions for the stresses are :

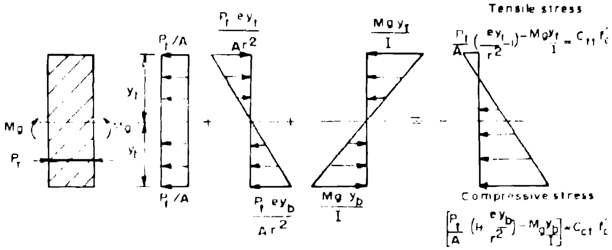

Tensile stress
$\frac{P_t}{A}\left(\frac{ey_t}{r^2}-1\right)-M_g\frac{y_t}{I}=C_{tt}f'_c$
$\frac{P_t\,ey_t}{Ar^2}$
$\frac{M_g y_t}{I}$
P_t/A
y_t
M_g
g
y_b
P_t
+
+
=
P_t/A
$\frac{P_t\,ey_b}{Ar^2}$
$\frac{M_g y_b}{I}$
Compressive stress
$\left[\frac{P_t}{A}\left(1+\frac{ey_b}{r^2}\right)-M_g\frac{y_b}{I}\right]=C_{ct}f'_c$

Fig. 3.4.1 : Stress conditions at transfer

$$\frac{P_t}{A}\left(\frac{ey_t}{r^2}-1\right)-M_g\frac{y_t}{I}=c_{tt}f'_c \leqslant c'_{tt}f'_c \quad \text{.. (3.4.1)}$$

$$\frac{P_t}{A}\left(\frac{ey_b}{r^2}+1\right)-M_g\frac{y_b}{I}=c_{ct}f'_c \leqslant c'_{ct}\,f'c \quad \text{.. (3.4.2)}$$

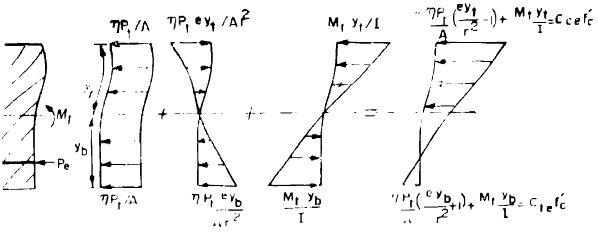
$\eta P_t/A$
$\eta P_t e y_t/Ar^2$
$M_t y_t/I$
$-\frac{\eta P_t}{A}(\frac{ey_t}{r^2}-1)+M_t\frac{y_t}{I}=c_{ce}f'_c$
M_t
y_t
y_b
P_e
$\eta P_t/A$
$\eta P_t\frac{ey_b}{Ar^2}$
$\frac{M_t y_b}{I}$
$\frac{\eta P_t}{A}(\frac{ey_b}{r^2}+1)+M_t\frac{y_b}{I}=c_{te}f'_c$

Fig. 3.4.2 : Stress conditions at working load

$$-\eta\frac{P_t}{A}\left(\frac{ey_t}{r^2}-1\right)+M_t\frac{y_t}{I}=c_{ce}f'_c \leqslant c'_{ce}f'_c \qquad .. \quad (3.4.3)$$

$$-\eta\frac{P_t}{A}\left(\frac{ey_b}{r^2}+1\right)+M_t\frac{y_b}{I}=c_{te}f'_c \leqslant c'_{te}f'_c \qquad .. \quad (3.4.4)$$

where

P_t = prestressing force at transfer
I = moment of inertia of the beam
M_g = moment due to self weight of the beam
L = length of span
M_t = bending moment at working load ($M_t = M_g + M_s + M_l$)
M_s = bending moment due to superimposed load
M_a = $M_s + M_l$
η = effectiveness of prestressing force ($=P_e/P_t$)

All values of c's are positive, so both the compressive as well as tensile stresses are given in magnitude without any sign attached to them. The centre of steel is also assumed to be below the centroidal axis of the beam. The quantities A, y_t, y_b and I in pre-tensioned bonded construction should be based on fully transferred cross-sectional area of the beam. In post-tensioned grouted beam, these quantities before and after grouting are different and the effect of the grout is to be considered in the working load condition only. For all practical purposes, the gross cross sectional area is a fairly good approximation and is adopted in this book for all purposes of calculations.

3.5. DIMENSIONLESS VARIABLES :

$y_t + y_b = h$ (over all height of the section)

$$\frac{y_t}{h}=\frac{y_t}{y_t+y_b}=\frac{1}{1+(y_b/y_t)}$$

Substitution of $M_t = M_a + M_g = (M_s + M_l + M_g)$ and $M_g = A\gamma \frac{L^2}{8}$ in the four equations yield nondimensionalised equations.

$$\frac{P_t}{Af'_c}\left[\frac{e}{h}\left(\frac{h}{r}\right)^2 \frac{1}{(y_b/y_t+1)} - 1\right] - \left(\frac{\gamma L^2}{8hf'_c}\right)\left(\frac{1}{(y_b/y_t+1)}\right)\left(\frac{h}{r}\right)^2 = c_{tt} \quad .. \quad (3.5.1)$$

$$\frac{P_t}{Af'_c}\left[\frac{e}{h}\left(\frac{h}{r}\right)^2 \frac{y_b/y_t}{(y_b/y_t+1)} + 1\right] - \left(\frac{\gamma L^2}{8hf'_c}\right)\left(\frac{y_b/y_t}{(y_b/y_t+1)}\right)\left(\frac{h}{r}\right)^2 = c_{ct} \quad .. \quad (3.5.2)$$

$$-\eta\frac{P}{Af'_c}\left[\frac{e}{h}\left(\frac{h}{r}\right)^2 \frac{1}{(y_b/y_t+1)} - 1\right] + \left(\frac{\gamma L^2}{8hf'_c}\right)\left(\frac{(1+M_a/M_g)}{(y_b/y_t+1)}\right)\left(\frac{h}{r}\right)^2 = c_{ce} \quad .. \quad (3.5.3)$$

$$-\eta\frac{P_t}{Af'_c}\left[\frac{e}{h}\left(\frac{h}{r}\right)^2 \frac{y_b/y_t}{(y_b/y_t+1)} + 1\right] + \left(\frac{\gamma L^2}{8hf'_c}\right)\left(\frac{y_b/y_t\ (1+M_a/M_g)}{(y_b/y_t+1)}\right)\left(\frac{h}{r}\right)^2 = c_{te} \quad .. \quad (3.5.4)$$

These four equations can further be simplified by introducing nondimensionalised parameters as suggested by Khachaturian and the equations are given below (3.1) :

$$m\left[\frac{\epsilon}{\rho(1+\Delta)} - 1\right] - \frac{1}{8\omega\rho(1+\Delta)} = c_{tt} \quad .. \quad (3.5.5)$$

$$m\left[\frac{\epsilon\Delta}{\rho(1+\Delta)} + 1\right] - \frac{\Delta}{8\rho\omega(1+\Delta)} = c_{ct} \quad .. \quad (3.5.6)$$

$$-\eta\, m\left[\frac{\epsilon}{\rho(1+\Delta)} - 1\right] + \frac{(1+R)}{8\omega\rho(1+\Delta)} = c_{ce} \quad .. \quad (3.5.7)$$

$$-\eta\, m\left[\frac{\epsilon\Delta}{\rho(1+\Delta)} + 1\right] + \frac{(1+R)\Delta}{8\rho\omega(1+\Delta)} = c_{te} \quad .. \quad (3.5.8)$$

Where

$\frac{hf'_c}{\gamma L^2} = \omega$ .. depth factor

$(r/h)^2 = \rho$ .. efficiency factor

$y_b/y_t = \Delta$ .. shape factor

$M_a/M_g = R$ .. moment ratio

} section properties

$P_t/Af'_c = m$ .. reinforcement ratio

$e/h = \epsilon$ .. eccentricity ratio

} steel properties

Known and unknown quantities of the above four governing equations may be classified as

c_{ct}, c_{tt}, c_{ce} and c_{te} ....known quantities

ρ, ω, Δ, ϵ, η, m and R..........unknown quantities

Out of the seven unknowns, η can reasonably be estimated and recomputed if necessary. With this assumption, there are six unknowns in the four equations which means that at least two of the nondimensionalised parameters must be estimated to get a unique solution. Arbitrary estimate of any of the two parameters is done based on practical and economic considerations.

To assume values of any two parameters, a constructive discussion is necessary. Four out of the six parameters (ω, ρ, Δ, R) are essentially associated with the property of the cross section and the other two parameters (m, ϵ) are associated with steel.

(a) *Depth factor* ($\omega = hf'_c/\gamma L^2$) : The expression contains three known quantities (f'_c, γ, L) and one unknown quantity h. Depth of the beam in many cases is controlled by architectural and site conditions. Even if it is not given, it can reasonably be assumed. It generally varies from L/15 to L/25. The effect of the depth of the beam on economy is discussed later.

(b) *Efficiency factor* ($\rho = r^2/h^2$) : For a given depth, the efficiency of the section increases with the increase of radius of gyration. The possible range of values of ρ are tabulated in table 3.5.1.

TABLE 3.5.1 : APPROXIMATE LIMITS OF ρ

No.	Section	Limits of ρ
(i)	All area concentrated at C.G.C	0
(ii)	All area concentrated at the extreme fibres	0.25
(iii)	Rectangular section	0.0833
(iv)	I-section	0.10 to 0.17
(v)	T-section	0.08 to 0.10

Higher the value of ρ, higher is the flexural efficiency of the section. The effect and mode of selection of efficiency ratio for design is discussed later.

(c) *Shape factor* ($\Delta = y_b/y_t$) : The range of shape factor for I-section is small. For symmetric I-sections (any symmetric sections) the value of shape factor is unity. Approximate range of shape factors for practical sections is given in table 3.5.2.

TABLE 3.5.2: LIMITS OF Δ

No.	Section	Limit of Δ
(i)	Symmetric sections (symmetry about centroidal axis)	1.0
(ii)	I-section—top flange heavy	1.0 to 1.6
(iii)	I-section—bottom flange heavy	0.6 to 1.0
(iv)	T-section	1.2 to 1.8
(v)	Inverted T	0.6 to 0.9

For heavy live loads and for long spans, the top flange has to be heavier in which case Δ should be chosen between 1.2 to 1.8. Even though the range of Δ is small, the effect on the limiting equations is considerable, so it is desirable that this value is not assumed to start with the design.

(d) *Moment ratio* $\left(R=\frac{M_a}{M_g}=\frac{M_s+M_l}{M_g}\right)$: It is difficult to fix any limit to the range of the value of R. As the length of the span increases, the ratio R decreases whereas M_g is indirectly a function of M_a. The value of R varies from 5.0 (for short spans) to 0.5 (for long spans). It should not be assumed but should be solved from the equations.

(e) *Reinforcement ratio* $(m=P_t/Af'_c)$: P_t/A may be defined as average stress. The reinforcement ratio is simply the ratio of average stress to the strength of concrete. For all practical purposes, it varies from 0.15 to 0.30. The value of m should be computed from the governing equations for economical section.

(f) *Eccentricity ratio* $(\epsilon=e/h)$: Eccentricity ratio is a measure of effective utilization of prestressing force. As the value of ϵ increases, the required prestressing force decreases. ϵ can be taken as high as possible but it has to be bounded by practical considerations such as cover, transfer condition etc. The two hypothetical limiting cases of ϵ are: (i) C.G.S. at the lower kern point, (ii) C.G.S. at the extreme of the lower fibre. These limits of eccentricity ratio vary from 0.25 to 0.55. The extreme value of ϵ is limited by cover distance. d′ is the minimum cover required then

$$\epsilon_{limit}=\frac{y_b-d'}{h}=\frac{y_b}{y_b+y_t}-\frac{d'}{h}=\left(\frac{\Delta}{\Delta+1}-\frac{d'}{h}\right).$$

If the value of d'/h is around 0.1, then

$$\epsilon_{limit}=\left(\frac{\Delta}{\Delta+1}\right)-0.1$$

This value varies from 0.35 to 0.40 for heavy bottom flange and 0.40 to 0.60 for heavy top flange of I-sections.

Table 3.5.3. gives approximate practical limits of various non-dimensionalised parameters.

TABLE 3.5.3 : LIMITING VALUES OF NONDIMENSIONALISED VARIABLE

S. No.	Section	h	ρ	Δ	R	m	ϵ
(i)	I-section with heavier top flange	L/15 to L/25	0.12 to 0.17	1.0 to 1.8	0.5 to 2.0 (long span)	0.15 to 0.30	0.40 to 0.60
(ii)	I-section with heavier bottom flange	L/15 to L/25	0.10 to 0.14	0.6 to 1.5	1.0 to 5.0 (short span)	0.15 to 0.30	0.35 to 0.40
(iii)	T-section	L/15 to L/25	0.08 to 0.10	1.2 to 1.8	0.5 to 2.5	0.15 to 0.30	

3.6. SOLUTION OF THE EQUATIONS: In many practical problems, values of ω and ρ may be assumed and then four unknowns with the four equations can be solved for a given set of values of c's. The four equations are rearranged below :

Multiply eq. 3.5.6 by η and add to eq. 3.5.8

$$\frac{\Delta(1+R-\eta)}{8\rho\omega(1+\Delta)}=\eta c_{ct}+c_{te} \quad .. \quad (3.6.1)$$

Multiply eq. 3.5.5 by η and add to eq. 3.5.7

$$\frac{(1+R-\eta)}{8\rho\omega(1+\Delta)}=\eta c_{tt}+c_{ce} \quad .. \quad (3.6.2)$$

Eq. 3.6.1 over eq. 3.6.2 yields

$$\Delta = \frac{\eta c_{ct} + c_{te}}{\eta c_{tt} + c_{ce}} \qquad .. \quad (3.6.3)$$

Addition of eqs. 3.6.1 and 3.6.2 yields

$$\frac{1+R-\eta}{8\rho\omega\,(1+\Delta)}(1+\Delta) = \eta\,(c_{ct}+c_{tt}) + (c_{te}+c_{ce})$$

or

$$R = 8\rho\omega\,[(c_{te}+c_{ce}) + \eta\,(c_{ct}+c_{tt})] - (1-\eta) \qquad .. \quad (3.6.4)$$

Dividing eq. 3.5.6 by Δ and subtracting from eq. 3.5.5 gives

$$m\left(-1-\frac{1}{\Delta}\right) = c_{tt} - \frac{c_{ct}}{\Delta}$$

or $$m = \frac{c_{ct} - \Delta\, c_{tt}}{1+\Delta} \qquad .. \quad (3.6.5)$$

Similarly from eqs. 3.5.7 and 3.5.8

$$m = \frac{\Delta\, c_{ce} - c_{te}}{\eta\,(1+\Delta)} \qquad .. \quad (3.6.6)$$

Substituting the value of Δ in eq. 3.6.5 yields

$$m = \frac{c_{ct} - c_{tt}\,(\eta c_{ct}+c_{te})/(\eta c_{tt}+c_{ce})}{1+(\eta c_{ct}+c_{te})/(\eta c_{tt}+c_{ce})}$$

$$= \frac{c_{ct}\,c_{ce} - c_{tt}\,c_{te}}{\eta(c_{tt}+c_{ct}) + (c_{te}+c_{ce})} \qquad .. \quad (3.6.7)$$

Adding eqs. 3.5.5 and 3.5.6 gives

$$\epsilon = \left[\rho\,(c_{tt}+c_{ct}) + \frac{1}{8\omega}\right]\left[\frac{(c_{te}+c_{ce}) + \eta(c_{tt}+c_{ct})}{(c_{ct}\,c_{ce} - c_{tt}\,c_{tc})}\right] \qquad .. \quad (3.6.8)$$

Eqs. 3.6.3 and 3.6.4 define the properties of the section and eqs. 3.6.7 and 3.6.8 define the prestressing steel and its location. An interesting aspect about the equations is that eqs. 3.6.3 and 3.6.7 are functions of stress coefficients and effectiveness of prestressing which can always be estimated reasonably well.

Rearrangement of the above equations are presented below. These equations will be used for discussion on the economy of the section.

$$\Delta = \frac{\eta c_{ct} + c_{te}}{\eta c_{tt} + c_{ce}} \qquad .. \quad (3.6.3)$$

$$R = 8\,\rho\omega\,(c_{te}+\eta c_{ct})\left(\frac{1}{\Delta}+1\right) - (1-\eta) \qquad .. \quad (3.6.9)$$

$$= 8\,\rho\omega\,(\eta c_{tt}+c_{ce})\,(\Delta+1) - (1-\eta) \qquad .. \quad (3.6.10)$$

$$m = \frac{c_{ct} - \Delta c_{tt}}{(1+\Delta)} = \frac{\Delta c_{ce} - c_{te}}{\eta\,(1+\Delta)}$$

$$\epsilon = \frac{1+\Delta}{c_{ct} - \Delta c_{tt}} \left[\rho\,(c_{tt}+c_{ct}) + \frac{1}{8\omega} \right] \quad \text{.. (3.6.11)}$$

3.7. ECONOMIC DESIGN: Economic design of a beam may be achieved by obtaining minimum concrete and steel with cost factor built in. But in most cases, the minimum weight design will cause minimum dead weight moments and consequently overall economy. Hence minimum weight design is discussed in this article.

Minimum weight will give minimum self weight moment and consequently maximum value of moment ratio ($R = M_a/M_g$). R will be maximum for maximum value of stress coefficients for any given values of ρ and ω i.e. R is maximum for

$c_{ct} = c'_{ct}$, $c_{tt} = c'_{tt}$

$c_{ce} = c'_{ce}$, $c_{te} = c'_{te}$

If area of steel is minimum, the eccentricity will be maximum and if area of steel is maximum, the eccentricity will be minimum. For long spans, the eccentricity computed from the solution of simultaneous equations is likely to fall beyond the bottom fibre. But the cable has to be kept within the cross section. The shape factor Δ could be so adjusted that the eccentricity of the cable is within the limits of the cross section. A marginal variation of some of the permissible stress coefficients would enable to modify the shape of the cross section. For example, by permitting tension stress at transfer less than the permissible stress, the shape of the cross section will adjust such that there will be more room available for accommodation of the cable.

The permissible stresses fix the shape of the cross section. The range of the Δ as per the permissible stresses of the Indian code of practice is given in table 1 of appendix A.

Indian code of practice for stress coefficients :

At transfer :

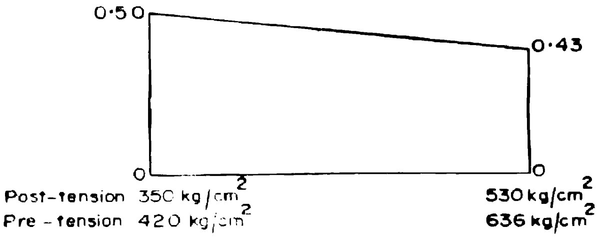

Fig. 3.7.1 : Stress coefficients (c'_{ct})

At working loads:

(1) Stresses in service not likely to increase

(2) Stresses in service likely to increase

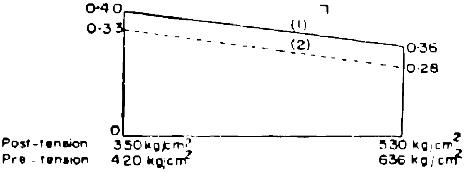
0·40
0·33
(1)
(2)
0·36
0·28
0
Post-tension 350 kg/cm² 530 kg/cm²
Pre-tension 420 kg/cm² 636 kg/cm²

Fig. 3.7.2 : Stress coefficients (c'_{ce})

Allowable tensile stress coefficients are

$$c'_{tt} = 0.1\ c'_{ct},$$

$$c'_{te} = 0.1\ c'_{ce}$$

or 14 kg/sq cm for pre-tensioned and 10 kg/sq cm for post-tensioned whichever is minimum.

3.8. PROPERTIES OF IDEALISED SECTIONS: Most shapes of sections in actual construction are of unsymmetrical I-section. Some typical prestressed concrete sections are shown in figs. 3.8.1, 3.8.2 and 3.8.3. For long spans, beams have normally heavier top flanges. Present section discusses sectional properties of idealised sections for the sake of simplicity.

Properties of cross section of an idealised unsymmetrical I-section.

$$A = (b_t\ t_t + b_b\ t_b + h_w\ b_w)$$

$$= b_t\ t_t + b_b\ t_b + (h - t_t - t_b)\ b_w \qquad \ldots \quad (3.8.1)$$

$$= (b_t h)[c_t + c_f c_b + (1 - c_t - c_b)\ c_w]$$

$$= c_a\ (b_t h) \qquad \ldots \quad (3.8.2)$$

Where

$$c_t = t_t/h,\ \ c_b = t_b/h$$

$$c_w = b_w/b_t,\ c_f = b_b/b_t \qquad \ldots \quad (3.8.3)$$

$$y_b = (1/A)\left[b_t\, t_t\left(h - \frac{t_t}{2}\right) + (h - t_t - t_b)\ b_w\left(\frac{h - t_t + t_b}{2}\right) + \frac{b_b\ t_b^2}{2}\right]$$

$$= \left(\frac{b_t h}{A}\right) h\left[c_t\left(1 - \frac{c_t}{2}\right) + c_w\ (1 - c_t - c_b)\left(\frac{1 - c_t + c_b}{2}\right) + \frac{c_f c_b^2}{2}\right]$$

$$= \frac{h\left[c_t\left(1 - \frac{c_t}{2}\right) + c_w\ (1 - c_t - c_b)\left(\frac{1 - c_t + c_b}{2}\right) + c_f\ \frac{c^2_b}{2}\right]}{[c_t + c_f c_b + (1 - c_t - c_b)\ c_w]}$$

$$= c_{yb} h \qquad \ldots \quad (3.8.4)$$

$y_t = h - y_b$

$$= \frac{h\left[c_b\left(1-\frac{c_b}{2}\right)c_f + c_w\,(1-c_t-c_b)\left(\frac{1-c_b+c_t}{2}\right)+\frac{c^2{}_t}{2}\right]}{[c_t + c_f c_b + (1-c_t-c_b)\,c_w]}$$

$$= c_{yt} h \qquad \text{..} \quad (3.8.5)$$

$$I = b_t h^3\left[\frac{1}{12}\{c_t{}^3 + c_f c^3{}_b + c_w\;(1-c_t-c_b)^3\} + c_t\left(\frac{y_t}{h}-\frac{c_t}{2}\right)^2\right.$$

$$\left. + c_w(1-c_t-c_b)\left(\frac{1+c_t-c_b}{2}-\frac{y_t}{h}\right)^2 + c_f c_b\left(\frac{y_b}{h}-\frac{c_b}{2}\right)^2\right]$$

$$= c_I\, b_t\, h^3$$

Where

c_a, c_I, c_{yb} and c_{yt} are nondimensional coefficients as given in the above expressions.

$$\Delta = \frac{y_b}{y_t} = \frac{c_t\left(1-\frac{c_t}{2}\right)+c_w\,(1-c_t-c_b)\left(\frac{1-c_t+c_b}{2}\right)+c_f\frac{c^2{}_b}{2}}{c_f c_b\left(1-\frac{c_b}{2}\right)+c_w\,(1-c_t-c_b)\left(\frac{1-c_b+c_t}{2}\right)+\frac{c^2{}_t}{2}} \quad \text{..}(3.8.7)$$

$$\rho = \frac{c_I}{c_a} \qquad \text{..} \quad (3.8.8)$$

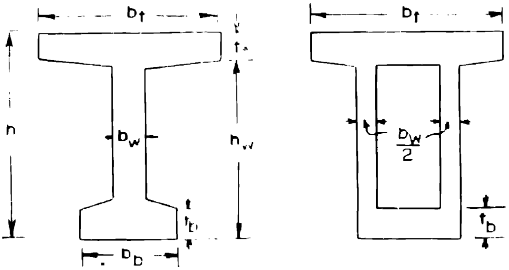

Fig. 3.8.1 : Typical I-Section for long spans

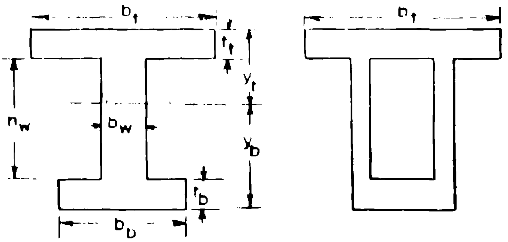

Fig. 3.8.2 : Idealised form of the I-section

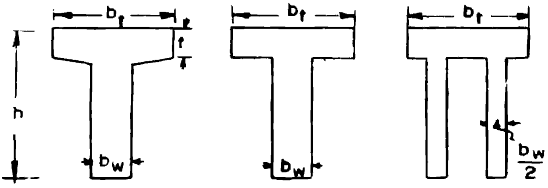

Fig. 3.8.3 : Typical T section

The expressions listed in eqs. 3.8.1 to 3.8.8 are useful in studying the various relationships of the section. Sectional properties for various values of c_t, c_b, c_w, c_f are given in table 2 (Appendix A).

3.9. CABLE PROFILE : Design procedure of a prestressed concrete beam consists of :

(i) Selection of area of cross section, shape of the section and determination of area of steel and maximum eccentricity.

(ii) Determination of layout of the cable to suit the other requirements.

The first part has been discussed in the previous section in which shape and size of the sections, area of steel and maximum eccentricity are obtained by solving the governing equations. Eccentricity given by the equations is applicable only at mid-span of the beam. It is now necessary to discuss the eccentricity of the cable at different locations along the span. End section has to be considered as another critical section as discussed in chapter I.

End section : End section of a simply supported prestressed concrete beam is subjected to prestressing force and external shear forces. Additional stresses due to secondary effects of anchorage block etc. are also induced at the end-section. To take care of all the secondary effects and practical limitations, area of the section is generally increased at the end.

The four requirements at the ends are

$$\frac{P_t}{\phi A}\left(\frac{ey_t}{r^2}-1\right)=c_{tt}\, f'_c \leqslant c'_{tt}\, f'_c \qquad \ldots \quad (3.9.1)$$

$$\frac{P_t}{\phi A}\left(\frac{ey_b}{r^2}+1\right)=c_{ct}\, f'_c \leqslant c'_{ct}\, f'_c \qquad \ldots \quad (3.9.2)$$

$$\frac{\eta P_t}{\phi A}\left(\frac{ey_t}{r^2}-1\right)=c_{te}\, f'_c \leqslant c'_{ce}\, f'_c \qquad \ldots \quad (3.9.3)$$

$$\frac{\eta P_t}{\phi A}\left(\frac{ey_b}{r^2}+1\right)=c_{ce}\, f'_c \leqslant c'_{ce}\, f'_c \qquad \ldots \quad (3.9.4)$$

Where ϕ =ratio of prestressing force at mid span to that at the end section of the beam. This is a measure of losses due to friction.

Eqs. 3.9.1 to 3.9.4 may be rearranged as

$$e < \left(\frac{\phi A}{P_t} c'_{tt} f'_c + 1 \right) r^2/y_t \qquad .. \quad (3.9.5)$$

$$e < \left(\frac{A\phi}{P_t} c'_{ct} f'_c - 1 \right) r^2/y_b \qquad .. \quad (3.9.6)$$

$$e < \left(\frac{A\phi}{\eta P_t} c'_{te} f'_c + 1 \right) r^2/y_t \qquad .. \quad (3.9.7)$$

$$e < \left(\frac{A\phi}{\eta P_t} c'_{co} f'_c - 1 \right) r^2/y_b \qquad .. \quad (3.9.8)$$

The lowest of the values of 'e' given by these four equations may be taken at the end support or it may be desirable to locate the steel at C. G. C. of the concrete. The value of ϕ may be estimated around 0.95.

Profile of the Prestressing Steel: The profile of the prestressing steel should be determined so that the four permissible stress requirements are satisfied at all points along the beam. Once the eccentricities at mid and end sections are determined, a reasonable shape of the profile may be made. A smooth curve of about second degree is reasonable for many practical problems because this curve will compensate uniformly distributed loads very effectively as a balancing load.

3.10. DESIGN PROCEDURE BASED ON FLEXURE: A discussion on the analysis of the beam has been made in the previous articles. It is desirable to consolidate the procedure for designing a prestressed concrete beam. A recommended design procedure is:

(i) Select the materials to be used and list the allowable stresses and stress coefficients as per the code requirements.

(ii) Select ω and ρ in the range as described in the previous articles. Value of ω is generally obtained by other criteria and value of ρ is selected as high as possible.

(iii) After selecting the stress coefficients, solve the eqs. 3.6.3, 3.6.4, 3.6.7 and 3.6.8 for Δ, R, m and ϵ.

(iv) Select the section for the values of ρ and Δ, from table 2 in Appendix A.

(v) Check the eccentricity obtained from the governing equations whether it is within the practical limitations of clear cover.

(vi) If the cover is not enough, change the stress coefficients or efficiency ratio to meet the reqirements.

(vii) Calculate steel area of cross section for the calculated P_t.

(viii) Select number of wires and check for: (a) accommodation of wires, (b) eccentricity, and (c) clear cover.

(ix) If all the three requirements mentioned in (viii) are satisfied, proceed to determine the losses of prestress. If the requirements are not satisfied, select another section to suit the requirements.

(x) Compute the losses in prestress if necessary.

(xi) Check the assumed value of η. If the computed value of η does not check with the estimated value, recheck the design with the new value of η.

(xii) Fix the profile of the cable as discussed in section 3.9.

(*Note*: Design for shear, anchorage, bond and other requirements are discussed later).

Design example 3.10.1: Design of a post-tensioned beam for the following data :

Data : effective span = 50 metres,

live load = 2000 kg/m,

depth of beam $\not>$ 2.2 metres,

a covering coat of about 5 cm thick to be over the top flange of the beam,

concrete of strength, $f'_c = 450$ kg/sq cm,

high tensile steel of 5 or 7 mm wire strands are available,

tensile strength of prestressing steel $(f'_s) = 15000$ kg/sq cm,

Code specifications :

density of concrete, $(\gamma) = 2400$ kg/m^3

Young's modulus, $E_c = 18000\sqrt{f'_c} = 3.82 \times 10^5$ kg/sq cm

$E_s = 2.1 \times 10^6$ kg/sq cm

Stress coefficients :

$$c'_{ct} = 0.47,\ c'_{tt} = \frac{10}{450} \simeq 0.02$$

$$c'_{ce} = 0.31,\ c'_{te} = \frac{10}{450} \simeq 0.02$$

f_s (at transfer) $= 0.7\ f'_s$

f_s (at working load) $= 0.6\ f'_s$

f_s (at anchorage) $= 0.8\ f'_s$

Design Procedure :

Trial 1 :—Assume efficiency ratio and depth of the beam.

Let

$$\rho=0.13$$

$$h=L/25=200 \text{ cm},$$

$$\eta=0.8$$

then, $\Delta_0=\dfrac{\eta c'_{ct}+c'_{te}}{\eta c'_{tt}+c'_{ce}}=\dfrac{0.396}{0.326}=1.21$

$$\omega=\frac{hf'_c}{\gamma L^2}=1.5$$

$$\epsilon_{(req)}=\frac{1+\Delta}{c_{ct}-\Delta c_{tt}}\left[\rho\,(c_{tt}+c_{ct})+\frac{1}{8\omega}\right]=0.63$$

$$\epsilon_{(limit)}=\frac{y_b-d'}{h}=\left(\frac{\Delta}{1+\Delta}-\frac{d'}{h}\right)=\left(\frac{\Delta}{1+\Delta}-0.1\right)$$

$$=0.448$$

$\epsilon_{(req)} > \epsilon_{(limit)}$, this condition states that the eccentricity is beyond the lower flange. There are few possibilities through which the eccentricity would be reduced :

(i) increase the depth, or

(ii) take $c_{tt} < c'_{tt}$

Trial 2 :—

Let $h=h_{(limit)}=220$ cm and

$c_{tt}=-0.05$ (i.e., allowing compression of $0.05\,f'_c$)

$$\therefore \quad \omega=\frac{hf'_c}{\gamma L^2}=1.65$$

$$\Delta=\frac{0.396}{0.27}=1.47$$

$$\epsilon_{(req)}=\left(\frac{2.47}{0.47+0.074}\right)[0.13\;(-0.05+0.47)+0.0763]=0.59$$

$$\epsilon_{(limit)}=\left(\frac{\Delta}{1+\Delta}-\frac{d'}{h}\right)=(0.595-0.1)=0.495$$

A preliminary design is suggested assuming eccentricity ratio as 0.5. Calculation of self weight and cross sectional area :

$$R=8\,\rho\,\omega\,(c_{te}+\eta c_{ct})\left(\frac{1}{\Delta}+1\right)-(1-\eta)$$

$$=1.716\;(0.396)\;(1.68)-0.2=0.94$$

Assume width of top flange as 2 metres for the purpose of calculation of superimposed load. Then

$w_s = 2 \times 2400 \times 0.05 = 240$ kg/m (say 250 kg/m)

$w_a = w_l + w_s = 2250$ kg/m

$$w_g = \frac{w_a}{R} = 2394 \text{ kg/m}$$

$$A = \frac{w_g}{\gamma} = 9975 \text{ sq cm}$$

Steel requirement:

$$m = \frac{c_{ct} - \Delta c_{tt}}{1 + \Delta} = 0.22$$

$$P_t = mA\, f'_c = 98.75 \times 10^4 \text{ kg}$$

$$A_s = \frac{P_t}{0.7 f'_s} = 94 \text{ sq cm}$$

Selection of section : The basic parameters obtained from the governing equation may be consolidated as

$\Delta = 1.47$, $\omega = 1.65$, $\rho = 0.13$, $\epsilon = 0.5$, $m = 0.22$

$A = 9975$ sq cm, $A_s = 94$ sq cm

A suitable section to suit the requirements could either be selected from table 2 (Appendix A) or could be obtained from eqs. 3.8.1 to 3.8.8. The closest suitable section for the nondimensionalised requirements from table 2 (Appendix A) is

$c_l = 0.5$, $c_w = 0.12$, $c_t = 0.12$, $c_b = 0.12$

and the corresponding coefficients of the section from table 2 (Appendix A) are

$\rho = 0.136$ $c_a = 0.2712$

$\Delta = 1.484$ $c_I = 0.0369$

$\omega = 1.65$ $c_{yb} = 0.5973$

$c_{yt} = 0.4027$

The stresses may now be checked for the selected section. The substitution of the various sectional parameter gives

$$c_{tt} = m\left[\frac{\epsilon}{\rho(1+\Delta)} - 1\right] - \frac{1}{8\rho\omega(1+\Delta)} = -0.119 < c'_{tt}$$

$$c_{ct} = m\left[\frac{\epsilon\,\Delta}{\rho(1+\Delta)} + 1\right] - \frac{\Delta}{8\rho\omega(1+\Delta)} = 0.37 < c'_{ct}$$

$$c_{ce} = -\eta m\left[\frac{\epsilon}{\rho(1+\Delta)} - 1\right] + \frac{1+R}{8\rho\omega(1+\Delta)} = 0.361 > c'_{ce} \text{ (not permissible)}$$

$$c_{te} = -\eta m\left[\frac{\epsilon\,\Delta}{\rho(1+\Delta)} + 1\right] + \frac{\Delta(1+R)}{8\rho\omega(1+\Delta)} = 0.1 > c'_{te} \text{ (not permissible)}$$

It can be seen from the above expression that the stresses at working load condition exceed the allowable stresses, and these stresses are computed based on the assumed value of η. If the actual stresses are marginal, then actual value of η should be computed for the particular section and the stresses be checked with the actual value of η.

Loss of prestress for calculation of η :

(i) Elastic shortening: A mean elastic shortening could be obtained by totaling the elastic strains at steel level over the length and dividing the total elongation by the length. Due to symmetry of the beam, only half the length of the beam is considered and the loss of prestress is computed.

Let

ϵ_e = mean elastic strain

e_x = eccentricity at distance x

then

$$\epsilon_e\left(\frac{L}{2}\right)=\frac{1}{E_c}\int_0^{L/2}\left(\frac{P_x}{A}+\frac{P_x e_x^2}{I}-\frac{M_x e_x}{I}\right)dx$$

Let $e_x=\frac{4e}{L^2}(Lx-x^2)$, assuming a parabolic cable profile

The bending moment is given by

$$M_x=\frac{w_g+w_s}{2}(Lx-x^2)$$

From the above three equations the value of ϵ_e is given as

$$\epsilon_e=\frac{(99+97-73.9)}{E_c}=0.00032$$

An approximate elastic strain may also be obtained without going through the integration.

$$(\epsilon_e)_{x=L/2}=\frac{c_{ct}\,f'_c}{E_c}\left(\frac{e}{y_b}\right)=0.000365$$

$$(\epsilon_e)_{x=0}=\frac{P_t}{AE_c}=0.000260$$

Taking a mean value of the above two

$$\epsilon_c=\frac{0.000365+0.000260}{2}=0.000313$$

which is fairly close to the mean elastic strain (0.00032) computed through integration.

Using $\epsilon_c=0.00032$, since the cables are strained at stages, the loss of strain due to elastic shortening is $\epsilon_c/2=0.00016$

(ii) Shrinkage strain $=\dfrac{3\times10^{-4}}{\log_{10}(T+2)}$

Taking transfer at 28 days, the loss due to shrinkage is given by

$$=\frac{0.0003}{\log_{10}(30)}=0.0002$$

(iii) Creep in concrete for a creep coefficient of 2.5

$= (2.5-1)\ \epsilon_c = 0.00048$

(iv) Creep in steel (3 %) $= 0.005 \times 0.03 = 0.00015$

(v) Anchorage take-up of 0.25 cm on either end gives loss due to

anchorage $=\frac{0.25}{2500}=0.0001$

(vi) Gain due to bending :

Max. gain of strain due to bending $=\frac{M_1 e}{IE_c} \simeq 0.000289$

If no bond is assumed, the actual gain in stress due to bending is

$$=\frac{2}{3}(0.000289)=0.000193$$

(vii) Frictional loss :

Let $k=0.0015$ (wobble effect per metre length)

$\mu=0.25$ (frictional coefficient)

$$e_x = y = \frac{4e}{L^2}(Lx - x^2)$$

$$\left(\frac{dy}{dx}\right)_{x=0} = \frac{110 \times 5000}{625 \times 10^4} = 0.088$$

$\therefore\ \alpha = 0.088$ (total change in the slope of the cable)

$$\frac{P_0 - P_t}{P_t} = \left(\mu\alpha + k\frac{L}{2}\right) = 0.0595$$

Strain loss $=\frac{P_0 - P_t}{E_s\, A_s} = 0.0003$

Summing up the losses in prestress :

Loss due to	Loss of strain	Percentage of loss
(i) Elastic shortening	0.00016	3.2
(ii) Shrinkage	0.00020	4.0
(iii) Creep in concrete	0.00048	9.6
(iv) Creep in steel	0.00015	3.0
(v) Anchorage take up	0.00010	2.0
(vi) Bending due to live load	−0.00019	−3.8
Total	0.00090	18.0

$$\therefore \quad \eta = \frac{0.005-0.0009}{0.005} = 0.82$$

The value of η works out to be slightly higher than assumed and the stress coefficients with new value of η are not altered very much. The computed stress coefficients are higher than the allowable with the actual $\eta = 0.82$, so a new section has to be selected. The depth of the beam is restricted, so the stress coefficients could be reduced by decreasing the efficiency factor ρ of the section. From table 2 (Appendix A) a lower efficient section is chosen and the corresponding values are given below:

New section and its properties:

Select $\rho = 0.1285$

$\Delta = 1.68$

then from table 2 (Appendix A)

$c_f = 0.5$, $c_w = 0.12$, $c_t = 0.12$, $c_b = 0.08$

and the sectional coefficients are

$c_n = 0.2560$, $c_i = 0.0329$, $c_{yb} = 0.6269$ and $c_{yt} = 0.3731$

Since the ranges of R, ϵ, m are known fairly well from the previous calculations, instead of starting with stress coefficients, let R, ϵ, m be assumed and allowable stress coefficients be checked.

Let

$\epsilon = 0.53$, $m = 0.24$, and $R = 0.94$, then

$$w_g = \frac{2250}{0.94} \simeq 2400 \text{ kg/m}$$

$$A = \frac{w_g}{\gamma} = 10{,}000 \text{ sq cm}$$

Calculation of stress coefficients: Using the parameters as selected in the previous section, the stress coefficients work out to be

$c_{tt} = -0.091 < (c'_{tt})$ (permissible)

$c_{ct} = 0.50 > (c'_{ct} = 0.47)$ (about 6.4% over stress)

$c_{ce} = 0.321 > (c'_{ce} = 0.31)$ (about 4.2% over stress)

$c_{te} = -0.007 < (c'_{te} = 0.02)$ (permissible)

$f_{se} = (0.005-0.0009)\, E_s = 8610$ kg/sq cm

$$\frac{f_{se}}{f'_s} = \frac{8610}{15000} = 0.57 < 0.6$$

Anchorage strain $= 0.005 + 0.0003$ (i.e. frictional loss)

$= 0.0053$

$f_{so} = 0.0053 \times E_s = 11130$ kg/cq cm

$$\frac{f_{so}}{f'_s} = \frac{11130}{15000} < 0.8$$

Actual stresses are slightly higher than the allowable. The small excess amount may be compensated by selecting an actual section which is slightly larger in area as compared to the idealised section.

Idealised section : All the coefficients of the section are given previously. Using these coefficients, dimensions could be obtained as

$A = 10000$ sq cm $\qquad t_t = 0.12\ h = 26.4$ cm

$\;\; = 0.2560\ b_t h \qquad t_b = 0.08\ h = 17.6$ cm

$\therefore\ b_t = 178$ cm $\qquad b_w = 0.12\ b_t = 21.4$ cm

$r^2 = 0.1285\ h^2 = 6219\ \text{cm}^2 \qquad b_b = 0.5\ b_t = 89$ cm

$y_b = 0.6269\ h = 138$ cm $\qquad e = 0.53\ h = 116.6$ cm

$y_t = 0.3731\ h = 82$ cm $\qquad P_t = mAf'_c = 108 \times 10^4$ kg

$$A_s = \frac{P_t}{0.7 f'_s} = 103 \text{ sq cm}$$

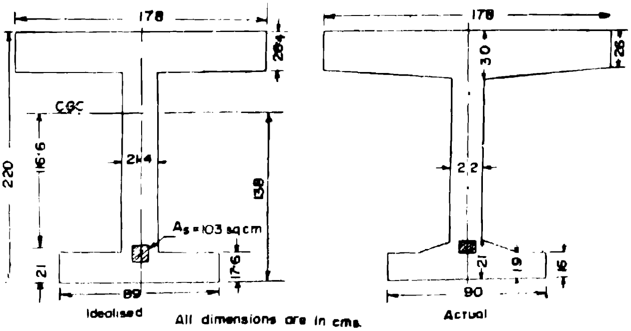

Use 7 mm wires (No. of wires required 268 or 30 strands of 9 wires)

Fig. 3.10.1 ; Section at mid span

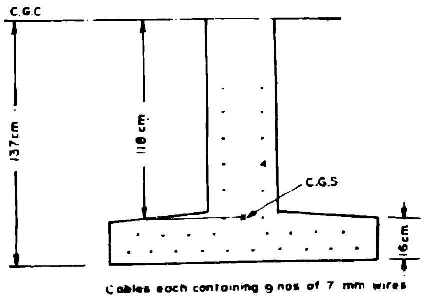

Cables each containing 9 nos of 7 mm wires

Fig. 3.10.2 : Approx. arrangement of cables at mid span

In case, it is not possible to increase the depth of the beam because of the above two reasons, it is possible to adjust the allowable stress coefficients to keep the eccentricity within the allowable limits. The eccentricity could be reduced by decreasing the value of c_{tt}. In other words the stress coefficients should be selected as

$$c_{ct} = c'_{ct},\ c_{tt} < c'_{tt},\ c_{ce} = c'_{ce},\ c_{te} = c'_{te}$$

A box section which is capable of accommodating many cables in the open box area is economical in providing flexibility for high eccentricity while achieving the maximum permissible stresses.

(c) *Effect of strength of concrete* : Variation in the area of cross section with strength of concrete is shown in fig. 3.11.4. As the strength of concrete increases, the area of cross section decreases. This straight forward conclusion could be made even without graphs. The graphs not only illustrate the qualitative nature, but also give quantitative values which are helpful in selecting the concrete strength. The decrease in the area of cross section with increase in the concrete strength is not rapid when compared with that of depth or efficiency ratio. It is desirable to use a high strength concrete. However the rate of cost of high strength concrete is more, so a proper selection of quality in the concrete is to be made such that the total cost of the structure is minimum. Other limitations in selecting a high strength concrete are the workability, availability of proper equipment and skilled man power for good and uniform compaction.

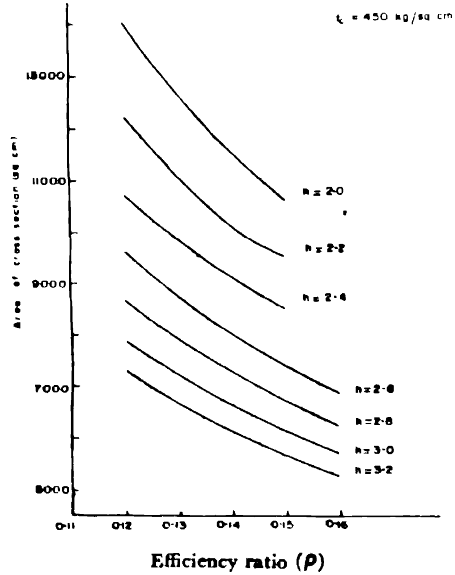

Fig. 3.11.1 : Variation of cross section with efficiency ratio

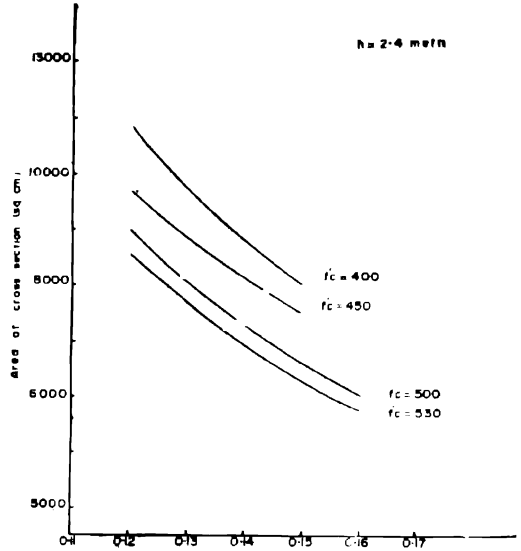

Efficiency ratio
Fig. 3.11.2 : Variation of cross section with efficiency ratio

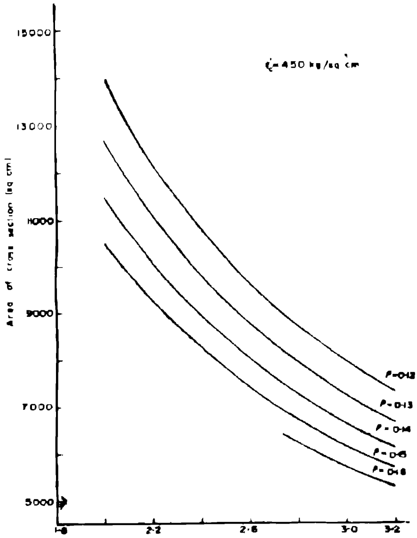

Depth of the beam (metre)
Fig. 3.11.3 : Variation of cross section with depth of the beam

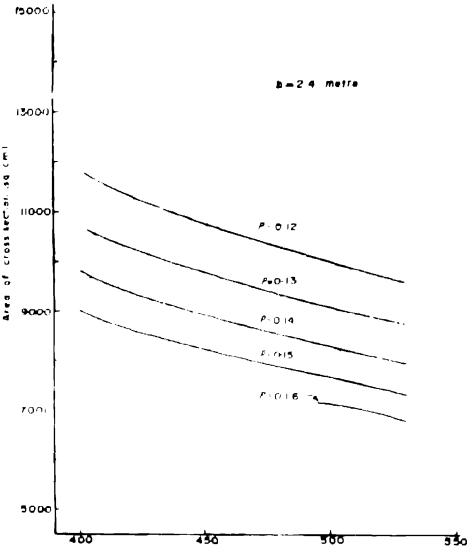

Cube strength in kg/sq cm

Fig. 3.11.4 : Variation of cross section with cube strength

3.12. GENERALISED ALLOWABLE STRESS EQUATIONS :

Governing equations established so far are only for simply supported beams. It is desirable to establish nondimensionalised design criteria for general bending moment conditions.

Let M_2 = maximum bending moment

M_1 = minimum bending moment

The values of M_1 and M_2 include moments due to self weight of the beam and are assumed to be of same sign.

The allowable stress equations are :

$$\frac{P_t}{Af'_c}\left(-1+\frac{ey_2}{r^2}\right)-\frac{M_1y_2}{Ar^2f'_c}=c_{tt}\leqslant c'_{tt} \quad .. \quad (3.12.1)$$

$$\frac{P_t}{Af'_c}\left(1+\frac{ey_1}{r^2}\right)-\frac{M_1y_1}{Ar^2f'_c}=c_{ct}\leqslant c'_{ct} \quad .. \quad (3.12.2)$$

$$-\frac{\eta P_t}{Af'_c}\left(-1+\frac{ey_2}{r^2}\right)+\frac{M_2y_2}{Ar^2f'_c}=c_{ce}\leqslant c'_{ce} \quad .. \quad (3.12.3)$$

$$-\frac{\eta P_t}{Af'_c}\left(1+\frac{ey_1}{r^2}\right)+\frac{M_2y_1}{Ar^2f'_c}=c_{te}\leqslant c'_{te} \quad .. \quad (3.12.4)$$

Notations for various quantities are shown in fig. 3.12.1.

Introducing the nondimensionalised values as already defined in the previous sections, the above equations reduce to :

$$m\left[-1+\frac{\epsilon}{\rho(1+\Delta)}\right]-\frac{x}{\rho(1+\Delta)}=c_{tt} \quad \text{.. (3.12.5)}$$

$$m\left[1+\frac{\epsilon\Delta}{\rho(1+\Delta)}\right]-\frac{x\Delta}{\rho(1+\Delta)}=c_{ct} \quad \text{.. (3.12.6)}$$

$$-\eta m\left(-1+\frac{\epsilon}{\rho(1+\Delta)}\right)+\frac{Rx}{\rho(1+\Delta)}=c_{ce} \quad \text{.. (3.12.7)}$$

$$-\eta m\left(1+\frac{\epsilon\Delta}{\rho(1+\Delta)}\right)+\frac{\Delta Rx}{\rho(1+\Delta)}=c_{te} \quad \text{.. (3.12.8)}$$

where

$$x=\frac{M_1}{Ah\,f'_c} \quad \text{.. (3.12.9)}$$

or

$$x=\left(\frac{M_1}{P_t h}\right)m,\ R=\frac{M_2}{M_1}\ \text{and}\ \Delta=\frac{y_1}{y_2} \quad \text{.. (3.12.10)}$$

Solution of the above equations gives the required beam dimensions. In any problem, the governing moments M_1 and M_2 are first located and then section is designed for the moments with the bending moment due to self weight as an unknown quantity. The set of equations is to be established for a critical section of the beam and solution of the equations can be obtained with some assumed parameters. This set of equations is useful in solving statically determinate beams such as overhang beams, cantilever beams.

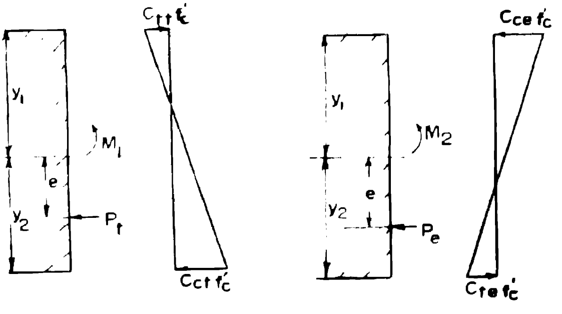

(a) Transfer (b) Service load

Fig. 3.12.1 : Sign conventions for allowable stresses

3.13. LOAD BALANCING METHOD : An introduction to load balancing method was discussed in chapter 1. The basic concept is that the external load at any point on the beam is balanced by the transverse component of the cable force. The load balancing method is very effective for beams subjected to constant load conditions. Even for variable load conditions, partial balance of the load will be affective. The example of section 3.10 is reworked here with load balancing method.

Example 3.13.1 : Same as example 3.10.1 by load balancing method

Given data :

effective span $=50$m, live load $=2000$ kg/m

superimposed load $=250$ kg/m

maximum allowable depth of the beam $=2.2$ m

$f'_c=450$ kg/cm^2, $f'_s=15000$ kg/cm^2

Allowable stress coefficients (for loads likely to increase) :

$c'_{tt}=c_{te}=0.022$, $c'_{ct}=0.47$, $c'_{ce}=0.31$

Design procedure :

Selection of equivalent balancing load : Assume self weight of the beam as 2400 kg/m. This assumption is to be based on the span of the beam and the live load on the beam. For a span of about 50 m, the self weight is likely to be close to live load unless the live load is really small.

$w_g=2400$kg/m, $w_s=250$ kg/m, $w_l=2000$ kg/m

$w_t=(w_g+w_s+w_l)=4650$ kg/m

If w_t is balanced completely, excessive stresses are likely to be developed at transfer condition. On the other hand, if only w_g is balanced completely excessive stresses are likely to be developed at working load conditions. Therefore, it is desirable to balance an average load of the two conditions of loading. The radial component of cable force at working is less than that at transfer load condition because of loss in prestress. Let the load to be balanced be w_b. Load to be balanced should be more than load at transfer but less than the working load.

Let w_{be} = load balanced at working condition $=3000$ kg/m

Cable force and profile : Let the cable profile be parabolic with maximum eccentricity e. The transverse component of prestressing force is given by

$$P_e \frac{d^2y}{dx^2} = \frac{8e\,P_e}{L^2} \text{ then :}$$

$$\frac{8eP_e}{L^2} = w_{be} = 3000$$

$$\therefore \quad eP_e = \frac{3000 \times 250000}{8} = 93.75 \times 10^6 \text{ kg cm}$$

If the external load is completely balanced, the stress at any section is given by

$$f_{ave} = \frac{P}{A}$$

In a partially balanced beam, the actual stresses will be on either side of f_{ave} so it is desirable to make a rough guess of f_{ave}.

Let $f_{ave} = 2/3$ of allowable working stress

$$= 2/3\ (0.31)\ f'_c$$

$$= 0.20\ f'_c$$

$$f_{ave} = 0.20\ f'_c = 90 \text{ kg/sq cm}$$

Since $w_g = 2400$ kg/m, $A = w_g/\gamma = 10{,}000$ sq cm

$$P_e = f_{ave}\ A$$

$$= 0.20 \times 450 \times 10000 = 90 \times 10^4 \text{ kg}$$

$$\therefore\quad e = \frac{93.75 \times 10^6}{90 \times 10^4} = 104.2 \text{ cm}$$

Stresses at transfer condition :

Let $\eta = 0.8$

$$P_t = P_e/0.8 = \frac{90 \times 10^4}{0.8} = 112.5 \times 10^4 \text{ kg}$$

Equivalent load balanced at transfer condition is

$$w_{bt} = \frac{w_{be}}{\eta} = \frac{8e\ P_e}{0.8\ L^2} = \frac{3000}{0.8} = 3750 \text{ kg/m}$$

Actual external load at transfer is the self weight, so the load that is not balanced at transfer condition is $-w_{bt} + w_g = -3750 + 2400 = -1350$ kg/m (acting upward). The stresses due to the load that is not balanced, can be calculated by beam theory and they are

$$f_{tt} = -\frac{P_t}{A} + \frac{My_t}{I}$$

Where M = bending moment due to the load that is not balanced

f_{tt} = stress at top fibre at transfer (tension)

$$f_{tt} = -\frac{P_t}{A} + \left(\frac{M}{A}\right)\left(\frac{y_t}{r^2}\right)$$

$$= -\frac{P_t}{A} + \left(\frac{M}{Ah}\right)\left(\frac{h}{r}\right)^2\left(\frac{y_t}{h}\right)$$

$$= -\frac{P_t}{A} + \frac{M}{Ah\ \rho\ (1+\triangle)}$$

$$\frac{P_t}{A} = \frac{P_e}{\eta A} = 112.5 \text{ kg/sq cm}$$

Let $\rho=0.1285$ and

$\triangle=1.68$

Then $f_{tt}=-112.5+\dfrac{1350\times2500\times1000}{8\times10000\times220\times0.1285\times2.68}$

$=-112.5+55.6=-56.9$ kg/sq cm (comp)

$f_{ct}=\dfrac{P_t}{A}+\dfrac{My_b}{I}=112.5+\dfrac{M}{Ah}\left(\dfrac{1}{\rho}\right)\left(\dfrac{\triangle}{1+\triangle}\right)$

$=112.5+93.4=205.9$ kg/sq cm

$c_{ct}=\dfrac{205.9}{450}=0.458$ (permissible)

Stresses at working load condition : Load balanced at working load condition $=3000$ kg/m. Load that is not balanced $=w_t-w_{bc}=$ 1650 kg/m.

$f_{te}=\dfrac{P_e}{A}+\dfrac{My_b}{I}$

$=-90+\left(\dfrac{1650\times250000}{8\times10000\times220\times0.1285}\right)\left(\dfrac{1.68}{2.68}\right)$

$=-90+1{,}14.33=24.33$ (10 kg/sq cm permissible)

$f_{ce}=\dfrac{P_e}{A}+\dfrac{My_t}{I}$

$=90+68.0=158.0$ kg/cm^2

$c_{ce}=\dfrac{158.0}{450}=0.351$ (not permissible)

Actual compressive stress at working load condition of this method is more than the allowed one. This could be easily avoided by increasing the eccentricity for the same prestressing force.

Revision of the design with eccentricity $=110$ cm

Transfer condition : (let prestressing force remain the same.) The load that is balanced due to 110 cm eccentricity instead of 104.2 cm is given by

$$w_{bt}=\frac{8P_te}{L^2}=3750\left(\frac{110}{104.2}\right)=3960 \text{ kg/m}$$

$\dfrac{P_t}{A}=f_{ave}=112.5$ kg/sq cm (remains same as before)

Load that is not balanced $=(2400-3960)$ kg/m $=-1560$ kg/m

$f_{ct}=-112.5+\dfrac{1560}{1350}(55.6)=-48.2$ (compressive stress)

$$f_{ct} = 112.5 + \frac{93.4 \times 1560}{1350} = 220.5 \text{ kg/cm}^2$$

$$c_{ct} = \frac{220.5}{450} = 0.49 \text{ (excess)}$$

(ii) Working load condition :

Load balanced at working load condition

$= 3960 \times 0.8 = 3168 \simeq 3170$ kg/m

Load that is not balanced $= 4650 - 3170 = 1480$ kg/m

$$\frac{P_c}{A} = f_{avc} = 90 \text{ kg/cm}^2 \text{ (as before)}$$

$$f_{te} = -90 + \frac{114.33 \times 1480}{1650} = 12.57 \text{ kg/sq cm}$$

(V_s 10 kg/sq cm permissible)

$$f_{ce} = 90 + \frac{68.0 \times 1480}{1650} = 151 \text{ kg/cm}^2$$

$$c_{ce} = \frac{151}{450} = 0.336 \text{ (not permissible, therefore revise)}$$

A comparison of the two solutions obtained from sections 3.10 and 3.13 is shown in table 3.13.1.

TABLE : 3.13.1 : COMPARISON OF SOLUTIONS OF A BEAM DESIGN BY TWO METHODS

Description	Method 1 (nondimensionalised parameters)	Method 2 (load balancing)
A	10000 sq cm	10000 sq cm
ρ	0.1285	0.1285
Δ	1.68	1.68
P_t	93.7×10^4 kg	112.5×10^4 kg
e	116.5 cm	110 cm
c_{tt}	−0.091	−0.107
c_{ct}	0.50	0.49
c_{te}	0.007	0.028
c_{ce}	0.321	0.336
A_s	103 sq cm	107.1 sq cm

The load balancing method is fairly easy ; it also gives an additional advantage of giving directly how much effective vertical shear force is existing. However it is not easy to assume a very economical section and some amount of trial and correction procedure is to be adopted.

Problems

3.1 Design a pre-tensioned prestressed concrete simply supported beam of span 24 m for a live load of 2400 kg/m. Design by nondimensionalised parameters and load balancing methods keeping the depth of the beam not exceeding 120 cm, use $f'_c = 450$ kg/sq cm, $f'_s = 15000$ kg/sq cm.

3.2 Design a post-tensioned prestressed concrete balanced cantilever bridge of spans as shown in Fig. 3.1. The bridge is used for two lane traffic with a moving load of 15000 kg/m. The girders are arranged such that the top flanges of the girders form the main slab of the bridge. A 5 cm thick wearing coat is to be provided on the top of the flanges. Use $f'_c = 400$ kg/sq cm.

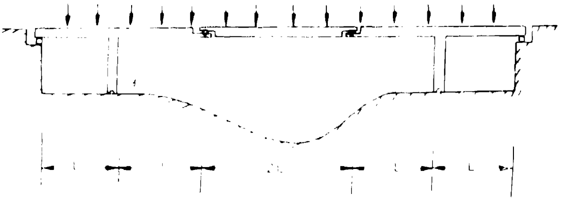

Fig. 3.1 : Problem 3.2

CHAPTER IV

PRESTRESSED CONCRETE COMPOSITE BEAMS

4.1. INTRODUCTION : A prestressed concrete composite beam consists of two essential parts, (i) a prestressed concrete beam either pre-tensioned or post-tensioned, and (ii) concrete slab reinforced, or prestressed or even of plain concrete. Usual construction procedure consists of two stages :

(i) A prestressed concrete beam is placed in position. The beam is either fully or partly prestressed.

(ii) A plain or reinforced concrete slab is cast in-situ over the top of the prestressed concrete beam.

If the beam is partly prestressed before casting the top slab, the remaining prestressing is done after casting the slab. Placing of the top slab is done in two ways. The slab is cast directly on the beam with or without overhang so that the total shuttering is wholly supported by the prestressed concrete beam itself. If the slab is fairly wide and the beam is not to be overstrained with the load of shuttering and wet concrete of the slab, the slab is cast partly supported by a shuttering not directly resting on the beam.

The concrete slab hardens and acts together with the girder to form a composite section. The precast beams are cast with controlled concrete of high strength, the slab with less strong concrete. If the slab has to act together with the precast beam, a strong bond has to be generated between the beam and the slab. When the composite section bends, the top fibre of the beam and the bottom fibre of the slab should have the strain compatibility of a single member. Some kind of connectors joining the two parts have to be provided to achieve single unit action. These connectors are essentially under shear force so they are called "shear connectors". The integral connection is achieved by providing shear keys at the top fibre of the beam along the span, or leaving the top of the beam unfinished and even sometimes roughened for casting the slab over the beam. Vertical ties are also provided along the span to prevent separation of the slab from the beam. It is desireable to treat the junction of the slab and the beam as a construction joint. The deformation of composite section with and without shear connectors is shown in fig. 4.1.1.

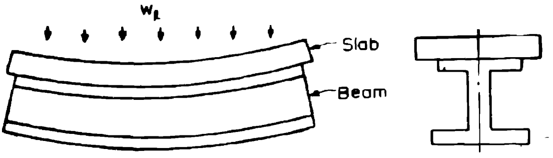

(a) Composite section without shear connectors

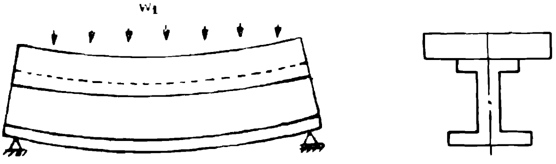

(b) Composite sectin with shear connectors

Fig. 4.1.1: Effect of shear connectors in composite construction

4.2. ALLOWABLE STRESS CONSIDERATIONS : There are three critical conditions of loading in composite construction which may be considered for design purposes:

(i) Transfer condition : The beam is subjected to the transfer prestressing force and self weight of the beam.

(ii) Casting of slab condition : The beam is subjected to transfer prestress, self weight of the beam, self weight of the wet slab and other superimposed loads due to shuttering etc.

(iii) Working load condition : The composite beam is subjected to effective prestressing force, self weight of the beam and the slab, other superimposed and external working loads.

In general, the third condition dominates the second condition so the first and the last conditions are real for design considerations. The stresses due to live loads are to be superimposed on the stresses caused due to second condition. This is a reasonably good and safe assumption because the slab hardens in the elastic deformed shape of the beam at second stage. The differential shrinkage of the slab and the beam affects the actual stress distribution. For the sake of simplicity of design, the shrinkage stresses are treated separately and superimposed on working load stresses. The expressions for stresses in the extreme fibre of the beam for these two critical conditions can be written as

$$\frac{P_t}{A}\left(\frac{ey_t}{r^2}-1\right)-M_g\frac{y_t}{I}=c_{tt}f'_c\leqslant c'_{tt}f'_c \qquad .. \quad (4.2.1)$$

$$\frac{P_t}{A}\left(\frac{ey_b}{r^2}+1\right)-M_g\frac{y_b}{I}=c_{ct}f'_c\leqslant c'_{ct}f'_c \qquad .. \quad (4.2.2)$$

$$-\eta\frac{P_t}{A}\left(\frac{ey_t}{r^2}-1\right)+(M_g+M_{gs}+M_{sl})\frac{y_t}{I}+M_a\left(\frac{y_{tc}}{I_c}\right)$$

$$=c_{ce}\,f'_c\leqslant c'_{ce}\,f'_c \qquad \ldots \quad (4.2.3)$$

$$-\eta\frac{P_t}{A}\left(\frac{ey_b}{r^2}+1\right)+(M_g+M_{gs}+M_{sl})\frac{y_b}{I}+M_a\left(\frac{y_{bc}}{I_c}\right)$$

$$=c_{tc}\,f'_c\leqslant c'_{tc}\,f'_c \qquad \ldots \quad (4.2.4)$$

Where

M_{gs} = bending moment due to self weight of the slab

M_{sl} = bending moment due to superimposed loads before the concrete hardens

I_c = moment of inertia of the gross composite section about its centroidal axis

y_{bc} = distance of the bottom fibre of the beam from the centroidal axis of the composite section

y_{tc} = distance of the top fibre of the beam from the centroidal axis of the composite section

The stress distribution at three conditions are shown in fig. 4.2.1.

The moment of inertia of the composite section is to be calculated by considering the relative properties of the materials of the slab and the beam. Since the strength of the slab is different from that of the beam, the stresses in the slab and the beam will differ for any given strain. It is desirable to transform the area of the slab based on relative strength. The transformed area of the slab is to be considered while working with the sectional properties of the composite section. Areas of the beam and the slab have to be transformed proportional to the modulus of elasticity of the two materials.

The total width of the slab will not be effective in acting together with the beam if the width of the slab exceeds certain limits, so the width of the slab should also be restricted. The width of the slab should not be greater than

(i) one fourth of the span of the beam,

(ii) centre to centre distance of the adjacent beams, and

(iii) twelve times the least thickness of the slab or web

The exact effective width of the slab has to be obtained based on shear lag and since the shear lag is not very well defined in the concrete

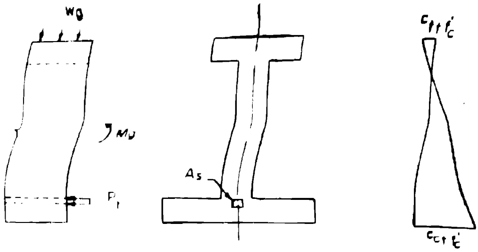

Transfer condition

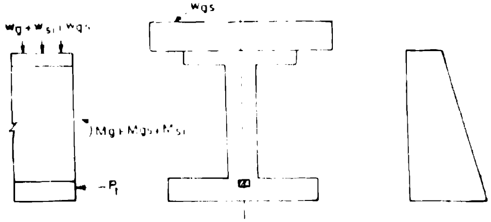

Casting of slab

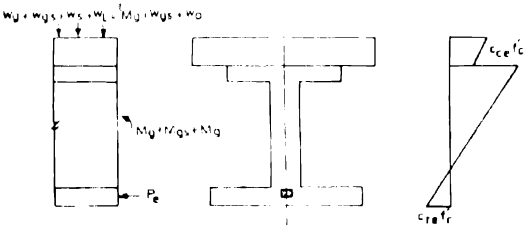

Working load condition

Fig. 4.2.1 : Loading conditions

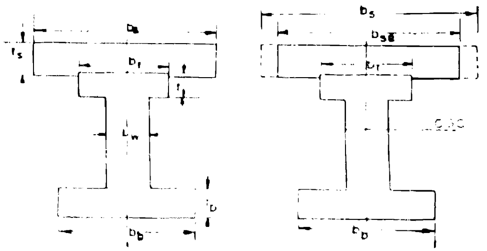

(a) Actual composite section (b) Effective composite section

b_s <1/4 span of the beam or <12 t_s or < centre to centre of the beam

Fig. 4.2.2 : Composite section

structures, the effective width is generally obtained from some approximate theoretical and experimental data. The effective slab width is illustrated in fig. 4.2.2.

4.3. NONDIMENSIONALISED ALLOWABLE STRESS EQUA*TIONS*:

It is observed in chapter III that the nondimensionalised equations *give* a basis to *establish an economical section. Eqs. 4.2.1 to* 4.2.4 are nondimensionalised by introducing the same parameters (Δ, m, ϵ, R, ρ and ω) which were discussed in the previous chapter. The nondimensionalised equations are very similar to the equations developed by Khachaturian (4.1).

Now

$$\frac{M_g}{I}(y_t)\frac{1}{f'_c} = \frac{\gamma AL^2}{8Ar^2}\left(\frac{h}{1+\Delta}\right)\frac{1}{f'_c}$$

$$= \left(\frac{\gamma L^2}{hf'_c}\right)\left(\frac{1}{8\rho}\right)\left(\frac{1}{1+\Delta}\right) = \frac{1}{8\,\omega\rho\,(1+\Delta)}$$

Eqs. 4.2.1 and 4.2.2 reduce to:

$$m\left(\frac{\epsilon}{\rho\,(1+\Delta)} - 1\right) - \frac{1}{8\,\rho\omega\,(1+\Delta)} = c_{tt} \qquad .. \quad (4.3.1)$$

$$m\left(\frac{\epsilon\Delta}{\rho\,(1+\Delta)} + 1\right) - \frac{\Delta}{8\,\rho\omega\,(1+\Delta)} = c_{ct} \qquad .. \quad (4.3.2)$$

Further

$$(M_g + M_{gs} + M_{sl}) = \frac{(\gamma A + \gamma A_{cs} + w_s)L^2}{8}$$

or
$$\frac{(M_g + M_{gs} + M_{sl})\ y_t}{f'_cI} = \frac{M_g y_t}{f'_cI}\left[1 + \frac{M_{gs}}{M_g} + \frac{M_{sl}}{M_g}\right]$$

$$= \frac{1}{8\,\omega\rho\,(1+\Delta)}\left[1 + \frac{A_{cs}}{A} + \frac{M_{sl}}{M_g}\right]$$

Let

$$I_c = u_{ic}\ I, \quad y_{bc} = u_{bc}\ y_b \text{ and } y_{tc} = u_{tc}\ y_t$$

Now
$$\frac{M_a\ y_{tc}}{f'_c\ I_c} = \frac{M_gR\ y_{tc}}{f'_c\ I_c}$$

$$= \left(\frac{M_g\ y_t}{f'_c\ I}\right)\left(\frac{R\ u_{tc}}{u_{ic}}\right)$$

$$= \left(\frac{1}{8\ \omega\rho\ (1+\Delta)}\right) R \left(\frac{u_{tc}}{u_{ic}}\right)$$

Let $\frac{M_{s1}}{M_g} = R_{s1}$ and $\frac{A_{cs}}{A} = \lambda$, then on substitution of the above quantities, the eqs. 4.2.3 and 4.2.4 reduce to :

$$-\eta m\left(\frac{\epsilon}{\rho(1+\Delta)}-1\right)+\frac{1}{8\,\omega\rho\,(1+\Delta)}\left(1+\lambda+R_{sl}+R\,\frac{u_{tc}}{u_{lc}}\right)=c_{ce} \qquad \text{(4.3.3)}$$

$$-\eta m\left(\frac{\Delta\epsilon}{\rho(1+\Delta)}+1\right)+\frac{\Delta}{8\,\omega\rho\,(1+\Delta)}\left(1+\lambda+R_{sl}+R\,\frac{u_{bc}}{u_{lc}}\right)=c_{te} \qquad \text{(4.3.4)}$$

For ready reference, all the governing equations are given here:

$$c_{tt}=m\left(\frac{\epsilon}{\rho(1+\Delta)}-1\right)-\frac{1}{8\,\rho\omega(1+\Delta)} \qquad \text{(4.3.1)}$$

$$c_{ct}=m\left(\frac{\epsilon\Delta}{\rho(1+\Delta)}+1\right)-\frac{\Delta}{8\,\omega\rho\,(1+\Delta)} \qquad \text{(4.3.2)}$$

$$c_{ce}=-\eta m\left(\frac{\epsilon}{\rho(1+\Delta)}-1\right)+\frac{1}{8\,\rho\,\omega\,(1+\Delta)}\left(1+\lambda+R_{sl}+\frac{Ru_{tc}}{u_{lc}}\right) \qquad \text{(4.3.3)}$$

$$c_{te}=-\eta m\left(\frac{\epsilon\Delta}{\rho(1+\Delta)}+1\right)+\frac{\Delta}{8\,\rho\,\omega\,(1+\Delta)}\left(1+\lambda+R_{sl}+\frac{Ru_{bc}}{u_{lc}}\right) \qquad \text{(4.3.4)}$$

Eqs. 4.3.1 and 4.3.3 give

$$\frac{\left[-\eta+1+\lambda+R_{sl}+R\,\dfrac{u_{tc}}{u_{lc}}\right]}{8\,\rho\,\omega\,(1+\Delta)}=\eta\,c_{tt}+c_{ce}$$

and eqs. 4.3.2 and 4.3.4 give

$$\frac{\Delta\left[-\eta+1+\lambda+R_{sl}+R\,\dfrac{u_{bc}}{u_{lc}}\right]}{8\,\rho\,\omega\,(1+\Delta)}=\eta\,c_{tt}+c_{ct}$$

A combination of the above two expressions yields

$$\frac{\Delta\left[(1-\eta)+\lambda+R_{sl}+R\,\dfrac{u_{tc}}{u_{lc}}\right]}{\left[(1-\eta)+\lambda+R_{sl}+R\,\dfrac{u_{bc}}{u_{lc}}\right]}=\frac{\eta\,c_{ct}+c_{te}}{\eta\,c_{tt}+c_{ce}}$$

$$\text{or } \Delta = \frac{\eta\, c_{ct} + c_{te}}{\eta\, c_{tt} + c_{ce}} \left(\frac{1 - \eta + \lambda + R_{sl} + R\,\dfrac{u_{tc}}{u_{lc}}}{1 - \eta + \lambda + R_{sl} + R\,\dfrac{u_{bc}}{u_{lc}}} \right) = \frac{\eta c_{ct} + c_{te}}{\eta c_{tt} + c_{ce}}\, \lambda_c \quad .. (4.3.5)$$

Where

$$\lambda_c = \frac{1 - \eta + \lambda + R_{sl} + R\,\dfrac{u_{tc}}{u_{lc}}}{1 - \eta + \lambda + R_{sl} + R\,\dfrac{u_{bc}}{u_{lc}}} \quad .. \quad (4.3.6)$$

From eqs. 4.3.1 and 4.3.2

$$m = \frac{c_{ct} - \Delta c_{tt}}{1 + \Delta} \quad .. \quad (4.3.7)$$

$$\frac{m\,\epsilon}{\rho\,(1+\Delta)} - m = c_{tt} + \frac{1}{8\,\rho\omega(1+\Delta)}$$

$$\frac{m\,\epsilon\,\Delta}{\rho\,(1+\Delta)} + m = c_{ct} + \frac{(1+\Delta)}{8\,\rho\omega(1+\Delta)}$$

A combination of the above two expressions yields

$$\frac{m\,\epsilon\,(1+\Delta)}{\rho(1+\Delta)} = (c_{tt} + c_{ct}) + \frac{(1+\Delta)}{8\rho\omega(1+\Delta)}$$

$$\text{or} \quad m\,\epsilon = (c_{tt} + c_{ct})\,\rho + \frac{1}{8\omega}$$

$$\text{Therefore,} \quad \epsilon = \frac{1}{m}\left[\rho\,(c_{tt} + c_{ct}) + \frac{1}{8\,\omega}\right] \quad .. \quad (4.3.8)$$

From eqs. 4.3.3 and 4.3.4

$$\left(1 + \lambda + R_{sl} + R\,\frac{u_{tc}}{u_{lc}}\right) = 8\,\omega\,\rho\,(1+\Delta)\left[c_{ce} + \eta\, m\left(\frac{\epsilon}{\rho\,(1+\Delta)} - 1\right)\right]$$

$$\left(1 + \lambda + R_{sl} + R\,\frac{u_{bc}}{u_{lc}}\right) = \frac{8\,\omega\rho\,(1+\Delta)}{\Delta}\left[c_{te} + \eta\, m\left(\frac{\Delta\,\epsilon}{\rho\,(1+\Delta)} + 1\right)\right]$$

$$\text{or} \quad \frac{R}{u_{lc}}\,(u_{tc} - u_{bc}) = 8\,\omega\rho\,(1+\ )\left[c_{ce} - \frac{c_{te}}{\Delta} + \eta\, m\left(-1 - \frac{1}{\Delta}\right)\right]$$

$$= 8\,\omega\rho\,\frac{(1+\Delta)}{\Delta}\left[(\Delta c_{ce} - c_{te}) - \eta\, m(1+\Delta)\right]$$

Therfore,

$$R = \frac{8\rho\omega u_{lc}(1+\Delta)}{(u_{tc} - u_{bc})\,\Delta}\left[(\Delta c_{ce} - c_{te}) - \eta\, m\,(1+\Delta)\right] .. \quad (4.3.9)$$

4.4. SOLUTION OF THE GOVERNING EQUATIONS: The four eqs. 4.3.1 to 4.3.4 give a criteria for design of a section. The unknown values in the four equations are η, Δ, m, ϵ, R, ρ, ω, λ, R_{sl}, u_{bc}, u_{tc}, u_{lc}. Out of these 12 unknowns, some of them are indirectly known. In general, the slab dimensions are known and, therefore, all the quantities associated with concrete slab are defined. Some quantities like η, ρ, ω could be assumed reasonably well. The four equations may now be solved with the following assumptions:

Assume quantities η, ρ, ω, λ, R_{s1}, u_{be}, u_{te}, u_{le} and then solve for Δ, ϵ, m, R which are the basic sectional details. On the above basis, the solution of the equations may now be written as:

$$\Delta = \lambda_e \frac{\eta c_{et} + c_{te}}{\eta c_{tt} + c_{ee}} \quad .. \quad (4.3.5)$$

$$m = \frac{c_{et} - \Delta c_{tt}}{1 + \Delta} \quad .. \quad (4.3.7)$$

$$\epsilon = \frac{1}{m}\left[\rho\,(c_{tt} + c_{et}) + \frac{1}{8\omega}\right] \quad .. \quad (4.3.8)$$

$$R = \frac{8u_{le}\,\omega\rho(1+\Delta)}{(u_{te} - u_{be})\,\Delta}\,[\Delta c_{ee} - c_{te} - \eta m(1+\Delta)] \quad .. \quad (4.3.9)$$

4.5. RANGES OF NONDIMENSIONALISED PARAMETERS:

(i) Depth factor ($\omega = hf'_c/\gamma h$); efficiency factor ($\rho = r^2/h^2$); shape factor ($\Delta = y_b/y_t$); eccentricity ratio ($\epsilon = e/h$); reinforcement factor ($m = P_t/Af'_c$); and moment ratio ($R = M_a/M_g$) have already been discussed in the previous chapter.

(ii) Composite section factor (λ_e): It can be observed from eq. 4.3.6 that the value of λ_e tends to unity for a non-composite section.

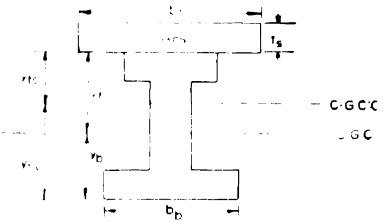

Fig. 4.5.1 : Composite section

It could be seen from fig. 4.5.1 that $u_{te} \leqslant 1$ and $u_{be} \geqslant 1$. The value of u_{te} is in the range of 0.80 to 1.0, u_{be} in the range of 1.0 to 1.20 and the value of R generally varies in the range of 0.7 to 3. Hence the range of λ_e will be from 0.90 to 1. For many practical purposes, λ_e may be assumed as 0.95 and Δ be solved from eq 4.3.5. The procedure for design is same as given in chapter III. All these equations reduce to a non-composite section by setting A_{cs} equal to zero.

4.6. SHRINKAGE STRESSES:

The composite construction consists of concrete of two different mixes cast at two different intervals. The shrinkage in the beam is more or less completed by the time the slab starts shrinking. The differential shrinkage causes stresses in composite construction. Assuming a certain shrinkage in the slab, strain compatibility has to be satisfied from which the stresses due to shrinkage are computed. Let ϵ_a = shrinkage strain in slab and if the slab is completely restrained, the force developed due to the restraint is given by

$$P_a = \epsilon_a E_{cs} A_{cs} \qquad \ldots. \ (4.6.1)$$

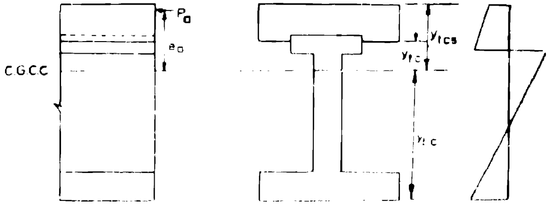

Fig. 4.6.1 : Differential shrinkage stress

The stresses due to shrinkage force are now computed using a simple beam theory. The extreme fibre stresses due to shrinkage are :

$$f_{bb} = \left(-\frac{P_a}{A_c} + \frac{P_a e_a y_{bc}}{I_c}\right) \qquad .. \ (4.6.2)$$

$$f_{tb} = -\left(\frac{P_a}{A_c} + \frac{P_a e_a y_{tc}}{I_c}\right) \qquad .. \ (4.6.3)$$

$$f_{bs} = -\left(\frac{P_a}{A_c} + \frac{P_a e_a y_{tc}}{I_c}\right) + f_a \qquad .. \ (4.6.4)$$

$$f_{ts} = -\left(\frac{P_a}{A_c} + \frac{P_a e_a y_{tcs}}{I_c}\right) + f_a \qquad .. \ (4.6.5)$$

Where

f_{bb} = stress at bottom fibre of the beam

f_{tb} = stress at the top fibre of the beam

f_{bs} = stress at bottom fibre of the slab

f_{ts} = stress at top fibre of the slab

y_{tcs} = distance of top fibre of the slab from the C. G. C. of the composite section

f_a = $\epsilon_a E_{cs}$

E_{cs} = Young's modulus of concrete of the slab

The stresses that are computed are approximate but are good for practical purposes. More exact stresses could be obtained by considering the mutual strain compatibility at the junction of the slab and the beam.

The shrinkage stresses are in addition to the stresses at working load conditions. It is necessary to superimpose the stresses at working load on the shrinkage stress and then check the allowable stresses. The allowable stress coefficients at working load condition in composite construction may be assumed less than those used in the non-composite construction.

Design example 4.6.1 : Design of a post-tensioned prestressed concrete composite beam for an effective span of 50 m to carry a uniformly distributed load of 2000 kg/m. The centre to centre of the girders is 200 cm. Assume the slab width as 200 cm. The maximum depth of the beam is not to exceed 220 cm.

Given data :

effective span = 50 m, live load = 2000 kg/m

depth of beam = 220 cm, superimposed load = 200 kg/m

concrete strength (f'_c) = 450 kg/sq cm and

tensile strength of prestressing steel (f'_s) = 15000 kg/sq cm

Code specifications :

density of concrete, (γ) = 2400 kg/m^3

Young's modulus, (E_c) = $18000\sqrt{f'_c} = 3.82 \times 10^5$ kg/sq cm

$E_s = 2.1 \times 10^6$ kg/sq cm

Stress coefficients (for loads likely to increase) be :

$c'_{ct} = 0.47$; $c'_{tt} = 0.022$; $c'_{ce} = 0.31$; $c'_{te} = 0.022$

f_s (at transfer) $= 0.7\, f'_s$

f_s (at working) $= 0.6\, f'_s$

f_s (at anchorage) $= 0.8\, f'_s$

Design procedure : Assume efficiency factor and other coefficients. Based on the experience of example 3.10.1, it is now possible to make an approximate estimate for efficiency and other factors. Factors used in example 3.10.1 are used in this example to make a comparison of the two beams.

Let $\rho = 0.1285$, $\Delta = 1.68$, and approximate values of

$u_{tc} = 0.92$, $u_{bc} = 1.04$

$u_{lc} = 1.20$, $\eta = 0.84$

$c_{tt} = -0.05$, $c_{ct} = 0.47$, $c_{ce} = 0.31$, $c_{te} = 0.02$

The values of u's have to be chosen from experience and then should be checked with the actual values obtained in the final selection. Area of cross section depends on the assumed values of u's. Any improper selection of u's will throw off the economy of the beam. Stress eqs. 4.3.1 to 4.3.4 could be written exactly in the form of simply supported beam eqs. 3.4 by introducing a modified $\overline{R}$ represented by

$$\bar{R} \simeq \left(1+\lambda+R_{sl}+R\frac{u_{tc}}{u_{lc}}\right)$$

$$\simeq \left(1+\lambda+R_{sl}+R\frac{u_{bc}}{u_{lc}}\right)$$

This modified $\bar{R}$ will give some guide line.

$$\omega = \frac{hf'_c}{\gamma L^2} = 1.65$$

$$\epsilon_{\text{req.}} \simeq \frac{1+\Delta}{c_{ct}-\Delta c_{tt}}\left[\rho\,(c_{tt}+c_{ct})+\frac{1}{8\,\omega}\right]=0.625$$

$$\epsilon_{\text{limit}} = \frac{\Delta}{1+\Delta} - 0.08=0.55$$

The value of m may be taken as 0.24 based on the example 3.10.1, then

$$R = \frac{8\,\rho\,\omega\,u_{ic}\,(1+\Delta)}{\Delta\,(u_{bc}-u_{tc})}\,[\eta m(1+\Delta) - (\Delta c_{ce}-c_{te})\,] = 1.068 \simeq 1.07$$

$$w_g = \frac{w_s}{R} = \frac{2200}{1.07} = 2050 \text{ kg/m}$$

$$A = \frac{2050}{2400} = 0.856 \text{ sq m}$$

Let the thickness of the slab be 8 cm (sometimes the thickness is fixed by practical criteria).

The area of the slab is given by

$$A_{cs} = b_s t_s = 200 \times 8 = 1600 \text{ sq cm}$$

Total area of c.s. = 8560 + 1600 = 10160 sq cm

It is now necessary to determine the various u's and check the allowable stresses. Various dimensions for the given efficiency and shape factors are given below (from table 2 in Appendix A).

For $\rho = 0.1285$, $\Delta = 1.68$, the sectional coefficients are

$c_a = 0.2560$, $c_i = 0.0329$, $c_{yb} = 0.6269$, $c_{yt} = 0.3731$,

$c_f = 0.5$, $c_w = 0.12$, $c_t = 0.12$, $c_b = 0.08$

$$\therefore\; b_t = \frac{8560}{0.256\,h} = 152 \text{ cm}$$

$$\begin{aligned}
r^2 &= 0.1285h^2 &&= 6219\\
y_b &= c_{yb}h &&= 138 \text{ cm}\\
y_t &= c_{yt}h &&= 82 \text{ cm}\\
t_t &= c_t h &&= 26.4 \text{ cm}\\
t_b &= c_b h &&= 17.6 \text{ cm}\\
b_w &= c_w b_t &&= 18.24 \text{ cm}\\
b_b &= c_f b_t &&= 76 \text{ cm}
\end{aligned}$$

$$\lambda = \frac{A_{cs}}{A} = \frac{1600}{8560} = 0.187$$

The properties of the composite section are calculated easily using the sectional properties of the beam.

Taking moments about the centroid of the beam cross section, the centroid of the composite section would be determined as

$$\bar{y} = \frac{1600\ (82+4)}{10160} = 13.6 \text{ cm}$$

$$y_{tc} = 82 - 13.6 = 68.4 \text{ cm}$$

$$y_{bc} = 138 + 13.6 = 151.6 \text{ cm}$$

$$u_{tc} = \frac{68.4}{82} = 0.835$$

$$u_{bc} = \frac{151.6}{138} = 1.09$$

$$\begin{aligned} I_c &= I\ 0 + A\bar{y}^2 + A_{cs}\ (4+68.4)^2 \\ &= 51146603 + 1878000 + 8380000 \\ &= 61404600 \text{ cm}^4 \end{aligned}$$

$$u_{Ic} = \frac{I_c}{I_p} = \frac{61404600}{51146600} = 1.2$$

Let the superimposed load at the time of casting of the slab be zero, then $R_{s1} = 0$. Using the values computed above, the allowable stresses could be checked with the help of eqs. 4.3.1 to 4.3.4.

Eqs. 4.3.1 to 4.3.4 for $m = 0.24$, $\eta = 0.84$, $R = 1.06$, $\rho = 0.1285$, $\Delta = 1.68$, $\epsilon = 0.53$, $\omega = 1.65$, $u_{tc} = 0.835$, $u_{bc} = 1.09$, $\lambda = 0.187$ and $u_{Ic} = 1.20$ give

$c_{tt} = -0.091$ (permissible)

$c_{ct} = 0.48$ (2.4% excess)

$c_{tc} = 0.025$ (11.3 kg/sq cm tension, excess)

$c_{cc} = 0.307$ (permissible)

$$P_t = mA\ f'_c = 0.24 \times 8560 \times 450 = 925000 \text{ kg}$$

$$A_s = \frac{925000}{0.6\ f'_s} = 102.8 \text{ sq cm}$$

$$\text{Percentage of steel} = \frac{102.8 \times 100}{10500} = 0.98\%$$

$$e = 0.53\ h = 116.6 \text{ cm}$$

Since some of the stresses in the selected section exceed the permissible limits, the reader is advised to try another section. The section should also be checked for shrinkage stresses.

Problems

4.1 A simply supported beam of span 20 m is carrying a load of 2400 kg/m. Design a composite beam with top slab of 15 cm thickness and 150 cm width. Use $f'_c = 400$ kg/sq cm and $f'_s = 15000$ kg/sq cm for beam and $f'_c = 200$ kg/sq cm for slab concrete. Make a comparative study of this design with problem 3.1.

4.2 The bridge described in problem 3.2 is provided with a top slab of 15 cm thickness using M 200 concrete. Design a composite beam bridge, using the data provided in the problem 3.2.

CHAPTER V

CONTINUOUS BEAMS

5.1. INTRODUCTION : It has been observed in the previous chapters that prestressing force causes deformation which can take place freely in a statically determinate structure without causing any change in the reactions. In a statically indeterminate structure, the deformation due to prestressing force will affect the support compatibility conditions resulting in some secondary stresses. This effect is explained through a simple example of two span continuous beam shown in fig. 5.1.1. Let the beam rest freely on three supports at same level and let it be prestressed with a straight tendon. The tendency of the tendon will be to lift the beam from the middle support. Hence, there should be a force at the middle support to keep the compatibility of the beam resting on all the three supports. This downward force 'R_b' has to be balanced by upward reactions at the extreme supports. The stresses caused due to these reactions are called secondary stresses.

Fig. 5.1.1 gives a complete picture of the problem. The shear force and bending moment caused by the prestressing force are also shown in the figure. The secondary stresses depend mainly upon the profile of the prestressing tendon and, if a proper profile is not chosen, the secondary stresses can be very large. On the other hand, if an appropriate profile of the tendon is chosen, the secondary stresses could be reduced to zero. A tendon of this profile is called "concordant cable". A concordant cable may be defined as the cable which will not produce any statically indeterminate reactions. The concordant cable profile is not unique in any given statically indeterminate structure but it is located within a certain narrow zone. The restriction to the concordant profile zone has the disadvantage of not utilising the depth of the beam effectively for a suitable profile in working load conditions. There are two possible important practical considerations: (i) the profile may be selected as a concordant profile which causes no secondary stresses, not considering economy, or (ii) the profile may be chosen as a compromise between the secondary stresses and the working load stresses based on economy. In other words, a concordant cable is a good choice but not necessarily the best. It is also important to note that creep is likely to cause some statically indeterminate reactions. Analysis of statically indeterminate prestressed concrete structures could be done by any of the methods used in structural analysis.

Flyover Bridge at Marine Drive, Bombay. Prestressed with Gifford Udall CCL Prestressing System. Consultants: Stup (India) Ltd.
(Courtesy of Killick, Nixon & Co., Ltd., Bombay)

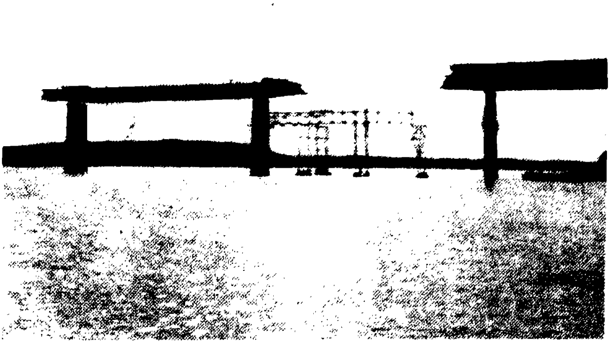

Sarangkheda Bridge under construction-launching
(Courtesy of the Hindustan Construction Co. Ltd., Bombay)

5.2. ANALYSIS OF TWO SPAN BEAM: A beam of constant cross section and having parabolic tendon profile may be considered for analysis. The derivations are developed using the prismatic beam theory. The tendon profile consists of two parabolas with sags g_1 and g_2. The two parabolas intersect at the middle support with an

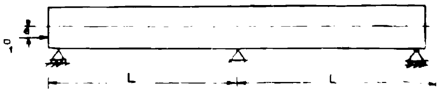

(a) Two span continuous beam (no external force including self weight)

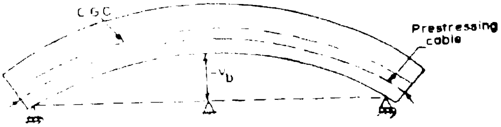

(b) Prestressing force acting and beam free to deform

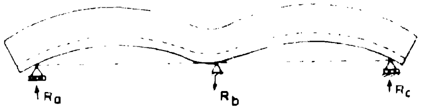

(c) Constraint due to the continuous supports

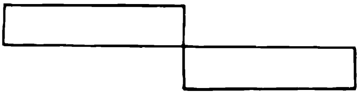

(d) Secondary shear force

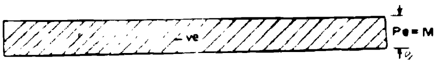

(e) Bending moment due to eccentric prestressing force

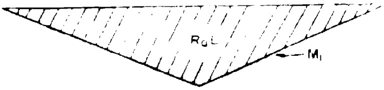

(f) Bending moment due to secondary reactions

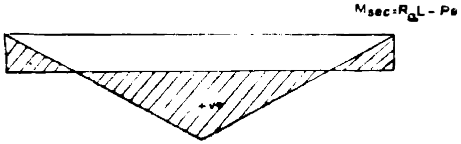

(g) Actual bending moments

Fig. 5.1.1. Two span continuous prestressed beam

eccentricity e. The intersection of the parabolas has to be rounded to a smooth transition curve without affecting the analysis. Sometimes the transition curve may be taken as a small parabola in which case three parabolas should be considered in the analysis.

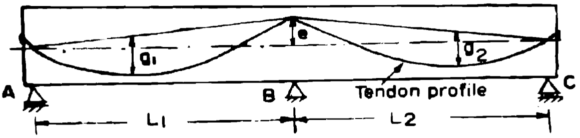

Fig. 5.2.1. Two span continuous beam

The problem is analysed by making the beam statically determinate by cutting it at the intermediate support and matching the compatibility.

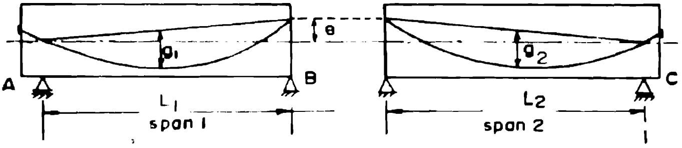

(a) Beam separated into two parts

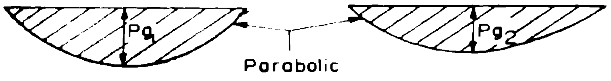

(b) B. M. due to parabolic profile only

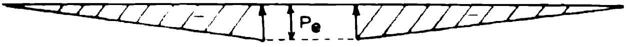

(c) B. M. due to middle eccentricity

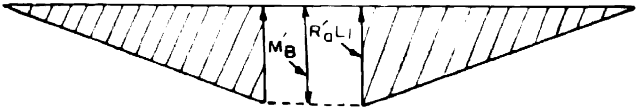

(d) B. M. due to indeterminate reactions

Fig. 5.2.2 : B. M. of separated sections due to prestressing only

Slopes at B of spans 1 and 2 are to be computed and matched to determine the indeterminate reactions. The slopes are computed using the bending moment curves shown in fig. 5.2.2.

$$EI\theta^0_{B1}=\frac{1}{2}\left(\frac{2}{3}L_1Pg_1\right)+\frac{2}{3}\left(\frac{1}{2}L_1P.e\right)$$

$$=\frac{PL_1}{3}(g_1+e) \quad .. \quad (5.2.1)$$

Similarly

$$EI\theta^0_{B2}=\frac{PL_2}{3}(g_2+e) \quad .. \quad (5.2.2)$$

Where

θ_B=slope of the beam at support B and the subscript 1 or 2 indicates span 1 or 2 respectively. The superscript 'o' refers to prestressing only. Profile distance measured downward from C.G.C. is considered positive.

Let

θ'_B=Slope due to statically indeterminate force

Then

$$\left.\begin{aligned} EI\theta'_{B1}&=\frac{1}{3}L_1\, M'_B \\ EI\theta'_{B2}&=\frac{1}{3}L_2\, M'_B \end{aligned}\right\} \quad .. \quad (5.2.3)$$

The condition of continuity is that the change of the slope to the right and left of the intermediate support should be zero i.e.,

$$\theta^o_{B1}+\theta^o_{B2}+\theta'_{B1}+\theta'_{B2}=0 \quad .. \quad (5.2.4)$$

$$\therefore \quad \frac{M'_B}{3}(L_1+L_2)+\frac{P}{3}[L_1(e+g_1)+L_2(e+g_2)]=0$$

$$\text{or} \quad M'_B=-P\left(\frac{L_1g_1+L_2g_2}{L_1+L_2}+e\right) \quad .. \quad (5.2.5)$$

$$\text{Now} \quad R'_A=\frac{M'_B}{L_1}$$

$$=-\frac{P}{L_1}\left(\frac{L_1g_1+L_2g_2}{L_1+L_2}+e\right) \quad .. \quad (5.2.6)$$

Final moments due to prestressing force can be obtained by superposition of the moments as shown in fig. 5.2.2. For example, the moment at support B is given by

$$M_B=Pe+M'_B$$

$$M_B=Pe-P\left(\frac{L_1g_1+L_2g_2}{L_1+L_2}+e\right)$$

$$=-P\left(\frac{L_1g_1+L_2g_2}{L_1+L_2}\right) \quad .. \quad (5.2.7)$$

It is important to note that the bending moment at the intermediate support due to prestressing force is independent of the eccentricity e at the support. It can be proved in general that in continuous beams, bending moment at an intermediate support due to prestressing force is independent of the eccentricity over the support but is governed by the maximum sag of the parabolas. Now it is clear that the tendon profile can be shifted, moving about the end points without affecting the bending moment at the intermediate support. For example, tendon profiles as shown in two cases of fig. 5.2.3 give the same moment at the intermediate support. Hence particular attention should be paid while fixing the sag.

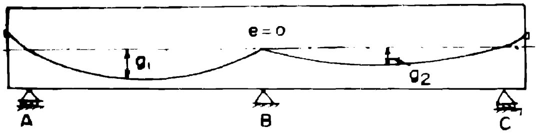

case 1

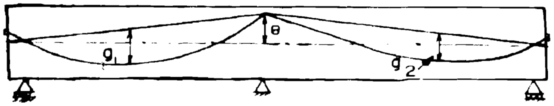

case 2

Fig. 5.2.3 : Two tendon profiles shown in the above two figures give the same moment at B

Let $R'_A = 0$, then from eq. 5.2.6,

$$e = -\left(\frac{L_1 g_1 + L_2 g_2}{L_1 + L_2}\right) \qquad \text{.. (5.2.8)}$$

A concordant cable can be obtained by providing the eccentricity as given in eq. 5.2.8.

Determination of shear forces: Shear force in the span AB due to prestress is

$$V_x = R'_A + P \sin \alpha = R'_A + P\left(\frac{dy}{dx}\right)$$

$$\text{Where} \quad y = x\left(\frac{4g_1 + e}{L_1} - \frac{4g_1 x}{L_1^2}\right)$$

$$V_x = -\frac{P}{L_1}\left[\frac{L_1 g_1 + L_2 g_2}{L_1 + L_2} + e\right] + P\left[\frac{4g_1 + e}{L_1} - \frac{8g_1 x}{L_1^2}\right]$$

$$= -\frac{P}{L_1}\left[\left(\frac{L_1 g_1 + L_2 g_2}{L_1 + L_2} + e\right) - \left(4g_1 + e - \frac{8g_1 x}{L_1}\right)\right]$$

$$= -\frac{P}{L_1}[L_1 g_1 (8x-3L_1)+L_2 (L_1 g_2-4g_1 L_1+8g_1x)]\frac{1}{L_1(L_1+L_2)}$$

$$= -\frac{P}{L_1}\left[\frac{g_1 (8x-3L_1)+L_2 (g_2-4g_1)}{L_1+L_2}+\frac{8g_1 xL_2}{L_1(L_1+L_2)}\right] \quad .. \quad (5.2.9)$$

The design for shear force should be done based on the shear force as obtained above.

The secondary moments can also be computed by considering the intensity of the radial force due to prestressing force. If the cable is parabolic, the intensity of the radial force is $(P\ d^2y/dx^2)$. The secondary moments are computed using this force, and illustrated in fig. 5.2.4. The method of load balancing technique is discussed later in which radial component force plays important role.

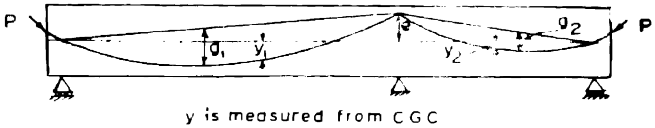

(a) Beam with parabolic cable

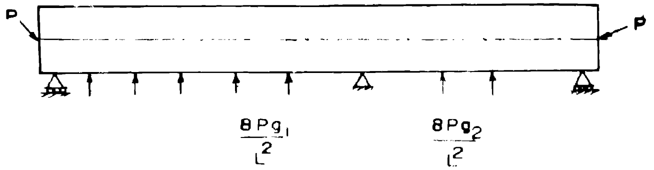

(b) Radial force due to P from which the secondary moments (M′) could be computed

Fig. 5.2.4 : Beam with equivalent radial force

5.3. ANALYSIS OF TWO SPAN CONTINUOUS BEAM WITH ECCENTRICITIES AT OUTER SUPPORTS :

For a cable profile having eccentricities at the end supports, the problem can be divided into two parts : (i) moment due to simple parabolic cable with zero eccentricities at outer supports plus (ii) moment due to straight cables with eccentricities at the end supports. The superposition of the two moments will give the resultant moment due to the cable profile. The slope compatibility can be obtained by considering the two parts separately. The moments are shown in fig. 5.3.1.

Summing up the slope at B

$$(\theta^o{}_{B1})_P+(\theta^o{}_{B2})_P+(\theta^o{}_{B1})_t+(\theta^o{}_{B2})_c+(\theta'{}_{B1})+(\theta'{}_{B2})=0$$

$$\frac{P}{3}[L_1 (g_1+e)+L_2 (g_2+e)+\frac{1}{2}(e_A L_1+e_C L_2)]+\frac{M'_B}{3} (L_1+L_2)=0$$

$$M'_B = -P\,[L_1(g_1+e)+L_2(g_2+e)+\frac{1}{2}(e_AL_1+e_CL_2)]/(L_1+L_2) \quad \ldots \quad (5.3.1)$$

$$M_B = M'_B + Pe$$

$$= -P\,\frac{L_1g_1+L_2g_2+\frac{1}{2}\,(e_AL_1+e_CL_2)}{L_1+L_2} \quad \ldots \quad (5.3.2)$$

(independent of 'e')

$$R'_A = \frac{M_B}{L_1} = -\frac{P}{L_1}\left(\frac{L_1g_1+L_2g_2+\frac{1}{2}\,(e_AL_1+e_CL_2)}{L_1+L_2}\right) \quad \ldots \quad (5.3.3)$$

Similarly

$$R'_C = \frac{M_B}{L_2} = -\frac{P}{L_2}\left(\frac{L_1g_1+L_2g_2+\frac{1}{2}\,(e_AL_1+e_CL_2)}{L_1+L_2}\right) \quad \ldots \quad (5.3\ 4)$$

$$R'_B = R'_A + R'_C$$

For concordant cable, set $M'_B = 0$. So from eq. 5.3.1

$$e = -[L_1g_1+L_2g_2+\frac{1}{2}\,(e_AL_1+e_CL_2)]/(L_1+L_2) \quad \ldots \quad (5.3.5)$$

Same procedure could be extended to three or more spans. However, relaxation at the supports leads to tedious calculations in solving simultaneous equations. Moment distribution procedure could be used to solve problems of higher indeterminacy.

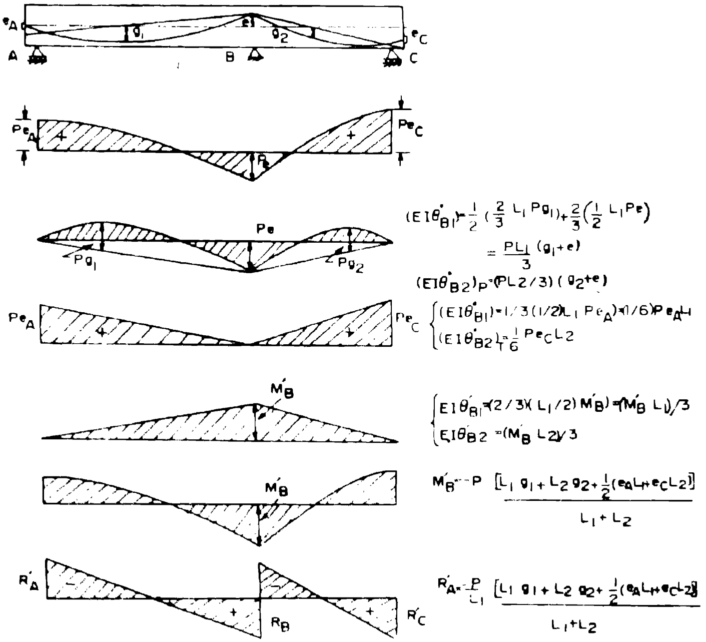

e_A
g_1
e
g_2
e_C
A
B
C
Pe_A
Pe_C
+
+
Pe
Pg_1
Pg_2
$(EI\theta_{B1})_P = \frac{1}{2}(\frac{2}{3}L_1Pg_1) + \frac{2}{3}(\frac{1}{2}L_1Pe)$
$= \frac{PL_1}{3}(g_1+e)$
$(EI\theta_{B2})_P = (PL_2/3)(g_2+e)$
$(EI\theta_{B1}) = 1/3(1/2)L_1Pe_A) = 1/6\,Pe_AL_1$
$(EI\theta_{B2}) = \frac{1}{6}Pe_CL_2$
M'_B
$EI\theta_{B1} = (2/3)(L_1/2)M'_B) = (M'_B L_1)/3$
$EI\theta_{B2} = (M'_B L_2)/3$
M'_B
$M'_B = -P\,\frac{[L_1g_1+L_2g_2+\frac{1}{2}(e_AL_1+e_CL_2)]}{L_1+L_2}$
R'_A
R_B
R'_C
$R'_A = -\frac{P}{L_1}\,\frac{[L_1g_1+L_2g_2+\frac{1}{2}(e_AL_1+e_CL_2)]}{L_1+L_2}$

Fig. 5.3.1 : Continuous beam

5.4. MOMENT DISTRIBUTION METHOD:

The moment distribution procedure starts by fixing the section at the supports against rotation and computing the fixed end moments. It is essential to calculate the fixed end moments due to prestressing force and distribute them in the same way as done for fixed end moments caused by external loads. Fig. 5.4.1 shows a fixed end beam with prestressing cable. The fixed end moments due to prestressing force are computed from rotation compatibility at the supports. All calculations are shown in fig. 5.4.1.

Summing up the slope at end A

$$\frac{PL}{6}\,[2g+2e_A+e_B]+\frac{L}{6}\,(2M'_A+M'_B)=0 \text{ i.e. for } \theta_A=0$$

or

$$P\,[2g+2e_A+e_B]+(2M'_A+M'_B)=0 \qquad \text{.. (5.4.1)}$$

Similarly for θ_B

$$P\,[2g+2e_B+e_A]+(M'_A+2M'_B)=0 \qquad \text{.. (5.4.2)}$$

The solution of the above two equations is

$$M'_A=-P\,(\tfrac{2}{3}\,g+e_A) \qquad \text{.. (5.4.3)}$$

$$M'_B=-P\,(\tfrac{2}{3}\,g+e_B) \qquad \text{.. (5.4.4)}$$

$$M_A=M^o_A+M'_A=Pe_A-P\,(\tfrac{2}{3}\,g+e_A)=-\tfrac{2}{3}\,Pg$$

$$M_B=M^o_B+M'_B=-\tfrac{2}{3}\,Pg \qquad \text{.. (5.4.5)}$$

$$M_C=Pg-\tfrac{2}{3}\,Pg=\tfrac{1}{3}\,Pg \qquad \text{.. (5.4.6)}$$

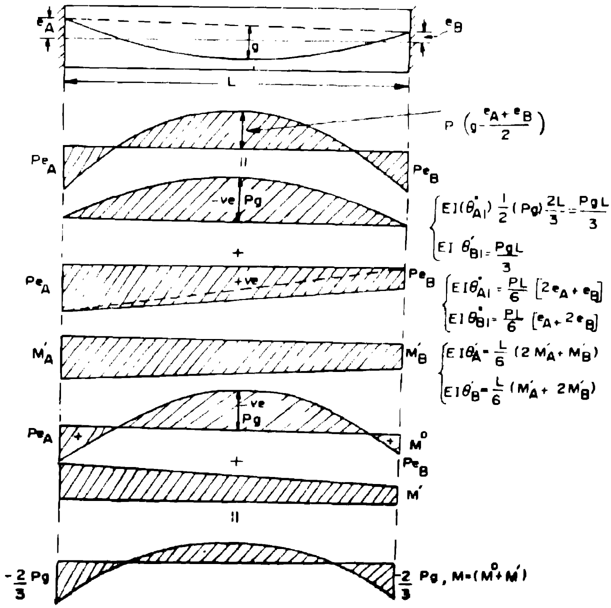
e_A
e_B
g
L
$P\left(g-\frac{e_A+e_B}{2}\right)$
Pe_A
Pe_B
=
-ve Pg
$EI(\theta'_{A1})=\frac{1}{2}(Pg)\frac{2L}{3}=\frac{PgL}{3}$
$EI\,\theta'_{B1}=\frac{PgL}{3}$
+
Pe_A
+ve
Pe_B
$EI\theta'_{A1}=\frac{PL}{6}[2e_A+e_B]$
$EI\theta'_{B1}=\frac{PL}{6}[e_A+2e_B]$
M'_A
M'_B
$EI\theta'_A=\frac{L}{6}(2M'_A+M'_B)$
$EI\theta'_B=\frac{L}{6}(M'_A+2M'_B)$
-ve Pg
Pe_A
+
+
M^o
Pe_B
+
M'
=
$-\frac{2}{3}Pg$
$\frac{2}{3}Pg$, $M=(M^o+M')$

Fig. 5.4.1 : **Bending moment in a fixed end beam due to prestressing force**

It is interesting to note that the end moments are independent of the end eccentricities. The prestressing force P is negative, so M_A and M_B are positive moments. (Same result can be obtained by considering the radial force.)

For a concordant profile, $M'_A = M'_B = 0$ that leads to

$$e_B - e_A = -\frac{2}{3} g \qquad \text{.. (5.4.7)}$$

The fixed end moments due to various tendon profiles are given in table 3 (Appendix A). For more detailed fixed end bending moments the reader is referred to references (5.1) and (5.2).

5.5. APPLICATION OF MOMENT DISTRIBUTION PROCEDURE: An example of three span continuous beam with external loads is shown in fig. 5.5.1 alongwith bending moment diagrams of individual spans in fixed end conditions. The moment distribution is given in table 5.5.1. The summation of moments due to external loads and prestressing force gives the moment that will exist in the beam. A concordant profile could also be obtained by setting the secondary bending moments due to the prestressing force equal to zero. The secondary moments are obtained as the difference of the balanced moments and moments due to eccentricity. The design should be checked for the final moments.

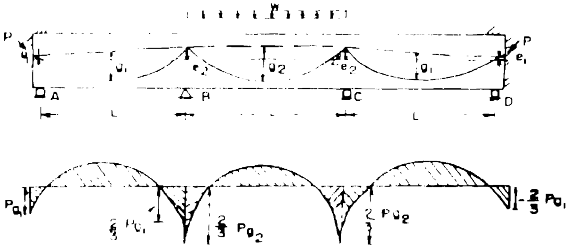

(a) Fixed end moments due to prestressing force

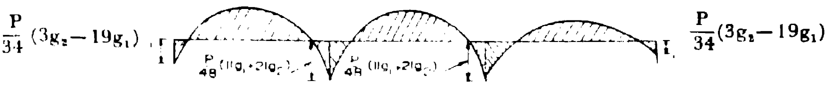
$\frac{P}{34}(3g_2-19g_1)$
$\frac{P}{48}(11g_1+21g_2)$
$\frac{P}{48}(11g_1+21g_2)$
$\frac{P}{34}(3g_2-19g_1)$

(b) Indeterminate moments due to prestressing force on continous beam (balanced)

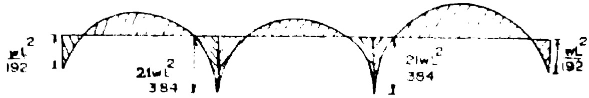

(c) Moments due to external loading

Fig. 5.5.1 : Moment in three span continuous beam

TABLE 5.5.1 : MOMENT DISTRIBUTION (DUE TO PRESTRESSING)

Joint	A	B		C		D
Member	AB	BA	BC	CB	CD	DC
Stiffness (relative)	1	1	1	1	1	1
Distrbution factor	0	0.5	0.5	0.5	0.5	0
Fixed end moment due to prestressing	$-\frac{2}{3}Pg_1$	$\frac{2}{3}Pg_1$	$-\frac{2}{3}Pg_2$	$\frac{2}{3}Pg_2$	$-\frac{2}{3}Pg_1$	$\frac{2}{3}Pg_1$
Balance	0	$-\frac{P}{3}(g_1-g_2)$	$-\frac{P}{3}(g_1-g_2)$	$-\frac{P}{3}(g_2-g_1)$	$-\frac{P}{3}(g_2-g_1)$	0
Carry over	$-\frac{P}{6}(g_1-g_2)$	0	$-\frac{P}{6}(g_2-g_1)$	$-\frac{P}{6}(g_1-g_2)$	0	$-\frac{P}{6}(g_2-g_1)$
Balance	0	$\frac{P}{12}(g_2-g_1)$	$\frac{P}{12}(g_2-g_1)$	$\frac{P}{12}(g_1-g_2)$	$\frac{P}{12}(g_1-g_2)$	0
Carry over	$+\frac{P}{24}(g_2-g_1)$	0	$\frac{P}{24}(g_1-g_2)$	$\frac{P}{24}(g_2-g_1)$	0	$-\frac{P}{24}(g_1-g_2)$
Balance	0	$-\frac{P}{48}(g_1-g_2)$	$-\frac{P}{48}(g_1-g_2)$	$-\frac{P}{48}(g_2-g_1)$	$-\frac{P}{48}(g_2-g_1)$	0
Total	$\frac{P}{24}(3g_2-19g_1)$	$\frac{P}{48}(11g_1+21g_2)$	$-\frac{P}{48}(11g_1+21g_2)$	$\frac{P}{48}(11g_1+21g_2)$	$-\frac{P}{48}(11g_1+21g_2)$	$-\frac{P}{24}(3g_2-19g_1)$

(contd.)

TABLE 5.5.1 : MOMENT DISTRIBUTION (DUE TO EXTERNAL LOAD)

Joint	A	B		C		D
Member	AB	BA	BC	CB	CD	DC
Fixed end moment due to external load	0	0	$\frac{wl^2}{12}$	$-\frac{wl^2}{12}$	0	0
Balance	0	$-\frac{wl^2}{24}$	$-\frac{wl^2}{24}$	$\frac{wl^2}{24}$	$\frac{wl^2}{24}$	0
Carry over	$-\frac{wl^2}{48}$	0	$\frac{wl^2}{48}$	$-\frac{wl^2}{48}$	0	$\frac{wl^2}{48}$
Balance	0	$-\frac{wl^2}{96}$	$-\frac{wl^2}{96}$	$\frac{wl^2}{96}$	$\frac{wl^2}{96}$	0
Carry over	$-\frac{wl^2}{192}$	0	$\frac{wl^2}{192}$	$-\frac{wl^2}{192}$	0	$\frac{wl^2}{192}$
Balance	0	$-\frac{wl^2}{384}$	$-\frac{wl^2}{384}$	$\frac{wl^2}{384}$	$\frac{wl^2}{384}$	0
Total	$-\frac{5wl^2}{192}$	$-\frac{21\,wl^2}{384}$	$\frac{21\,wl^2}{384}$	$-\frac{21\,wl^2}{384}$	$\frac{21\,wl^2}{384}$	$\frac{5wl^2}{192}$

5.6. CONTINUOUS BEAMS WITH VARIABLE SECTION:

In continuous beams, the magnitude of moment is comparatively large at intermediate supports, so efficiency of construction may be obtained by increasing the thickness of the beam at the intermediate supports. The variable moment of inertia affects the distribution of moments in a continuous beam. The cable profile 'y' is measured from the centroidal axis and if it is to be a smooth curve, should follow the profile of the centroidal axis. As shown in fig. 5.6.1, the centroidal axis has a kink at a distance $\xi_1 L_1$ so the cable profile should also have the same amount of kink.

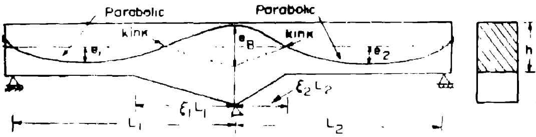

$$g_1 = e_1 + \frac{e_B}{2}$$

$$g_2 = e_2 + \frac{e_B}{2}$$

(a) Actual profiles

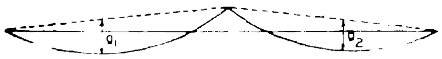

(b) Centroidal axis straightened

Fig. 5.6.1 : Beam with varible thickness

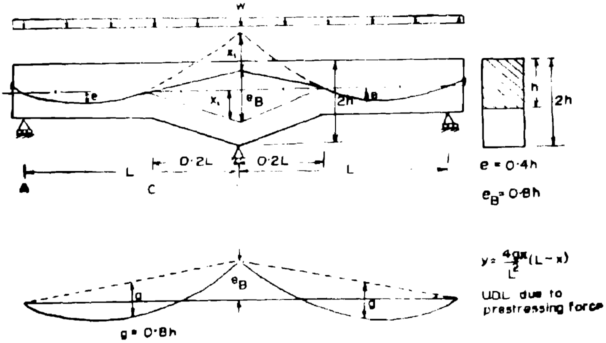

Fig. 5.6.2 : Example 5.6.1

Example 5.6.1: Analysis of a haunch beam as shown in fig. 5.6.2.

Solution of the problem by moment distribution procedure is shown in table 5.6.1. The stiffness and carry-over factors are obtained from tables of haunch sections. The beam is symmetrical about the middle support so the moment distribution is done for one span only.

$M_B = M'_B + Pe_B$

M_B (due to P) $= -0.169$ (8 Pg) (vide table 5.6.1)

$M^o_B = Pe_B$

If a concordant cable is desired, then

$M'_B = M_B - M^o_B = -0.169 \times 8Pg - Pe_B = 0$

$\therefore e_B = -0.169 \times 8g$

TABLE 5.6.1 : MOMENT DISTRIBUTION—example 5.6.1.

Joint	A	B
Member	AB	BA
Carry over factor	0.7	0.5
Relative stiffness	4.4	6.67
Distribution factor	1	0.5
Fixed end moment due to P	0.069 (8 Pg)	−0.12 (8 Pg)
Balance	−0.069	0
Carry over	0	−0.049
Total B. M.	0	−0.169 (8 Pg)
Fixed end moment due to UDL	$0.069\ wL^2$	$-0.12\ wL^2$
Balance	−0.069	0
Carry over	0	−0.049
Total B. M.	0	$-0.169\ wL^2$

Transfer condition (neglecting the dead load moments):

$M_B = -0.169 \times 8\ Pg = -1.352\ Pg$

L. L. Condition: $M_B = 1.352\ Pg - 0.169w\ L^2$

5.7. **DESIGN OF STATICALLY INDETERMINATE SRTUCTURES :** In statically indeterminate structures, it is desirable to locate the cable zone based upon the zero tension on extreme fibres. The limiting curves of cable zone are described below :

Let M_1 = maximum bending moment at transfer condition
M_2 = maximum bending moment at effective working load condition
k_b = bottom kern distance = r^2/y_t
k_t = top kern distance = r^2/y_b

Considering the zero tension at top and bottom fibres

$$\frac{P_t}{A}\left(1+\frac{M_1 y_t}{P_t\,r^2}-\frac{e y_t}{r^2}\right)\geqslant 0 \qquad \text{.. (5.7.1.)}$$

$$\frac{\eta P_t}{A}\left(1-\frac{M_2 y_b}{\eta\,P_t r^2}+\frac{e y_b}{r^2}\right)\geqslant 0 \qquad \text{.. (5.7.2)}$$

Eqs. 5.7.1 and 5.7.2 reduces to

$$e\leqslant\left(\frac{M_1}{P_t}+k_b\right) \qquad \text{.. (5.7.3)}$$

$$e\geqslant\left(\frac{M_2}{\eta\,P_t}-k_t\right) \qquad \text{.. (5.7.4)}$$

Eqs. 5.7.3 and 5.7.4. could be shown diagramatically as in fig. 5.7.1.

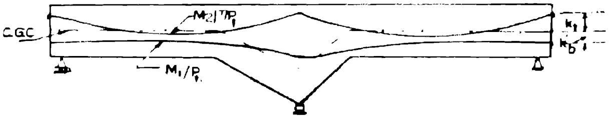

(a) Beam with limiting eccentricity zone

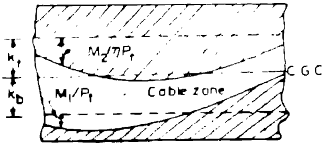

(b) A small portion of the beam

Fig. 5.7.1: Cable zone

Having determined the cable zone as shown in fig. 5.7.1, the eccentricities may be adjusted as discussed in the previous section so that there are no secondary moments.

This procedure calls for (i) selection of section, (ii) assumption of η and (iii) value of P_t calculated from the variation between the maximum and minimum bending moment and the kern distance available to accommodate it.

Let the maximum variation between M_1 and $M_2 = (M_2 - M_1)_{max}$

then, $$P_t = \frac{(M_2 - M_1)_{max}}{k_b + k_t} \quad \text{.. (5.7.5)}$$

Typical cable profiles for statically indeterminate structures are shown in figs. 5.7.2 to 5.7.4. For more detailed continuity connections, the reader is referred to references (5.3) and (5.4).

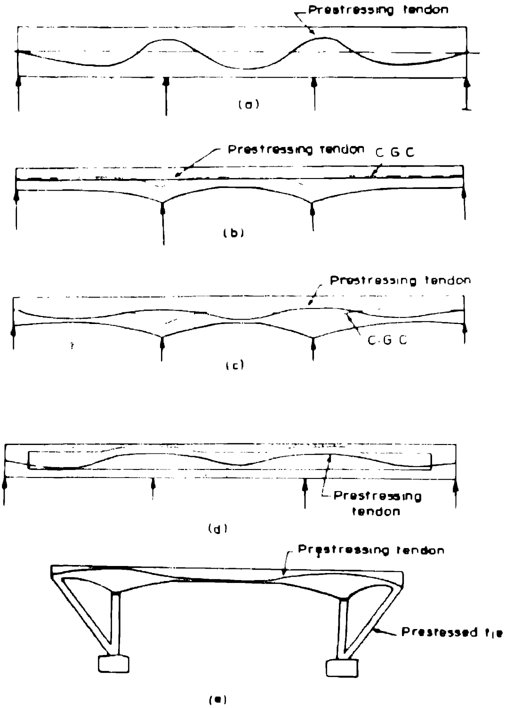

Fig. 5.7.2 : Typical profiles in continuous beams

5.8. LOAD BALANCING METHOD: Analysis and design of continuous beams is very much simplified by load balancing method. If the external load on each span is balanced by the prestressing force of the span, then the stress at any point in the beam is P/A. However, the external load is not constant in most of the problems, so the complete balancing of external load for all conditions of loading is not possible. A partial balancing has to be done deriving the maximum benefit out of this method. The procedure is best illustrated by the following example.

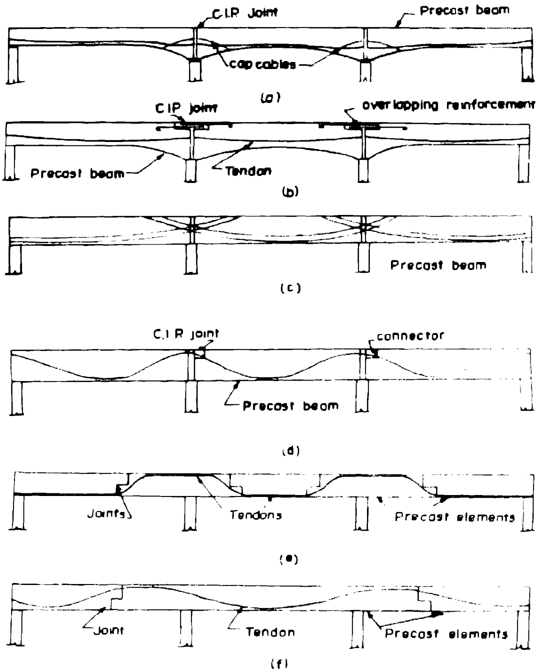

Fig. 5.7.3 : Continuous beams of precast elements

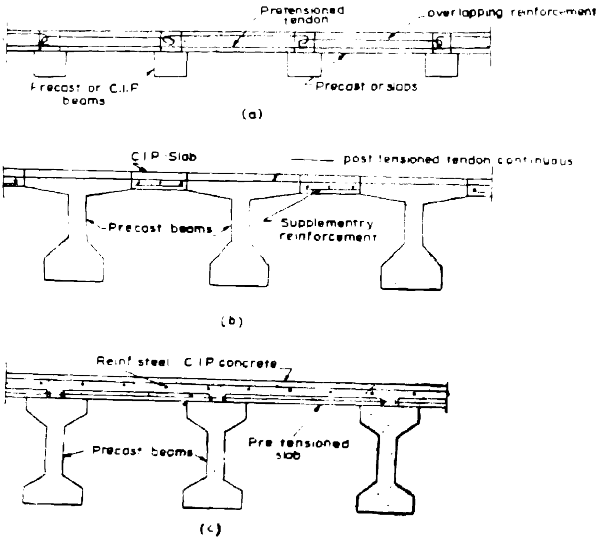

Fig. 5.7.4 : Various types of continuous prestressed slabs

Design example 5.8.1: Design of a post-tensioned two span continuous beam of 30 m each span and subjected to an external load of 2000 kg/m over the entire beam for loads not likely to increase.

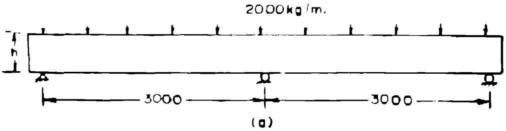

Fig. 5.8.1 : Example 5.8.1

Given data: $f'_c = 450$ kg/sq cm, $f'_s = 15000$ kg/sq cm

Design procedure :

(a) Select $h = L/25 = 1.20$ m
Let the self weight = 1000 kg/m

(b) Load conditions are self weight of 1000 kg/m at transfer and total weight of 3000 kg/m at working.
Select a balancing load of 1800 kg/m at working condition.

∴ unbalance load at working = 1200 kg/m

(c) Cable profile: Maximum sag in a cable gives maximum efficiency with minimum steel requirements. Let 20 cm cover be assumed both at top and bottom flanges of the beam which would provide a maximum sag of about 50 cm. The actual maximum sag will be slightly greater than 50 cm and will be about 14 m from support. An approximation of maximum sag of 50 cm at mid-span is assumed.

Load balancing equation is given by

$$w_{bo} = \frac{8\,P_e\,g}{L^2}$$

$$\therefore \quad P_e = \frac{1800 \times 900}{8 \times 0.50} = 405000 \text{ kg}$$

Let $f_{ave} = 100$ kg/cm^2

Then $A = \dfrac{P_e}{f_{ave}}$

$= 4050$ sq cm

Let the area, $A = 4000$ sq cm

and $P_e = 400000$ kg

Self weight $w_g = 2400 \times 0.4 = 960$ kg/m (Vs 1000 kg/m assumed)

$$f_{ave} = \frac{P_e}{A} = \frac{400,000}{4000} = 100 \text{ kg/sq cm}$$

(d) Transfer condition:

Let $\eta = 0.82$

$$\therefore \quad P_t = \frac{P_e}{0.82} = 487,700 \text{ kg}$$

Load balanced at transfer $= 1800/0.82 = 2200$ kg/m.

Load that is not balanced $= (-2200 + 960) = -1240$ kg/m.

The load that is not balanced is the effective load on the beam. Hence the bending moments for the continuous beam should be computed based on this effective load.

At transfer, maximum +ve bending moment 'M_{bt}' occurs at support, and it is

$$M_{bt} = -(w_g - w_b)\left(\frac{L^2}{8}\right) = 139500 \text{ kgm}$$

Maximum −ve bending moment M_d occurs near point D, and it is

$$M_d = (w_g - w_b)\, L^2/16 = -69750 \text{ kgm}$$

Stresses at support (transfer condition):

$$\frac{P_t}{A} = \frac{487700}{4000} = 121.9 \text{ kg/sq cm}$$

$$f_{ct} = \frac{P_t}{A} + \frac{M_{bt}\, y_b}{I} = \frac{P_t}{A} + \frac{M_{bt}}{Ah}\left(\frac{\Delta}{1+\Delta}\right)\frac{1}{\rho}$$

Let $\rho = 0.165$, $\Delta = 1.0$

Then

$$f_{ct} = 121.9 + \frac{13950000}{4000 \times 120} \times (1/0.33) = 121.9 + 87.8$$

$$= 209.7 \text{ kg/sq cm}$$

$$c_{ct} = \left(\frac{209.7}{450}\right) = 0.465 \text{ (permissible)}$$

$$f_{tt} = -121.9 + 87.8 = -34.1 \text{ (permissible)}$$

Stresses at mid section (at transfer):

$$f_{tt} = -121.9 + \frac{87.8}{2} = -88.0 \text{ kg/sq cm (permissible)}$$

$$f_{ct} = 121.9 + \frac{87.8}{2} = 165.8 \text{ kg/sq cm (permissible)}$$

(e) Working load condition: The load that is not balanced at working load is 1200 kg/m. The stresses due to bending can be computed in proportion to the unbalanced loads. The load that is not balanced at working load is (1200/1480) times at transfer.

Stresses at support:

$$f_{ave}=\frac{P_e}{A}=\frac{400{,}000}{4000}=100 \text{ kg/sq cm}$$

$$f_{te}=-100+\left(\frac{12}{14.8}\right)\times 87.8$$

$$=-100+71=-29 \text{ kg/sq cm (permissible)}$$

$$f_{ce}=100+71=171 \text{ kg/sq cm}$$

$$c_{ce}=171/450=0.38 \text{ (marginal over stress)}$$

Stresses at mid section (D):

$$f_{te}=-100+\frac{71}{2}=-64.5 \text{ kg/sq cm (permissible)}$$

$$f_{ce}=100+35.5=135.5 \text{ kg/sq cm (permissible)}$$

(f) Selection of section:

The given quantities are

$\Delta=1$, $\rho=0.165$, $A=4000$ sq cm, $h=120$ cm,

$P_t=487700$ kg, $w_l=2000$ kg/m, $f'_s=15000$ kg/sq cm

The sectional properties for

$\Delta=1.0$, $\rho=0.1668$, the coefficients are

$c_f=1$, $c_w=0.08$, $c_t=0.08$, $c_b=0.08$

$c_a=0.2272$, $c_I=0.0379$

$c_a b_t h=A=4000$ sq cm

$$\therefore \quad b_t=\frac{4000}{0.2272\times 120}=142 \text{ cm}$$

$b_w=0.08\times 142=11.36$ cm

$e_b=40$ cm

$e_a=30$ cm

$g=50$ cm

$$A_s=\frac{P_t}{0.7f'_s}=\frac{487700}{10500}=46.4 \text{ sq cm}$$

$t_t=0.08\times 120=9.6\simeq 10$ cm

$t_b=0.08\times 120\simeq 10$ cm

Note:—It is to be noted that since the stresses at support govern the section, it may be desirable to increase the height of the beam at support to 125 cm and then check for stress.

Problems

5.1 Determine the secondary moments developed in the *prestressed* concrete beam shown in fig. 5.1. of square section.

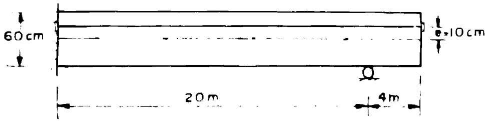

Fig. 5.1

5.2 A three span continuous beam of equal spans is subjected to a uniformly distributed load. Determine a cable profile which will not cause any secondary moments.

5.3 A two span continuous beam of 20 m each span, fixed at one end and simply supported at the other end is subjected to a uniformly distributed load of 1600 kg/m. Design the beam as a pre-tensioned concrete structure with 450 kg/sq cm concrete.

CHAPTER VI

MISCELLANEOUS STRUCTURAL MEMBERS

6.1. INTRODUCTION : Several structural elements or simple members such as columns, piles, tie rods for arches, tension elements, retaining walls, portal and building frame members are being designed and constructed in prestressed concrete. Recent trends in prefabricated construction have opened several areas of structural elements being made by prestressed concrete (6.1 to 6.6). This chapter discusses simple structures and structural members of prestressed concrete construction. Members are classified into two major groups : (i) members essentially subjected to compressive forces, and (ii) members subjected to tensile forces.

6.2. COMPRESSION MEMBERS : The prestressing concept was originally developed to take care of the low tensile capacity of concrete. So prestressing a concrete compression member appears to be redundant and superfluous. However, most of the compressive members like columns and piles are subjected to handling and combined axial and bending force. The prefabricated columns are subjected to bending stresses during transportation and erection. For these reasons, it has been found necessary to use reinforcement to take care of secondary stresses. Prestressing a compressive member subjected to handling or bending moments results in using less steel with higher efficiency.

(1) Prestressed concrete columns subjected to combined bending and axial force : Consider a column subjected to axial and bending moment as shown in fig. 6.2.1. There are two conditions of loading : (i) transfer condition and (ii) working load condition.

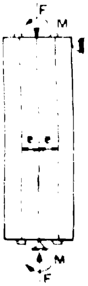

Fig. 6.2.1 : Column under external forces

Let F = axial force

M = bending moment (assumed to be small)

Assuming the same notations as discussed in the previous chapters, the stresses at the two load conditions may be written as follows :

(i) *At transfer condition (assuming axial prestress force)* :

$$f_{ct} = P_t/A_c,\ P_t = f_{st}A_s \qquad \text{.. (6.2.1)}$$

where A_c = area of the column

(ii) *At working load condition :* The member is subjected to compressive force. In addition to the losses of prestress with time, there will be a further loss of prestress due to elastic shortening caused by the external loads (in case of beams, there is a gain in prestress due to external loads). Considering the failure condition, the compressive strain in the column at the time of failure will be in the order of 0.003. If the effective prestress strain in steel is about 0.004, then the effective prestress strain at ultimate load is about 0.001. This illustrates that most of the prestressing force is released when the ultimate load on the column is reached, thus the ultimate strength of the column is not much affected by the precompression.

Let the compressive force dominate at working load conditions ; then the approximate strain in steel is given by

$$\epsilon_s = \epsilon_{se} - \frac{F}{A_cE_c}$$

$$\begin{aligned} P &= (\epsilon_sE_s)\,A_s \\ &= A_s\,E_s\left(\epsilon_{se} - \frac{F}{A_cE_c}\right) \\ &= P_e - \left(\frac{A_sE_s}{A_cE_c}\right)F \\ &= P_e - pnF = \eta P_t - pnF \end{aligned} \qquad \text{.. (6.2.2)}$$

where $p = A_s/A_c$ (reinforcement ratio)

$n = E_s/E_c$ (modular ratio)

Compressive stress is given by

$$\begin{aligned} f_{ce} &= \frac{P}{A_c} + \frac{F}{A_c} + \frac{My}{I} \\ &= \frac{P}{A_c} + \frac{F}{A_c} + \frac{MD}{2I} \end{aligned} \qquad \text{.. (6.2.3)}$$

Where D = total depth of the section

On substituting the value of P in eq. 6.2.3

$$\begin{aligned} f_{ce} &= \eta\frac{P_t}{A_c} - \frac{pnF}{A_c} + \frac{F}{A_c} + \frac{MD}{2I} \\ &= p\,\eta\,f_{st} - \frac{pnF}{A_c} + \frac{F}{A_c} + \frac{MD}{2I} \end{aligned}$$

$$=p\eta f_{st}+\frac{F}{A_c}(1-pn)+\frac{MD}{2I} \qquad .. \quad (6.2.4)$$

Eqs. 6.2.1 and 6.2.3 are the governing equations from which the column design is to be determined. Here the known quantities are F and M, while stresses (f_{st}, f_{ct}, f_{ce}) may be selected either from code or economical considerations. Value of η is to be assumed which, if necessary, could be checked after completion of the design. So only three quantities (A_s, A_c, shape and size of the section) are to be determined.

From eq. 6.2.1, the percentage of steel is given by

$$p=(f_{ct}/f_{st}) \qquad .. \quad (6.2.5)$$

Eq. 6.2.4 may be modified for rectangular section as

$$f_{ce}=p\,\eta\,f_{st}+\frac{F}{A_c}(1-pn)+\frac{6M}{A_cD}$$

$$=p\,\eta\,f_{st}+\frac{F}{A_c}\left(1-pn+\frac{6M}{FD}\right) \qquad .. \quad (6.2.6)$$

Assuming the value of depth D is given by other considerations, the area of the section is given by

$$A_c=\frac{F\left(1-pn+\frac{6M}{FD}\right)}{(f_{ce}-p\eta\,f_{st})} \qquad .. \quad (6.2.7)$$

All the quantities on the right hand side of the above equation are known, so the area of the concrete section could be obtained.

Allowable stress in steel at transfer is usually taken as 0.7 f'_s. Precompression is mainly for the secondary stresses so it may be taken in the range of 0.05 f'_c to 0.2 f'_c. Allowable compressive force under working load may be taken in the range of 0.40 to 0.50 f'_c depending upon the utility of the member.

Example 6.2.1 : Design of a prestressed concrete column of 5 metres high for a combined, axial force of 50,000 kg and bending moment of 100,000 kg cm.

(a) Selection of stresses :

Let $f'_c=450$ kg/sq cm
$f'_s=15000$ kg/sq cm
$f_{st}=0.7\,f's=10500$ kg/sq cm
$f_{ct}=21$ kg/sq cm
$f_{ce}=0.4\,f'_c=180$ kg/sq cm

(b) Selection of section : Let a rectangular section of depth 25 cm be assumed, i.e., D = 25 cm

(c) Calculation of areas :

$$p=\frac{f_{ct}}{f_{st}}=\frac{21}{10500}=\frac{1}{500}=0.002$$

$$n = \frac{E_s}{E_c} = \frac{2.1 \times 10^6}{3.82 \times 10^6} = 5.5$$

Let $\eta = 0.8$, then from eq. 6.2.7

$$A_c = \frac{50000\left(1 - \frac{5.5}{500} + \frac{6 \times 100000}{50000 \times 25}\right)}{\left(180 - \frac{0.8 \times 10500}{500}\right)}$$

$$= 50000\left(\frac{1.469}{163.2}\right) = 449 \text{ sq cm}$$

Let breadth of the section be = B, then $B = A_c/D$

$$\therefore \quad B = \frac{449}{25} = 18 \text{ cm}$$

$A_s = 0.002 \times 449 = 0.89$ sq cm and

$P_t = A_s f_{st} = 9450$ kg

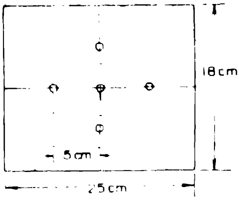

(Five wires of 5 mm dia)

Fig. 5.2.2 : Section of the column

Example 6.2.2 : Design a column subjected to an eccentric load of 50000 kg acting at 2 cm eccentric with the column axis and determine the factor of safety.

Solution : The eccentric loading could be separated into axial force and bending moment as

F = 50,000 kg, and M = 100,000 kg cm

Adopt the same section as designed in the example 6.2.1.

Let $f'_c = 450$ kg/sq cm, $\epsilon_u = 0.003$

Determination of ultimate load capacity : As the stress-strain curve upto the crushing of concrete is not linear, eq. 6.2.7 cannot be used directly. Eq. 6.2.3 is general and the same can be used here.

$$\epsilon_{se} = 0.8 \times \frac{10500}{21 \times 10^5} = 0.004$$

$$\epsilon_{ce} = \frac{P_e}{A_c E_c} = \frac{0.80 \times 9450}{477 \times 3.82 \times 10^5} = 0.000042$$

$$P = A_s f_s = A_s E_s \epsilon_s = A_s E_s (\epsilon_{se} - \epsilon_u + \epsilon_{ce})$$

$$= 0.89 \times 2.1 \times 10^6 \times (0.004 - 0.003 + 0.000042)$$

$$= \mathbf{1790 \text{ kg}}$$

Now

$$0.64\, f'_c = \left(\frac{P}{A_c} + \frac{F_u}{A_c} + \frac{2\, F_u 6}{A_c\, D} \right)$$

or

$$\frac{F_u}{A_c}\left(1 + \frac{12}{D} \right) = 0.64\, f'_c - \frac{P}{A_c}$$

Where $0.64\, f'_c$ is the ultimate compressive stress of concrete prism.

$$\frac{F_u}{A_c}\left(1 + \frac{12}{D} \right) = 288 - \frac{1790}{449}$$

$$\therefore \quad F_u = \frac{449 \times 25}{37}(288-4) = 86000 \text{ kg}$$

$$\text{Factor of safety} = \frac{F_u}{F} = \frac{86000}{50000} = 1.72$$

(*Note :*—It could be observed from this example that effective compression due to prestressing force at the ultimate load is 4 kg/sq cm)

Ultimate load for a column without prestress :

$$F_{ult} = \left(\frac{288}{288-4} \right) 86000 = 87200$$

$$\frac{F_{ult}}{F} = \frac{87200}{50000} = 1.744$$

The factor of safety of a non-precompressed column is 1.744 against 1.72 of a precompressed column. It shows that the factor of safety is not much affected by precompressing the column. This is more or less true in most cases. Therefore it is desirable to use prestressed columns when it is expected that the column will be subjected to bending moments either during working or handling conditions.

(2) Typical column subjected to different conditions : Axial prestressing force is applied in case of a column subjected to small bending moments. A more effective prestressing could be obtained by providing some eccentricity to the prestressing cable if the bending moment is constant. Similarly in case of columns subjected to handling, if the exact handling is specified, it is possible to select a cable profile which would be more effective. In most cases of handling and transportation, the members are subjected to random handling so it is always desirable to introduce axial prestressing instead of eccentric prestressing. Typical possible cable profiles of column are shown in fig. 6.2.3.

Columns subjected to large eccentric loads have to be designed as beam columns. The deformation of the axis of the column may be included while computing the bending moment.

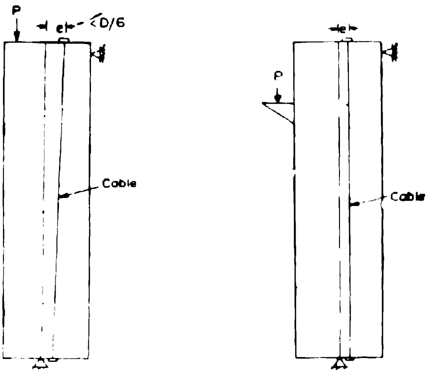

(a) Column under eccentric load

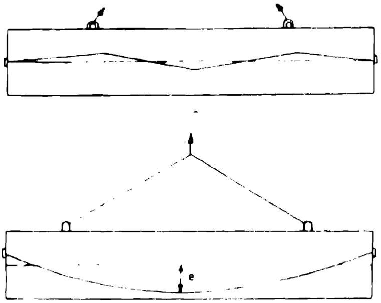

(b) Column handled with two pickup points

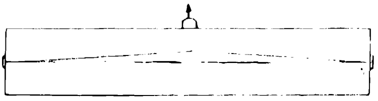

(c) Column handled with one pickup point

Fig. 6.2.3 : Typical cable profiles of precast columns

(3) **Prestressed concrete piles :** Piles are usually cast and cured in the factory and then transported to the site. Such piles are subjected to four load conditions: (i) transfer of prestress, (ii) transportation, (iii) driving, and (iv) service. Out of these four conditions, the transfer condition is not a dominant condition. The piles are likely to be subjected to tensile stresses during transportation and driving conditions. It is hard to obtain a true vertical position of the pile during driving. Any small tilting of the pile during the driving operation will result in undesirable stresses. So the allowable stresses during service conditions are taken low. Special precautions have to be taken at the top of the pile where pile cap and driving force come into contact. Foundation piles cannot be cast in long lengths because of transporta-

tion problems ; in such cases suitable joints have to be designed. Sheet piles are also made of prestressed concrete construction which are precompressed axially. If post-tensioning is done, the ducts must be grouted before driving (6.7, 6.8).

(4) **Prestressed concrete poles and towers:** Prestressed concrete poles are gaining their use as transmission poles and towers. The transmission poles are generally cast at factory and supplied to the site. The design of poles is simple but the main problem is their transportation. Since the length of poles that could be transported is very much restricted, the long poles are cast in small lengths and assembled at site. The connections have to be designed using simple slices, extension pieces or additional reinforcements. Long prestressed concrete poles are used for radio and other communication towers (6.9).

(5) **Prestressed concrete piers and abutments:** Piers and abutments are prestressed for two reasons. Prestressing is used as a means of anchoring the pier to bed rock, and in some cases, if the bending moment due to water or soil pressure is large, the piers are prestressed against any possible tension. During the worst cases of bending moments, if the piers are subjected to vibrations due to moving loads, the piers are likely to crack. The prestressing force not only stops cracking but also reduces deformations. In most cases of prestressed piers, the prestressing is relatively nominal.

6.3. TENSION MEMBERS: If a member is subjected to tensile forces only, it appears superfluous to use any concrete construction because the tensile resistance of concrete is negligible. Even though the steel takes all the tension force, a prestressed concrete construction for tension member has distinct advantage of small deformations. Except for a small variety of tension members, most members requires rigidity. For example, tie rods of arches and ring beams of water tanks require rigidity in addition to strength.

(1) **Tie members:** Analysis and design of direct tension member is very simple and the governing equations for design can be written by considering the transfer and service load conditions.

Let F = direct tension force to be carried by the member

Then

$$f_{ct}=\frac{P_t}{A_c}=\frac{A_s\, f_{st}}{A_c}=p\, f_{st} \qquad \text{.. (6.3.1)}$$

$$f_{ce}=\frac{P}{A_c}-\frac{F}{A_c}=\frac{(P-F)}{A_c} \qquad \text{.. (6.3.2)}$$

Where

$$P=\eta\, P_t+\left(\frac{F\, E_s}{A_c\, E_c}\right)$$

$$=\left(\eta\ f_{st}+\frac{nF}{A_c}\right)A_s$$

$$=(P_e+pnF) \qquad \ldots \quad (6.3.3)$$

and $$f_s=\left(\eta\ f_{st}+\frac{Fn}{A_c}\right) \qquad \ldots \quad (6.3.4)$$

Eqs. 6.3.3 and 6.2.2 are similar, except for change in sign

$$f_{ce}=\frac{1}{A_c}(\eta\ P_t+p\ n\ F-F)$$

$$=\frac{1}{A_c}[\eta\ P_t-F\ (1-np)] \qquad \ldots \quad (6.3.5)$$

$$=\eta\ p\ f_{st}-\frac{F}{A_c}\ (1-np) \qquad \ldots \quad (6.3\ 6)$$

Allowable stresses: f_{ct} could be taken as high as 0.5 f'_c as the member will be relieved of the compression as soon as the external loads act. In service load conditions, allowable stress of concrete may be taken as practically equal to zero. To have a good serviceability, the member may be designed to have small compression even at working load condition. The value of f_{ce} may be taken in the range of 0.1 f'_c to 0. The stress in steel at working load condition should also be checked.

Example 6.3.1 : Design a tie member of 20 m length subjected to 40000 kg axial tension and determine the factor of safety.

Assume :

$f'_c=450$ kg/sq cm

$c_{ct}=0.48$, $c_{ce}=0.1$

$f_{ce}=0.1\times450=45$ kg/sq cm

$f'_s=15000$ kg/sq cm

$f_{st}=0.6\ f'_s=9000$ kg/sq cm

$\eta=0.85$

$n=5.5$

Selection of section :

$$f_{ct}=p\ f_{st}$$

$$\therefore\quad p=\frac{f_{ct}}{f_{st}}=\frac{0.48\times450}{0.6\times15000}=0.024$$

From eq. 6.3.6

$$f_{ce}=\eta\ p\ f_{st}-\frac{F}{A_c}(1-np)$$

or $$A_c=\frac{F\ (1-np)}{\eta\ p\ f_{st}-f_{ce}}$$

then

$$A_c=\frac{40000\,(1-5.5\times 0.024)}{0.85\times 0.024\times 9000-45}=251 \text{ sq cm}$$

Using 16×16 cm tie rod section, $A_c=256$ sq cm

$$A_s=256\times 0.024=6.14 \text{ sq cm}$$

$$P_t=6.14\times 9000=55260 \text{ kg}$$

Calculation of factor of safety : cracking load—Let ultimate tensile stress of concrete = 40 kg/sq cm and ultimate tensile strain = 0.00015.

At cracking load

$$\epsilon_s=\epsilon_{se}+\epsilon_{ce}+\epsilon_t$$

$$=\left(\frac{0.85\times 9000}{2.1\times 10^6}+\frac{\eta\, P_t}{A_c\, E_c}+0.00015\right)$$

$$=(0.00364+0.00057+0.00015)=0.00436$$

$$f_s=0.00436\times 2.1\times 10^6=9156 \text{ kg/sq cm}$$

If F_c = load at cracking, then equilibrium condition at craking gives

$$-40=\frac{1}{256}\,(9156\times 6.14-F_c)$$

or $$F_c=10240+56218=66458 \text{ kg}$$

$$\text{Factor of safety at cracking}=\frac{F_c}{F}=\frac{66458}{40000}=1.66$$

Total elongation at cracking load = $(0.00057+0.00015)\times 2000$
= 1.44 cm

If only high tensile steel is used instead of prestressed concrete tie, the elongation at the cracking load is

$$\frac{F_c L}{A_s E_s}=\frac{66458\times 2000}{6.14\times 2.1\times 10^6}=10.3 \text{ cm}$$

Deformation of steel tie-bar at a load of 66458 kg is as high as 10.3 cm and will affect the arch, whereas the deformation of a prestressed concrete tie-bar is 1.44 cm for the same load.

The effect of concrete is lost as soon as the cracking takes place and then all the load is to be taken by steel.

$$\therefore\quad F_{ult}=f'_s A_s=15000\times 6.14=92100 \text{ kg}$$

$$\text{Factor of safety}=\frac{92100}{40000}=2.303$$

The factor of safety is not affected by providing the concrete.

(2) Prestressed concrete ring beams and circular tanks : Ring beams are used in domes, water tanks and in similar constructions. These ring beams are subjected to tensile forces caused by radial pressure. Similarly, circular tanks are also subjected to radial pressures which cause hoop tensions in the tank walls. If P is the prestressing force, then the radial component is given by

$$P \frac{d^2y}{dx^2} = \frac{P}{R}, \text{ where R is the radius.}$$

Most of the load is taken by the steel and the concrete acts like a a stiffener with impervious medium. The relation between the hoop force and the radial pressure could be obtained from simple statics as shown in fig. 6.3.1. There are two conditions of loading and the governing equation can be written directly for the two conditions.

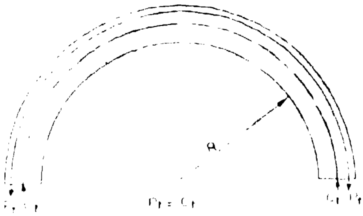

(a) Transfer condition : Prestress could be replaced by equivalent radial component P_t/R.

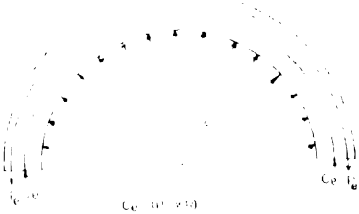

(b) Service load condition where w = intensity of radial pressure

Fig. 6.3.1 : Free body diagrams at two load conditions

The govering equations are :

At transfer condition :

$$f_{ct} = \frac{P_t}{A_c} = \frac{A_s f_{st}}{A_c} = p f_{st} \qquad .. \quad (6.3.7)$$

$$\therefore \quad p = \left(\frac{f_{ct}}{f_{st}}\right) \qquad .. \quad (6.3.8)$$

At service condition :

$$f_{ce} = \frac{C_e}{A_c} = \frac{P - wR}{A_c} \qquad .. \quad (6.3.9)$$

Now

$$\epsilon_s = \epsilon_{se} + \frac{wR}{A_c E_c}$$

$$= P_e + pnwR \qquad .. \quad (6.3.10)$$

$$f_{ce} = \frac{(\eta P_t + pnwR) - wR}{A_c}$$

$$= \frac{\eta P_t - wR\,(1-pn)}{A_c}$$

or $$A_c = \frac{\eta P_t - wR\,(1-pn)}{f_{ce}} \quad \ldots \quad (6.3.11)$$

The above expressions are exactly similar to the expressions derived in the previous section. Eq. 6.3.11 can also be written as

$$A_c = \frac{wR\,(1-pn)}{\eta\, p\, f_{st} - f_{ce}} \quad \ldots \quad (6.3.12)$$

Allowable stresses : f_{st} is taken in the range of $0.6\,f'_s$ to $0.7f'_s$. The value of f_{ct} could be taken from $0.4\,f'_c$ to $0.5\,f'_c$. In case of circular tanks, no cracking should be allowed. Hence the stress at working load condition should be in the range of $0.10f'_c$. The value of η will also be low because of losses due to shrinkage and creep will be high since structure will be under wet and dry conditions.

Example 6.3.2: Design of a free edge water tank of 20 metre radius to store 5 metre head of water.

Assume:

$f'_c = 450$ kg/sq cm, $f'_s = 15000$ kg/sq cm

$f_{st} = 0.7\,f'_s = 10500$ kg/sq cm

$f_{ct} = 0.5\,f'_c$, $f_{ce} = 0.1\,f'_c$

$\eta = 0.8$, $n = 5.5$

Solution :

$$p = \frac{f_{ct}}{f_{st}} = \frac{0.5 \times 450}{0.7 \times 15000} = 0.021$$

$$A_c = \frac{wR\,(1-pn)}{\eta\, p\, f_{st} - f_{ce}}$$

$$w = \gamma\, h = (0.001 \times 500) \text{ kg/sq cm}$$

$$A_c = \frac{(0.001 \times 500) \times 2000\,(1-0.116)}{0.8 \times 0.021 \times 10500 - 90} = 10.2 \text{ sq cm}$$

Considering 1 cm height, the thickness is

$t_c = A_c/1 = 10.2$ cm

$A_s = 0.021 \times 10.2 = 0.2142$ sq cm

The pressure of the water reduces to zero at the top of the tank. Keeping the thickness of the wall almost constant, the percentage of steel could be reduced practically to zero at the top of the wall. A nominal steel of 0.1 % is kept at the top. Use 5 mm wires at 9 mm centre to centre at the bottom and 40 mm centre to centre at the top of the wall.

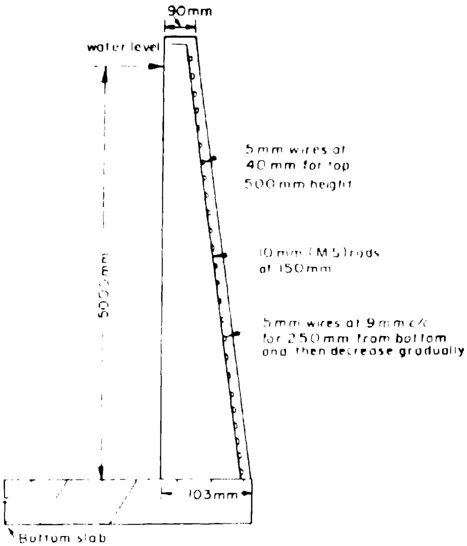
90mm
water level
5 mm wires at 40 mm for top 500 mm height
10 mm (M.S.) rods at 150 mm
5 mm wires at 9 mm c/c for 250 mm from bottom and then decrease gradually
5000 mm
103mm
Bottom slab

Fig. 6.3.2 : Section of vertical wall of the water tank

$$P_t = 0.218 \times 10500 = 2289 \text{ kg}$$

Cracking load and factor of safety at cracking: Let tension crack occur at 0.00015 strain and 40 kg/sq cm stress of concrete.

At cracking load

$$\epsilon_s = \epsilon_{se} + \epsilon_{ce} + \epsilon_t$$

$$= \frac{0.8 \times 10500}{2.1 \times 10^6} + \frac{2289}{10.2 \times 3.82 \times 10^5} + 0.00015$$

$$= 0.004 + 0.00059 + 0.00015 = 0.00474$$

$$P = E_s \epsilon_s A_s = 0.00474 \times 0.218 \times 2.1 \times 10^6$$

$$= 2170 \text{ kg}$$

Now $f_{ce} = (P - w_c R)/A_c$

or $-40 = \dfrac{(2170 - 2000 w_e)}{10.2}$

or $w_e = 1.289$ kg/sq cm

Factor of safety at cracking $= \dfrac{1.289}{0.5} = 2.58$

Factor of safety at zero stress in concrete:

$$= \frac{2170}{2000 \times 0.5} = 2.17$$

This example gives only an approximate design.

(3) Circular tanks with fixed base: Previous section deals with circular tanks having bottoms which can translate freely. This type of boundary condition does not exist in reality. Most of the tanks have fixed or hinged bases. The effect of clamping at the base gives practically zero hoop stress and maximum negative bending moment at the base. A typical bending moment and hoop forces in circular tanks are shown in fig. 6.3.3. Vertical prestressing force should be provided to compensate the bending moment. Bending moments and hoop stresses should be worked out for any particular tank and the necessary prestressing force be applied. An elastic analysis of these cylindrical tanks can be used for the design purposes and is discussed in chapter XI.

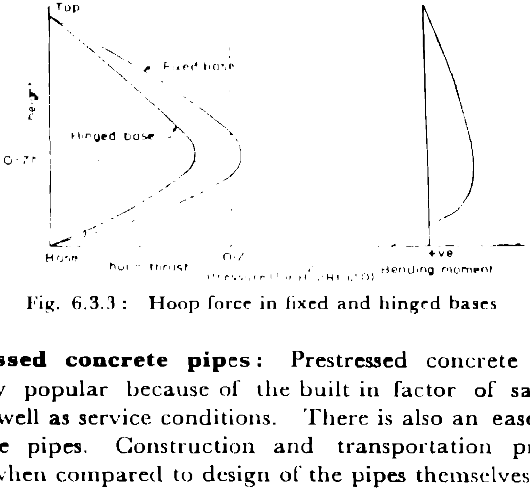

Fig. 6.3.3 : Hoop force in fixed and hinged bases

(4) Prestressed concrete pipes: Prestressed concrete pipes have become very popular because of the built in factor of safety during handling as well as service conditions. There is also an ease in manufacturing the pipes. Construction and transportation problems are major ones when compared to design of the pipes themselves (6.10).

6.4. PRESTRESSED CONCRETE PAVEMENTS: (1) Roads and Runways:

Roads and runways have thin slabs which are generally treated as plates on elastic foundation. The working load stresses are not very high in most cases. The thickness of the slab is very small as compared to the length. Secondary effects due to temperature and shrinkage are considerable. The prestressing cables are generally put at the bottom of the slab with sufficient cover and the prestressing is done in the longitudinal direction with ordinary or prestressing steel in the transverse directions. Special precautions have to be taken at the ends of the slab against warping. The expansion and contraction of the pavements is very much reduced by prestressing force.

Prestressed concrete construction is also used for revetments of canals. Precast units to suit the profile of canal are manufactured in factory, transported and then placed in position. Cast in site concrete is more expensive because of the form-work involved along the canal whereas small precast units could very well be used with sufficient care at the joints. Construction and expansion joints call for attention in this problem (6.11 to 6.15).

(2) **Prestressed concrete sleepers:** Prestressed concrete sleepers are made in mass scale and are used on the rail roads. As the train loads are fixed, the design is done once for a particular track. The great advantage of prestressed sleepers is their high resilience with small deformation.

Problems

6.1 A bridge pier is to carry an axial load of 400,000 kg with a horizontal pressure of 1000 kg/m for a height of 4 m from the base of the pier. The height of the pier is 8 m above foundation. Design a prestressed concrete pier with 400 kg/sq cm concrete.

6.2 A cylindrical barrel pipe line of 2 m diameter is to carry water at a pressure of 30 kg/sq cm. Design a prestressed concrete pipe with a factor of safety of 3. At working load condition, the pipe should be at 20 kg/sq cm hoop compressive stress. Use M450 concrete.

6.3 Design a tie-bar member of a tied arch, in which the tie is subjected to an axial force of 100,000 kg. Adopt 450 kg/sq cm concrete without cracking at working load and 200 kg/sq cm compressive stress at transfer condition. Also determine the factor of safety for this member.

CHAPTER VII

DEFLECTION OF PRESTRESSED CONCRETE BEAMS

7.1. INTRODUCTION: Complete load deformation characteristic upto failure of a prestressed concrete beam is desirable in some situations but not very essential for most practical problems. It is desirable to check the deflections of a structure at least upto working load conditions. In case of prestressed concrete beams, it is possible to calculate the deflections with good accuracy upto working load since the concrete does not crack in working load conditions. The basic assumptions used in elastic beam theory will hold good for prestressed concrete beams. Concrete could be considered as a homogeneous and isotopic material even though there is bound to be some amount of non-homogeneity in the material. That plane sections normal to the axis of the beam remains plane even after bending is a sound assumption applicable to prestressed concrete beams. The stress-strain relation is assumed to be linear in the simple beam theory whereas the stress-strain relation in concrete is not absolutely linear. The effect of approximation of linearization of the stress-strain in concrete could be large if the stress level under investigation is high. For low stress, the linearization does not matter very much. The modulus of elasticity of concrete has to be estimated accurately to get good results on deformations. The relation between the Young's modulus and the cube strength has been investigated and a reasonable basis is set up between these two properties.

7.2. DEFLECTIONS BASED ON LOAD BALANCING METHOD: Replacement of prestress force into a statically equivalent system of forces was discussed in chapter I. The transverse and horizontal components of prestress force can be considered independently as external loads and coupled with self weight and super imposed loads. The method of calculation of stresses in prestressed concrete beam based on load balancing technique was discussed in chapter I. The deflection theory can be developed exactly in the same way as the bending theory. This method does not call for further development of separate set of expressions associated with prestressed concrete beams; the deflection equation of elastic beam columns could be used in the deflection theory of prestressed concrete beam. Theory and procedure of deflection predictions are illustrated through examples.

Example 7.2.1 : Determine maximum deflection at transfer and at working load conditions of a prestressed concrete beam as shown in fig. 7.2.1 subjected to a load of 5000 kg/m.

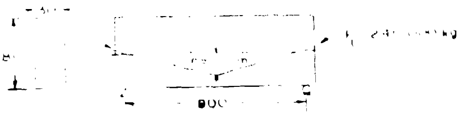

Fig. 7.2.1 : Example 7.2.1

Solution : Prestressed concrete beam at transfer and working conditions may be represented as a statically equivalent system like that shown in fig. 7.2.2. The two conditions may be treated as beam column problems ; maximum deflection could be predicted using beam column formula. An approximate maximum deflection equation for beam column may be given as

$$y_{\max} = y_0 \left(\frac{1}{1-\alpha} \right) \qquad \ldots (7.2.1)$$

Where

y_0 = maximum deflection of a simple beam with same transverse loading

$y_{\max}$ = maximum deflection for a beam column

α = P/P_E,

Where P = axial load and P_E = Euler's buckling load

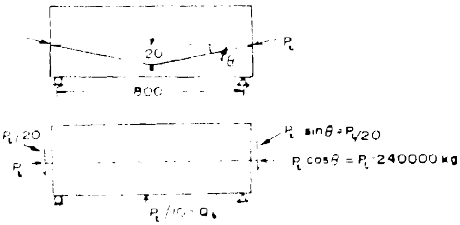

Equivalent beam column at transfer condition

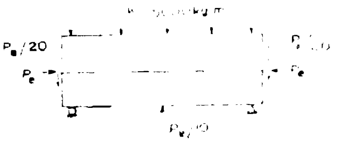

Fig. 7.2.2 : Equivalent beam column at working load

Deflection at transfer condition:

Let $E_c = 4 \times 10^5$ kg/sq cm

$$y_{max} = y_o\left(\frac{1}{1-\alpha}\right) = \left(\frac{W_{bt}L^3}{48\,EI}\right)\left(\frac{1}{1-\alpha}\right)$$

where

W_{bt} = transverse force at mid span

$$\frac{W_{bt}L^3}{48\,E\,I} = -0.5$$

$$\alpha = \frac{P_t}{P_E} = \frac{240{,}000}{\pi^2 EI/L^2} = 0.03$$

$$y_{max} = 0.5\left(\frac{1}{1-0.03}\right) = -0.515 \text{ cm (upward)}$$

Deflection at working load:

Let $\eta = 0.85$ then

$$\frac{P_e}{P_E} = 0.0255$$

$$y_{max} = \frac{5w_{be}L^4}{384\,EI}\left(\frac{1}{1-\alpha}\right) + \frac{W_{be}L^3}{48\,EI}\left(\frac{1}{1-\alpha}\right)$$

$$= 0.098 \text{ cm}$$

The deflection calculation at working load condition includes loss of prestress due to various reasons. It can be observed that the actual deflection at working load condition is very small as compared to the deflection of a reinforced concrete beam under the same conditions of loading.

Example 7.2.2: A prestressed concrete beam as shown in fig. 7.2.3 is provided with a parabolic cable profile. Determine the deflections at transfer and working load conditions with a working load of 5000 kg/m.

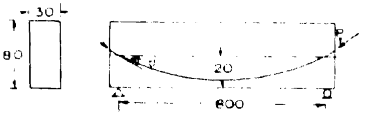

Fig. 7.2.3

$$y = \frac{4e}{L^2}(Lx - x^2)$$

$$\frac{dy}{dx} = \frac{4e}{L^2}(L - 2x)$$

$$\theta = \left.\frac{dy}{dx}\right]_{x=0} = \frac{4e}{L} = \frac{1}{10}$$

Solution: A statically equivalent prestressed beam is shown in fig. 7.2.4.

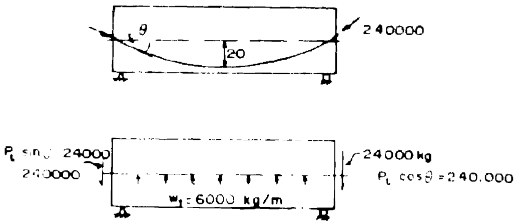

(a) Statically equivalent beam at transfer condition

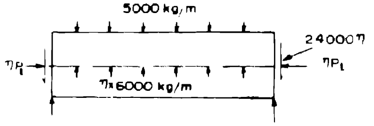

(b) Statically equivalent beam at working load
Fig. 7.2.4

Deflection at transfer condition:

Let $E_c = 4 \times 10^5$ kg/sq cm, then

$$\alpha = \frac{P_t}{P_E} = 0.03$$

$$y_{max} = \frac{5\, w_{bt}\, L^4}{384\, EI}\left(\frac{1}{1-\alpha}\right)$$

Where $w_{bt} = -6000$ kg/m (intensity of transverse load)

$\therefore\ y_{max} = -0.644$ cm

Deflection at working condition:

Let $\eta = 0.85$, then

$$\alpha = \frac{P_e}{P_E} = 0.0255$$

Effective transverse load at working condition is $w_{be} = (w_l - w_{bt}\,\eta)$ $(5000\text{-}6000\,\eta) = -100$ kg/m

$$y_{max} = \frac{5 w_{be}\, L^4}{384\, EI}\left(\frac{1}{1-\alpha}\right) = -0.0106$$

In this example, the balancing load is more than the working load so the deflection is always upwards. The upward deflection due to the prestressing force is sometimes called camber.

7.3. EFFECT OF CAMBER: In general, the deflection caused due to prestressing force is opposite to that caused by external loads. This type of deformation gives two distinct advantages: (i) Deformations at working load conditions are very much reduced; and (ii) stability and the resistance of the structure is improved. The negative curvature of a structure gives a structural form which withstands external loads more efficiently. In addition to the two distinct advantages already mentioned, the structure is likely to gain in architectural appearance. Long span bridge and shell structures of ordinary construction will have large deformations at working load. Hence the prestressing cable can also be used to give such deformations which will give better appearances. Structures with large overhangings will derive greater architectural and structural stability from proper prestressing. In light structures creep deflection could become a problem, so camber should also be restricted to about L/300.

Problems

7.1 A cantilever beam of span 4 m is subjected to a uniformly distributed load of 1000 kg/m. The beam is designed with 400 kg/sq cm concrete. If it is desirable to keep the beam in horizontal position at the working load, design the cross section, showing the prestressing force and profile.

7.2 Determine the deflections at transfer and working loads of the 50 m span beam discussed in chapter III.

CHAPTER VIII

FLEXURAL ULTIMATE STRENGTH AND ULTIMATE LOAD DESIGN OF PRESTRESSED CONCRETE BEAMS

8.1. INTRODUCTION: The study of ultimate strength of prestressed concrete construction is very important due to the nature of stress-strain characteristics of the materials used and permissible stresses in the construction. The stress in steel at transfer condition is comparatively large. Structural safety in working load condition is assured by not exceeding a permissible stress which is equal to certain fraction of the ultimate stress. The factor of safety applied to stresses will not assure the same factor of safety against ultimate loads since the stress and external load relations do not vary linearly. Propagation of cracks in concrete also plays an important role in connecting the sectional properties with the external load and thus affecting the factor of safety provided in the permissible stresses. It is therefore essential to predict the actual failure of the member in order to get a good factor of safety involved in the construction. For ultimate load design, the safety factors are called load factors and defined in eq. 8.1.1.

$$w_u = N_l w_l + N_g w_g \qquad \ldots \qquad (8.1.1)$$

where

w_u = ultimate load

w_l = live load (working condition)

w_g = load due to self weight

N_l = load factor for live load

N_g = load factor for self weight (also superimposed load)

The self weight or the superimposed load is fairly defined so the value of N_g is slightly greater than unity. The approximate values of N_g and N_l are :

$N_g = 1.20$ to 1.80, $N_l = 1.50$ to 2.40

These values differ depending upon various factors such as the utility and type of the construction, type of material and the knowledge of the uncertainties such as

(i) inaccuracies and errors in construction
(ii) inaccurate positioning of the steel
(iii) inaccuracies in load calculations
(iv) validity of basic assumptions used in the analysis
(v) non-uniformity in the materials of construction
(vi) defects in materials either due to manufacturing or due to handling and storage
(vii) supporting and other static considerations
(viii) principal stress considerations due to the three dimensional effect
(ix) secondary stresses due to shrinkage, temperature
(x) probabilisting over load considerations and so on.

Failure of a structure may be defined as the exhausting of serviceability condition. It may be due to either excessive deformation or ultimate strength capacity. In general, the failure load calculation is based on the ultimate strength consideration and then the serviceability criterias are checked. In addition to the flexural failure, there are other possibilities of failures. The failure possibilities of prestressed concrete members are :

(i) failure due to anchorage stresses
(ii) flexural failure
(iii) combined shear and moment failure
(iv) failure due to lateral or torsional buckling.

The present chapter discusses the flexural failure only. The other types of failures from strength considerations are discussed later.

8.2. FLEXURAL FAILURE : Flexural failure is essentially taken as the ultimate strength capacity. The flexural failure could be divided into two parts.

(i) *Failure due to yielding of steel:* The steel yields first and results in excessive deformation; ultimately the beam collapses. This type of failure is called ductile failure and gives sufficient notice before actual collapse. If the breaking strain of steel is not high enough, even failure from yielding of steel may not give enough notice. This is likely to happen in prestressed concrete construction.

(ii) *Failure due to crushing of concrete:* Compressive strength of concrete is reached before the yielding of steel. The crushing takes place instantaneously so the failure is without notice and is called brittle failure.

The type of failure depends upon the initial compression and percentage of steel. It is desirable to have a ductile failure rather than sudden failure (or compression failure).

8.3. ULTIMATE MOMENT: Assumptions used in the derivation are

(i) plane sections remain plane during bending

(ii) failure occurs when the top fibre reaches the ultimate compressive strain

(iii) average strain in steel even after cracking is not far from the maximum strain

(iv) force due to tension in concrete is neglected.

Equations for strains are

$$\epsilon_{su}=\epsilon_{se}+\frac{\epsilon_{se}\,\epsilon_{ce}}{\epsilon_{se}-\beta_1\,\epsilon_{ce}}+\frac{\epsilon_u}{a}(d-a)\,\beta_2 \qquad \text{.. (8.3.1)}$$

$$\epsilon_{s1}=\frac{\epsilon_u}{a}(a-d_1) \qquad \text{.. (8.3.2)}$$

$$\epsilon_{s2}=\frac{\epsilon_u}{a}(d_2-a) \qquad \text{.. (8.3.3)}$$

where

ϵ_{ce} = strain in concrete at steel level at working load condition

ϵ_{se} = effective strain in steel

ϵ_{s1} = strain in ordinary tension reinforcement

ϵ_{s2} = strain in ordinary compressive reinforcement

ϵ_{su} = strain in prestressing steel at ultimate strength

ϵ_u = ultimate compressive strain of concrete

β_1, β_2 = compatibility factors

a = distance between the neutral axis and the top fibre

d_1, d_2 = distance of ordinary reinforcements from the top fibre

Equilibrium equations have to be written for two possible conditions:

(i) Neutral axis in the top flange

(ii) Neutral axis in the web.

Case 1: Neutral axis in the top flange:

$$\frac{ab_t}{\epsilon_u}\int_0^{\epsilon_u} f(\epsilon)\,d\epsilon=A_s f_s \qquad \text{.. (8.3.4)}$$

$$\frac{a^2 b_t}{\epsilon_u^2}\int_0^{\epsilon_u} f(\epsilon)\,\epsilon\,d\epsilon+A_s f_s (d-a)=M_u \qquad \text{.. (8.3.5)}$$

Case 2: Neutral axis in the web:

$$\frac{ab_w}{\epsilon_u}\int_0^{\epsilon_u(a-t_t)/a} f(\epsilon)\,d\epsilon+\frac{ab_t}{\epsilon_u}\int_{\epsilon_u(a-t_t)/a}^{\epsilon_u} f(\epsilon)\,d\epsilon=A_s f_s \qquad \text{.. (8.3.6)}$$

$$\frac{a^2 b_w}{\epsilon_u^2}\int_0^{\epsilon_u(a-t_t)/a} f(\epsilon)\,\epsilon d\,\epsilon+\frac{a^2 b_t}{\epsilon_u^2}\int_{\epsilon_u(a-t_t)/a}^{\epsilon_u} f(\epsilon)\,\epsilon d\,\epsilon+A_s f_s (d-a)=M_u \qquad \text{.. (8.3.7)}$$

The ultimate moment could be determined from the above set of equations.

Example 8.3.1 : Determination of ultimate moment capacity of a simply supported beam of span 16 m loaded with central concentrated load. The cross section and other particulars are given in fig. 8.3.1. Use the stress strain relations as given in figs. 8.3.2 and 8.3.3.

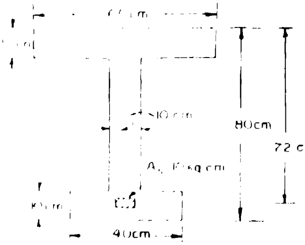

Fig. 8.3.1 : Beam section

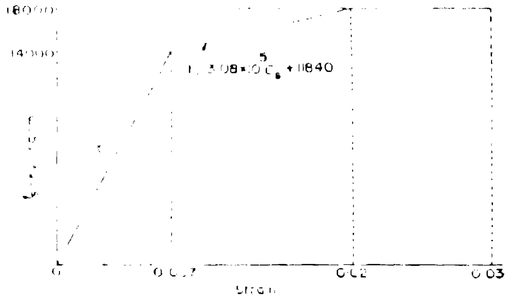

Fig. 8.3.2 : Stress strain relation for steel

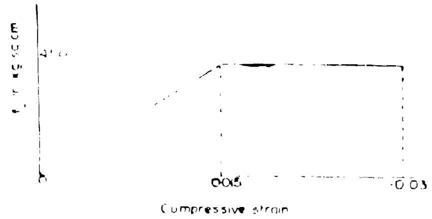

Fig. 8.3.3 : Stress strain relation for concrete

Use :

$f_{se} = 8000$ kg/sqcm, $A_s = 10$ sq cm,

$\epsilon_u = 0.003$, $\epsilon_{su} = 0.03$,

$\beta_1 = \beta_2 = 1$, $E_c = 3 \times 10^5$ kg/sq cm

Solution

Assuming that the neutral axis is in the top flange, from eqs. 8.3.4 and 8.3.5

$$\frac{60a}{0.003}\left[\frac{E_c}{2}(0.0015)^2+450\,(0.003-0.0015)\right]=10\,f_s$$

$$\therefore\ f_s=2025\ a \qquad \ldots \quad (8.3.8)$$

and

$$\frac{60\ a^2}{0.003^2}\left[\frac{E_c}{3}(0.0015)^3+\frac{450}{2}\,(0.003^2-0.0015^2)\right]$$
$$+10\,f_s\,(72\text{-}a)=M_u$$

$$\therefore\quad 12375\ a^2+10\,f_s\,(72\text{-}a)=M_u \qquad \ldots \quad (8.3.9)$$

Let

$f'_s=18000$ kg/sq cm, then from eq. 8.3.8

$a=8.9$ (the assumption $a<t_f$ is true)

From eq. 8.3.9

$M_u=(963{,}000+11{,}400{,}000)=12.338\times10^6$ kg cm

Note : –If 'a' happened to be greater than 10 cm, then equation of case 2 has to be used. It is also necessary to check the strain of steel for $\epsilon_u=0.003$. Eq. 8.3.1 can be used to compute final ϵ_{su}. This would involve determination of ϵ_{ce} and an approximate ϵ_{ce} could be found from the lever arm which is computed with the help of fig. 8.3.4.

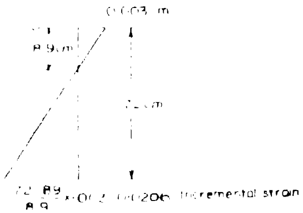

Fig. 8.3.4 : Strain distribution

$$\epsilon_s=\epsilon_{se}+\frac{\epsilon_{se}\ \epsilon_{ce}}{\epsilon_{se}-\epsilon_{ce}}+0.0206$$

$$=0.004+0.0206+\frac{\epsilon_{se}\ \epsilon_{ce}}{\epsilon_{se}-\epsilon_{ce}}.$$

In many cases, ϵ_{ce} is very small as compared to ϵ_{se} and it is approximately about 1/8 to 1/10 of ϵ_{se}.

So $\frac{\epsilon_{se}\ \epsilon_{ce}}{\epsilon_{se}-\epsilon_{ce}}\simeq\epsilon_{ce}$, this is negligible as compared to 0.0246.

Hence,

$\epsilon_s=0.0246<\epsilon_{su}$

The failure is by crushing of concrete.

Maximum curvature$=\epsilon_u/a=0.003/8.9=3.37\times10^{-4}$ rad/cm. Maximum deflection could be calculated only after finding the values of the curvature at various points and then by double integration. Determination of ultimate load capacity is usually simple but the prediction of the deformation involves numerable calculations.

8.4. SIMPLIFIED METHOD FOR DETERMINATION OF ULTIMATE MOMENT: The method described in the previous section for determination of ultimate load is general and the calculations involved for determination of ϵ_s may not worth the accuracy involved. Some modification in stress-strain relation of concrete could be done by assuming an equivalent stress block. A rectangular stress block modification is done in this chapter. The two equilibrium equations regarding the compression zone are modified as follows (see figs. 8.4.1 and 8.4.2). The two cases as discussed in the previous section are investigated.

Case 1: Neutral axis in the top flange ($t_f > a$)

Let $a = k_u d$

Considering the equilibrium equations we have

$$C=\frac{ab_t}{\epsilon_u}\int_0^{\epsilon_u} f(\epsilon)\,d\epsilon=k_1\,k_3\,f'_c\,b_t\,a=A_s\,f_{su} \qquad .. \quad (8.4.1)$$

Where

$C=$compressive force

$k_1=$ the ratio of average to maximum stress

$k_3=$ratio of equivalent stress block

$$\therefore k_u = \left(\frac{1}{k_1\,k_3}\right)\left(\frac{A_s\,f_{su}}{f'_c\,b_t\,d}\right) \qquad .. \quad (8.4.2)$$

Let the centroid of the stress block be at k_2a from the top fibre, then

$$k_2\,a = \frac{\dfrac{b_ta^2}{\epsilon_u^2}\displaystyle\int_0^{\epsilon_u} f(\epsilon)\,\epsilon\,d\epsilon}{\dfrac{b_ta}{\epsilon_u}\displaystyle\int_0^{\epsilon_u} f(\epsilon)\,d\epsilon} = \frac{a}{\epsilon_u}\,\frac{\displaystyle\int_0^{\epsilon_u} f(\epsilon)\,\epsilon\,d\epsilon}{\displaystyle\int_0^{\epsilon_u} f(\epsilon)\,d\epsilon} \qquad .. \quad (8.4.3)$$

The value of k_2 for rectangular stress block is 1/2 and for triangular block 1/3. Ultimate moment is given by

$$M_u=A_s\,f_{su}\,d\,(1-k_2\,k_u) \qquad .. \quad (8.4.4)$$

Other strain relations are

$$f_{su}=f_s\,(\epsilon_{su}) \qquad .. \quad (8.4.5)$$

$$\epsilon_{su}=\epsilon_{se}+\frac{\epsilon_{se}\,\epsilon_{ce}}{\epsilon_{se}-\beta_1\,\epsilon_{ce}}+\frac{\epsilon_u}{k_u}(1-k_u)\,\beta_2 \qquad .. \quad (8.4.6)$$

Eqs. 8.4.2, 8.4.4, 8.4.5 and 8.4.6 involve four unknowns (f_{su}, k_u, k_2, ϵ_{su}) and they are further simplified by eliminating k_u.

$$f_{su} = \frac{\beta_2\,(k_1\,k_3)\,\epsilon_u\,f'_c\,(b_t\,d)}{[\epsilon_{su}-\epsilon_{se}-\epsilon_{se}\,\epsilon_{ce}/(\epsilon_{se}-\beta_1\,\epsilon_{ce})+\beta_2\,\epsilon_u]\,A_s} \quad .. \quad (8.4.7)$$

Solve eqs. 8.4.7 and 8.4.5 for f_{su} and ϵ_{su}, then k_u from eq. 8.4.2 and M_u from eq. 8.4.4.

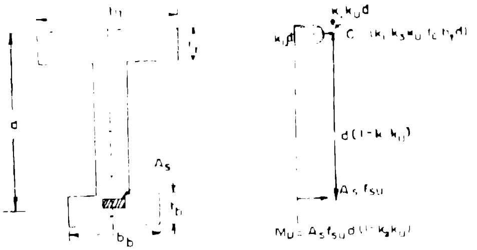

Fig. 8.4.1 : Ultimate moment—case 1 (neutral axis in top flange)

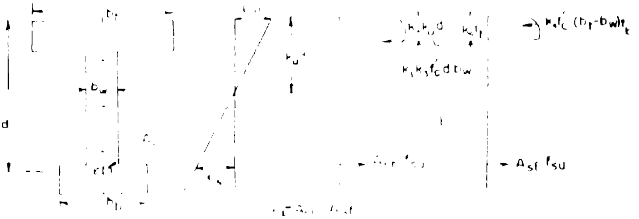

Fig. 8.4.2 : Ultimate moment—case 2 (neutral axis in the web)

Case 2: Neutral axis in the web :

The forces and moments of case 2 are shown in fig. 8.4.2. New coefficients k_4 and k_5 which are to be estimated are introduced. The stress block on the flange can be assumed close to a rectangular block. Equilibrium equations can be written as

$$k_u\,k_1k_3\,f'_c\,d\,b_w+k_4\,f'_c\,(b_t-b_w)\,t_t=A_s\,f_{su} \quad .. \quad (8.4.8)$$

$$M_u=k_1k_3\,k_u\,f'_c\,d^2\,b_w\,(1-k_2\,k_u)+k_4\,f'_c\,(b_t-b_w)\,t_t\,(d-k_5\,t_t) \quad (8.4.9)$$

Above equations have to be solved alongwith the steel strain and steel stress eqs. 8.4.5 and 8.4.6. The ranges of various k's are:

$k_1\,k_3=0.64$ to 0.70, $k_2=0.45$ to 0.50

$k_4=0.70$ to 0.85, $k_5=0.45$ to 0.50

The use of values of k_1, k_2, k_3, k_4, k_5 are illustrated by assuming a rectangular stress block shown in fig. 8.4.3. The value of k_1 is obtained from experimental data and found to be about 0.7 if cube strength of concrete is used and, 0.85 when cylinder strength is used. The value of k_3 can be found by knowing the stress strain relation of concrete and is approximated to 0.85 by considering a statically equivalent stress block. The value of k_2 for rectangular stress block is 0.5.

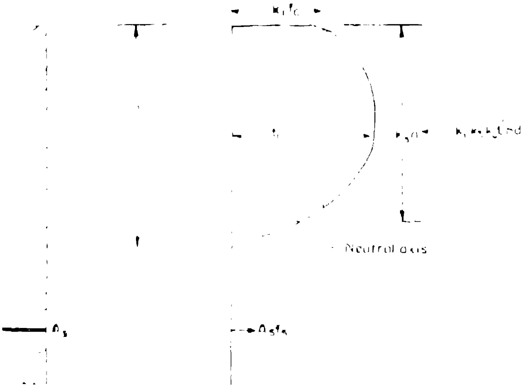

Fig. 8.4.3 : Approximation by rectangular stress block

Example 8.4.1: Determination of the ultimate moment capacity of the beam given in example 8.3.1.

Assuming a rectangular stress block, the coefficients may be taken as

$k_1 = 0.70,\ k_2 = 0.50,\ k_3 = 0.85,\ k_4 = 0.65,\ k_5 = 0.5$

let $a = t_f$ then from eqs. 8.4.8 and 8.4.9

$0.7 \times 0.85 \times 450 \times 72 \times 10 k_u + 0.65 \times 450 \times 50 \times 10 = 10 f_{su}$

$\therefore\ f_{su} = 19278\, k_u + 14625$

Similarly eq. 8.4.9 reduces to

$M_u = 19.3 \times 10^5 (k_u - 0.5\, k_u^2) + 9.8 \times 10^6$

$\epsilon_{su} = 0.0014 + (0.003)(1 - k_u)/k_u$

$f_{su} = f_s(\epsilon_{su})$

The above four equations have to be solved simultaneously. Since they are non-linear equations, it is desirable to solve them by trial. Easiest guess could be made about ϵ_{su}.

Let $\epsilon_{su} > 0.02$, so $f_{su} = 18000$ kg/sq cm

$$\therefore\ k_u = \frac{3375}{19278} = 0.175 \text{ and } a = 12.6 \text{ cm}$$

Check for ϵ_{su} by substituting the value of k_u in stress strain relation.

$$\epsilon_{su} = 0.0014 + \frac{0.003}{0.175} \times 0.824 = 0.0184 < (0.02 \text{ assumed})$$

Now assume $\epsilon_{su} = 0.019$

Then $f_{su} = 11840 + 3.09 \times 10^5 \times 0.019 = 17700$ kg/sq cm

$$k_u = \frac{3075}{19278} = 0.160 \text{ and } a = 11.5 \text{ cm}$$

Recheck for ϵ_{su} by substituting

$\epsilon_{su} = 0.0044 + 0.0165 = 0.0209$ (slightly more than assumed)

$M_u = 19.3 \times 10^5\ (0.147) + 9.8 \times 10^8 = 100.8 \times 10^5$ kg cm

8.5. ULTIMATE DESIGN OF PRESTRESSED CONCRETE BEAMS :

The ultimate moment relation based on the live loads can be written as

$$M_u = N_g\,(M_g + M_s) + N_l\,M_l \qquad \ldots \quad (8.5.1)$$

$$f_{su} \leqslant f_{sl} \qquad \ldots \quad (8.5.2)$$

Where f_{sl} = allowable ultimate stress in steel

From eqs. 8.5.1 and 8.5.2. it could be seen that the ultimate moment capacity and the ultimate steel stress must be equal or greater than the ultimate designed moment and steel stress. Introducing non-dimensionalised factors such as (8.1)

$$Q = \frac{M_u}{b_t\, d^2\, f'_c} \qquad \ldots \quad (8.5.3)$$

$$c_a = \text{shape factor} = \frac{A}{b_t\, h}$$

$$= \frac{b_b\, t_b + b_t\, t_t + b_w\,(h - t_b - t_t)}{b_t\, h}$$

$$= c_b\,(c_f - c_w) + c_t\,(1 - c_w) + c_w \qquad \ldots \quad (8.5.4)$$

Eq. 8.5.1 may be written as

$$M_g = \frac{\gamma\, A L^2}{8} = \left(\frac{Q A}{h c_a}\, d^2\, f'_c \times \frac{1}{N_g}\right) - \frac{N_l}{N_g}\, M_l - M_s$$

$$\text{or} \quad A = \frac{\left(M_s + \dfrac{N_l}{N_g}\, M_l\right)}{\left(\dfrac{d^2 f'_c\, Q}{h c_a\, N_g} - \dfrac{\gamma\, L^2}{8}\right)} \qquad \ldots \quad (8.5.5)$$

Eq. 8.5.5 gives the area of section in which the values of Q and c_a are unknowns. Assuming h to be already fixed by some other criteria, the value of 'd' will be about 85 to 90 percent of h. If a reasonable estimate is made for c_a and Q, the area of the section will be known. The economy of the structure depends upon area of cross section which is directly proportional to c_a and inversely proportional to Q. For an economical section the value of c_a has to be decreased, the value of Q increased, or the value of Q/c_a increased.

c_a increases with, (i) increase of c_f $(= b_b/b_t)$

(ii) increase of c_w

(iii) increase of c_b $(= t_b/h)$ and

(iv) increase of c_t $(= t_t/h)$

The aim should be to keep the above four conditions close to the limiting practical considerations.

For uniformity in procedure, the equilibrium equations are also put in the non-dimensionalised form and given below (8.1).

Case 1: Neutral axis within the top flange :

$$\left(\frac{a}{d}\right)\left(\frac{1}{\epsilon_u f'_c}\right)\int_0^{\epsilon_u} f(\epsilon)\,d\epsilon = \frac{f_{su}}{f'_c}\,q \qquad \ldots (8.5.6)$$

$$Q = \frac{M_u}{b_t d^2 f'_c} = \left[\left(\frac{a}{d}\right)^2 \frac{1}{\epsilon_u^2 f'_c}\int_0^{\epsilon_u} \epsilon f(\epsilon)\,d\epsilon + q\,\frac{f_{su}}{f'_c}\left(1-\frac{a}{d}\right)\right] \qquad \ldots (8.5.7)$$

where $$q = \frac{A_s}{b_t d} \qquad \ldots (8.5.8)$$

Case 2: Neutral axis within the web :

$$\frac{b_w}{b_t}\left(\frac{a}{d}\right)\frac{1}{\epsilon_u f'_c}\int_0^{\epsilon_u} f(\epsilon)\,d\epsilon +$$

$$\left(1-\frac{b_w}{b_t}\right)\left(\frac{a}{d}\right)\frac{1}{\epsilon_u f'_c}\int_{\epsilon_u(1-t_t/a)}^{\epsilon_u} \epsilon f(\epsilon)\,d\epsilon = q\,\frac{f_{su}}{f'_c} \qquad \ldots (8.5.9)$$

$$\frac{M_u}{b_t d^2 f'_c} = \frac{b_w}{b_t}\left(\frac{a}{d}\right)^2 \frac{1}{\epsilon_u^2 f'_c}\int_0^{\epsilon_u} \epsilon f(\epsilon)\,d\epsilon +$$

$$\left(1-\frac{b_w}{b_t}\right)\times\left(\frac{a}{d}\right)^2 \frac{1}{\epsilon_u^2 f'_c}\int_{\epsilon_u(1-t_t/a)}^{\epsilon_u} \epsilon f(\epsilon)\,d\epsilon + q\,\frac{f_{su}}{f'_c}\left(1-\frac{a}{d}\right) \qquad \ldots (8.5.10)$$

From the moment equilibrium eqs. 8.5.7 and 8.5.10, it can be seen that the value of Q ($= M_u/b_t d^2 f'_c$) increases with a/d. To have maximum ultimate load, (a/d) has to be maximum. ϵ_{su} will be minimum for maximum value of (a/d) and should then be equal to ϵ_{sl}.

Hence $$\epsilon_{sl} = \epsilon_{su} - \epsilon_{se} + \epsilon_{ce} + \epsilon_u\left(\frac{d}{a}-1\right) \qquad \ldots (8.5.11)$$

Where ϵ_{sl} = allowable steel strain at ultimate moment from which (a/d) could be determined as

$$\frac{a}{d} = \frac{-\epsilon_u}{(-\epsilon_{sl} + \epsilon_{se} + \epsilon_{ce} - \epsilon_u)} \qquad \ldots (8.5.12)$$

8.6. ULTIMATE LOAD DESIGN PROCEDURE: The quantities usually furnished are:

(i) span ;
(ii) load acting on the span;
(iii) strength of the materials ;
(iv) load factors from code ; and
(v) stress-strain relations of the materials.

Quantities to be determined are:

(i) area of cross section (A), its shape and dimensions;
(ii) prestressing force (P_t) ;
(iii) area of steel (A_s) ; and
(iv) profile of the cable.

Approximate procedure to be adopted for design of prestressed concrete beam by ultimate moment method may be taken as

(i) select the over-all depth of the beam (h) ;
(ii) assume a reasonable value of d (approximately 0.85 to 0.90 times h) ;
(iii) assume some values of c_f, c_t, c_w etc. and calculate c_a from eq. 8.5.4 or obtain from tables. While assuming these values, the economical sizes have to be selected based on the previous discussion ;
(iv) calculate a/d from eq. 8.5.12 ;
(v) from the value of 'a', investigate to which case does this belong to;
(vi) now calculate q f_{su}/f'_c from the force equilibrium equation ;
(vii) calculate Q from the moment equilibrium equation ;
(viii) compute b_f from Q, then b_b etc.

Example 8.6.1 : Design of a prestressed concrete beam by ultimate load method.

Data given : span = 16 m

live load = W_l = 10,000 kg concentrated at the mid span

$N_g = 1.2$, $N_l = 2.4$ and the stress strain relations as given in example 8.3.1.

Design :

$$\text{Let } h = \frac{L}{20} = 80 \text{ cm}, \ d = 0.9\, h = 72 \text{ cm},$$

$$c_f = 0.6, \ c_b = 0.125, \ c_t = 0.125, \ c_w = 0.175, \ \epsilon_{se} = 0.004$$

$$\therefore \quad c_a = c_b\,(c_f - c_w) + c_t\,(1 - c_w) + c_w = 0.331$$

$$\frac{a}{d} = \frac{-\epsilon_u}{(-\epsilon_{sl} + \epsilon_{se} + \epsilon_{ce} - \epsilon_u)} = 0.161$$

$$\therefore \quad a = 11.6 \text{ cm whereas } t_t = \frac{80}{8} = 10 \text{ cm}$$

Since a > t_t, this problem belongs to case 2, i.e., neutral axis is in the web.

$$\epsilon_u\left(1-\frac{h}{a}\right)=-0.00042$$

From eq. 8.5.9

$$\frac{0.175\times0.161}{0.003\times450}\left[\frac{1}{2}\times3\times10^5\times(0.0015)^2+3\times10^5\times(0.003-0.0015)\right.$$

$$\left.\times0.0015\right]+\frac{0.825\times0.161}{0.003\times450}\left[\frac{1}{2}\times3\times10^5\,(0.0015^2-0.00042^2)\right.$$

$$\left.+3\times10^5\times0.0015\,(0.003-0.0015)\right]=\frac{18000}{450}\,q$$

$$\therefore\quad q=0.0029$$

From moment eq. 8.5.10

$$Q=\frac{M_u}{b_t\,d^2\,f'_c}=\frac{0.175\,(0.161)^2}{0.003^2\times450}\left[\frac{3\times10^5}{3}\,(0.0015)^3+\frac{450}{2}\,(0.003^2-\right.$$

$$\left.0.0015^2)\right]+\frac{0.825\times(0.161)}{0.003^2\times450}\left[\frac{3\times10^5}{3}\,(0.0015)^3+\frac{450}{2}\times\right.$$

$$\left.(0.003^2-0.0015^2)\right]+\frac{18000}{450}\,(0.839)\times0.0029=0.109$$

Let $\gamma=0.0024$ kg/cm³, $M_g=0$

$$M_l=10000\times\frac{1600}{4}=4\times10^6\ \text{kg cm}$$

From eq. 8.5.5

$$A=\frac{N_l}{N_g}\,M_l\Big/\left[\frac{d^2\,f'_c\,Q}{h\,c_B\,N_g}-\frac{\gamma\,L^2}{8}\right]$$

$$=\frac{2\times4\times10^6}{\dfrac{72\times72\times450\times0.109}{80\times0.331\times1.2}-0.0024\times\dfrac{2560000}{8}}$$

$$=1106\ \text{sq cm}$$

$$b_t=\frac{A}{h\,c_B}=\frac{1106}{80\times0.331}=41.5\ \text{cm}$$

$b_b=0.6\,b_t=25$ cm, $t_b=t_t=10$ cm,

$b_w=0.175\times80=$ **14** cm

$A_s=0.0029\times1106=3.20$ sq cm

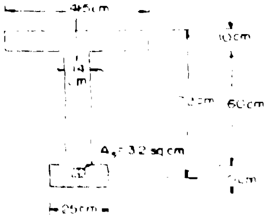

Fig. 8.6.1 : Section of example 8.6.1

8.7. ULTIMATE MOMENT BY I. S. CODE OF PRACTICE (I. S.: 1343—1960):

Section 6.8 of I. S : 1343—1960 discusses different types of failure of prestressed concrete beam in which percentage of reinforcement governs the type of failure. The procedure is best illustrated by working out an example.

Example 8.7.1: Determination of the ultimate moment capacity of a pretensioned concrete section shown in fig. 8.7.1 by I. S. code of practice. Use $f'_c = 450$ kg/sq cm, $f'_s = 15000$ kg/sq cm.

Solution :

(a) Check for percentage of steel :

$$A_{tsf} = \frac{0.68\, f'_c\, b_t\, t_t}{f'_s}$$

$$= \frac{0.68 \times 450 \times 60 \times 11}{15000} = 13.46 \text{ sq cm}$$

$$A_{tsw} = A_{ts} - A_{tsf} = 20 - 13.46 = 6.54 \text{ sq cm}$$

$$\frac{A_{tsw} f'_s}{b_w d\, f'_c} = \frac{6.54 \times 15000}{10 \times 72 \times 450} = 0.3 \; (>0.24)$$

Since the above value is greater than 0.24, the beam will fail by compression and the corresponding ultimate load is given by

$$M_u = 0.75\, f'_c\, (0.25\, b_w d^2 + 0.68\, t_t\, (b_t - b_w))\, (d - 0.5\, t_t)$$

$$= 12.2 \times 10^6 \text{ kg cm}$$

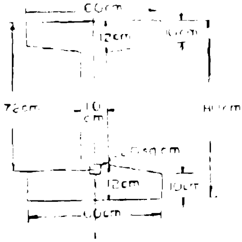

Fig. 8.7.1 : Example 8.7.1

Problems

8.1 Determine the ultimate moment capacity of the 50 m span beam of the design example given in chapter III. Determine the factor of safety.

8.2 Determine the ultimate moment capacity of the composite beam example discussed in chapter IV.

CHAPTER IX

ANALYSIS AND DESIGN OF PRESTRESSED CONCRETE BEAMS FOR SHEAR

9.1. INTRODUCTION : The previous chapters discuss analysis and design of prestressed concrete beams subjected to bending moments. Bending moments in beams are usually accompanied by shear forces, so such members are designed for combined bending and shear. Because of simplicity and limited theoretical and experimental data, design of members subjected to combined bending and shear is done independently for bending and for shear. The failure load is generally predicted by taking the combined effect of bending and shear forces. Extensive research is being done in this direction to predict failure due to combined bending and shear forces. The problem is rather complex and depends upon several variables. Even though a large amount of experimental data is available, the exact prediction of the behaviour of the beams under combined moment and shear forces has not reached a satisfactory stage. A good qualitative behaviour is well established and attempts are being made to set up a realistic design procedure based on the combined action of moment and shear forces. This chapter presents some methods of analysis and design for combined shear and moment forces. Ultimate load capacity based on shear moment failure is also discussed in this chapter.

9.2. SHEAR STRESS : Uncracked sectional properties are used while calculating the shear stress at working load.

Let τ = shear stress

V = shear force

Q_y = first moment of area about the point under consideration

$$= \int_{y}^{y_t} b_y y \, dy$$

Then the shear stress τ for a prismatic member is given by

$$\tau = \frac{VQ_y}{I\,b_y} \qquad \text{.. (9.2.1)}$$

where b_y = width of the section at the point

9.3. PRINCIPAL STRESSES: Beams are essentially two dimensional problems and the principal stresses in plane stress problem are given by

$$\sigma_1 = \frac{\sigma_x + \sigma_y}{2} + \sqrt{\left(\frac{\sigma_x - \sigma_y}{2}\right)^2 + \tau^2} \quad .. \quad (9.3.1)$$

$$\sigma_2 = \frac{\sigma_x + \sigma_y}{2} - \sqrt{\left(\frac{\sigma_x - \sigma_y}{2}\right)^2 + \tau^2} \quad .. \quad (9.3.2)$$

where

σ_1 = maximum principal stress

σ_2 = minimum principal stress

σ_x = normal stress on x plane

σ_y = normal stress on y plane

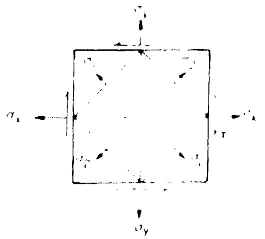

Fig. 9.3.1 : Plane stress notations

σ_y is transverse stress, very small in most cases. If transverse prestressing is done, then σ_y may be considered, otherwise σ_y may be neglected as compared to σ_x. In such cases, the principal stresses are expressed from eqs. 9.3.1 & 9.3.2 as

$$\sigma_1 = \frac{1}{2}\left[\sigma_x + \sqrt{\sigma_x^2 + 4\tau^2}\right] \quad .. \quad (9.3.3)$$

$$\sigma_2 = \frac{1}{2}\left[\sigma_x - \sqrt{\sigma_x^2 + 4\tau^2}\right] \quad .. \quad (9.3.4)$$

The principal stress plane is given by

$$\text{Tan } 2\alpha = \frac{(2\tau)}{\sigma_x} \quad .. \quad (9.3.5)$$

Where α = angle of principal stress plane

One of the principal stresses is likely to be tensile and will act at an angle 'α' with the horizontal axis. For very efficient use of shear steel, reinforcement should be laid at an angle α with the horizontal. However the practical and economical considerations often suggest vertical stirrups.

9.4. STIRRUPS FOR WORKING LOADS : Total shear force at any section is

$$V_t = V_g + V_s + V_l \qquad .. \quad (9.4.1)$$

where

V_g = shear force due to self weight

V_s = shear force due to superimposed load

V_l = shear force due to live load and

V_t = total shear force.

In case the tendon is inclined, the vertical component of the tendon force will take a part of the shear force and is given by

$$V_p = P_e \frac{dy}{dx} \qquad .. \quad (9.4.2)$$

where V_p = shear force taken by the tendon

The effective shear force at any section is given by

$$V = (V_t - V_p) \qquad .. \quad (9.4.3)$$

where V = effective shear force at the section

The tensile principal stress, sometimes called diagonal tension, acts approximately at 30 (The inclination is generally 20° to 40°). The horizontal component of this tensile force is generally withstood by the prestressing force and the vertical component by vertical shear steel or concrete.

Let

A_{sv} = area of vertical stirrup

f_{sv} = allowable stress in steel stirrups

s = spacing of the stirrups

Area of shear steel is given by

$$A_{sv} = \frac{\sigma_1 (s b_w)}{f_{sv}} \qquad .. \quad (9.4.4)$$

If A_{sv} is already selected, then the spacing of the stirrups is given by

$$s = \left(\frac{A_{sv} \, f_{sv}}{\sigma_1 \, b_w} \right) \qquad .. \quad (9.4.5)$$

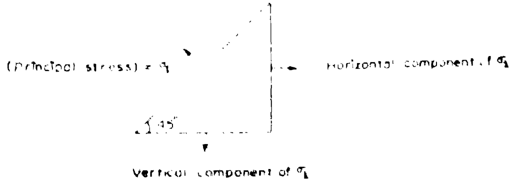
(Principal stress) = σ_1
Horizontal component of σ_1
45°
Vertical component of σ_1

Fig. 9.4.1 : Components of principal stresses

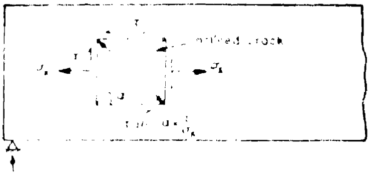

Fig. 9.4.2 : Beam with element forces with inclined cracks

9.5. FAILURE DUE TO SHEAR : Failure of a prestressed concrete beam caused by shear can be divided into two groups :

(i) failure caused by pure shear and

(ii) failure caused by combined shear and flexure.

Failure caused by pure shear is very rare and practically never occurs in most of the prestressed concrete structures. Failure caused by the combined action of shear and bending moment is common. Therefore it is desirable to design or check beams for "shear-moment failure".

It has been observed that a vertical crack starts at the lower fibre during overload conditions at maximum bending moment location. In simply supported beam vertical cracking propagates towards supports as the load increases. Then shear-moment cracks begain to develop. Shear moment cracks are normally developed as a continuation of vertical cracks and those cracks in general are from 'h to 4h' distance from a simple support or from '0.5h to h' distance from intermediate supports. Shear moment cracks develop large deformation, distorting the horizontal reinforcement. Then the distorted longitudinal reinforcement starts resisting the vertical shear force. The location and development of cracks affect the deformation characteristics of the beam. Specifically, diagonal cracks develop some kind of rotational hinges about which the cracked elements rotate. A typical crack development and beam rotation is shown in figs. 9.5.1 and 9.5.2.

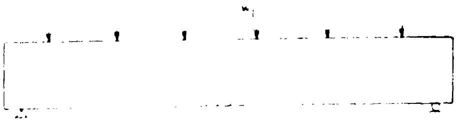

(a) Crack initiation

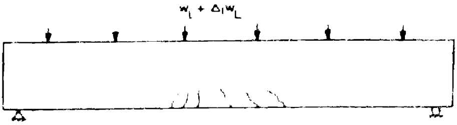

(b) Vertical crack propagation

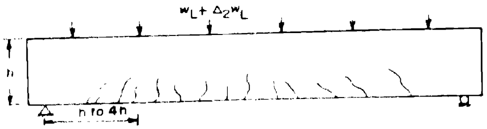

(c) Inclined cracks—shear moment cracks

Fig. 9.5.1 : Typical crack development

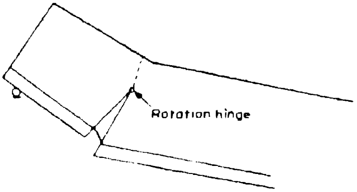

Widening of shear—moment crack (rotation hinge)

Fig. 9.5.2 : Hinge development due to inclined cracks just before failure

9.6. COMPRESSIVE STRENGTH OF CONCRETE SUBJECTED TO COMBINED BENDING AND SHEAR : If f'_c is the ultimate stress of a concrete cube, the ultimate compressive stress available in beams will generally be less than f'_c because of shape, length and other segregation effects. Ultimate concrete stress is generally given by $k_p f'_c$, where k_p is a factor approximately in the range of 0.64 (9.1). If a beam is subjected to both bending as well as shear forces, then the allowable ultimate compressive stress is further reduced. An approximate interaction formula has been suggested based on experimental data (9.2) and it is

$$f'_{cs} = (k_p\, f'_c) / \left[1 + 3.2\left(\frac{Vh}{M}\right)\right] = k_p\, k_7\, f'_c \qquad \text{.. (9.6.1)}$$

$$k_7 = 1 / \left[1 + 3.2\left(\frac{Vh}{M}\right)\right] \qquad \text{.. (9.6.2)}$$

where

f'_{cs} = ultimate concrete stress in a beam subjected to combined bending and shear

$k_p f'_c$ = ultimate concrete prism strength (in many cases, the prism strength is taken equal to bending compressive strength)

Interaction curve for k_7 is shown in fig. 9.6.1. The values of Vh/M are in the order of 0.1 to 0.4 in most of the practical problems.

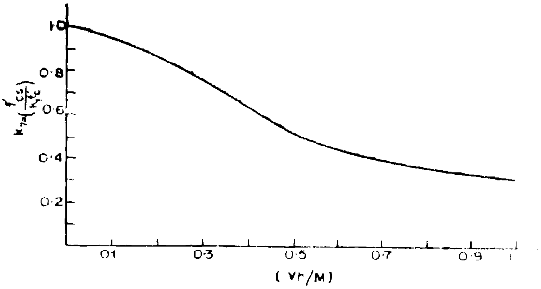

Fig. 9.6.1 : Interaction curve for combined shear and bending moment

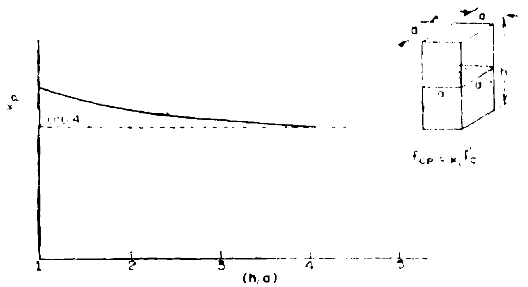

Fig. 9.6.2 : Concrete prism strength

Value of k_p decreases as the length to side ratio increases. This variation may be attributed to three factors : (i) size effect, (ii) consistency variation in the concrete and (iii) effect of friction at the surface of test specimens. In case of concrete subjected to pure bending, ultimate bending strength in compression is assumed to be higher than that of a prism strength. The relation is given by (9.3)

$$f'_{cb} = k_p \ k_6 \ f'_c \qquad .. \quad (9.6.3)$$

Where

f'_{cb} = compressive strength of concrete in bending

k_6 = nondimensionalised coefficient and its value is suggested to be about 1.2 to 1.25

The practice in working load design assumes a higher strength in bending as compared to direct compression. If the compressive strength in bending is considered to be higher than that in direct compression, then compressive strength in shear and bending is also increased accordingly. All the calculations in this text are made assuming that the compressive strength in bending is the same as the compressive strength of prism.

9.7. ULTIMATE BENDING MOMENT UNDER COMBINED MOMENT AND SHEAR (MOMENT SHEAR FAILURE) :

Rectangular cross Section with Straight Tendons : Combined moment and shear crack (principal stress) is generally inclined at 20° to 40° to the bending axis depending upon the relative magnitude of the quantities. This crack is idealised at 45° for the purpose of calculation and to be on the safe side of the design. An idealised crack and various forces acting at the time of failure are shown in fig. 9.7.1.

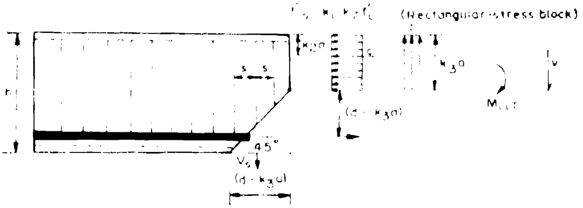

Fig. 9.7.1 : Forces at combined bending and shear failure (straight tendon)

Vertical component of the stirrup forces at failure is

$$V_s=\left[\frac{(d-k_3a)}{s}A_{sv}\,f'_{sv}\right]$$

$$=d\left[\frac{1-k_3\,k_u}{s}\right]A_{sv}\,f'_{sv} \qquad .. \quad (9.7.1)$$

where

V_s = shear force taken by the stirrup steel

Equations of equilibrium at ultimate load capacity of the section are

$$V=\frac{d}{s}\,(1-k_3\,k_u)\,A_{sv}\,f'_{sv}+\tau\,(k_3\,k_u db) \qquad .. \quad (9.7.2)$$

$$f_s\,A_s=k_1\,k_7\,k_3\,k_u\,bd\,f'_c \qquad .. \quad (9.7.3)$$

$$M_u=\left[\frac{d}{s}\,(1-k_3\,k_u)\,A_{sv}\,f'_{sv}\right]\left(\frac{d-k_3\,a}{2}\right)+(k_1\,k_7\,f'_c)\,(k_3\,k_u\,d)\,(b)\,(d-k_2a)$$

$$=(k_1\,k_7\,k_3\,k_u)\,(1-k_2\,k_u)\,bd^2\,f'_c+\frac{1}{2}(1-k_3\,k_u)^2\,\frac{d^2}{s}\,A_{sv}\,f'_{sv} \qquad .. \quad (9.7.4)$$

$$f'_s=f_{su}\ \text{(for all practical purposes)} \qquad .. \quad (9.7.5)$$

or

$$f_s=f_s\,(\epsilon_s) \qquad .. \quad (9.7.6)$$

$$\epsilon_s=\epsilon_{se}+\epsilon_{ce}+\epsilon_u\left(\frac{d}{a}-1\right)$$

$$=\epsilon_{se}+\epsilon_{ce}+\epsilon_u\left(\frac{1}{k_u}-1\right) \qquad .. \quad (9.7.7)$$

Above set of eqs. 9.7.3 to 9.7.7 gives the ultimate moment for a beam of rectangular cross section subjected to combined bending and shear. For all practical purposes, the value of f'_s could be assumed equal to f_{su}. However with such an approximation, ultimate capacity of the beam is on the unsafe side.

Example 9.7.1: A simply supported 8 m long prestressed concrete beam of rectangular cross section (30 × 80 cm) is provided with a straight cable of 10 sq cm having 20 cm eccentricity. Mild steel stirrups of 1 cm wires at 15 cm are provided for shear. Determine the ultimate capacity of the beam.

Use f'_c = 450 kg/sq cm

f_{su} = 15000 kg/sq cm

$k_1 = 0.85$, $k_3 = 0.85$, $k_2 = 0.5$ and $k_7 = 1$

Solution :

Since the beam is rectangular in section and simply supported, the critical section is at mid span.

From eq. 9.7.3

$$k_u = (A_s f_s)/(k_1\ k_7\ k_3\ bd\ f'_c) = 0.295$$

$$k_3\ a = k_3\ k_u\ d = 0.295 \times 0.85 \times 80 = 20 \text{ cm}$$

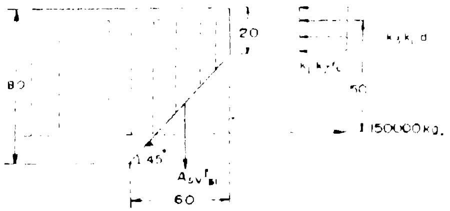

Fig. 9.7.2 : Example 9.7.1

The following computations are made with reference to fig 9.7.2.

$$A_{sv} = \left(\frac{60}{15}\right) \frac{\pi}{4} = 3.14 \text{ sq cm}$$

Let the ultimate stress of mild steel be 3000 kg/sq cm

$$M_u = 150000 \times 50 + 3.14 \times 3000 \times 30 = 77.83 \times 10^5 \text{ kg cm}$$

9.8. ULTIMATE BENDING MOMENT UNDER COMBINED BENDING AND SHEAR OF A RECTANGULAR CROSS-SECTION WITH INCLINED TENDONS:

Fig. 9.8.1 gives the detail of forces acting at the time of shear-moment failure of a beam. The inclined crack is assumed to be at 45° to the horizontal axis. Ultimate strength of concrete and steel are assumed to be effective at the time of failure. This assumption is made to simplify the solution. A rigorous solution could be obtained by calculating the stress in steel based upon the assumption that plane sections remain plane.

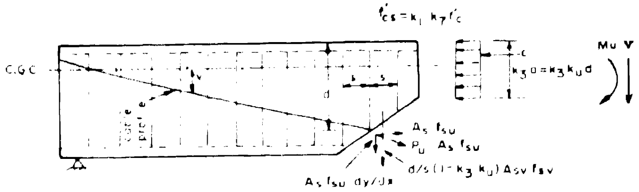

Fig. 9.8.1. Forces at combined bending and shear failure of a beam with inclined cable

Applying the equilibrium equations at shear moment failure (fig. 9.8.1)

$$A_s f_{su} = (k_1 k_7 k_3 k_u)\, bd\, f'_c \qquad \text{.. (9.8.1)}$$

$$M_u = (k_1 k_7 k_3 k_u\, bd\, f'_c)\,(d - k_2 k_3 a) + \left(A_s f_{su} \frac{dy}{dx}\right) d + \frac{1}{2}(1 - k_3 k_u)^2 \frac{d^2}{s} A_{sv} f'_{sv}$$

$$= bd^2\left[k_1 k_7 k_3 k_u (1 - k_2 k_3 k_u) f'_c + p\left(\frac{dy}{dx}\right) f_{su} + \frac{1}{2}(1 - k_3 k_u)^2 \frac{A_{sv}}{sb} f'_{sv}\right]$$

$$= \left[k_1 k_7 k_3 k_u (1 - k_2 k_3 k_u) f'_c + p\left(\frac{dy}{dx}\right) f_{su} + \frac{1}{2}(1 - k_3 k_u)^2 p_s f'_{sv}\right] bd^2 \qquad \text{.. (9.8.2)}$$

where

p_s = ratio of shear reinforcement

$$= \left(\frac{A_{sv}}{sb}\right) \qquad \text{.. (9.8.3)}$$

k_u has to be obtained from eq. 9.8.1 and the ultimate moment could be obtained from eq. 9.8.2.

9.9 ULTIMATE MOMENT UNDER COMBINED BENDING AND SHEAR OF I-GIRDER: Expressions for shear moment failure could be written in the same way as done for the previous section. There are two possible cases of failure in I-girders: (i) neutral axis within the top flange, and (ii) neutral axis in the web of the girder. If the neutral axis is in the top flange, then ultimate moment is given by the previous section by substituting b_t for b.

Fig. 9.9.1 gives complete details at the time of failure of an I-section where the neutral axis is in the web portion.

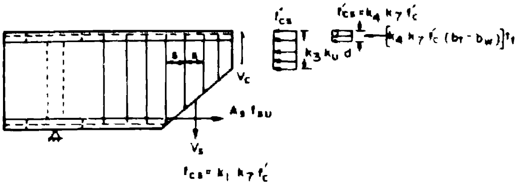

Fig. 9.9.1 : Forces at combined bending and shear failure (I-section with neutral axis in the web)

Assume $f'_s = f_{su}$ at the time of failure, then the equilibrium equations are given as

$$A_s f_{su} = k_1\ k_7\ k_3\ k_u\ f'_c\ db_w + k_4\ k_7\ t_t\ (b_t - b_w)\ f'_c \qquad .. \quad (9.9.1)$$

$$M_u = k_1\ k_7\ k_3\ k_u\ (1 - k_2\ k_u)\ b_w d^2 f'_c + k_4\ k_7\ (d - k_5\ t_t)\ (b_t - b_w)\ t_t\ f'_c$$
$$+ (A_{sv} f'_{sv}\ (1 - k_3\ k_u)^2/2s)\ d^2 + A_s f_{su} \left(\frac{dv}{dx}\right) d \qquad .. \quad (9.9.2)$$

The values of k_u and M_u are the two unknowns and these two quantities could be obtained from eqs. 9.9.1 and 9.9.2.

Example 9.9.1 : Determination of ultimate load capacity of a prestressed concrete cantilever beam of 8 m with the cross section as shown in fig. 9.9.2 subjected to a uniformly distributed load.

Given data :

$f'_c = 450$ kg/sq cm and $f's = 15000$ kg/sq cm

$k_2 = 0.5$, $k_3 = 0.85$, $k_1 = 0.85$, $k_4 = 0.85$, $f_{su} = f'_s$

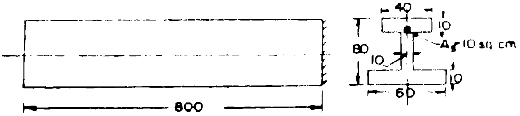

Fig. 9.9.2 : Example 9.9.1

Solution :

The section at support is subjected to maximum shear and bending moment, so the allowable compressive stress depends upon the relative ratio.

$$\frac{Vh}{M} = \frac{8 \times 0.8}{8 \times 4} = 0.2$$

$$k_7 = \frac{1}{1 + 3.2 \times 0.2} = 0.61$$

Assuming the neutral axis in the web portion, from eq. 9.9.1

$$k_u = [A_s\ f'_s - k_4\ k_7\ t_b\ (b_b - b_w)\ f'_c]/(k_1\ k_7\ k_3\ f'_c\ d\ b_w) = 0.18$$

$$k_3\ k_u\ d = 12.2\ (> t_b)$$

Strain compatibility to find the type of failure is

$$\epsilon_s = 0.0044 + 0.003\left(\frac{72-12.2}{12.2}\right)$$

$$= 0.0193 = \text{yield strain of steel}$$

$$M_u = k_1\ k_7\ f'_c\ [(t_b\ b_b) \times (72-5) + b_w\ (12.2-t_h) \times (62-1.1)]$$

$$= 963730 \text{ kg cm}$$

$$w_u = (M_u \times 2)/(L^2) = \frac{963730 \times 2}{800 \times 800} = 30 \text{ kg/cm} = 3000 \text{ kg/m}$$

9.10. LOCATION OF FAILURE SECTION: In the last section the failure was assumed to occur at a section where the value of k_7 is calculated from the shear and moment relation at the section. In any problem, it is necessary to locate the likely failure and establish the value of k_7 at that section. In statically determinate structures, location of shear moment failure can be estimated or derived. An example of a well-defined situation is shown in fig. 9.10.1, where shear force and bending moment are maximum at a particular section (c c). Hence shear-moment failure will also occur at that section.

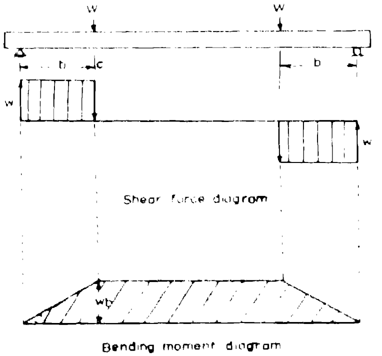

Fig. 9.10.1 : Defined problem of shear moment failure (Failure occurs at section c c where bending moment and shear force are maximum)

In some problems, the zone of failure is not well defined. In a simple problem like a simply supported beam subjected to uniform loading, maximum bending moment occurs at mid-span although the maximum shear force is near the support. Investigations have to be made to locate the maximum combined effect. Since the section will develop cracks due to bending, it is difficult to establish a generalised principal stress equation of the beam. Independent moment and shear force diagrams of a simply supported beam are shown in fig. 9.10.2. The figure also gives the effective shear resisted by the cross section and tendon. Location of maximum damage due to the combined effect of moment and shear is rather undefined. In such a case as this, failure could be either (i) moment failure or (ii) shear-moment failure. Shear-moment failure is likely to occur near a heavy concentrated load if it is present. Trial analysis generally gives a satisfactory result even though it may not give an exact section where the failure occurs (9.3 to 9.5).

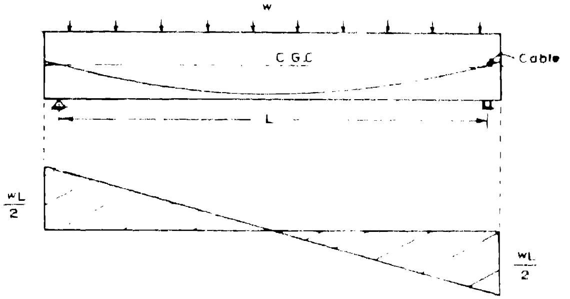

(a) External shear force diagram

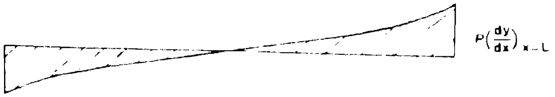

(b) Shear force taken by tendon

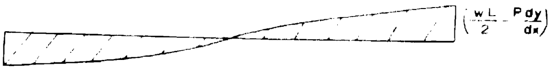

(c) Shear force resisted by the section

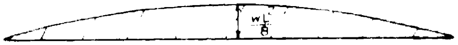

(d) Bending moment diagram

Fig. 9.10.2 : Shear and moment diagrams

Location of shear moment failure in a statically indeterminate structure is not easy to predict because of the nature of the shear and bending moment distribution. The effects of secondary bending force and the curvature in the cable make the problem more complicated. Even though a particularly critical section exists at which the failure starts, the real failure of a structure is not due to failure of a single section but due to a localised effect. An investigation near the critical section gives fairly close approximation of failure load. Shear and moment are maximum near the intermediate supports so the shear-moment failure is likely to occur at about h/2 to 2h from an intermediate support. A statically indeterminate structure collapses when sufficient number of sections yield into a collapsable mechanism. Determination of real ultimate load capacity should be based on limit design.

9.11. SUGGESTIONS FROM EXPERIMENTAL INVESTIGATIONS: Extensive experimental investigations have been done on shear failures and a large amount of data is being accumulated on the subject. In spite of the large experimental data, it is still difficult to suggest any exact procedure for design against shear moment failure. Design is done independently for bending moment and shear force while shear-moment failure load is computed based on the designed section. Effect of different parameters on the shear-moment failure, as suggested by McGregor, Sozen and Siess (9.6), are given here to help in the design of shear reinforcement.

(i) *Effect of prestress :* Increase in prestressing force increases the inclined cracking loads. Even though certain amount of increase in cracking load is obtained by increasing the prestressing force, the warning against ultimate failure is reduced. A typical behaviour of cracking load relative to effective prestressing force is shown in fig. 9.11.1.

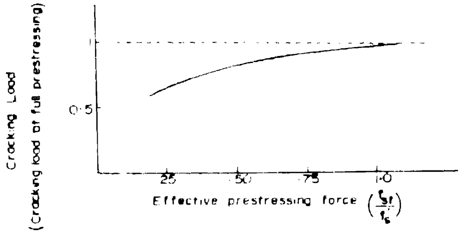

Fig. 9.11.1 : Effect of prestress on cracking load

(ii) *Effect of web thickness :* The inclined cracking load appears to be independent of the thickness of the web. In most cases, the web thickness is in a narrow range so that three dimensional effects do not come into play. Web could be treated as a plane stress problem without any loss of accuracy for design purposes.

(iii) *Effect of web reinforcement :* Rate of propagation of the shear crack depends on web reinforcement. The initation of a crack starts near the bottom fibre and is generally independent of the vertical (web) reinforcement. However, the propagation of the crack depends upon the shear reinforcement. Ultimate shear-moment capacity could be increased by increasing the shear reinforcement.

In beams without web reinforcement, the beam distorts and causes kink in the main prestressing force. The vertical component of the

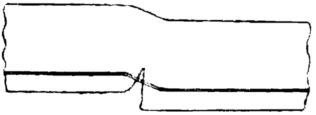

Fig. 9.11.2 : Kink at vertical crack in a beam with web reinforcement

prestressing force at the kink contributes towards shear force. The kink action reduces the ultimate bending moment capacity even though it increases the ultimate shear capacity. The overall ultimate capacity of the beam is affected by the kink. The deformation of a beam is also affected by vertical reinforcement. A typical load deflection curve with different percentages of shear reinforcement is shown in fig. 9.11.3. It can be seen that the increase of shear reinforcement decreases the deflection to some extent and increases the ultimate load capacity of the beam. Even in the case of problems where the reinforcement is not needed based upon the working load design, it is still desirable to provide some nominal shear reinforcement. It will increase the ultimate capacity of the beam and also avoid a sudden failure of the beam due to fast propagation of inclined crack.

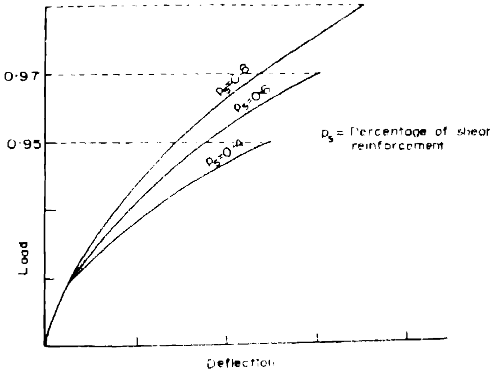

Fig. 9.11.3 : Qualitative behaviour of a prestressed concrete beam based on shear reinforcement

(iv) *Effect of vertical prestressing :* Vertical prestress reduces the tensile principal stress as shown in the following equation :

$$\sigma_1 = \frac{\alpha_x + \sigma_y}{2} - \left[\frac{(\sigma_x + \sigma_y)^2}{4} + \tau^2 \right]^{1/2} \qquad .. \ (9.11.1)$$

Effect of σ_y is same as of σ_x as far as the principal stresses are concerned. The inclined crack load decreases with increased vertical prestressing. The shear-moment failure load could be increased by about 5 to 10% by introduction of vertical prestressing, whereas the moment failure load is not affected by the vertical prestressing force. The effect of vertical prestress on the behaviour of a beam is shown in fig. 9.11.4.

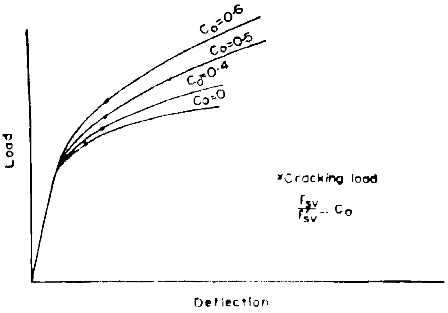

Fig. 9.11.4 : Typical behaviour of prestressed concrete beam with vertical prestressing

(v) *Effect of draping of longitudinal steel:* Upward inclination of longitudinal reinforcement takes vertical shear and it is proportional to the inclination. If the failure is due to shear domination, then the ultimate capacity could be increased by draping of the wires. If the failure is a moment failure, draping of wires decreases the ultimate load capacity.

Problems

9.1 A bridge slab is to be supported by two frames shown in Fig. 9.1. Draw bending moment and shear force diagrams for the structure and suggest a cable profile to balance the external forces.

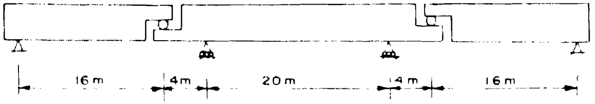

Fig. 9.1 : Problem 9.1

9.2 The beam of problem 9.1 is subjected to a distributed load of 3000 kg/m. Design prestressing and shear steel for the beam. Determine the ultimate strength of the cantilever and the overhang beam sections.

CHAPTER X

PRESTRESSED CONCRETE FLOORS AND SLABS

10.1. INTRODUCTION : Slab construction is suitable for building floors, small bridges and culverts. The slab bridge or culvert construction is adopted when the span of the bridge is small. In such cases the design is simple and could be done as explained in previous chapters. There are several types of slab construction, the designs of which present interesting and challenging problems. The three major groups of slab construction are :

(i) beam and slab construction ;
(ii) flat slab-panel construction ; and
(iii) flat plate construction.

The different types of slab constructions are shown in fig. 10.1.1. Any slab may be classified as one-way or two-way slab based upon the structural action of the slab. If the span ratio (also called as aspect ratio) is large, the slab acts in one direction as a very wide beam. If the width of the slab is small as compared to the length, most of the load is carried by the short span. Such a slab is called a one-way slab and designed as a very wide beam. If the span ratio is in the neighbourhood of 1, the load is carried by both the spans and the slab is called two-way slab. The inherent continuity of the structure which has a built-in load distributing and sharing capacity gives a factor of safety much higher than the safety factor adopted to working stresses. This

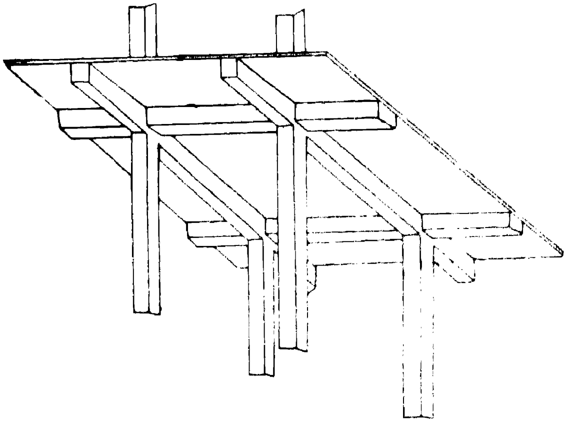

(a) Beam and slab construction

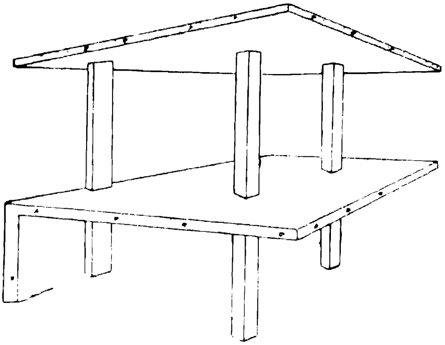

(b) **Flat** slab construction

Fig. 10.1.1 : Different types of slab construction

chapter discusses only an approximate analysis of slabs so that the readers who are not familiar with classical theory can design the slabs easily.

10.2. ONE-WAY SLAB : The bending moment at any point of a slab is represented by bending moments along the two perpendicular directions and twisting moment in the plane. Neglecting the Poisson's effect, the resisting moments along the two spans may be written as

$$M_x = -\frac{Et^3}{12}\frac{\partial^2 w}{\partial x^2} = \frac{Et^3}{12R_x} \quad \text{.. (10.2.1)}$$

$$M_y = -\frac{Et^3}{12}\frac{\partial^2 w}{\partial y^2} = \frac{Et^3}{12R_y} \quad \text{.. (10.2.2)}$$

where

w = deflection of the slab

R_x, R_y = radii of curvature of the bent slab

M_x = bending moment on x-plane

M_y = bending moment on y-plane

t = thickness of the slab

The bending moment curvature relations given in eqs. 10.2.1 and 10.2.2 could be obtained using a simple beam theory. Fig. 10.2.1 gives the sign convensions assumed in arriving at the moment curvature relations.

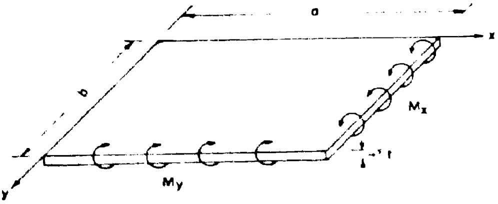

Fig. 10.2.1 : Slab notations

Bending moment is proportional to curvature. To compare the relative magnitudes of the bending moments, let the slab be bent in a shallow spherical surface for calculating the curvature. From fig. 10.2.2 the maximum curvatures could be written as

$$R_x \simeq \frac{a^2}{8\, w_{max}}$$

$$R_y \simeq \frac{b^2}{8\, w_{max}}$$

where

a = span of the slab in x-direction

b = span of the slab in y-direction

w_{max} = maximum deflection of the slab

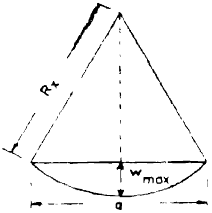

Fig. 10.2.2 : Curvature deflection relation

On substitution of the curvature relations, the ratio of moments works out to be

$$\frac{M_y}{M_x} = \frac{a^2}{b^2} \qquad \text{.. (10.2.3)}$$

Eq. 10.2.3 illustrates an approximate relative magnitude of bending moments in two directions. It can be seen that the moment in short span direction is much greater than that in the long span direction. For slabs where the span ratio is more than two, most of the load is carried by the short span, and the slab should be designed as one-way slab. An illustrative example of one-way slab is given below.

Example 10.2.1 : Design a prestressed concrete slab 5 by 20 m to carry a live load of 900 kg/sq m. The slab is simply supported on four sides.

Given data is

$f'_c = 450$ kg/cm, $f'_s = 15000$ kg/sq cm, and $\eta = 0.85$

Solution : The aspect ratio of the slab is 4 so the slab should be designed as one-way slab. Load balancing method is used by considering one unit width of the slab.

Let

$$t = \frac{\text{short span}}{40} = 12.5 \text{ cm, use } t = 12 \text{ cm}$$

All calculations are made considering one cm width of the slab with a parabolic cable profile.

Let

q_l = intensity of live load
q_g = intensity of self load
q_t = intensity of total load, then
$q_l = 9$ kg/m
$q_g = 0.01 \times 0.12 \times 24 = 2.88$ kg/m
$q_t = (q_l + q_g) = 11.88$ kg/m

Let the load balanced at working load condition be

$q_{be} = 7.5$ kg/m and $e = 3.0$ cm, then

$$P_e = \frac{q_{be} b^2}{8e} = 781 \text{ kg/cm width}$$

$$P_t = \frac{781}{\eta} = 920 \text{ kg/cm width}$$

$$q_{bt} = \frac{q_{be}}{\eta} = 8.8 \text{ kg/m}$$

Check for stresses at transfer condition:

Load not balanced = 2.88 − 8.8 = − 5.92 kg/m

$$f_{ct} = \frac{P_t}{A} + \frac{M}{Z} = \frac{920}{12} + \frac{5.92 \times 2500 \times 6}{8 \times 12 \times 12} = 137.4 \text{ kg/sq cm}$$

$$f_{tt} = -\frac{920}{12} + \frac{5.98 \times 2500 \times 6}{8 \times 12 \times 12} = -15.8 \text{ kg/sq cm (comp)}$$

Check for stresses at working load:

Load not balanced = 11.88 − 7.5 = 4.38 kg/m

$$f_{ce} = \frac{P_e}{A} + \frac{M}{Z} = \frac{781}{12} + \frac{4.38 \times 2500 \times 6}{8 \times 12 \times 12} = 110.6 \text{ kg/sq cm}$$

$$f_{te} = -\frac{P_e}{A} + \frac{M}{Z} = -19.4 \text{ kg/sq cm (comp)}$$

All the stresses are compressive and less than the permissible stresses; hence the section is suitable. The eccentricity at the mid-span is taken as 3 cm which gives a cover of 3 cm to centre of the steel. The clear cover provision is satisfied for 7 mm wires.

$$A_s = \frac{P_t}{0.7\, f'_s} = \frac{920}{10500} = 0.0875 \text{ sq cm}$$

Use 7 mm wires at 4.5 cm spacing.

Note : (a) Minimum clear cover of 2 cm is desired.

(b) Any additional reinforcement will lead to excessive stresses at transfer condition, so the steel requirement should be kept close to the design.

(c) A nominal longitudinal reinforcement of mild steel of 6 mm at 30 cm spacing should be used for temperature and secondary stresses.

There are two practical limitations in adopting load balancing design for slab constructions : (i) setting up a curved profile for a thin slab is difficult and more so if the eccentricity of the cables have to be changed along the long span ; (ii) in a slab which is supported on four edges, the maximum bending moment occurs at the middle of the short span and decreases slowly towards the edge. To adjust the cables and cable profiles to suit the varying bending moment along the long span is not easy. Straight cables in the slab may prove to be more economical in many small constructions.

Example 10.2.2 : Design a simply supported slab to cover an area of 20 by 5 m and to carry a load of 900 kg/sq m, using a straight cable profile. Compare this design with the design made by load balancing method of example 10.2.1.

Data given:

$f'_c = 450$ kg/sq cm, $f'_s = 15000$ kg/sq cm, and $\eta = 0.85$

Solution :

Let $t = \frac{\text{span}}{40} = 12.5$ cm, then $q_g = 0.125 \times \frac{2400}{100} = 3$ kg/m/cm

$\therefore$ $q_t = 12$ kg/m/cm width

Let the cable be placed at 2.0 cm eccentricity and with no tensile stress at working load. This leads to (by considering 1 cm width)

$$f_{te} = -\frac{P_e}{A} - \frac{P_e\,e}{Z} + \frac{M}{Z} = 0$$

$$= -P_e\left[\frac{1}{12.5} + \frac{2\times 6}{12.5\times 12.5}\right] + \frac{12\times 2500\times 6}{8\times 12.5\times 12.5} = 0$$

or $P_e = 920$ kg/cm

$\therefore$ $P_t = 920/\eta = 1080$ kg/cm

$$f_{ct} = \frac{P_t}{A} + \frac{P_t e}{Z} - \frac{M_g}{Z} = 137.0 \text{ kg/sq cm}$$

$$f_{tt} = -\frac{P_t}{A} + \frac{P_t e}{Z} - \frac{M_g}{Z} = -41 \text{ kg/sq cm (comp)}$$

$$f_{ce} = \frac{P_e}{A} - \frac{P_e e}{Z} + \frac{M_t}{Z} = 143 \text{ kg/sq cm}$$

$$f_{te} = 0$$

All the stresses at the middle of the span are within the limits. The eccentricity at the edge of the span is 2 cm so it is desirable to check for stresses at the end section. Eccentricity is within the kern distance so no tensile stresses are developed. The compressive stress at transfer will dominate and is given by

$$f_{ct} = \frac{P_t}{A} + \frac{P_t e}{Z} = 169.3 \text{ kg/sq cm}$$

All the stresses at any cross section are within the permissible limits.

$$A_s = \frac{P_t}{0.7 f'_s} = \frac{1080}{10500} = 0.103 \text{ sq cm}$$

Use 7 mm wires at 3.75 cm apart. A nominal mild steel reinforcement of 6 mm wires at 30 cm apart should be provided in the longitudinal direction.

A straight cable profile increases the area of steel and concrete requirements by 17.5% and 4.17% respectively as compared to balanced load design (curved cable profile). If a controlled curved cable profile can be set at less expense, then the curved cable profile is more economical.

10.3. TWO-WAY SLAB: The external load on a slab is distributed on both the spans if the span ratio of the slab is in the range of 1 to 2. In such slab construction, prestressing is to be done in both the directions. If z define the cable profiles for cable running in both the directions, the effective vertical component of the cable force is then given by

$$q_b = P_{ta} \frac{\partial^2 z}{\partial x^2} + P_{tb} \frac{\partial^2 z}{\partial y^2} \quad \text{.. (10.3.1)}$$

where

P_{tb} = prestressing force in short span

P_{ta} = prestressing force in long span

q_b = balancing load

z = discrete function defining the cable profiles both in x and y directions.

Let

e_b = maximum eccentricity of cable in short span direction

e_a = maximum eccentricity of cable in long span direction,

then for parabolic cable profiles, the balancing load is given by

$$q_b = 8 \left[\frac{P_{ta}\, e_a}{a^2} + \frac{P_{tb}\, e_b}{b^2} \right] \quad \text{.. (10.3.2)}$$

The load that is not balanced should be considered for calculation of bending moment stresses and deflections.

There are several approximate formulae developed for calculation of bending moments in slabs. The moment coefficient of slabs based on orthotropic plate theory are used in the present calculations. In the absence of these coefficients, the designer can use the regular plate theory coefficients. A modified orthotropic plate theory (10.1) divides the slab into middle and end strips and suggests bending moment coefficients. The strip partitions are shown in fig. 10.3.1 and the bending moment coefficients are given in fig. 10.3.2. The design bending moments are given by

$$
\begin{aligned}
M_{b1} &= \beta_1 q\, b^2 \\
M_{b2} &= \beta_2 q\, b^2 \\
M_{a1} &= \beta_3 q\, b^2 \\
M_{a2} &= \beta_4 q\, b^2 \\
M_{ab} &= \beta_5 q\, b^2
\end{aligned}
\qquad \text{.. (10.3.3)}
$$

where

β_1, β_2, β_3, β_4 and β_5 are the bending moment coefficients (fig. 10.3.2)

M_{b1} = maximum bending moment for middle half of the short span

M_{b2} = maximum bending moment for extreme quarter of the short span

M_{a1} = maximum bending moment for middle half of the long span

M_{a2} = maximum bending moment for the extreme quarter of the long span

M_{ab} = maximum twisting moment which occurs at the corners

b = short span length

The design of two-way slab is illustrated through an example.

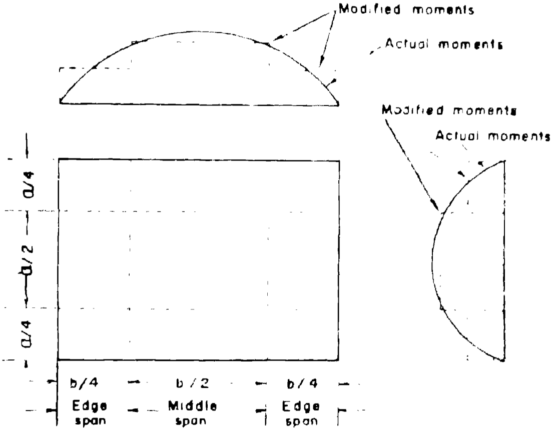

Fig. 10.3.1 : Modified and actual moments in a two-way slab

Example 10.3.1 : Design of a 8 by 10 m simply supported slab to carry a load of 600 kg/sq m.

Given data :

$f'_c = 450$ kg/sq cm, $f'_s = 15000$ kg/sq cm

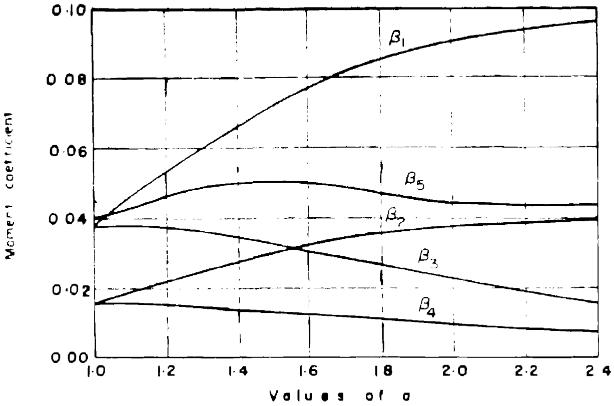

Fig. 10.3.2 : Moment coefficient graphs

Let $t = b/50 = 16$ cm

cover in short span = 3 cm, $\therefore e_b = 5$ cm and

cover in long span = 3.7 cm, $\therefore e_a = 4.3$ cm

Solution : (Design for one cm width of each strip)

$q_g = 0.16 \times 0.01 \times 24 = 0.0384$ kg/sq cm

$q_l = 0.06$ kg/sq cm

Let $q_B = 0.004$ kg/sq cm

$\therefore$ $q_t = 0.1024$ kg/sq cm

It is desirable to select the balancing load proportional to the external load distribution. The bending moment is shown to be inversely proportional to the square of the span of the corresponding direction. Therefore the load taken by the span would be inversely proportional to the fourth power of the span. (The load is directly proportional to the moment and inversely proportional to the square of the span).

$\therefore$ The load on span is proportional to $\left(\dfrac{a^4 q}{a^4 + b^4}\right)$ and

the balancing load is $\dfrac{8\, P_{tb} e_b}{b^2}$

$$\frac{8\, P_{tb} e_b}{b^2} = \frac{a^4\, q_{bt}}{a^4 + b^4} \qquad \text{.. (10.3.4)}$$

$$\text{or} \quad P_{tb} = \frac{a^4\, b^2\, q_{bt}}{8\,(a^4 + b^4)\, e_b} \qquad \text{.. (10.3.5)}$$

Similarly

$$P_{ta} = \frac{b^4\, a^2\, q_{bt}}{8\,(a^4 + b^4) e_a}$$

Let $q_{bt}=0.07$ (vs $q_g=0.0384$ and $q_t=0.1024$)

Then from eq. 10.3.5

$$P_{tb}=\left(\frac{10^4}{10^4+8^4}\right)\left(\frac{64}{8\times5}\right)(10000\ q_{bt})=800 \text{ kg/cm width}$$

$$P_{ta}=\left(\frac{8^4}{10^4+8^4}\right)\left(\frac{100}{8\times4.3}\right)10000\ q_{bt}=700 \text{ kg/cm width}$$

Load that is not balanced at transfer condition

$$=0.0384—0.07=-0.0316 \text{ kg/sq cm}$$

The bending moment coefficients for two-way slab from fig. 10.3.2 can be obtained as (for $a/b=1.25$)

$$\beta_1=0.055,\ \beta_2=0.025,\ \beta_3=0.038$$
$$\beta_4=0.018,\ \beta_5=0.046$$

Therefore corresponding bending moments from eq. 10.3.3 are

$M_{b1}=0.055\times0.0316\times640000=1110$ kg cm/cm

$M_{b2}=505$ kg cm/cm

$M_{a1}=765$ kg cm/cm

$M_{a2}=365$ kg cm/cm

$M_{ab}=930$ kg cm/cm

Check for stresses at transfer :

$$f=\frac{P_{tb}}{A}\pm\frac{M_{b1}}{Z}=\frac{800}{16}\pm\frac{1110\times6}{256}=50\pm26$$

$f_{ct}=50+26=76$ kg/sq cm

$f_{tt}=-50+26=-24$ kg/sq cm (comp)

It is not necessary to check for the stresses in the extreme quarter strip as the stresses in the middle strip are within the allowable limits.

Check for stresses at working load condition :

$P_{eb}=\eta\ P_{tb}=0.85\times800=680$ kg/cm width

Load that is not balanced $=q_t-0.85\ q_{bt}=0.0429$ kg/sq cm

$$f_{ce}=\frac{P_{eb}}{A}+\frac{M_{b1}}{Z}=42.5+35.2=77.7 \text{ kg/sq cm}$$

$f_{te}=-42.5+35.2=-7.3$ kg/sq cm (comp)

As the stresses at the critical section are much below the limiting stresses, it is not necessary to check for the stresses at the other sections. The area of steel may be obtained as

$$A_{sb}=\frac{P_{tb}}{f_{st}}=\frac{800}{10500}=0.071 \text{ sq cm/cm width}$$

$$A_{sa}=\frac{P_{ta}}{f_{st}}=\frac{700}{10500}=0.067 \text{ sq cm/cm width}$$

Since the stresses are much below the allowable limits, the thickness of the slab could be reduced to 15 cm. With 15 cm thick slab, the stresses are found to be within the limits.

Adopt the following:

Thickness of slab $= 15$ cm,

$A_{sb} = 0.071$ sq cm, $A_{sa} = 0.067$ sq cm

in which A_{sa} and A_{sb} are the reinforcement in the long and short span directions.

Maximum percentage of reinforcement is about 0.5 percent. Additional reinforcement to take care of twisting moment has to be provided.

Check for deflection : Elastic theory of plates can be applied to prestressed concrete slabs even for deflection measurements. The deflection coefficients can be taken from the theory of plates. In the present section, the deflection coefficients are taken from "Theory of plates and shells" by Timoshenko (10.2).

Let

δ_t = maximum deflection at transfer condition

δ_e = maximum deflection at working load condition

The deflection for a plate of aspect ratio 1.25 is given as

$$\delta = \frac{0.006\, q\, b^4}{E_c I}$$

$$\therefore \quad \delta_t = \frac{0.006 \times (-0.0316) \times 800^4}{1/12 \times 15^3 \times 3.82 \times 10^5} = -0.78 \text{ (upward)}$$

(prorating the deflection for unbalanced load)

$$\delta_e = (0.78)\left(\frac{4.29}{3.16}\right) = 1.06 \text{ cm.}$$

(The unbalanced loads are taken same as the original because there is not much deviation in the final section).

A reinforced cement concrete slab will deflect by about 2.3 cm for the same live load conditions assuming an uncracked section. So the deflection of prestressed concrete slab is very small as compared to a reinforced concrete slab. This characteristic behaviour is very useful for large spans.

Ultimate load capacity of a slab is much higher than the ultimate capacity of the section. A slab will not fail by yielding at any one particular cross section but fails by yielding at several sections in a pattern so that the total slab forms into a collapsable mechanism. Calculation of the ultimate load of a slab by yield line theory is not discussed in this section.

10.4. PRESTRESSED CONCRETE BEAM AND SLAB CONSTRUCTION: Prestressed concrete beam and slab construction is not very popular because of the constructional difficulties and economical considerations. Prestressing operations in beam and slab construction are too involved to be very economical. Use of precast prestressed beams appear to be a more logical method of construction and has gained some popularity in the field. In such a case of construction, the design could be done independently for beams and for slab, treating the beam as a composite construction.

10.5. PRESTRESSED CONCRETE FLAT SLAB: Prestressed concrete flat slab construction gained great importance because of several reasons that yielded in economy. Flat slab constructions has the adaptability for any type of building requirements, ease in form work, casting of concrete and prestressing operations (10.3 to 10.7). Lift slab construction which forms a part of flat slab construction has gained importance because of the ease in prestressing and form work operations. Lift slab construction is the one in which all the floors are cast in sequence at ground level, prestressed and lifted to the corresponding floor level by proper hoisting arrangements. There are three positive advantages in lift slab construction: (i) the flat surface of the slab gives an advantage and economy in casting the slabs at one level, one over the other with practically no money and time involved in shuttering arrangements; (ii) prestressing operations do not involve in any temporary hoisting and supporting arrangements; and (iii) the self weight of the slab is small as compared to any other construction. The methods for lift slab construction are changing fast to suit the availability of equipment and personnel.

Lifting of the slab is done with a mechanical or hydraulic jacking system using the building columns as supports. Fastening the slab to columns and other details are not discussed in this chapter.

Design of Prestressed Concrete Flat Slab: Flat slabs are invariably continuous so it is desirable to discuss the design of continuous flat slabs. Analysis of continuous flat plate supported on column presents a complex statically indeterminate structural problem. An exact analysis is difficult, so an approximate analysis based on wide beam theory is presented here. Approximate moment coefficients are available in "Theory of plates and shells" by Timoshenko (10.3) which can be used in design. The flat slab could be treated as two sets of continuous beams, each set spanning in one direction. Fig. 10.5.1 illustrates the approximation made. The approximation of beam theory assumes that the flat slab is treated as a wide beam rigidly supported along the column line.

The design bending moments either at support or at middle of any span are computed based on continuous beam theory treating the total width of the slab as the width of the beam. The total bending moment is then redistributed along the width giving a higher weightage

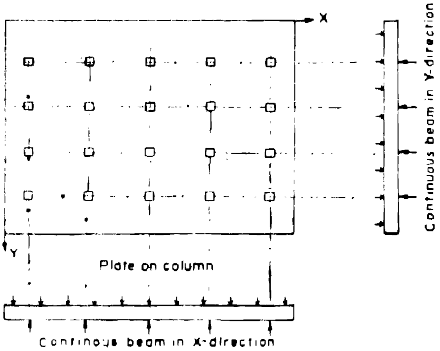
X
Continuous beam in Y-direction
Y
Plate on column
Continuous beam in X-direction

Fig. 10.5.1 : Flat slab on columns approximated as beams in two directions

to the column strip as compared to the middle strip. The weightage of column and middle strip bending moments depend upon the number of columns along the width of the assumed continuous beam. The bending moment is proportional to the rate of change of slope of the deflected slab profile. The rate of change of slope of column strip is much higher than that of a middle strip. The division of strips, its qualitative behaviour and approximate bending moments along the width of the slab are shown in fig. 10.5.2.

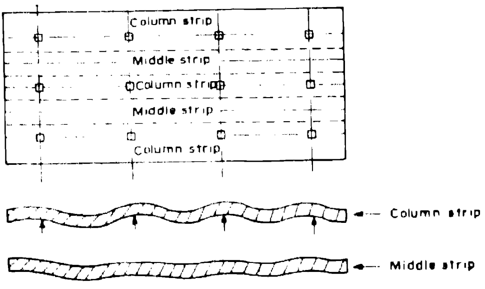

(a) Deformation of column and middle strips

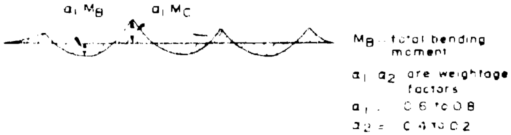

(b) Bending moments on column strip

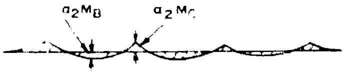

(c) Bending moments on middle strip

Fig. 10.5.2 : Column middle strip distribution in flat slab

Two methods of design are discussed in this section: (i) if the cable profile could be made in a curved form, then load balancing method of design is used; (ii) if a straight cable profile is adopted, then simple beam column theory is adopted. The bending moment profile is not very well known in a flat slab and even if an approximate moment profile is determined, it changes very rapidly so the adjustment of cable profile to suit the bending moment profile in balancing the load is not an easy practicable task and the loss of prestress due to curvature is relatively high. Hence a straight cable profile appears to be a more realistic and practicable solution in flat slab. An illustrative example using the two methods is given.

Example 10.5.1 : An area of 32 by 40 m is to be covered by a flat slab for a live load of 500 kg/sq m. Design a prestressed concrete flat slab.

Given data :

$f'_c = 450$ kg/sq cm, $f'_s = 15000$ kg/sq cm
column spacing $= 800$ cm and

$$\text{thickness of slab} = \frac{800}{40} = 20 \text{ cm}$$

Solution: The spacing of the columns and the corresponding bending moments based on beam theory are shown in fig. 10.5.3. The design is worked out by load balancing method with parabolic cable profile.

It is desirable to assume a parabolic cable profile with constant radii in all the spans. This keeps the balancing loads constant in the slab. The design is done for column and middle strip in one direction,

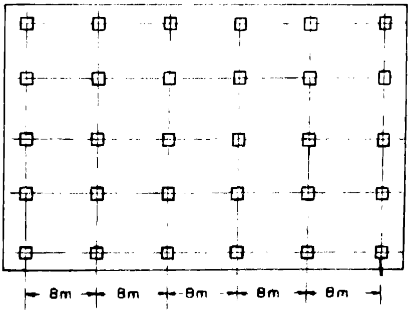

(a) Position of columns

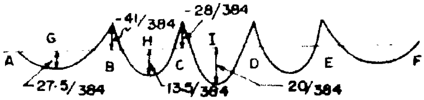

(b) Bending moment coefficient (qL^2)

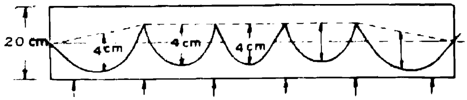

(c) Cable profile of column strip

Fig. 10.5.3 : Flat slab design example

and since the bending moments in the second direction are of same order as those in other direction, the same prestressing is adopted in second direction.

Design of column strip :

$q_g = 2400 \times 0.20 = 480$ kg/sq m

$q_l = 500$ kg/sq m, $\therefore q_t = 480+500=980$ kg/sq m

Let $g = 4$ cm (where g is maximum sag) and the intensity of load balanced at transfer be q_{bt} and it is

$q_{bt} = 1000$ kg/sq m

Now $q_{bt} = \dfrac{8g}{a^2}(P_{ta}+P_{tb})$

As the spans are equal, let $P_{ta}=P_{tb}=P_t$

Then $P_t = \dfrac{1000 \times 64}{16 \times 0.04} = 100000$ kg/m width

$f_{ave} = P_t/A$

$= \dfrac{100000}{20 \times 100} = 50$ kg/sq cm

The prestressing cable changes its direction giving a downward component along the column line which increases the bending moments at working load conditions of the column strip. To reduce the vertical component along the column line, it is desirable to take minimum eccentricity of the cable. It will also be seen that the compressive stresses are not really governing so the prestressing force could be increased and the eccentricity decreased. A free body diagram of prestressing cable force is shown in fig. 10.5.4. An exact analysis and design for this type of force system is difficult. It may be observed that the vertical component of the prestressing force at column line is $[8P_tg/L]$. For the particular slab, this component force distributed over the entire area of the column strip (8×4) gives intensity of load equal to 1000 kg/sq m. The analysis should be done by including this vertical component force.

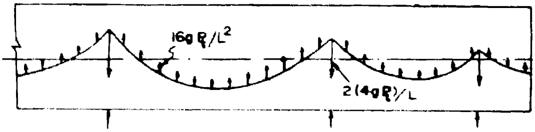

(a) Vertical force component of the cable

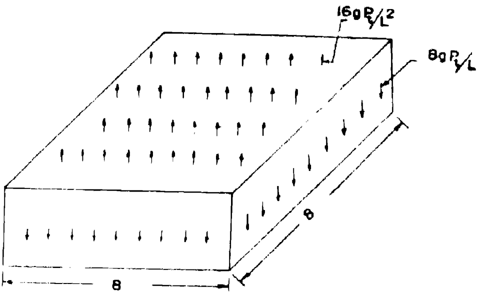

(b) One unit of slab

Fig. 10.5.4 : Free body diagram of one panel slab with equivalent prestressing forces

Load not balanced on the column strip at transfer

$$= 480 - \frac{1000}{2} + \frac{1000}{2} = 480 \text{ kg/sq m}$$

Load not balanced on the middle strip at transfer

$$= 480 - 1000 = -520 \text{ kg/sq m}$$

(The —ve sign indicates load acting upward)

The effective intensity of load on one panel width may be taken as the mean of the intensities on the column and middle strips.

The effective intensity of load on the slab at transfer

$$= \frac{480-520}{2} = -20 \text{ kg/sq m}$$

This effective load at transfer is negligibly small, therefore the stresses caused due to flexure are very small. The stresses at top and bottom of the slab be taken equal to

$$\frac{P_t}{A} = 50 \text{ kg/sq cm}$$

The maximum bending moment occurs at the support B and this moment at transfer (fig. 10.5.3 for moment coefficient)

$$M_{bt} = -\frac{41\, q\, a^2}{384} = \frac{41 \times 20 \times 8 \times 8}{384} = 137 \text{ kg m/m}$$

$$= 13700 \text{ kg cm/m}$$

This moment is shared by the column and middle strips. Let the column strip be assumed to carry 70 percent of the moment while the middle strip carries the rest of the moment. The bending moments of column and middle strips are denoted by a superscript of c and m respectively.

$$M^c_{bt} = 0.7 \times 13700 = 9590 \text{ kg cm/50 cm}$$

$$M^m_{bt} = 0.3 \times 13700 = 4110 \text{ kg cm/50 cm}$$

Check for stresses in the column strip at transfer condition :

$$f_{ct} = \frac{P_t}{A} + \frac{M^c_{bt}}{Z} = \frac{100000}{20 \times 100} + \frac{9590 \times 6}{50 \times 20 \times 20}$$

$$= 50 + 2.8 = 52.8 \text{ kg/sq cm}$$

$$f_{tt} = -\frac{P_t}{A} + \frac{M^c{}_{bt}}{Z} = -50+2.8 = -47.2 \text{ kg/sq cm.}$$

Both the stresses are within the permissible limits.

Check for stresses in the column strip at working load :

$$P_e = 0.85\ P_t = 85000 \text{ kg/m}$$

Load not balanced in the column strip

$$= 980 - \frac{850}{2} + \frac{850}{2} = 980 \text{ kg/sq m}$$

Load not balanced in the middle strip

$$= 980-850 = 130 \text{ kg/sq m}$$

$$\text{Mean intensity of load} = \frac{980+130}{2} = 555 \text{ kg/sq m}$$

$$M^c{}_{be} = (0.7)\left(-\frac{41}{384}\,qa^2\right)$$

$$= -\frac{0.7 \times 41 \times 555 \times 8 \times 8}{384} = -2570 \text{ kgm/50 cm}$$

$$= -257000 \text{ kg cm/50 cm}$$

$$f_{ce} = \frac{P_e}{A} + \frac{M^c{}_{be}}{Z} = \frac{85000}{100 \times 20} + \frac{257000 \times 6}{50 \times 20 \times 20}$$

$$= 42.5+77.2 = 119.7 \text{ kg/sq cm}$$

$$f_{te} = -\frac{P_e}{A} + \frac{M^c{}_{be}}{Z} = -42.5+77.2 = 34.7 \text{ kg/sq cm}$$

Similar computation for stresses for the middle strip both for positive and negative bending moments is to be made.

To keep the balancing force constant throughout the slab, it is desirable to keep the prestressing force and eccentricity same both in the middle and column strips. This adoption is not very economical as it takes higher steel content. An approximate and effective economy could be obtained by redistributing the cables so that a higher intensity is provided in the column strip as compared to the middle strip.

$$A_s = \frac{P_t}{0.7\,f'_s} = 8.88 \text{ sq cm/m}$$

The load balancing method discussed in this example is an approximate method. The approximations could be justified because of symmetry in loads and also the number of spans are more than three. There are some practical difficulties in setting up the alignment. The loss of prestress due to the curvature is also considerable. To avoid the design and the practical difficulties, it is some times advantageous to provide a straight cable across the slab. Such a cable when provided eccentrically will generate secondary bending moments. Determination of the secondary bending moments is difficult. Therefore it is desirable to keep the cable at the centroidal axis or at least very close to it. The secondary bending moments may be negligible in case of very small eccentric straight cables. The method is illustrated through an example.

Example 10.5.2 : An area of 32 × 40 m is to be covered by a flat slab and it is subjected to 500 kg/sq m of live load. Design a slab assuming a straight cable profile (same as example 10.5.1 with a change in the cable profile).

Given data :

$f'_c = 450$ kg/sq cm, $f_{st} = 10500$ kg/sq cm
$f'_s = 15000$ kg/sq cm, column spacing = 800 cm and
thickness of slab = 24 cm

Solution :

The spacing of the columns and the corresponding bending moment based on beam theory are shown in fig. 10.5.3 (same as adopted in example 10.5.1). The slab is subjected to positive and negative bending moments and the negative bending moment dominates the design. So adopt a negative eccentricity of 1 cm straight cable.

$$q_g = 2400 \times 0.24 = 576 \text{ kg/sq m}$$
$$q_l = 500 \text{ kg/sq m}$$
$$\therefore \quad q_t = 1076 \text{ kg/sq m}$$

Design of column strip at support B : Let there be no tensile stress, present at working load condition at the support B then

$$f_{te} = 0 = \left(\frac{P_e}{A} + \frac{P_e e}{Z} - \frac{M^c_{be}}{Z}\right) \text{ or } \frac{P_e}{A} = 0.2\,f'_c \quad \ldots (10.5.1)$$

It is assumed that 70 percent of the moment is taken by the column strip and 30 percent by the middle strip. Then

$$M^c_{be} = \frac{41}{384} \times 1076 \times 8 \times 800 \times 0.7 = 513000 \text{ kg cm/50 cm}$$

$$M^m_{be} = \frac{41}{384} \times 1076 \times 8 \times 800 \times 0.3 = 221000 \text{ kg cm/50 cm}$$

The substitution of M^c_{be} in eq. 10.5.1 gives

$$\frac{P_e}{A} = 0.2\,f'_c$$

$$\therefore \quad P_e = 102600 \text{ kg/50 cm}$$

$$P_t = \frac{102600}{0.85} = 121000 \text{ kg/50 cm}$$

Check for stress at support B of the column strip :

$f_{te} = 0$

$$f_{ce} = \frac{P_e}{A} - \frac{P_e e}{Z} + \frac{M^c_{be}}{Z} = \frac{102600}{50 \times 24} - \frac{102600 \times 6}{50 \times 24 \times 24} + \frac{513000 \times 6}{50 \times 24 \times 24}$$
$$= 85.8 - 21.5 + 107 = 171.3 \text{ kg/sq cm}$$

Check for stresses at mid span of column strip :

M^c_{ge} = moment coefficient = 27.5/384

$$f_{te} = -\frac{P_e}{A} + \frac{P_e e}{Z} + \frac{M^c_{ge}}{Z} = -85.8+21.5+72 = 7.7 \text{ kg/sq cm}$$

$$f_{ce} = \frac{P_e}{A} + \frac{P_e e}{Z} + \frac{M^c_{ge}}{Z} = 85.8+21.5\times72 = 179.3 \text{ kg/sq cm}$$

Stresses at other points of the span need to be checked.

$$A_s = \frac{121000}{10500} = 11.5 \text{ sq cm/50 cm}$$

Use 60 wires of 7 mm diameter per metre width in two or three rows or in strand.

Design of middle strip : The bending moments at the middle strip are 3/7 of the column strip. Therefore the prestressing force could be about half of the column strip and the stresses be checked.

Let

$$P_e = \frac{102600}{2} = 51300 \text{ kg/50 cm}$$

Check for stresses at support of middle strip :

$$f_{te} = -\frac{P_e}{A} - \frac{P_e e}{Z} + \frac{M^m_{be}}{Z} = -42.6-10.8+48$$

$$= -7.4 \text{ kg/sq cm}$$

$$f_{ce} = 42.6 - 10.8 + 46 = 78.1 \text{ kg/sq cm}$$

$$f_{tt} = -\frac{P_t}{A} + \frac{P_t e}{Z} - \frac{M^m_{bt}}{Z} < \text{(permissible)}$$

$$f_{ct} = \frac{P_t}{A} - \frac{P_t e}{Z} - \frac{M^m_{bt}}{Z} < \text{(permissible)}$$

Check for stresses at middle of the middle strip :

$$f_{te} = -\frac{P_e}{A} + \frac{P_e e}{Z} + \frac{M^m_{ge}}{Z} = -42.6+10.8+31$$

$$= -0.8 \text{ kg/sq cm} \qquad \text{(permissible)}$$

$$f_{ce} = \frac{P_e}{A} + \frac{P_e e}{Z} + \frac{M^m_{ge}}{Z} < \text{(permissible)}$$

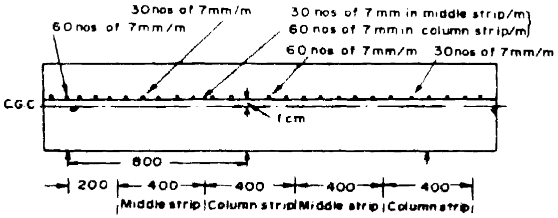

Fig. 10.5.5 : Reinforcement in slab—Example (10.5.2)

Use 30 wires of 7 mm diameter for one metre width. Fig. (10.5.5) gives steel distribution in half of the slab.

Problems

10.1 There are three parallel walls of 20 m long and spaced at 3m apart with two end walls. Design a prestressed concrete slab to cover the area. Use $f'_c=400$ kg/sq cm, $f'_s=15000$ kg/sq cm. The working load on the slab be taken as 500 kg/sq m.

10.2 Design a two-way slab to cover an area of 4 by 6 m and to carry a working load of 600 kg/sqm. The slab be designed as prestressed in both the directions with straight cables. Use $f'_c=400$ kg/sq cm and $f'_s=15000$ kg/sq cm.

10.3 A small building consists of three rooms and the plan of which is shown in fig. 10.1. The live load to be carried by the roof is 240 kg/sqm. Design a single flat slab to cover the entire area. Use $f'_c=400$ kg/sq cm and $f'_s=15000$ kg/sq cm.

Hint : The slab is to be assumed as simply supported on the outer walls. The continuity of the slab over the intermediate walls be idealised as fixed edge support. The appropriate bending moment coefficients for slabs with different edge conditions may be taken from the code specifications. The fixed end bending moments for two adjacent slabs at the common support are likely to be different. Take a mean of the fixed edge bending moments at the intermediate support and design a cable going from one end of the slab to the other end. Do not curtail the cables at the intermediate wall level.

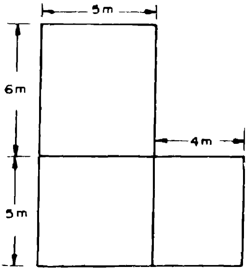

Fig. 10.1—Problem 10.3

10.4 An area of 30 by 40 m is to be covered by a flat slab with a working load of 400 kg/sq m over the slab. Design the slab as supported on columns spaced at 6 m and 8 m in the 30 m and 40 m directions respectively. Use $f'_c=400$ kg/sq cm and $f'_s=15000$ kg/sq cm.

CHAPTER XI

FOLDED PLATE AND SHELL STRUCTURES

11.1. INTRODUCTION : The efficiency of a structure depends upon the effective use of materials in the structure. Shell structures have an inherent advantage in their geometry to distribute the load effectively to all the material instead of concentrating the load resistances to any particular portion. The load carrying capacity of the shells depends basically on the shape of the structure rather than on the mass of materials used. Even though the shells are very efficient structures, their use is limited to specific purposes due to other utility criteria. They are generally used as roof structures and sometimes as foundation structural elements. There is a positive aesthetic advantage in using these structures for roof elements. The architect has a great flexibility in adopting any desired shape and curve to express the human imagination through the structures. Conventional shells such as cylindrical and spherical shells are not very difficult to analyse for given standard boundary conditions. Shells of double curvature and shells of arbitrary curves accommodate the imagination of architects but are rather difficult to analyse. Approximate methods or experimental techniques are used as a basis of design in such complicated shell structures. Analysis of prestressed concrete shell structures presents much more sophistication as compared to the reinforced concrete shells. The use of prestressing is commonly adopted for conventional shells such as cylindrical, spherical and folded plates without much difficulty. This chapter presents some simplified and approximate analysis which are good for most of the practical problems. The book is designed essentially for those who are not familiar with the theory of shells. Readers who would like to have more detailed information are referred to some of the standard books on shell theory (11.1—11.6).

11.2. ANALYSIS OF FOLDED PLATES : Folded plates may be broadly classified into three groups such as long, intermediate and short folded plates. When the length to rise ratio of the folded plate is greater than 10, it is called long plate ; otherwise it falls into one of the two remaining categories. Methods of analysis of folded plates are generally classified as (i) beam method ; (ii) folded plate theory neglecting the relative joint displacements ; (iii) folded plate theory considering relative joint displacements ; and (iv) elasticity approach. Beam method which comes out of simple statics uses the beam formula, treating the folded plate as a beam. This method, which is based on linear stress variation in cross-section of the fold, neglects the transverse slab bending moments and therefore the method is dependable for long folded plates. Folded plate theory neglecting the relative joint displacements assumes that the plates are relatively deep in their own plane so as to provide transverse supporting reactions at the folds. Thus the folded plate in the transverse direction is treated as continuous one-way slab. This method, even though it makes a better approximation than beam theory, is still an approximate method and likely to give transverse bending moments of the slab higher than the actual ones. The third folded plate theory which considers the relative joint displacements, is much improved and more accurate. It can be applied to most of the folded plates except very short plates. The fourth method which is the most accurate of all, treats the structure as a continuum and uses an elasticity approach. The presentation of this method is beyond the scope of this book. The first two methods are fairly straight forward and do not need much explanation. Therefore only the third method—folded plate theory considering relative joint displacements, is described in this book.

The folded plate theory considering the relative joint displacements separates the structure into two structural actions. The slab in the transverse direction is treated as a continuous slab on elastic supports and the forces in the slab are evaluated using slope-deflection equations. The plate in the longitudinal direction is treated as a beam subjected to the forces in its plane. Displacements at the folds are used as compatibility conditions between the transverse slab and longitudinal beam actions (11.7).

(*i*) *Slab action* : Fig. 11.2.2 illustrates the two actions of folded plate, (a) slab action, and (b) beam action. Plane of any plate is taken as xy plane while x-axis is considered to be the longitudinal axis of the plate. For the purpose of analysis, all external loads on the plate are resolved into two perpendicular directions. One is transverse to the plate and the other is in the plane of the plate. All external loads are assumed to be of harmonic function (sin $n\pi x/L$) so as to simplify the analysis of force and deformation relations in the longitudinal section of the folded plate. Any distributed load is approximated as an equivalent harmonic load and the results are deduced from it.

Analysis : Let the load on any slab connecting i and i+1 joints be represented by

$$q_{ii+1} = q \sin \frac{\pi x}{L}$$

where

L=length of the folded plate

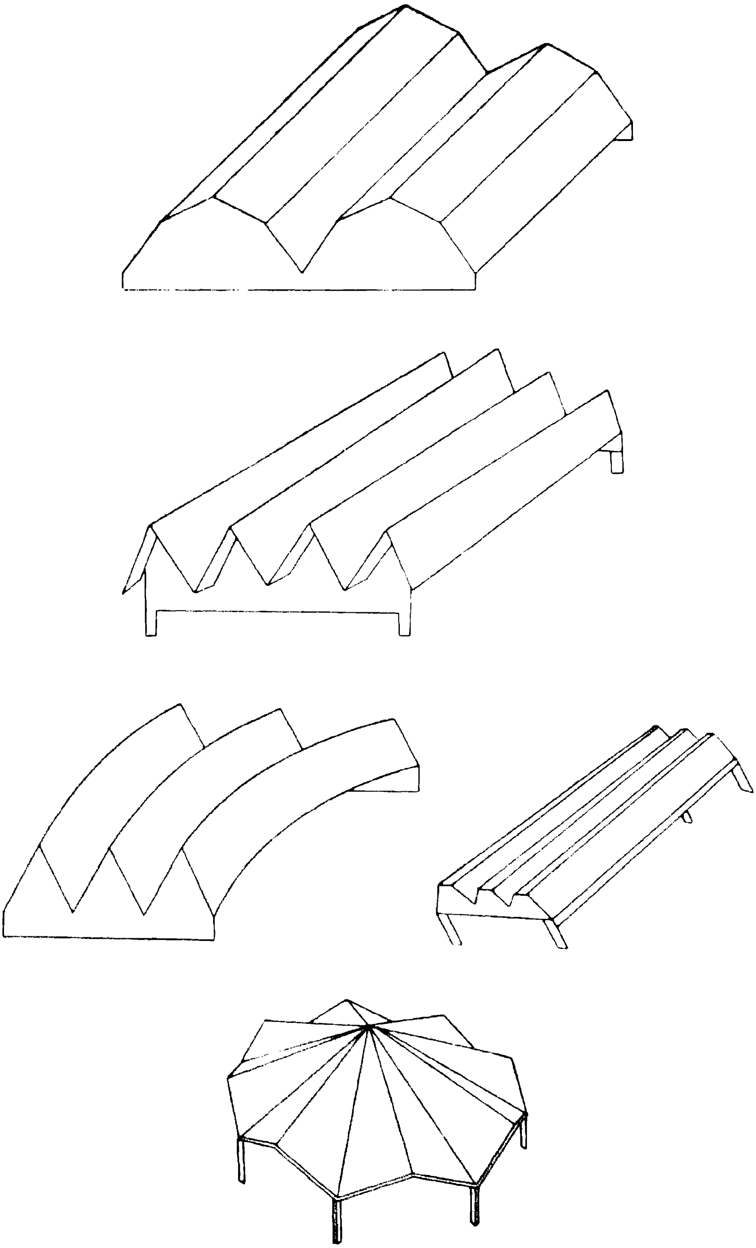

Fig. 11.2.1 : Typical folded plate

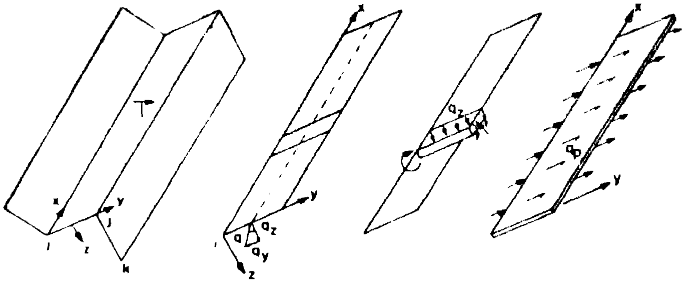

Folded plate, Load components, Slab strip action in yz plane Beam action in xy plane

Fig. 11.2.2 : Folded plate structural action

q_{ii+1}=intensity of load acting vertically downwards

Let q_z and q_y be the components of the distributed load q in z and y-directions respectively. The forces and deformations used in the derivations are shown in fig. 11.2.3.

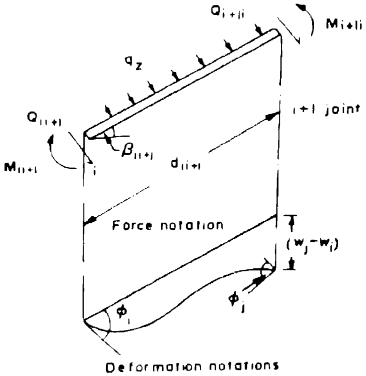

Fig. 11.2.3 : Slab strip spanning between i and i+1 joints

Considering a unit width of the slab spanning between i and i+1 joints, the force deformation relations could be written as

$$\left.\begin{aligned}
m_{ii+1} &= m_{fii+1} + k_{ii+1}\,(2\phi_i + \phi_{i+1} - 3\delta_{ii+1}) \\
m_{i+1i} &= m_{fi+1i} + k_{ii+1}\,(2\phi_{i+1} + \phi_i - 3\delta_{ii+1}) \\
Q_{ii+1} &= \frac{(m_{ii+1} - m_{i+1i})}{d_{ii+1}} - \frac{q_z d_{ii+1}}{2} \\
Q_{i+1i} &= \frac{m_{i+1i} - m_{ii+1}}{d_{ii+1}} - \frac{q_z d_{ii+1}}{2}
\end{aligned}\right\} \quad \ldots \quad (11.2.1)$$

where

m_{ii+1}=bending moment at joint i of slab connecting i and i + 1 joints

Q_{ii+1} =shear force at joint i of slab connecting i and i+1 joints

ϕ_i =rotation of joint i

$k \quad = \frac{2Et^3}{12d}$

$d \quad =$ width of slab

Moment compatibility at joint i yields

$$m_{ii-1} = m_{ii+1} = m_i$$

The compatibility equations lead to three moment equations as

$$\frac{m_{i-1}}{k_{i-1i}} + m_i\left(\frac{1}{k_{i-1i}} + \frac{1}{k_{ii+1}}\right) + \frac{m_{i+1}}{k_{ii+1}} = 6\left(\delta_{i-1i} - \delta_{ii+1}\right)$$

$$+ \frac{1}{k_{i-1i}}\left(2\,m_{fi} + m_{fi-1}\right) + \frac{1}{k_{ii+1}}\left(2\,m_{fi} + m_{fi+1}\right) \quad .. \quad (11.2.2)$$

Eq. 11.2.2. is essentially a governing equation of the ith joint, containing one moment and deflection of the joint. If there are N joints, there will be N equations involving 2N unknowns. N unknowns could be evaluated from the N joint equations and the other N unknowns will have to be determined from the deflection compatibility of the slab and the longitudinal beam action.

(*ii*) *Beam action* The three types of loads acting on the beam element are shown in fig. 11.2.4.

(i) Component of the distributed load (q_y) in the plane of the plate ;

(ii) component of the slab transverse shear force (Q) ;

(iii) component of the line load acting at the joint or fold.

The line load at the joint is first resolved into components along with the transverse shear (Q). The effect of the plane force is determined as shown in fig. 11.2.4.

Let

S_i -- line load at the ith joint

$$= S \sin \frac{\pi x}{L}$$

R_{ii-1} = combined effect of the line load and the transverse shear Q at the ith joint, transverse to plate ii−1

Similarly R_{ii+1}

Then the forces at the fold are given by

$$\left.\begin{aligned} R_{ii-1} &= S_{ii-1} + Q_{ii-1} \\ R_{ii+1} &= S_{ii+1} + Q_{ii+1} \end{aligned}\right\} \quad .. \quad (11.2.3)$$

The components of fold forces in the plane of the plates are given by

$$\left.\begin{aligned} P_{ii-1} &= -\left(R_{ii-1}\,\mathrm{Cos}\,\alpha_i + R_{ii+1}\right)\mathrm{cosec}\,\alpha_i \\ P_{ii+1} &= \left(R_{ii-1} + R_{ii+1}\cos\alpha_i\right)\mathrm{cosec}\,\alpha_i \end{aligned}\right\} \quad .. \quad (11.2.4)$$

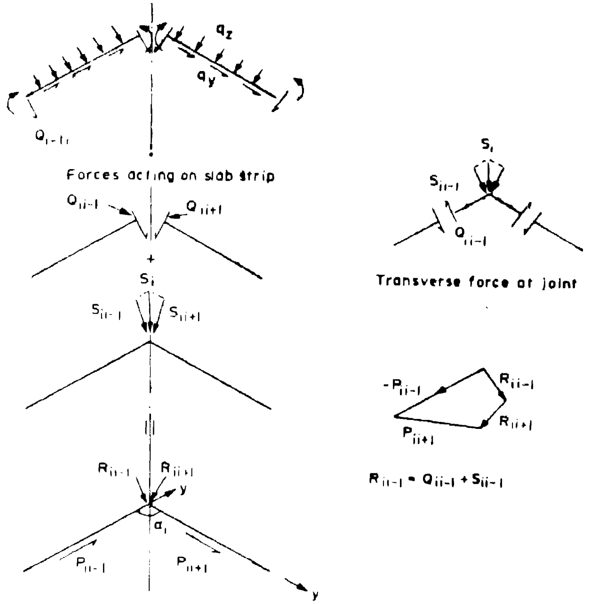

Fig. 11.2.4 : Forces at joints and their components in the plane of the plates

where

α_i = angle of deviation of the plates

P_{ii-1} = force acting at the ith joint in the plane of the plate i, i − 1

On any plate there will be two forces acting one at each of the two joints of the plate as shown in fig. 11.2.5.

Let P_i = total effective force on the plate ii − 1, then

$$P_i = P_{ii-1}+P_{i-ii}+\int_0^d q_y dy = \left(P_i \sin \frac{\pi x}{L}\right) \qquad .. \quad (11.2.5)$$

Considering only shallow plates where depth (d) is small as compared to the length (L), the plate could be treated as a beam loaded with P_i. Then the mid-span bending moment for the loading is

$$M_{ip} = \frac{P_i L^2}{\pi^2} \qquad .. \quad (11.2.6)$$

The corresponding extreme fibre stresses based on simple beam theory are

$$\left.\begin{aligned} f_{pi-ii} &= \frac{M_{ip}}{Z_{i-ii}} \\ f_{pii-1} &= \frac{-M_{ip}}{Z_{i-ii}} \end{aligned}\right\} \qquad .. \quad (11.2.7)$$

where

M_{ip} = bending moment of mid-span of plate i — 1, i.

f_{pi-1i} = bending stress due to load P at i — 1 th joint of plate i — 1, i and similarly f_{pii-1}

Z_{i-1i} = modulus of section of the plate about z-axis

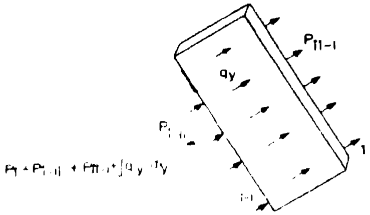

Fig 11.2.5 : Effective force acting in the plane of plate

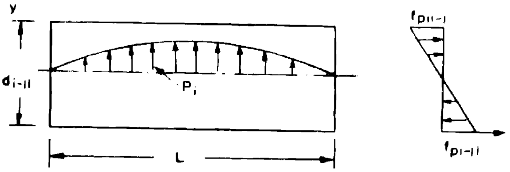

Fig. 11.2.6 : Plate acting as a beam

Bending stresses of the two adjacent plates at the common edge or fold should cause equal strains. If the extreme fibre strains of the two adjacent plates due to P forces are not compatible at the fold, then a secondary set of stresses will be generated within the plate. Such stresses could be generated by a self equilibrium shear force system.

Let T_{i-1} and T_i be the self equilibrium shear forces developed at the i — 1 and i folds of the structure. These must vary in sin πx/L form to be compatible with the other stress system. The bending moment and normal forces due to the shear forces are given by

$$M_{it} = -\frac{d_{i-1i}}{2}\,(T_{i-1}+T_i) \qquad \ldots (11.2.8)$$

$$N_{it} = T_{i-1}-T_i \qquad \ldots (11.2.9)$$

where

M_{it} = bending moment on the plate i — 1, i due to shear force T

N_{it} = normal force on the plate due to shear force T

Stresses due to the shear force system may be obtained as

$$\left.\begin{aligned} f_{ti-1i} &= \frac{N_{it}}{A_{i-1i}} - \frac{M_{it}}{Z_{i-1i}} \\ f_{tii-1} &= \frac{N_{it}}{A_{i-1i}} + \frac{M_{it}}{Z_{i-1i}} \end{aligned}\right\} \qquad \ldots (11.2.10)$$

where

f_t = stress in the plate due to shear force T

Final extreme fibre stresses can now be obtained from eqs. 11.2.7 and 11.2.10

$$\left.\begin{aligned} f_{i-li} &= f_{pi-ti} + f_{ti-li} = \frac{-M_{ip} - M_{it}}{Z_{i-li}} + \frac{N_{it}}{A_{i-li}} \\ f_{li-i} &= f_{pli-i} + f_{tli-i} = \frac{M_{ip} + M_{it}}{Z_{i-li}} + \frac{N_{it}}{A_{i-li}} \end{aligned}\right\} \quad \ldots \quad (11.2.11)$$

Eq. 11.2.11 could also be expressed as

$$\left.\begin{aligned} f_{i-li} &= \frac{-M_{ip}}{Z_{i-li}} + \frac{4T_{i-1} + 2T_i}{A_{i-li}} \\ f_{li-i} &= \frac{M_{ip}}{Z_{i-li}} - \frac{4T_i + 2T_{i-1}}{A_{i-li}} \end{aligned}\right\} \quad \ldots \quad (11.2.12)$$

Assuming the Poisson's ratio is zero, the longitudinal strain compatibility reduces to equivalence of the stresses at the fold. A diagramatic representation of the two adjacent stresses is shown in fig. 11.2.7.

The strain compatibility then gives

$$f_{li-i} = f_{li+1} \quad \text{or}$$

$$\frac{T_{i-1}}{A_{i-li}} + 2\left(\frac{1}{A_{i-li}} + \frac{1}{A_{li+1}}\right)T_i + \frac{T_{i+1}}{A_{li+1}}$$

$$= \frac{M_{ip}}{2\,Z_{i-li}} + \frac{M_{i+1p}}{2\,Z_{li+1}} \quad \ldots \quad (11.2.13)$$

Eq. 11.2.13, when applied to each of the folds, will generate sufficient number of equations to determine the shear forces T.

Displacement compatibility of the slab and beam actions : The plate edges go through deflection which should be compatible with slab and beam actions. The deflection in slab action is already indicated by δ_i. The loading on the beam action of the plate vary as sin $\pi x/L$ so the mid-span deflection in the plane of the plate due to sin $\pi x/L$ load is given by

$$v_{li-i} = \frac{M_i L_i^2}{\pi^2 EI} = \frac{12}{\pi^2 E}\left(\frac{M L^2}{t d^2}\right)_i \quad \ldots \quad (11.2.14)$$

where

v_{li-i} = deflection in the plane of the plate i − li

$M_i = M_{ip} + M_{it}$

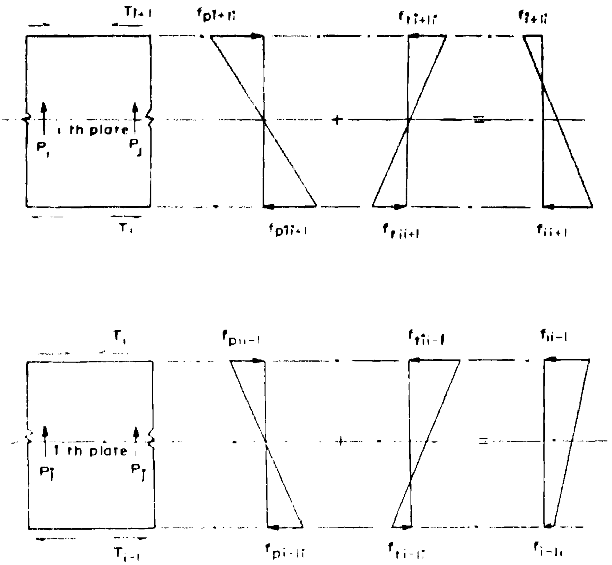

Fig. 11.2.7 : Longitudinal strain compatibility condition (Poisson's ratio = 0)

Deflections of plates adjacent to joint i should together produce a compatible deflection as shown in fig. 11.2.8.

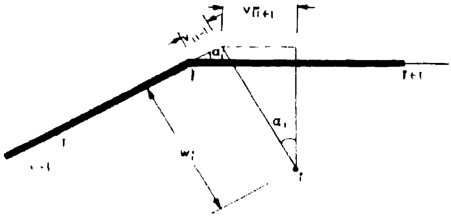

Fig. 11.2.8 : Deflection of fold i

From fig. 11.2.8, deflection relation could be written as

$$w_i = (v_{ii+1} - v_{ii-1} \cos \alpha_i) \operatorname{cosec} \alpha_i \qquad .. \quad (11.2.15)$$

$$\delta_i = \left[\frac{w_i - w_{i-1}}{d_{ii-1}} \right]$$

$$= \frac{(v_{ii+1} - v_{ii-1} \cos \alpha_i) \operatorname{cosec} \alpha_i - (v_{i-1i} + v_{i-1i-2} \cos \alpha_{i-1}) \operatorname{cosec} \alpha_{i-1}}{d_{ii-1}}$$

$$= \frac{v_{ii+1} \operatorname{cosec} \alpha_i - (\cot \alpha_i + \operatorname{cosec} \alpha_{i-1}) \, v_{ii-1} + v_{i-1i-2} \cot \alpha_{i-1}}{d_{ii-1}}$$

$$.. \quad (11.2.16)$$

The derivation apparently looks pretty involved. However the solution could be obtained from the series of simultaneous equations, or through an iterated scheme.

11.3. DESIGN OF FOLDED PLATES: The load balancing method is a good approach to the design of folded plates. Folded plates are to be designed for transfer load and working load conditions. The external load acting on the folded plate is essentially due to self-weight of the plate with relatively small live load. These two loads could be taken as acting vertically downwards and resolved into perpendicular coordinates, one normal to the plate and another in the plane of the plate. Span of the slab is usually small and it is also not convenient to impose prestressing force along the slab profile. Therefore, the slab is designed as a simple reinforced concrete slab and the prestressing is done in the longitudinal direction of the plate to compensate the beam action (11.8—11.12).

Design example 11.3.1: Design of a folded plate structure to cover an area of 30 by 10 m using a single fold of 90° included angle. Live load on the plate is 100 kg/sq m.

Given data:

$L=30$ m, $H=5$ m, $d=5\sqrt{2}=7.07$ m

$q_1=100$ kg/sq m

Solution:

Let $t=L/250\simeq 12.5$ m

$$\text{then } q_d=\sqrt{2}\left(\frac{12.5}{100}\times 2400\right)=423 \text{ kg/sq m}$$

Let the uniformly distributed load be converted into a statically equivalent sinsoidal load, then the maximum amplitude is given by (the first term coefficient of the series)

$$q=\frac{4}{\pi}\times(\text{uniformly distributed load})$$

The effect of the hormonic loading is obtained if the uniformly distributed load intensity is multiplied by $\frac{4}{\pi}$.

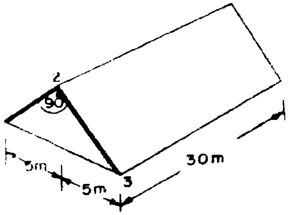

Fig. 11.3.1 : Example 11.3.2

The longitudinal edges of the plate are assumed to be free, so

$$T_1 = T_2 = 0$$

Let

$$\left.\begin{array}{l} A_{12} = A_{23} = A \\ t_{12} = t_{23} = t \\ Z_{12} = Z_{23} = Z \end{array}\right\} \text{because of symmetry}$$

From eq. 11.2.13

$$2\left(\frac{1}{A} + \frac{1}{A}\right)T_2 = \frac{M_{1p} + M_{2p}}{2Z}$$

$$T_2 = \frac{A}{8Z}(M_{1p} + M_{2p}) = \frac{3}{4d}(M_{1p} + M_{2p}) \qquad \ldots (11.3.1)$$

There is no line load at the fold and the extreme edge of the fold is free, so all the transverse components of the load will be transmitted directly to the adjacent plate. The plates are perpendicular to each other so the transverse shear on one plate would act wholly on the other plate in its plane. Due to symmetry, only one plate of the structure is designed. Additional advantage in this example is that the deformations and transverse shears are uncoupled because of the symmetry and single fold.

$M_{1p} = -M_{2p}$ and

$\therefore$ $T_2 = 0$ (from eq. 11.3.1)

Load at transfer (self weight only)

$$= (q_g\, d + Q_g)\frac{4}{\pi}$$

$$= \left[\frac{423}{\sqrt{2}} \times 7.07 + \frac{423}{\sqrt{2}} \times 7.07\right]\frac{4}{\pi} = 5360 \text{ kg/m}$$

Load at working condition $= (q_t\, d + Q_t)\dfrac{4}{\pi} = 6650$ kg/m

Let P_{be} = load balanced at transfer condition. Transfer load should be chosen so as to keep allowable stresses at transfer and working conditions about the same. The allowable compressive stress at working condition is about 0.8 times to that transfer load condition. Then a good load balance may be obtained by

$$0.8\,(q_{bt} - 5360) = (6650 - .85\, q_{bt})$$

$$\therefore \quad q_{bt} = \frac{10950}{1.65} = 6660 \text{ kg/m}$$

Let the cable profile be parabolic and maximum eccentricity equal to 3 m. Then the equivalent balancing load is given by

$$\frac{8eP_t}{L^2}=q_{bt}$$

$$\therefore\quad P_t=\frac{6660\times900}{8\times3}=251000 \text{ kg}$$

$$A_s=\frac{P_t}{0.7f'_s}=\frac{251000}{10500}=23.8 \text{ sq cm}$$

Check for stresses at transfer:

Load not balanced $=5360-6660=-1300$ kg/m

bending moment $M_t=1300\frac{L^2}{\pi^2}=104000$ kg m

average stress $=\frac{P_t}{A}=\frac{250000}{12.5\times707}=28.6$ kg/sq cm

bending stress $=\frac{M_t}{Z}=\frac{6\times10400000}{12.5\times707\times707}=10$ kg/sq cm

$f_{ct}=28.6+10=38.6$ kg/sq cm (permissible)

$f_{tt}=-28.4+10=-18.6$ kg/sq cm (permissible)

Check for stresses at working load:

$P_e=0.85\ P_t=212000$ kg

Load not balanced, $q_{be}=6660-6660=-10$

bending moment $M_e=\frac{10\ L^2}{\pi^2}$

average stress $=\frac{212000}{12.5\times707}=26$ kg/sq cm

bending stress $=\frac{M_e}{12.5\times707\times707}\simeq0$

The stresses are much below the permissible limits so the prestressing force may even be reduced.

Percentage of prestressing reinforcement $=\frac{23.8\times100}{12.5\ \times707}=0.27$

Design of slab: At transfer condition load that is not balanced $=-1300$ kg/m, $\therefore$ $P_2=1300$ kg/m (line load at fold)

$M_{1p}=M_t=104000$ kg m

$$q_z=\left(\frac{423}{\sqrt{2}}\right)\frac{4}{\pi}=380 \text{ kg/sq m}$$

From eq. 11.2.16

$$=\frac{[v_{23}-(0+1)\ v_{21}+0]}{d}=\frac{v_{23}-v_{21}}{d}$$

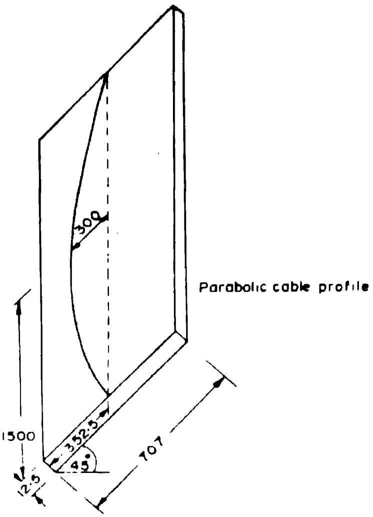

Fig. 11.3.2 : Longitudinal plate and cable profile

and from eq. 11.2.14

$$v_{21} = \frac{12}{\pi^2 E}\left(\frac{ML^2}{td^3}\right)$$

$$\delta_{21} = \frac{12}{\pi^2 E}\left(\frac{L^2}{td^3}\right)(M_{2p} - M_{1p})$$

$$= -\frac{24L^2M_{1p}}{\pi^2E\ td^3}$$

Similarly $\delta_{23} = \dfrac{24\,L^2M_{1p}}{\pi^2Et\ d^3}$

Bending moment on the slab is given by eq. 11.2.2 as

$$\frac{m_1}{k_{12}} + 2m_2\left(\frac{1}{k_{12}} + \frac{1}{k_{23}}\right) + \frac{m_3}{k_{23}} =$$

$$\frac{1}{k_{12}}(2m_{f21} + m_{f12}) + \frac{1}{k_{23}}(2m_{f23} + m_{f32}) + 6\,(\delta_{21} - \delta_{23})$$

where $m_1 = m_3 = 0$

$$k_{12} = k_{23} = k = \frac{Et^3}{12d}$$

$$m_{f12} = -m_{f21} = -\frac{q_z\ d^2}{12}, \text{ and}$$

$$m_{f23} = -m_{f32} = -\frac{q_z\ d^2}{12}$$

The substitution of various quantities in the three moment equations gives

$$2m_2\left(\frac{2}{k}\right)=\frac{1}{k}\left(\frac{qd^2}{12}-\frac{qd^2}{12}\right)-6(2)\left(\frac{24\,L^2\,M_{1p}}{\pi^2\,Et\,d^3}\right)$$

$$m_2=-\left(\frac{72\,M_{1p}\,L^2}{\pi^2\,Et\,d^3}\right)\left(\frac{Et^3}{12\,d}\right)=-\left(\frac{6\,M_{1p}\,L^2\,t^2}{\pi^2\,d^4}\right)$$

It may be of importance to note that the slab bending moment is a function of the length of the plate which is essentially caused due to relative displacements of the slab edges.

$$m_2=-\frac{6\times104000\times900\times0.125\times0.125}{\pi^2\times7.07\times7.07\times7.07\times7.07}=-491\ \text{kgm/m}$$

Use 1 cm wires, 12 nos. per metre width near joint as negative reinforcement.

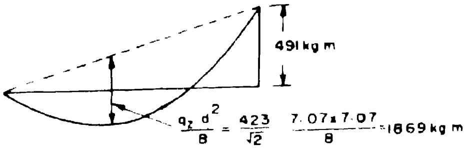
491 kg m
$\frac{q_z d^2}{8}=\frac{423}{\sqrt{2}}\ \frac{7.07\times7.07}{8}=1869$ kg m

Fig. 11.3.3 : Bending moment on slab profile

Design of mid section :

$$\text{Bending moment at middle of the slab}=1869-\frac{491}{2}$$

$$=1623.5\ \text{kgm}$$

Use 1 cm wires, 22 nos. per metre width

The negative bending moment increases gradually near the longitudinal end support. It is desirable to extend the positive reinforcement into the negative moment zone near the support.

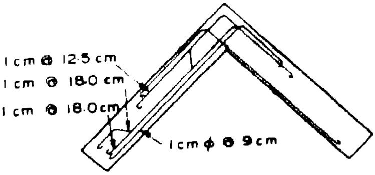

Fig. 11.3.4 : Slab reinforcement

The solution of this example can also be obtained with good accuracy by treating the folded plate as a beam with inverted V as the cross section. The following example will indicate an approximate design procedure of long folded plate based on the simple beam theory.

Example 11.3.2: A folded plate is to be designed to cover an area of 32 by 35 m. The service and superimposed loads are 100 and 50 kg/sq m respectively. The length of the folded plate is to be taken as 32 m.

Solution:

An inverted v type of fold with 7 m fold width as shown in fig. 11.3.5 is selected. Five folds of this type will cover 35 m width and also give a wider top flange. It is desirable to have a wider top flange to meet the working load compressive force at the top fibre. The span to fold width of the folded plate is 32/7 and span to height ratio is 32/2. Therefore the folded plate can be treated as a long folded plate and be designed as a beam.

The thickness of the flanges and web are usually governed by practical limitations. So the sizes of the various elements are assumed subject to practical limitations and shown in fig. 11.3.6. Various sectional properties of the fold, such as area, moment of inertia, are computed in table 11.3.1.

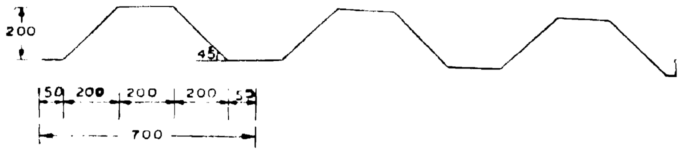

Fig. 11.3.5 : Typical folded plate selected for the roof

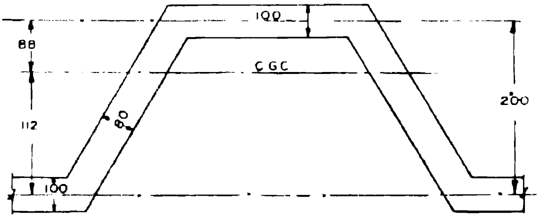

Fig. 11.3.6 : Fold slab dimensions

The loads are taken for one fold width instead of the intensity of load.

$\therefore \quad w = q \times 7$

self weight $= w_g = 0.75184 \times 2400 = 1804$ kg/m

$w_g + w_s = 1804 + 50 \times 7 = 2154$ kg/m

$w_t = w_g + w_s + w_l = 2154 + 100 \times 7 = 2854$ kg/m

Let the load to be balanced be approximately the mean of the loads at transfer and working load

TABLE 11.3.1 : SECTIONAL PROPERTIES OF A FOLD OF 7 M WIDTH

Section	area	distance from bottom flange	moment of the area	moment of inertia about C.G.C
	cm^2	cm	cm^3	cm^4
1. Top flange	200×10 $= 2000.0$	200	400000	2000×88^2 $= 154.88 \times 10^6$
2. Inclined web	$(282.4 \times 8) \times 2$ $= 2 \times 2259.2$ $= 4518.4$	100	451840	$\left(\frac{1}{12} \times 2259.2 \times 200^2 + 2259.2 \times 12^2\right) \times 2$ $= 157.15 \times 10^6$
3. Bottom flange	$(50 \times 10)2$ $= 1000$	0	0	1000×112^2 $= 125.44 \times 10^6$
Total	7518.4	—	851840	437.47×10^6

$$\bar{y} = \frac{851840}{7518.4} = 112 \text{ cm}$$

$$\therefore \quad w_{be} \simeq \left(\frac{2154 + 2854}{2}\right) = 2504 \simeq 2500 \text{ kg/m}$$

Some of the prestressing cables can be supposed to be straight in the bottom flange and the remaining have parabolic profile in the plane of the inclined web. The vertical component of the balancing cable force in the web should be treated as the balancing load. The relative sizes of the bottom flange and the web suggest that about two-thirds of the cables could be accommodated in the web portion and the remaining in the bottom flange.

Let the effective sag in the inclined plane of the web $= 1.00$ m Equating the load balancing forces in the vertical direction, gives

$$\frac{1}{\sqrt{2}}\left(\frac{2}{3}\right)\left(\frac{8 P_e g}{L^2}\right) = w_{be}$$

$$\therefore \quad P_e = \frac{2500 \times 3 \times \sqrt{2} \times 32 \times 32}{2 \times 8 \times 1.0} = 676800 \text{ kg/fold width}$$

$$P_t = \frac{P_e}{\eta} = \frac{676800}{0.85} = 795000 \text{ kg/fold width}$$

Check for stresses at transfer :

Load not balanced at transfer condition

$$= 2154 - \frac{2500}{\eta} = 2154 - \frac{2500}{0.85} = -786 \text{ kg/fold}$$

$$f_{ct} = \frac{P_t}{A} + \frac{M\,y_b}{I} = \frac{795000}{7518.4} + \frac{786 \times 32 \times 32 \times 100 \times 112}{437.47 \times 10^6}$$

$$= 105.5 + 20.5 = 126 \text{ kg/sq cm}$$

$$f_{tt} = -\frac{P_t}{A} + \frac{My_t}{I} = -105.5 + (20.5)\ 88/112 = -88.8 \text{ kg/sq cm}$$

Check for stresses at working load :

Load not balanced at working load is

$$= 2854 - 2500 = 354 \text{ kg/fold}$$

$$f_{ce} = \frac{P_e}{A} + \frac{My_t}{I} = \frac{676800}{7518.4} + \frac{354 \times 32 \times 32 \times 100 \times 88}{437.47 \times 10^6}$$

$$= 89.7 + 7.3 = 97 \text{ kg/sq cm}$$

$$f_{te} = -\frac{P_e}{A} + \frac{My_b}{I} = -89.7 + 7.3\ (112/88) = -80.4 \text{ kg/sq cm (comp)}.$$

Use M 400 concrete with 7 mm high tensile wires

Area of steel in the bottom flange $= \frac{1}{3}\ (P_t/0.7\ f's)$

$$= \frac{1 \times 795000}{3 \times 10500} = 25.2 \text{ sq cm}$$

Area of steel in the two inclined webs

$$= \frac{2}{3}\ (P_t/0.7\ f's) = \frac{2 \times 795000}{3 \times 10500} = 50.4 \text{ sq cm}$$

The area of steel $(50.4/2) = 25.2$ sq cm should be set up in parabolic profile in each of the inclined webs with 100 cm effective eccentricity.

This example gives the design of the longitudinal prestressing force only. The folded plate is to be treated as a continuous beam supported at each of the folds along the width of 35m and be designed as a reinforced concrete slab.

11.4. INTRODUCTION TO PRESTRESSED CONCRETE SHELLS : The aim of this book is only to present a basic concept of design of simple shell structures such as spherical and cylindrical shells. Prestressed concrete cylindrical water tanks have become very popular so an attempt is made on the design of cylindrical water tanks. Because spherical domes are used for building and tank roofs, a typical design of a spherical shell is also presented. Cylindrical shell roofs are prestressed in the longitudinal direction as done in the folded plate construction. The edge beams of cylindrical barrel which are generally subjected to high tensile and torsional stresses are prestressed to increase the working strength and stiffness. A detailed design of prestressed concrete cylindrical shell is discussed here.

11.5 DESIGN OF CYLINDRICAL TANKS: Four types of cylindrical tanks are in current use. Their classification is essentially based on structural behaviour caused by the boundary conditions at the base of the tank. Theoretically, the base of a tank could be fixed even though it is practically impossible to enforce a rigid restraint against rotation at the base. The footing or the bottom slab and the soil on which the footing rests are elastic materials, so only an elastic restraint is offered against rotation at the base of the cylindrical wall. Design of such tanks should be done on partially restrained base condition. An illustration of this example is shown in fig. 11.5.1. Hinged base (fig. 11.5.2), which is free to rotate about the joint, is reasonable to obtain in practice, and if designed as an idealised hinge, it is safe even if some partial restrains are enforced at the joint. The third type of base, the sliding base as shown in fig. 11.5.3, is very simple in its structural design but not so easy to attain in practice. There will always be some frictional restrain between the base and the wall which will introduce secondary bending moments. The fourth type of base, as shown in fig. 11.5.4, is an extension of sliding base with more flexibility for rotation and sliding.

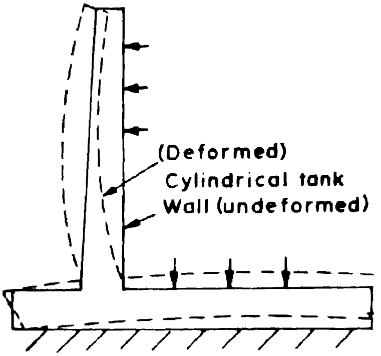

Fig. 11.5.1 : Fixed base which essentially acts as partially fixed base

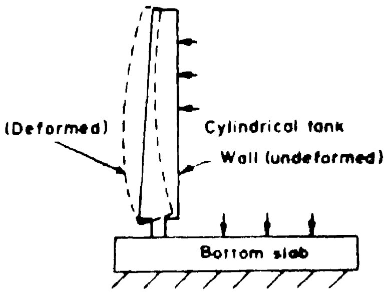

Fig. 11.5.2 : Hinged base

Design example 11.5.1: Design of a prestressed water tank wall for storage of 2×10^6 litres of water. The tank may be assumed to be free at top and fixed or hinged at the base.

Given data: $f'_c = 450$ kg/sq cm, $f_{ct} = 0.5\, f'_c$, $f_{ce} = 0.1 f'_c$

$f'_s = 15000$ kg/sq cm, $\eta = 0.8$, $n = 5.5$

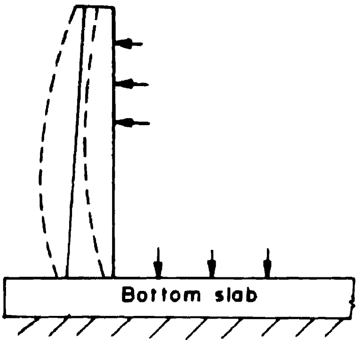

Fig. 11.5.3 : Sliding base

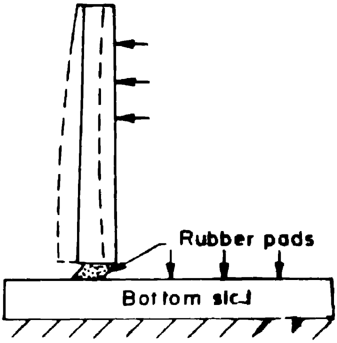

Fig. 11.5.4 : Base on rubber pads

Solution :

Let the height (h) to diameter (D) ratio of the tank be 0.25 i.e. (h/D = 1/4)

Volume $= \left(\dfrac{\pi D^2 h}{4}\right) = 2 \times 10^6 \text{m}^3$ by substituting D=4h

$$D^3 = \frac{4 \times 4 \times 2000000}{\pi}$$

or $\qquad D = 21.6 \text{ m}$

$\therefore$ R=10.8 m and h=5.4 m

Determination of prestressing force: The formulae developed in chapter VI based on load balance technique are used here.

$$p = \frac{f_{ct}}{f_{st}} = 0.021$$

$$A_c = \frac{qR\ (1-pn)}{\eta p\ f_{st} - f_{ce}}$$

Hydrostatic thrust at base is

$$q = \gamma h = 0.001 \times 540 = 0.54 \text{ kg/sq cm}$$

$$A_c = \frac{0.54 \times 1080\ (1-0.116)}{0.8 \times 0.021 \times 10500 - 45} = 3 \text{ sq cm/cm}$$

Use a minimum wall thickness of 10 cm to take care of bending moments and reinforcement.

Let all the hydrostatic thrust be balanced by prestressing force and further induce 0.1 f′c compression in the wall to avoid any possible cracking or water leakage.

Then

$$f_{ce} = \frac{C_c}{A_c} = \frac{P - qR}{A_c} \qquad \text{.. (11.5.1)}$$

From eq. 6.3.10

$$P = E_s A_s \left(\epsilon_{se} + \frac{qR}{A_c E_c} \right)$$

$$P = P_e + A_s \frac{q\,Rn}{A_c} \qquad \cdots \quad (11.5.2)$$

From eq. 11.5.1

$$P = f_{ce} A_c + qR$$

$$= 45 \times 10 + 0.54 \times 1080 = 450 + 583 = 1033 \text{ kg}$$

From eq. 11.5.2

$$A_s = \frac{1033}{8400 + 320.8} = 0.118 \text{ sq cm/cm}$$

It may be observed that by increasing the area of concrete, the area of steel requirement is also increased, to keep a minimum of 45 kg/sq cm of compression at working load condition.

$$P_t = A_s f_{st} = 1240 \text{ kg cm}$$

$$f_{ct} = \frac{P_t}{A_c} = \frac{1240}{10} = 124 \text{ kg/sq cm}$$

Bending reinforcement: There is always a radial thrust inward and it is maximum at transfer condition. The fixed bending moment and shear force at the base of the wall are given by Timoshenko (11.13) as

$$M_0 = \frac{q_r\,Rt}{\sqrt{12\,(1-\upsilon^2)}} \left(1 - \frac{1}{h\beta} \right) \qquad \cdots \quad (11.5.3)$$

$$Q_0 = \frac{q_r\,Rt}{\sqrt{12\,(1-\upsilon^2)}} \left(2\beta - \frac{1}{h} \right) \qquad \cdots \quad (11.5.4)$$

Where

M_0 = fixed end bending moment

Q_0 = shear force at fixed base

$$\beta = \sqrt[4]{\left[\frac{3\,(1-\upsilon^2)}{R^2\,t^2} \right]}$$

q_r = radial thrust

The hydrostatic thrust q should be replaced by radial thrust caused due to prestressing force and such a balancing condition gives

$$q_r = \frac{P_t}{R} = \frac{1240}{1080} = 1.15 \text{ kg/sq cm}$$

Substitution of various quantities in eqs. 11.5.3 and 11.5.4 gives

$\eta M_0 = -\ 6985$ kg cm/cm

and $Q_0 = -\ 2.13$ kg/cm

The fixed end bending moment is 6985 kg cm/cm and is too high for 10 cm thick slab. Thus the tank should be designed with hinged base rather than fixed base.

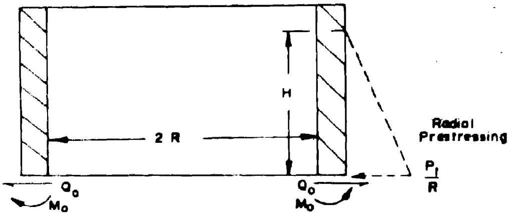

Fig. 11.5.5 : Fixed end forces at transfer

Design of reinforcement at hinged base: Let Q_0 be shear force at hinged base, then it can be obtained from Theory of Plates and Shells by Timoshenko (11. 13) that

$$Q_0 = \frac{q_r\,\beta^3\,t^3\,R^2}{6t\sqrt{(1-\upsilon^2)}} = 46 \text{ kg/cm}$$

The reinforcement should be designed so as to take all the shear forces. A typical reinforcement for hinged base is shown in fig. 11.5.6. Assuming that the weight of the wall is transferred directly to base but not through the reinforcement, the force in the inclined wire due to shear force could be obtained from fig. 11.5.7.

Let there be two inclined wires at the base and depending upon the direction of shear force, one wire will be in tension and the other in compression. Let F_0 be the force (comp. or tension) in the the wire then,

$$4\,F_0 \cos 60 = Q_0 = 46$$

$$\therefore \quad F_0 = 11.5 \text{ kg}$$

$$\text{Area of steel} = \frac{11.5}{1400} = 0.009 \text{ sq cm/cm width}$$

Provide a minimum shear key mild steel reinforcement of 1 cm wire at 20 cm.

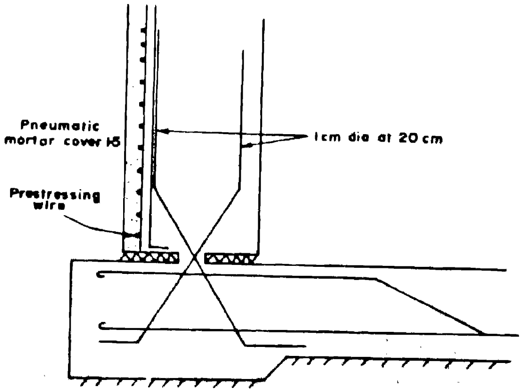

Fig. 11.5.6 : Hinged base

Note.—The prestressing wire should be wound round the tank in helical manner with a minimum clear spacing of 2.5 times the diameter. In case of tanks when the height of the tank is large, the number of wires may have to be arranged in layers so as to provide the minimum spacing. Minimum thickness of the pneumatic mortar in between any two successive wire layers should be at least 8 mm. The thickness of the pneumatic mortar or the wire diameter should not be counted in the thickness of the wall which is generally indicated by core of the wall. The splicing of the wires should be designed properly. A minimum of about 0.15 precent reinforcement has to be provided to take care of the thermal stresses.

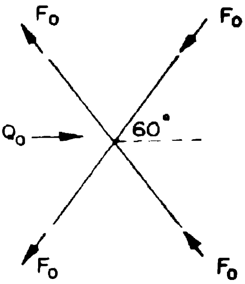

Fig. 11.5.7 : Reinforcement forces at hinge

11.6. DOME-RING CONSTRUCTION :

A typical spherical dome with edge ring beam is shown in fig. 11.6.1. Forces due to membrane analysis are superimposed on the forces due to bending and horizontal line loads on the dome and then the design is done for the resulting force system.

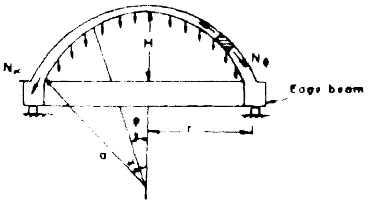

Fig. 11.6.1 : Dome with ring beam

The resultant forces and deformations due to membrane theory are given by (11.14) as

$$N_{\phi m} = -\frac{aq}{1+\cos\phi} \quad .. \quad (11.6.1)$$

$$N_{\theta m} = aq\left(\frac{1}{1+\cos\phi} - \cos\phi\right) \quad .. \quad (11.6.2)$$

$$v_{od} = \frac{a^2 q}{Eh}\left(\frac{1+\upsilon}{1+\cos\phi} - \cos\phi\right) \quad .. \quad (11.6.3)$$

$$\theta_{od} = \frac{aq}{Et}(2+\upsilon)\sin\theta \qquad \ldots \quad (11.6.4)$$

where

a = radius of the sphere

$N_{\phi m}$ = meridinal stress resultant at ϕ on the surface of the shell

$N_{\theta m}$ = hoop stress resultant at ϕ on the surface of the shell

q = load intensity proportional to the self weight of the shell

t = thickness of the shell

v_{od} = horizontal displacement of the dome due to external load

θ_{od} = rotation of the dome due to external load

υ = Poisson's ratio

Subscript 0 indicates external load and d indicates the dome.

The stress resultants and displacements due to constant line loads acting along the boundary of the shell are given in table 11.6.1.

TABLE 11.6.1 : STRESS RESULTANTS AND DISPLACEMENT COEFFICIENTS DUE TO LINE LOADS

	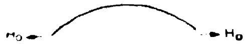	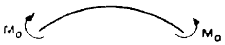
N_ϕ	$-\sqrt{2}\,e^{-\lambda\psi}\cot\phi\,\sin\left(\lambda\psi-\frac{\pi}{4}\right)\sin\alpha$	$-\frac{2}{a}\lambda e^{-\lambda\psi}\cot\phi\,\sin\lambda\psi$
N_θ	$-\sqrt{2}\,e^{-\lambda\psi}\sin\left(\lambda\psi-\frac{\pi}{2}\right)\sin\alpha$	$-\frac{2\sqrt{2}}{a}e^{-\lambda\psi}\sin\left(\lambda\psi-\frac{\pi}{4}\right)$
M_ϕ	$ae^{-\lambda\psi}\sin\lambda\psi\sin\alpha$	$\sqrt{2}\,e^{-\lambda\psi}\sin\left(\lambda\psi+\frac{\pi}{4}\right)$
v	$v_{hd}=\frac{2a\lambda}{Et}\sin^2\alpha$	$v_{md}=\frac{2\lambda^2}{Et}\sin\alpha$
θ	$\theta_{hd}=\frac{2\lambda^2}{Et}\sin\alpha$	$\theta_{md}=\frac{4\lambda^3}{Eat}$

Where

M_ϕ = bending moment on the meridian

v_{hd} = edge horizontal displacement coefficient due to horizontal line load

v_{md} = edge horizontal displacement coefficient due to edge bending moment

θ_{hd} = edge rotation coefficient due to horizontal line load

θ_{md} = edge rotation coefficient due to edge moment

$$\lambda^4 = 3\,(1-\upsilon^2)\left(\frac{a}{t}\right)^2$$

$$\psi = \alpha - \phi$$

Horizontal displacement outward and rotation in clockwise direction are taken as positive. The second subscript d indicates the dome.

The force notations acting on the combined dome-ring system are shown in fig. 11.6.2 and the corresponding displacements due to these forces are given in table 11.6.1.

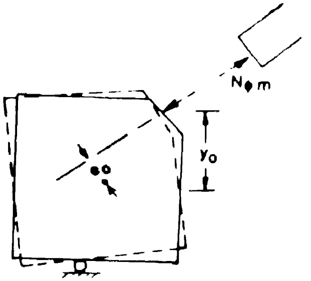

Fig. 11.6.2 : Dome-ring force system

The ring beam is subjected to membrane thrust of the shell and the line load due to bending forces. The membrane thrust which acts eccentrically on the ring cross section may be subdivided into centroidal thrust and bending moment as shown in fig. 11.6.3. These forces cause deformations of the ring, their relation is given in eq. 11.6.5. Compatible conditions at the junction of the ring beam and the shell give sufficient conditions to evaluate the edge corrections, and thus the resultant forces acting on the shell could be developed.

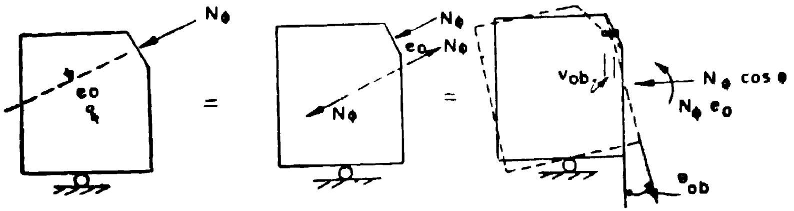

Fig. 11.6.3a : Effective membrane equivalent forces on the ring beam

$$v_{ob} = \frac{r^2}{E}\left(\frac{\cos\alpha}{A_b} + \frac{y_o\,e_o}{I_b}\right) N_\alpha$$

$$\theta_{ob} = -\frac{r^2 e_o}{E I_b}\, N_\alpha$$

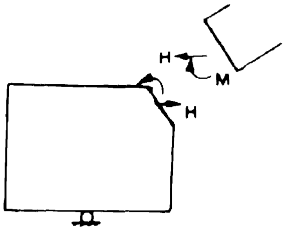

Fig. 11.6.3b : Bending correction forces at the junction of the ring and shell

Deformation coefficients on the ring are

$$\left.\begin{aligned} v_{hb} &= \frac{r^2}{E}\left(\frac{1}{A_b} + \frac{y^2_o}{I_b}\right), & \theta_{mb} &= \left(\frac{r^2}{EI_b}\right) \\ v_{mb} &= -\left(\frac{r^2 y_o}{EI_b}\right), & \theta_{hb} &= -\left(\frac{r^2 y_o}{EI_b}\right) \end{aligned}\right\} \quad \ldots \quad (11.6.5)$$

where

v = horizontal displacement coefficient

y_o = distance of the junction of ring beam and dome from the centroid of the ring beam

e_o = perpendicular distance of the membrane force from centroid

A_b = area of ring beam

I_b = moment of inertia of ring beam about vertical plane

The subscript h or m indicates line forces horizontal or moments and b indicates the beam.

The deformation compatibility relation between the ring beam and the dome are given by eq. 11.6.6. This set of equations when solved with the appropriate coefficients will result in the moment M_l and thrust H_l for which the beam to be designed.

$$\left.\begin{aligned} (v_{od}+v_{ob}) + (v_{hd}+v_{hb})\, H_l + (v_{md}+v_{mb})\, M_l &= 0 \\ (\theta_{od}+\theta_{ob}) + (\theta_{hd}+\theta_{hb})\, H_l + (\theta_{md}+\theta_{mb})\, M_l &= 0 \end{aligned}\right\} \quad \ldots \quad (11.6.6)$$

An illustrative example is given with complete details.

Example 11.6.1 : An area of 30 m diameter is to be covered by a dome. Design a prestressed concrete spherical dome with ring beam for a live load intensity of 200 kg/sq m of the dome surface acting vertically downwards.

Given data :

Poisson's ratio = 0.15, dome angle = 30°

average thickness, t = 10 cm, f'_c = 450 kg/sq cm

q_l (live load) = 200 kg/sq m

Solution:

$$r = \text{radius of the ring beam} = 15 \text{ m}$$

$$a = \text{radius of sphere} = 15/\sin 30 = 30 \text{ m}$$

$$q_g = 240 \text{ kg/sq m},\ q_t = q_g + q_l = 440 \text{ kg/sq m}$$

$$N_{\phi m} = -\frac{aq}{1+\cos\alpha} = -\frac{30q}{1+0.867} = -16 \text{ q kg/m}$$

$$v_{od} = \frac{a^2}{t}\left(\frac{1+\upsilon}{1+\cos\alpha} - \cos\alpha\right)(\sin\alpha)\left(\frac{q}{E}\right) = -1130.4\ (q/E)$$

$$\theta_{od} = -\frac{a}{t}(2+\upsilon)(\sin\alpha)\ (q/E) = -322.5\left(\frac{q}{E}\right)$$

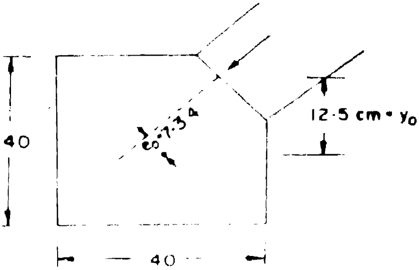

Fig. 11.6.4 : Ring beam

Let the ring beam be square in cross-section of size 40 cm.

$$A_b = 0.4 \times 0.4 = 0.16 \text{ sq m}$$

$$I_b = (1/12 \times 0.4)\ (0.4)^3 = 0.00213 \text{ m}^4$$

$$v_{ob} = -\frac{30 \times 225}{1.867}\left(\frac{0.867}{0.16} + \frac{0.125 \times 0.0734}{0.00213}\right)\frac{q}{E} = -35178\ (q/E)$$

$$\theta_{ob} = \frac{225 \times 0.0734}{0.00213} \times 16\left(\frac{q}{E}\right) = 124000\frac{q}{E}$$

$$v_o = (v_{od} + v_{ob}) = -(1130.4 + 35178)\frac{q}{E} = -36308.4\frac{q}{E}$$

$$\theta_o = (\theta_{od} + \theta_{ob}) = (-322.5 + 124000)\frac{q}{E} = 123677.5\frac{q}{E}$$

$$\lambda^4 = 3\ (1-\upsilon^2)\left(\frac{a}{h}\right)^2$$

$$= 3\ (1-0.0225)\left(\frac{3000}{10}\right)^2 = 263925$$

$$\lambda^2 = 513.73 \text{ or } \lambda = 22.7$$

$$v_{hd} = \frac{2a\lambda}{Et}\sin^2\alpha$$

$$Ev_{hd} = \frac{2 \times 30 \times 22.7 \times 10}{4} = 3405$$

$$Ev_{md} = \frac{2\lambda^2}{t}\sin\alpha = \frac{2\times 513.73\times 10}{2} = 5137.5$$

$$E\theta_{md} = \frac{4\lambda^3}{at} = 15549$$

$$Ev_{bb} = r^2\left(\frac{1}{A_b} + \frac{y_0^2}{I_b}\right) = 225\ (6.25+7.34) = 3057.8$$

$$Ev_{mb} = \frac{r^2\,y_0}{I_b} = -\frac{225\times 0.125}{0.00213} = -13204$$

$$E\theta_{mb} = \frac{r^2}{I_b} = \frac{225}{0.00213} = 105634$$

$$Ev_h = E\ (v_{hd}+v_{hb}) = 6463$$

$$Ev_m = E\ (v_{md}+v_{mb}) = -\ 8067$$

$$E\theta_m = E\ (\theta_{md}+\theta_{mb}) = 121183$$

Compatibility eq. 11.6.6 yields

$$6463\ H_l - 8067\ M_l - 36308\ q = 0$$

$$-8067\ H_l + 121183\ M_l + 123678\ q = 0$$

$$H_l - 1.248\ M_l = 5.617\ q$$

$$\underline{-H_l + 15.02\ M_l = -15.33\ q}$$

$$13.772\ M_l = -9.713\ q$$

$$M_l = -\frac{9.713}{13.772}\,q = -0.705\ q\ \text{kg m/m}$$

$$H_l = (5.617 - 1.248\times 0.705)\ q = 4.74q$$

Design of prestressing and reinforced steel :

The horizontal thrust on the ring beam is

$= H_l = 4.74\ q = 2085 \simeq 2100$ kg/m (for $q = q_t$)

Hoop force in the ring beam = 2100 × 15 = 31500 kg

The prestressing wire can be provided in two different ways.

(i) Prestressing may be done both in ring beam as well as in dome so that the horizontal thrust in the ring beam is resisted by ring prestressing and the dome hoop stress by the dome prestressing. However, prestressing of dome is not as convenient as prestressing of the ring beam. (ii) Hence prestressing may be designed so that a part of the hoop stress of the dome, along with the hoop stress in the ring beam, may be resisted by the prestressing force. Let the hoop stress in the first one metre width from the ring beam be covered by the prestressing force in the ring beam. Average hoop force in the first one metre width from table (11.6.3).

$$= \frac{42620 + 10279}{2} = 26450\ \text{kg}$$

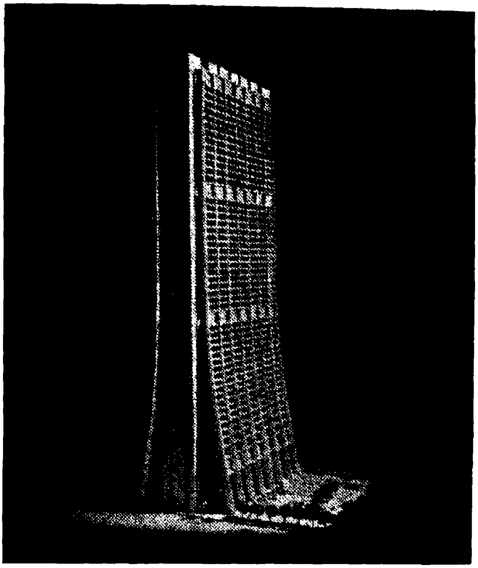

The First National Bank of Chicago

Sixty-story highrise office and bank building with exterior columns splayed outward at the bottom. Outward thrust of columns resisted by 40 Ryerson BBRV tendons, delivering a total effective force of 6,500 tons. On each of two outer column lines there are two tendons. On each of six intermediate column lines there are six 46-wire tendons. Tendons go completely across the building, a distance of about 200 ft. at the plaza level, one storey below the street level.

(*Courtesy of Joseph T. Ryerson and Son, Inc., USA*)

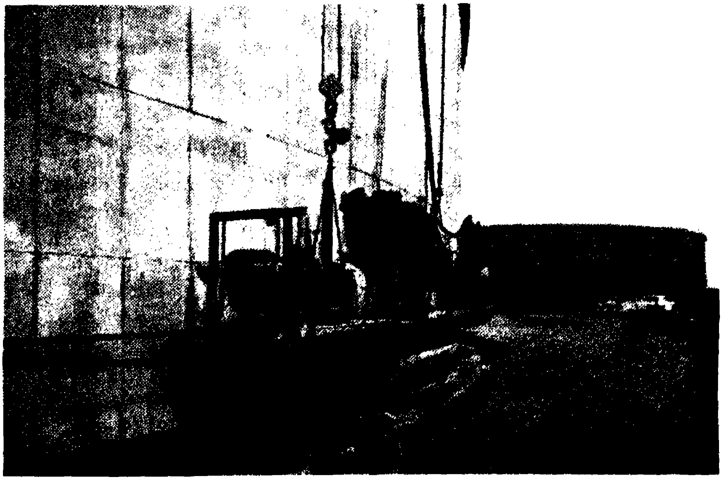

Redwood City, California....Wire winding operation on two 4 000,000 gallon prestressed concrete reservoirs $165\frac{1}{2}$ ft. inside diameter × 26 ft. high.

(*Courtesy of The Preload Company, Inc., New York*)

TABLE 11.6.2: COEFFICIENTS OF RESULTANT FORCES

ϕ	ψ		$\lambda\psi$		$e^{-\lambda\psi}$	cot ϕ	Sin $\lambda\psi$	Sin $(\lambda\psi-\pi/4)$	Sin $(\lambda\psi+\pi/4)$	Sin $(\lambda\psi+\pi/2)$	Coeff. of H_0			Coeff. of M_0		
	Deg	Rad	Deg	Rad							N_ϕ	N_θ −22.7 (6)(11)	M_ϕ .655 (8)(6)	N_ϕ −1.52 (6)(7) (8)	N_θ −49 (6)(9)	M_ϕ 1.44 (6)(10)
1	2	3	4	5	6	7	8	9	10	11	12	13	14	15	16	17
30	0	0	0	0	1.0	1.732	0	—.707	.707	—1.0	.865	22.9	0	0	37.6	1.0
28	2	.0349	45.4	0.804	0.449	1.881	.7169	.014	.999	—.697	—.0083	7.15	.210	—.92	—.307	0.63
24	6	.1047	136.2	2.4	0.091	2.246	.6769	.999	—.042	.736	—.143	—1.53	.0405	—.21	—4.45	—.005
20	10	.1745	227	4.01	.0018	2.748	—.7547	—.669	—.997	.665	.0002	—.027	—.0009	.0056	.006	0
10	20	.3491	454	8.0	.0002	5.675	.9903	.799	.602	.139	0	0	0	0	0	0
0	30	.5236	681	12.0	0	∞	.544	—.978	.208	—.839	0	0	0	0	0	0

TABLE 11.6.3 : STRESS RESULTANTS WITHOUT PRESTRESSING FORCE

ϕ	Cos ϕ	$\frac{1}{1+\cos\phi}$	N_ϕ (kg/m)				N_θ (kg/m)				M_ϕ (kgm/m)		
			Membrane	H_0	M_0	Total	Membrane	H_0	M_0	Total	H_0	M_0	Total
(1)	(2)	(3)	(4)	(5)	(6)	(7)	(8)	(9)	(10)	(11)	(12)	(13)	(14)
30	0.866	0.536	−7080	1820	0	−5460	−4300	48000	−1080	42620	0	−29.04	−29.04
28	0.883	0.525	−6920	−17	−6	−6943	−4730	15000	9	10279	440	−18.3	421.7
24	0.914	0.512	−6760	−300	−1	−7061	−5300	3200	133	−1967	85	0.15	85.15
20	0.940	0.504	−6680	4	0	−6676	−5780	58	0	−5722	0	0	0
10	0.985	0.492	−6520	0	0	−6520	−6500	0	0	−6500	0	0	0
0	1.0	0.500	−6600	0	0	−6600	−6600	0	0	−6600	0	0	0

Note : Table is prepared using the membrane equations and the table of coefficients from table (11.6.2).

Total hoop force to be resisted by the ring beam prestressing

$= 31500+26450 = 57950$ kg

Let allowable working stress in steel be $0.6f'_s = 9000$ kg/sq cm

$$\therefore \text{ Area of steel} = \frac{57950}{9000} = 6.66 \text{ sq cm}$$

Use 18 Nos. of 7 mm wires, then prestressing force $P_e = 18\times3450 = 62000$ kg taking 3450 kg as the effective prestressing capacity of 7 mm wire. It is now necessary to calculate the stress resultants due to thrust caused by the actual prestressing force and also due to the moment caused by the eccentricity of the prestressing force. It is desirable to provide the cables so that there is a counter acting eccentricity. Let the prestressing be done in one layer of cables with an eccentricity of 6 cm as shown in fig. 11.6.5.

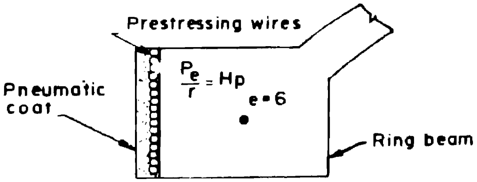

(a) Prestressing force on the ring beam

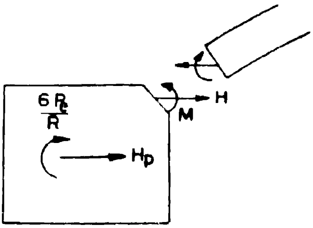

Fig. 11.6.5 : Compatible forces due to prestressing only

The horizontal thrust H and the moment M have to be calculated by considering prestressing force as an external force. The corresponding deformation coefficients are computed in order.

$$H_p\,(Ev_{hb}) = -r^2\left(\frac{1}{A_b}+\frac{y_0\,e}{I_b}\right)H_p$$

$$= -225\left(6.25+\frac{0.14\times0.06}{0.00213}\right)H_p = -2239\,H_p$$

(The negative sign is used because of the negative action of horizontal thrust H_p)

$$H_p\,(E\theta_{hb}) = \left(-\frac{r^2\,y_0\,e}{I}\right)H_p = 888\,H_p$$

The influence coefficients are taken from the previous section :

$$Ev_{hb} = 6463,\ E\theta_{hb} = -8067,\ E\theta_{mb} = 121183$$

The compatibility equation yields

$$6463\ H_l - 8067\ M_l = -2293\ H_p$$

$$-8067\ H_l + 121183\ M_l = -0.888\ H_p$$

or

$$H_l - 1.248\ M_l = -0.355\ H_p$$

$$\underline{-H_l + 15.22\ M_l = \ 0.110\ H_p}$$

$$13.972\ M_l = -0.245\ H_p$$

$$M_l = \frac{-0.245\ H_p}{13.972} = -0.018\ H_p$$

$$H_l = (-0.355 - 1.248 \times 0.018)\ H_p = -0.377\ H_p$$

$$\text{Where } H_p = \frac{P_e}{r} = \frac{62000}{15} = 4133 \text{ kg/m}$$

$$M_l = 74 \text{ kg m/m}$$

$$H_l = -0.377 \times 4133 = -1558 \text{ kg/m}$$

The stress resultants are now computed in table 11.6.4 using table 11.6.2.

Design of ring beam : The forces acting on the ring beam at working load condition are shown in fig. 11.6.5. The ring beam is subjected to axial thrust and twisting moment for which the beam is designed.

$$\text{Radial thrust} = \frac{P_e}{R} - H_p$$

$$\text{Axial thrust} = \left(\frac{\frac{P_e}{R} - H_p}{R}\right)$$

$$\text{Axial stress} = \left(\frac{\frac{P_e}{R} - H_p}{R A_b}\right) = \text{negligible}$$

Design of dome reinforcement :

The dome has to be designed to resist the axial thrust, hoop tension and the bending moment. The critical section is essentially at the junction of the shell and ring beam, so the thickness of the shell near the edge is increased to give higher flexural stiffness. As the disturbance damps from the edge beam, the thickness of the shell is gradually decreased from 13 cm at the edge beam to 9 cm at 5 m from edge.

$$\text{Max. axial force} = N_\theta = 7006 \text{ kg}$$

$$\text{Axial stress} = \left(\frac{7006}{100 \times 13}\right) = 5.4 \text{ kg/sq cm}$$

No meridinal reinforcement is required except for shrinkage and temperature effects. Provide 0.18% reinforcement for shrinkage

$$A_s = 0.0018 \times 100 \times 13 = 2.34 \text{ sq cm/m}$$

Use 10 numbers of 6 mm mild steel wire per metre width.

TABLE 11.6.4 : STRESS RESULTANTS AT WORKING LOADS

ϕ	N_ϕ (kg/m)				N_θ (kg/m)				M_ϕ (kg m/m)			
	Dome*	H_1 (−1558)	M_1 (74)	Total	Dome	H_1 (−1558)	M_1 (74)	Total	Dome	H_1 (−1558)	M_1 (74)	Total
(1)	(2)	(3)	(4)	(5)	(6)	(7)	(8)	(9)	(10)	(11)	(12)	(13)
30	−5460	−1350	0	−6410	42620	−35700	2800	9720	29.04	0	74	45
28	−6943	13	−68	−7013	10279	−11700	−23	−1444	421.70	−3270	47	−2801
24	−7061	222	−15	−6854	−1967	2380	−330	83	85.15	−630	0	−545
20	−6676	0	0	−6676	−5722	420	0	−5302	0	1	0	1
10	−6520	0	0	−6520	−6500	0	0	−6500	0	0	0	0
0	−6600	0	0	−6600	−6600	0	0	−6600	0	0	0	0

***Note** : 1. Dome indicates stress resultants taken from dome-ring analysis without prestressing force. Table 11.6.3.

2. The resultant stress due to H_1 and M_1 are obtained using table 11.6.2.

TABLE 11.6.5: STRESS RESULTANTS AT TRANSFER CONDITION

ϕ	N_ϕ (kg/m)				N_θ (kg/m)				M_ϕ (kg m/m)			
	Dome*	H_1	M_1	Total	Dome	H_1	M_1	Total	Dome	H_1	M_1	Total
(1)	(2)	(3)	(4)	(5)	(6)	(7)	(8)	(9)	(10)	(11)	(12)	(13)
30	−2970	−1590	0	−4560	23300	−42020	3300	15420	−16	0	87	71
28	−3800	15	−80	−3865	5600	−13770	−27	−8197	225	−385	55	−105
24	−3850	260	−17	−3607	−108	2800	−390	2302	46	−742	0	−696
20	−3650	0	0	−3650	−3100	494	0	−2606	0	1	0	1
10	−3550	0	0	−3550	−3550	0	0	−3550	0	0	0	0
0	−3600	0	0	−3600	−3600	0	0	−3600	0	0	0	0

*Note: 1. External load at transfer is 240 kg/sqm, so the dome stresses are prorated to 240/440.

2. Loss of prestress is assumed to be 15% so the stresses due to prestress at working load given in table (11.6.4) are divided by $\eta = 0.85$.

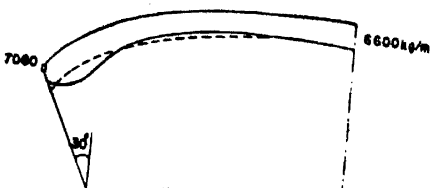

Values of N_ϕ

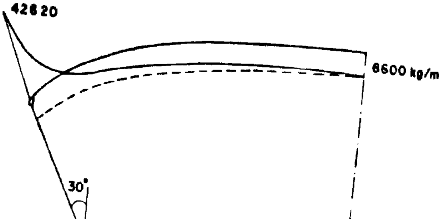

Values of N_θ

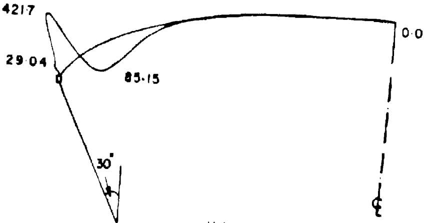

Values of M_ϕ

Fig. 11.6.6 : Stress resultants for spherical dome-ring without any prestressing

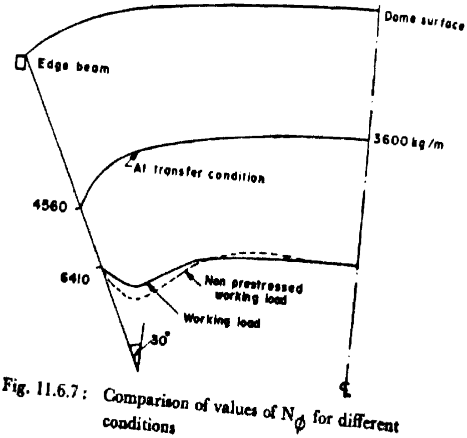

Fig. 11.6.7 : Comparison of values of N_ϕ for different conditions

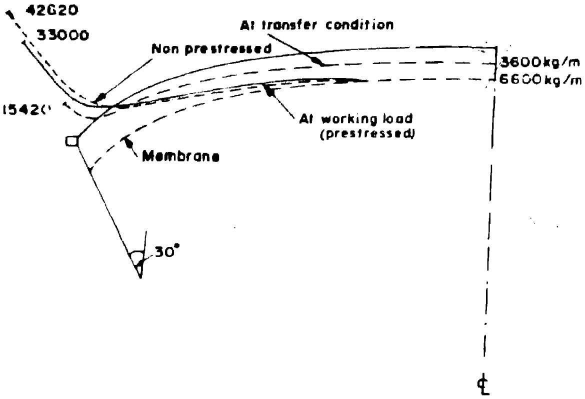

Fig. 11.6.8 : Comparison of N_θ, prestressed and non-prestressed

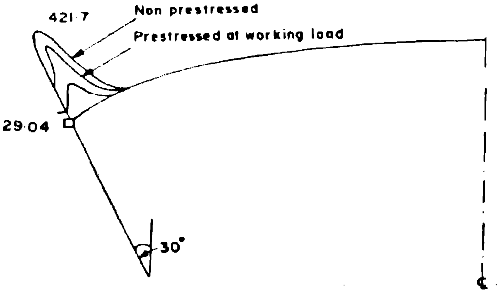

Fig. 11.6.9 : Comparison of M_ϕ, prestressed and non-prestressed

Hoop reinforcement :

Hoop force for the first 1 m width near the edge

$$= \frac{33000+6406}{2} = 19703 \text{ kg/m}$$

$$\text{Area of steel} = \frac{19703}{1400} = 14 \text{ sq cm}$$

Use 18 numbers of 10 mm mild steel wires in two rows per metre width.

Bending reinforcement :

Maximum bending moment = 354.7 kg m/m

Let the effective depth = 11 cm

$$\therefore A_s = \frac{35470}{0.9 \times 11 \times 1400} = 2.56 \text{ sq cm/m}$$

Use 4 numbers of 10 mm mild steel wires per metre width upto 2 m into the shell, and then curtail two of the four wires.

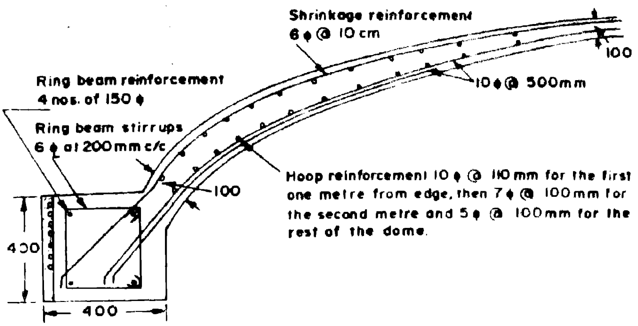
Shrinkage reinforcement
6 ϕ @ 10 cm
100
10 ϕ @ 500mm
Ring beam reinforcement
4 nos. of 150 ϕ
Ring beam stirrups
6 ϕ at 200mm c/c
100
Hoop reinforcement 10 ϕ @ 110mm for the first one metre from edge, then 7 ϕ @ 100mm for the second metre and 5 ϕ @ 100mm for the rest of the dome.
400
400

Fig. 11.6.10 : Reinforcement details (all dimensions in mm)

11.7. INTRODUCTION TO PRESTRESSED CONCRETE CYLINDRICAL SHELL: A cylindrical shell may be defined as a singly curved shell formed by a straight line generator moving on a curve. The cylindrical shell discussed in this section is a thin circular one used for roof construction. A shell may be considered as a thin shell if the ratio of the radius to the thickness of the shell is greater than 20. Most shells built for roof construction have this ratio greater than 20 and therefore thin shell analysis is applicable. Thin cylindrical shells are generally classified into two groups: (i) long, and (ii) short shells. There are different methods to classify long and short shells sometimes including even intermediate shells. Ratio of radius to the length of the shell is generally accepted as a basis for classification of shells used in roof construction. *ASCE* Manual on design of cylindrical concrete shell roofs suggests that the shells having R/L ratio less than 0.6 may be classified as long shells, otherwise short barrels (11.15). There is no exactness to this ratio, so *ASCE* Manual classification may be considered good for practical purposes.

Several types of approximations based on various parameters were made in the analysis of cylindrical shells. Each theory or solution has its limitations and advantages. Any attempt to discuss the cylindrical shell analysis is beyond the scope of the book since the main aim of this book is to present the design of cylindrical shell in a simplified manner so that readers, who have not studied any analysis of shell structures, can follow and do the design computations.

ASCE Manual 31 presents certain coefficients of forces and deformations of the shell for different types of load conditions. These coefficients are used for the design of the shell. Rational use of these coefficients needs certain understanding in the basic analysis and notations.

11.8. METHOD OF ANALYSIS OF CYLINDRICAL SHELL: The cylindrical shell roof is first assumed to be a complete cylinder resisting the external loads in plane forces (no bending and transverse stresses). These in plane forces are called membrane forces. A set of correction forces which compensate the unbalanced boundary forces are then introduced and a separate solution for such line loads is obtained by bending analysis. The superposition of these two solutions gives the final solution for design. Basic notations used in the cylindrical shells are shown in fig. 11.8.1, and the superposition of two linear solutions to obtain stress resultants is shown in fig. 11.8.2. Membrane stress resultants and deformations for various load conditions are given in tables 4 to 6 (Appendix A). Similarly, stress resultants due to line loads are given in tables 7 to 9 (Appendix A). The shell which has no edge beams is called free edge shell. Prestressing is adopted for a long shell in which edge beams are provided. The edge beam essentially acts as a tie which will resist most of the longitudinal tension developed in the shell. Analysis of such prestressed concrete shells is done by superposition of the two solutions.

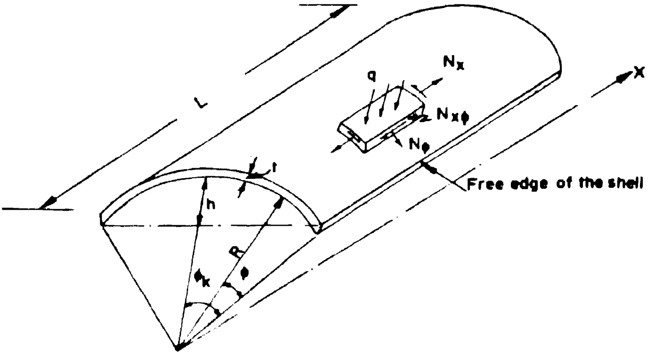

R = radius, L = length (span), ϕ_k = shell angle,
t = thickness, q = external load, h = rise,
N_x and N_ϕ = stress resultants in x and ϕ directions,
$N_{x\phi}$ = shear force

Fig. 11.8.1 : Shell dimensions and notations

(i) The cylindrical shell and the prestressed concrete edge beams are analysed as two independent structural systems.

(ii) Four possible forces—(a) vertical force (V_1), (b) horizontal force (H_1), (c) transverse moment on the curved axis of the shell or torque on the beam (M_1), and (d) the force along the longitudinal axis (S_1), i.e., shear force on the shell and longitudinal force on the beam—are likely to act at the intersection of the shell and the edge beam. This set of forces are introduced in the two independent shell and beam systems. The shell and the beams are analysed independently for this

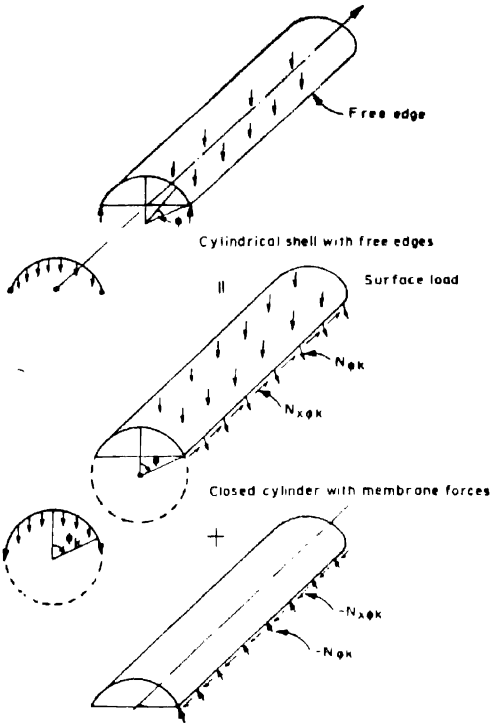
Free edge
Cylindrical shell with free edges
Surface load
||
$N_{\phi K}$
$N_{x\phi K}$
Closed cylinder with membrane forces
+
$-N_{x\phi K}$
$-N_{\phi K}$
Cylinder with edge compensating force

Fig. 11.8.2 : Superposition of two shells to get free edge conditions of a shell

set of line loads. The free body diagrams of the two independent systems are shown in figs. 11.8.2 and 11.8.3. The line forces at the intersection of the shell and beam are obtained through the four deformation compatibility conditions. Each of the algebraic sums of the (i) vertical, (ii) horizontal, (iii) rotational, and (iv) extensional longitudinal strain deformations must be equal to zero. Poisson's ratio for concrete is small so the fourth condition of compatibility of longitudinal strain may be assumed same as longitudinal stress equivalence.

Let w, v and θ be the displacements taken positive in the directions of forces V_l, H_l and M_l respectively. The first subscript '0' indicates deformations of the individual shell and beam systems subjected to external loads. The first subscripts v, h, m and s (for some deformation quantities) indicate deformations due to vertical, horizontal, moment and shear line forces respectively. The second subscript s or b indicates shell or beam system.

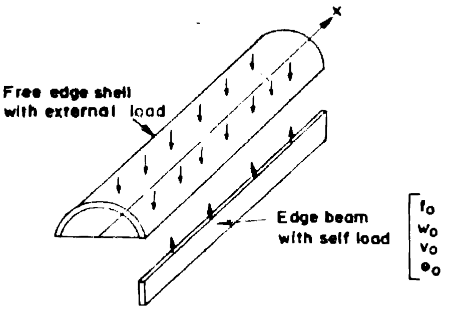

Free edge shell and edge beam with external force

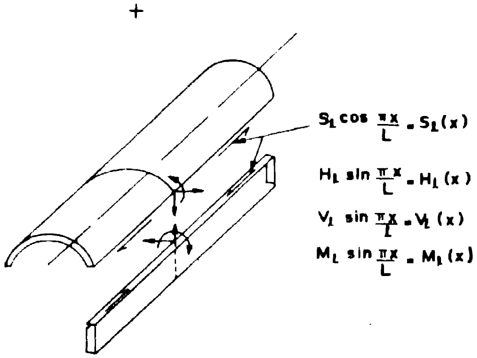
+
$S_L \cos \frac{\pi x}{L} = S_L(x)$
$H_L \sin \frac{\pi x}{L} = H_L(x)$
$V_L \sin \frac{\pi x}{L} = V_L(x)$
$M_L \sin \frac{\pi x}{L} = M_L(x)$

Shell and edge beam under line loads

Fig. 11.8.3 (a) : Cylindrical shell with edge beam compatible forces

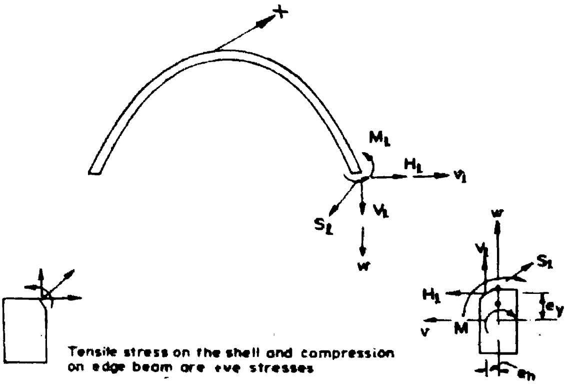

Tensile stress on the shell and compression on edge beam are +ve stresses

Fig. 11.8.3 (b) : Line loads and deformations with +ve sign conventions

The compatibility equations using the notations as described above may now be written as :

$$(w_o+w_v+w_h+w_m+w_s)_s+(w_o+w_v+w_h+w_m+w_s)_b=0 \quad .. \quad (11.8.1)$$

$$(v_o+v_v+v_h+v_m+v_s)_s+(v_o+v_v+v_h+v_m+v_s)_b=0 \quad .. \quad (11.8.2)$$

$$(\theta_o+\theta_v+\theta_h+\theta_m+\theta_s)_s+(\theta_o+\theta_v+\theta_h+\theta_m+\theta_s)_b=0 \quad .. \quad (11.8.3)$$

$$(f_o+f_v+f_h+f_m+f_s)_s+(f_o+f_v+f_h+f_m+f_s)_b=0 \quad .. \quad (11.8.4)$$

The deformations of the shell for various load conditions can be obtained directly from *ASCE* Manual 31. So only the deformations of prestressed concrete beam system are derived in this section.

The deformation compatibility at the intersection of beam and shell should be satisfied for all values of x. To meet this restraint, the external loads are expressed in Fourier expansion, with the result that the deformations will also be of the same form.

Let $q(x)$ = intensity of load

Then q may be expressed in Fourier expansion as

$$q(x)=\Sigma q_n \sin\frac{n\pi x}{L} \quad .. \quad (11.8.5)$$

The corresponding edge forces and deformations are of the same form.

$$\begin{aligned}
N_\phi &= \Sigma N_{\phi n} \sin\frac{n\pi x}{L}\\
N_{x\phi} &= \Sigma N_{x\phi n} \cos\frac{n\pi x}{L}\\
N_x &= \Sigma N_{xn} \sin\frac{n\pi x}{L}\\
V_l &= \Sigma V_{ln} \sin\frac{n\pi x}{L}\\
H_l &= \Sigma H_{ln} \sin\frac{n\pi x}{L} \qquad . \quad (11.8.6)\\
S_l &= \Sigma S_{ln} \cos\frac{n\pi x}{L}\\
M_l &= \Sigma M_{ln} \sin\frac{n\pi x}{L}\\
w &= \Sigma w_n \sin\frac{n\pi x}{L}\\
v &= \Sigma v_n \sin\frac{n\pi x}{L}\\
\theta &= \Sigma \theta_n \sin\frac{n\pi x}{L}
\end{aligned}$$

If $q(x)=q$ (constant), then expansion of Fourier series gives

$$q\,(x)=\frac{4}{\pi}q\Sigma\frac{1}{n}\sin\frac{n\pi x}{L} \quad .. \quad (11.8.7)$$

It is desirable to work with as many terms of the series as possible.

However, it was observed that approximation of the loads with first term of the series gave fairly good results, so the design is presented using this approximation. Hence

$$q(x)=\frac{4}{\pi}q\ \sin\frac{\pi x}{L} \qquad ..\ (11.8.8)$$

Similarly other quantities are expressed through first term of the series.

Force and deformations computed due to a uniform load intensity should always be multiplied by $(4/\pi \sin \pi x/L)$ if first term approximation is made for the uniform load. The line loads at the intersection of the shell and edge beam are always taken in the form as given in eq. (11.8.6) in which case the value $(4/\pi)$ does not appear.

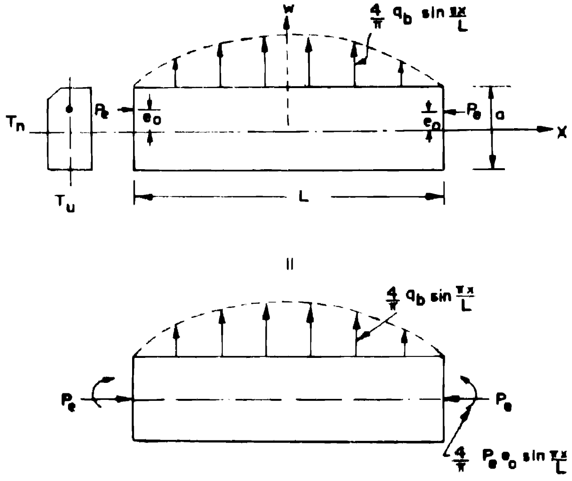
W
$\frac{4}{\pi} q_b \sin\frac{\pi x}{L}$
T_n
T_u
P_e
e_0
e_0
P_e
a
X
L
=
$\frac{4}{\pi} q_b \sin\frac{\pi x}{L}$
P_e
P_e
$\frac{4}{\pi} P_e e_0 \sin\frac{\pi x}{L}$

$$M_x = \frac{4}{\pi} q_b \int^x\!\!\int^x q_b \ \mathrm{Sin}\frac{\pi X}{L}\, dx - \frac{4}{\pi} P_e e_0 \,\mathrm{Sin}\frac{\pi X}{L}$$

Fig. 11.8.4 : External loads acting on the edge beam

Deformation of edge beam :

Let q_{gb} = self weight intensity of beam acting downward

q_{pb} = prestressing force balancing component which is given by

$$=\frac{8P_e g}{L^2}$$

P_e, g and L are already defined in Chapter III for load balancing design. The effective balancing force acting upward is given by

$$q_b(x)=q_{pb}-q_{gb}=\left(\frac{8P_e g}{L^2}-q_{gb}\right) \qquad ..\ (11.8.9)$$

q_b is assumed to be uniform and then approximated by the first term of the series as

$$q_b\,(x) = \frac{4}{\pi} q_b \sin\frac{\pi x}{L} \qquad .. \quad (11.8.10)$$

External forces acting on the edge beam are shown in fig. 11.8.4 and the corresponding deformations can easily be obtained using

$$q\,(x) = \frac{4}{\pi} q \sin\frac{\pi x}{L}$$

$$M_x = \frac{4}{\pi}\left(\frac{q L^2}{\pi^2} - P_e e_o\right) \sin\frac{\pi x}{L} \qquad .. \quad (11.8.11)$$

$$w_{ob} = \frac{4}{EI_h}\left(\frac{q_b L^4}{\pi^4} - \frac{P_e e_o L^4}{\pi^2}\right) \sin\frac{\pi x}{L} \qquad .. \quad (11.8.12)$$

$$\theta_{ob} = v_{ob} = 0$$

where I_h = moment of intertia of the beam about horizontal axis

The deformations due to various line loads are derived independently due to various forces.

(*i*) *Deformations due to V* $\left(V_1 \operatorname{Sin}\frac{\pi x}{L}\right)$: Considering fig. 11.8.5a

$$\text{Torque on the beam at } x = \int_0^x V_1 e_h \operatorname{Sin}\frac{\pi x}{L}\,dx$$

$$= \frac{L}{\pi} V_1 e_h \cos\frac{\pi x}{L}$$

$$\text{rotation due to torque} = \frac{1}{GJ}\int_0^x \left(\frac{V_1 e_h L}{\pi} \cos\frac{\pi x}{L}\right) dx$$

$$= \frac{L V_1 e_h}{\pi GJ}\left(x - \frac{L}{\pi} \sin\frac{\pi x}{L}\right)$$

The twist at the middle section of the beam is given by substituting $x = L/2$ in the above expression.

$$\theta_{vb} = \frac{L^2 V_1 e_h}{\pi GJ}\left(\frac{1}{2} - \frac{1}{\pi}\right) = (\pi - 2)\frac{L^2 e_h V_1}{2\pi^2 GJ} \qquad .. \quad (11.8.13)$$

where GJ = torsional rigidity of the beam

$$w_{vb} = \frac{V_1 L^4}{\pi^4 EI_h} + \theta_{vb} e_h = \frac{L^2}{\pi^2}\left(\frac{L^2}{\pi^2 EI_h} + \frac{(\pi-2) e_h^2}{2 GJ}\right) V_1 \quad .. \quad (11.8.14)$$

$$v_{vb} = \theta_{vb} e_v = \frac{(\pi-2) L^2}{2\pi^2 GJ} e_v e_h V_1 \qquad .. \quad (11.8.15)$$

$$f_{vb} = -\frac{M_{ev}}{I_h} = -\frac{L^2 e_v V_1}{\pi^2 I_h} \qquad .. \quad (11.8.16)$$

(*ii*) *Deformations due to horizontal load* $H_1\left(H_1 \sin\frac{\pi x}{L}\right)$:

Considering fig. 11.8.5b,

$$\text{Torque on edge beam} = \int_0^x \left(H_l\, e_v \sin \frac{\pi x}{L} \right) dx$$

$$= \frac{L}{\pi} H_l\, e_v \left(1 - \cos \frac{\pi x}{L} \right)$$

Rotation of the beam at middle section (θ_{hb}) is

$$\theta_{hb} = -\frac{1}{GJ} \int_0^{L/2} \frac{L}{\pi} H_l\, e_v \left(1 - \cos \frac{\pi x}{L} \right) dx$$

$$\theta_{hb} = -\frac{(\pi - 2)}{2\pi^2 GJ} L^2 e_v H_l \qquad \ldots (11.8.17)$$

$$w_{hb} = \theta_{hb}\, e_h = \frac{(\pi - 2) L^2}{2\pi^2 GJ} e_v\, e_h H_l \qquad \ldots (11.8.18)$$

$$v_{hb} = \frac{H_l L^4}{\pi^4 EI_v} - \theta_{hb}\, e_v$$

$$= \frac{L^2}{\pi^2} \left[\frac{L^2}{\pi^2 EI_v} + \frac{(\pi - 2)}{2\,GJ} e_v\, e_h \right] H_l \qquad \ldots (11.8.19)$$

$$f_{hb} = -\frac{M\, e_h}{I_v} = -\frac{L^2 e_h}{\pi^2 I_v} H_l$$

(*iii*) *Deformations due to Twist* $M_l \left(M_l \sin \frac{\pi x}{L} \right)$:

Considering Fig. 11.8.5c,

$$\text{Torque on the edge beam} = \int_0^x M_l \sin \frac{\pi x}{L}\, dx$$

$$= \frac{L}{\pi} \left(1 - \cos \frac{\pi x}{L} \right) M_l$$

$$\theta_{mb} = \frac{L}{\pi} \left(\frac{M_l}{GJ} \right) \int_0^{L/2} \left(1 - \cos \frac{\pi x}{L} \right) dx$$

$$= \frac{(\pi - 2) L^2}{2\pi^2 GJ} M_l \qquad \ldots (11.8.20)$$

$$w_{mb} = \theta_{mb}\, e_h = \frac{(\pi - 2) L^2}{2\pi^2 GJ} e_h M_l \qquad \ldots (11.8.21)$$

$$v_{mb} = \theta_{mb}\, e_v = \frac{(\pi - 2) L^2 e_v M_l}{2\pi^2 GJ} \qquad \ldots (11.8.21)$$

$$f_{mb} = 0$$

(*iv*) *Deformation due to shear forces* $S_l\left(S_l \sin\frac{\pi x}{L}\right)$:

Considering fig. 11.8.5d, axial force at distance x is

$$F_x = \int_0^x S_l \cos\frac{\pi x}{L} dx = \frac{L S_l}{\pi} \sin\frac{\pi x}{L}$$

$$M_{xh} = F_x e_v = \frac{L}{\pi} e_v S_l \sin\frac{\pi x}{L}$$

$$M_{xv} = F_x e_h = \frac{L}{\pi} e_h S_l \sin\frac{\pi x}{L}$$

$$\theta_{sb} = 0$$

$$w_{sb} = -\frac{L}{\pi} e_v S_l\left(\frac{L^2}{\pi^2 EI_h}\right) = -\frac{L^3 e_v S_l}{\pi^3 EI_h} \quad \ldots \quad (11.8.22)$$

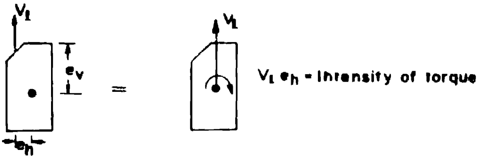

(a) Vertical line load

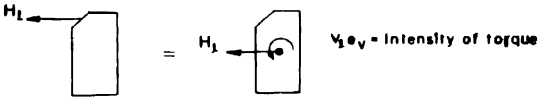

(b) Horizontal line load

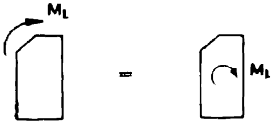

(c) Moment

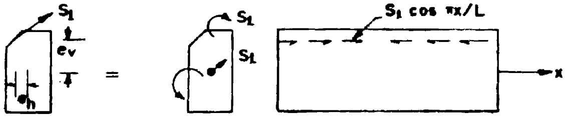

(d) Shear force

Fig. 11.8.5 : Various line loads acting on the edge beam at the intersection of the shell and beam

$$\begin{bmatrix} \omega \\ v \\ \theta \\ f \end{bmatrix} = \begin{bmatrix} \frac{L^2}{\pi^2}\left(\frac{L^2}{\pi^2 EI_h}+\frac{(\pi-2)e_h^2}{2GJ}\right) & \frac{L^2(\pi-2)\,e_v e_h}{2\pi^2 GJ} & \frac{L^2(\pi-2)e_h}{2\pi^2 GJ}-\frac{L}{E\pi}\left(\frac{L^2 e_v}{\pi^2 I_h}\right) \\ \frac{L^2(\pi-2)e_v e_h}{2\pi^2\,GJ} & \frac{L^2}{\pi^2}\left(\frac{L^2}{\pi^2 EI_v}+\frac{(\pi-2)e_v e_h}{2GJ}\right) & -\frac{L^2(\pi-2)e_v}{2\pi^2 GJ}-\frac{L}{E\pi}\left(\frac{L^2 e_h}{\pi^2 I_v}\right) \\ \frac{L^2(\pi-2)e_h}{2\pi^2\,GJ} & -\frac{L^2\,(\pi-2)e_v}{2\pi^2\,GJ} & \frac{L^2(\pi-2)}{2\pi^2\,GJ} \qquad 0 \\ -\frac{L^2 e_v}{\pi^2 I_h} & -\frac{L^2 e_h}{\pi^2 I_v} & 0 \qquad \frac{L}{\pi}\left(\frac{1}{A}+\frac{e_v^2}{I_h}+\frac{e_h^2}{I_v}\right) \end{bmatrix} \begin{bmatrix} V \\ H \\ M \\ S \end{bmatrix} \qquad ..(11.8.25)$$

$$v_{sb} = -\frac{L^3 e_h S_l}{\pi^3 E I_v} \qquad .. \quad (11.8.23)$$

$$f_{sb} = \frac{F_x}{A} + \frac{M_{xh} e_v}{I_h} + \frac{M_{xv} e_h}{I_v}$$

$$= \frac{L}{\pi}\left(\frac{1}{A} + \frac{e_v^2}{I_h} + \frac{e_h^2}{I_v}\right) \qquad .. \quad (11.8.24)$$

All the deformations due to live loads are shown in matrix form in eq. 11.8.25. This matrix is a stiffness matrix and so symmetric. Symmetry in the stiffness coefficients can be obtained from Maxwells reciprocal theorem

11.9. DESIGN EXAMPLE: Design of a prestressed concrete cylindrical shell to cover an area of about 40 by 16 m.

Basic dimensions: Let span of the shell, (L) be 40 m; then the chord of the shell will be 16 m. Some basic dimensions such as rise, thickness of the shell and edge beam dimensions have to be assumed based on architectural and practical considerations.

Let rise of the shell, (h) = 3.0 m; then the radius (R) of the shell will be given by $(2R-h)h = 8 \times 8$

$\therefore$ R = 12.17 m, $\sin \phi_k = (8/12.17) = 0.658$ or $\phi_k = 41°$

Value of ϕ_k is chosen as 45° so that the coefficients of *ASCE* Manual 31 can be used directly.

$\therefore$ $R = 8 \operatorname{cosec} \phi_k = 11.31$ m

Let the thickness of shell = 10 cm

width of the beam = 15 cm

depth of the beam = 200 cm

$\therefore$ $(R/L) = 0.283$, or $(L/R) = 3.54$, and $(L/R)^2 = 12.5$

Membrane analysis:

Weight of the shell = $0.10 \times 2400 = 240$ kg/sq m

Surface load on the shell be distributed like the self weight } = 120 kg/sq m

Total load on the shell, (q) = 360 kg/sq m

$qR = 360 \times 11.31 = 4070$ kg/m

The unbalanced stress resultants at the edge of the shell are computed using table 4 (Appendix A).

$N_{\phi k} = 4qR$ col (9) $= -5200 \times 0.707 = -3670$ .. (11.9.1)

$N_{x\phi k} = 4qR\ (L/R)$ col (8) $= 5200 \times 3.54\ (-0.4502)$

$= -8300$ kg/m .. (11.9.2)

$N_{xk} = 4\ qR\ (L/R)^2$ col (7) $= 5200 \times 12.53 \times (-0.1433)$

$= -9300$ kg/m .. (11.9.3)

Similarly the deformation (w_{0sm}) at the middle of the free edge due to membrane forces is

$$Ew_{0sm} = \frac{4\,qR}{\pi}\left(\frac{L^4}{R^3\,t}\right)\left[\left(\frac{2R}{L}\right)^2 + \frac{2}{\pi^4} + \left(\frac{R}{L}\right)^4\right] \text{col (10)}$$

$$= 5200 \times 17700\ (0.0324 + 0.0205 + 0.0032)$$

$$= 5.16 \times 10^6 \qquad \text{.. (11.9.4)}$$

M_x and N_ϕ at $x=L/2$ and $N_{x\phi}$ at $x=0$ due to membrane forces are calculated using the coefficients of the *ASCE* Manual 31 and are shown in table 11.9.1. These membrane stress resultants will be used for final stress resultants.

TABLE 11.9.1 : MEMBRANE STRESS RESULTANTS

ϕ	N_x at ($x=L/2$)		N_ϕ at ($x=L/2$)		$N_{x\phi}$ at ($x=0$)	
	Coeff.	Force (65000)	Coeff.	Force (5200)	Coeff.	Force (18400)
45	−.2026	−13200	−1.0	−5200	−0.0555	−102
30	−.1957	−12650	−0.9659	−5010	−0.1648	−3020
20	−.1837	−11910	−0.9063	−4710	−0.2690	−4950
10	−.1660	−10800	−0.8191	−4250	−0.3652	−6720
0	−.1443	−9300	−0.7071	−3670	−0.4502	−8300

Correction to membrane edge forces :

Slender edge beam will have negligible stiffness against horizontal and torsional forces. The problem with slander edge beams then reduces to two free edge boundary conditions :

(i) free horizontal displacement, and

(ii) free torsional rotation.

Only the remaining two compatibility conditions have to be satisfied in the present shell as the edge beam is very slender.

Correction forces applied to force a free edge condition on the shell are $-N_{\phi k}$ and $-N_{x\phi k}$ and these forces are resolved in the vertical and horizontal directions.

$$V_l = -N_{\phi k} \sin \phi_k = 3670 \times 0.707 = 2600$$

$$H_l = -N_{\phi k} \cos \phi_k = 2600$$

$$S_l = -N_{x\phi k} = 8300$$

The particular shell parameters are $(R/t)=113.1$ and $(R/L)=0.283$ whereas the closest corresponding values in the Manual are 100 and 0.3 respectively. Errors from taking $R/t=100$ and $R/L=0.3$ for the purpose of coefficients are negligibly small, so the coefficients used in this analysis are for

$R/t=100$ and $R/L=0.3$

Using the table 8 (Appendix A)

$$Ew_{osl} = \frac{L^4}{R^3 t}(46.06\ V_1+1.073\ S_1-30.12\ H_1) \qquad \ldots \quad (11.9.5)$$

$$=815000\ V_1+18990\ S_1-533000\ H_1=891\times 10^6$$

$$N_{xl} =(L/R)^2\ (11.24\ V_1-5.257\ H_1+0.8743\ S_1)=290000 \quad \ldots \quad (11.9.6)$$

The effective forces and deformations of the free edge shell at the middle of the free edge are

$Ew_{os} =E\ (w_{osm}+w_{osl})=(5.16+890)\ 10^6=895\times 10^6$

$N_{ox} = N_{xl}-N_{xm} \quad =290000-9300 \ =280700$ kg/m

$f_{os} =(280700/.10) \ =2807000$ kg/sq cm

Corrections to the shell deformation due to edge load :

Let V_1 and S_1 be the forces developed at the intersection of the beam and shell due to the edge beam.

Then

$(N_{xv}+N_{xs})_s=12.50\ (11.24\ V_1+0.8743\ S_1)$

$$f_{vs}+f_{ss} \quad =125 \quad (11.24\ V_1+0.8743\ S_1) \qquad \ldots \quad (11.9.7)$$

$$E(w_{vs}+w_{ss})=17700\ (46.06\ V_1+1.073\ S_1) \qquad \ldots \quad (11.9.8)$$

Deformations of the edge beam due to external loads :

$I=I_b=(1/12)\times 0.15\times 2^3=0.1\ m^4$

Self weight of beam $=0.15\times 2\times 2400=720=720$ kg/m

Membrane correction force in the vertical direction is 2600 kg/m acting vertically downward. To obtain internal forces, a vertical balancing force of about 2600 kg/m should be applied through the prestressed concrete beam.

Let the effective balancing load $=2500$

Actual balancing prestressing force

$q_b=2500+720=3220$ kg/m

Let the sag of the cable, $(g)=120$ cm with eccentricity at the middle as 80 cm.

The prestressing force corresponding to the balancing force is given by

$$(8gP_e/L^2)=3220$$

$$\therefore \quad P_e=\frac{3220\times 40\times 40}{8\times 1.2}=536700 \text{ kg}$$

$$Ew_{ob} = \frac{4}{\pi I_b}\left(\frac{L^4 q_b}{\pi^4}-\frac{P_e e_o L^2}{\pi^2}\right)$$

$$= \frac{4}{\pi}\,(262400\ q_b - 347.8\times10^6) = 392\times10^6$$

$$f_{ob} = -\frac{4e_v}{\pi\, I_h}\left(\frac{L^2}{\pi^2}\ q_b - P_e\ e_o\right) + \frac{P_e}{A}$$

$$= -\frac{4}{\pi}\,(1620\ q_b - 2150000) + 1790000$$

$$= -634000 \text{ (Compressive)}$$

$$Ew_{vb} = 263000\ V_l$$

$$Ew_{sb} = -\frac{L^3\, e_v}{\pi^3\, I_h} S_l = -21000\ S_l$$

$$f_{vb} = 1620\ V_l$$

$$f_{sb} = \frac{L}{\pi}\left(\frac{1}{A} + \frac{e_v^2}{I}\right) S_l = 170\ S_l$$

Compatibility conditions :

The vertical deflection compatibility yields

$$w_{os} + w_{vs} + w_{ss} + w_{ob} + w_{vb} + w_{sb} = 0$$

$$895\times10^6 + 17700\ (46.01\ V_l + 1.073\ S_l) + 428\times10^6$$
$$+263000\ V_l - 21000\ S_l = 0$$

or $1.077\ V_l - 0.002\ S_l = -1248$ .. (11.9.9)

The longitudinal strain compatibility yields

$$f_{os} + f_{vs} + f_{ss} + f_{ob} + f_{sb} = 0$$

$$2767000 + 124.9\ (11.24\ V_l + 0.8743\ S_l) - 650000 - 1620\ S_l + 170\ S_l = 0$$

or $-0.212 V_l + 0.280\ S_l = -2174$ .. (11.2.10)

Solution of eqs. (11.9.9) and (11.9.10) gives:

$V_l = 1200$ kg/m

$S_l = 6880$ kg/m

Final stress resultants :

There are two sets of correction line loads to be applied to the membrane solutions:

(i) Correction line load forces to develop free edge in the membrane solution

(ii) Correction line load forces due to compatibility of the edge beam

The final correction forces are

$V_l = 2600 - 1200 = 1400$ kg/m

$H_l = 2600$ kg/m

$S_l = 8300 - 8680 = -380$ kg/m

Stress resultants in the shell due to these correction forces are given in table 11.9.2 using table 7 (Appendix A). Table 11.9.3 give final resultant forces in the shell which are obtained from tables 11.9.1 and 11.9.2.

TABLE 11.92: STRESS RESULTANTS DUE TO CORRECTION FORCES

ϕ	N_x at (x=L/2)		$N_{x\phi}$ at (x=0)		N_ϕ at (x=L/2)		M_ϕ at (x=L/2	
	Coeff.	Force	Coeff.	Force	Coeff.	Force	Coeff.	Force
Due to vertical edge loads (1400)								
45	1.400	1970	0	0	−1.178	−1660	−0.257	−362
30	−1.044	−1460	0.432	610	−1.454	−2050	−0.230	−325
20	−3.110	−4380	−0.788	−1110	−1.326	−1880	−0.174	−245
10	−0.946	−1330	−2.214	−3120	−0.330	−460	−0.090	−126
0	11.240	15900	0	0	0.707	995	0	0
Due to horizontal edge load (2600)								
45	−1.970	−5110	0	0	0.306	793	0.159	414
30	−0.047	−122	−1.061	−2760	0.839	2180	0.155	403
20	1.941	5050	0.505	−1316	1.279	3330	0.134	349
10	1.513	9330	0.633	1650	1.158	3010	0.082	213
0	−5.257	−13700	0	0	0.707	1840	0	0
Due to shear edge load (−380)								
45	−0.119	44	0	0	0.072	−28	−0.006	2
30	−0.077	29	−0.085	33	−0.033	12	−0.004	1
20	0.038	−14	−0.101	38	0.024	−9	−0.002	0
10	0.321	−122	−0.013	5	0.024	−9	0	0
0	0.870	−327	0.300	−114	0	0	0	0

TABLE 11.9.3: FINAL STRESS RESULTANTS

θ	N_x at $(x=L/2)$ kg/m Due to Membrane	 V_1	 H_1	 S_1	Final
45	−13200	1970	−5110	44	−16296
30	−12650	−1460	−122	29	−14209
20	−11910	−4380	5050	−14	−11154
10	−10800	−1330	3930	−122	−8322
0	−9300	15900	−13700	−327	−7427
			$N_{x\phi}$ at $(x=0)$		
45	−102	0	0	0	−102
30	−3020	610	−2760	33	−5137
20	−4950	−1110	−1316	38	−7338
10	−6720	−3120	1650	5	−8185
0	−8300	0	0	−114	−8414
			N_ϕ at $(x=L/2)$		
45	−5200	−1660	793	−28	−6095
30	−5010	−2050	2180	12	−4868
20	−4710	−1880	3330	−9	−3269
10	−4250	−460	3010	−9	−1707
0	−3670	995	1840	0	−865
			M_ϕ at $(x=L/2)$		
45	0	−362	414	2	54
30	0	−325	403	1	79
20	0	−245	349	0	104
10	0	−126	213	0	87
0	0	0	0	0	0

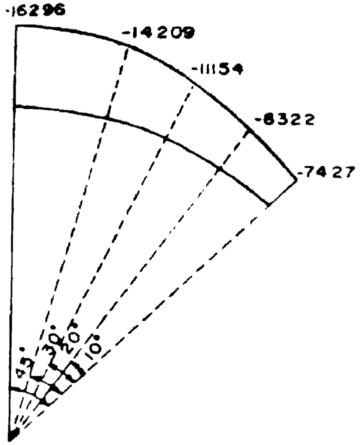

Fig. 11.9.1 : Variation of N_x at x=L/2

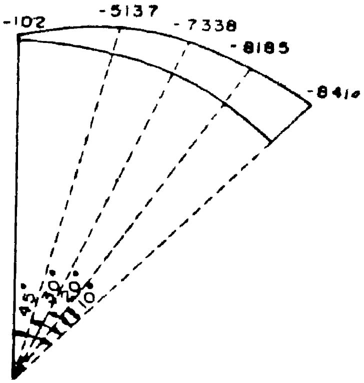

Fig. 11.9.2 : Variation of N_x at x=0

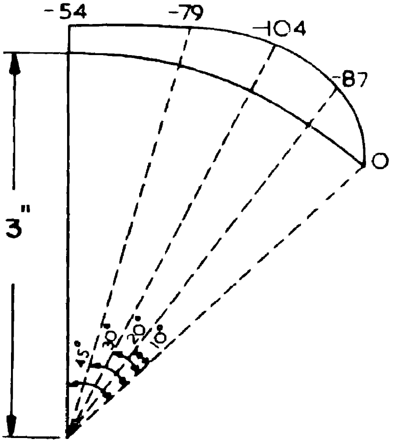

Fig. 11.9.3 : Variation of N_ϕ at x=L/2

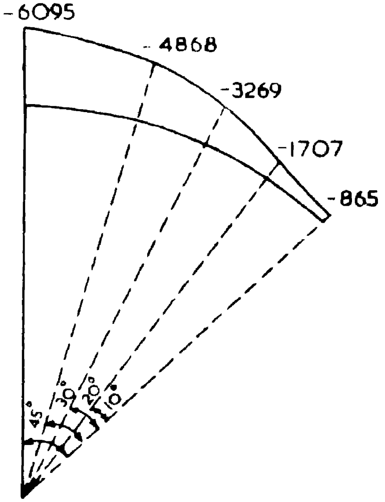

Fig. 11.9.4 : Variation of M_ϕ at x=L/2

Reinforcement details :

(a) Longitudinal reinforcement:

The shell is subjected to longitudinal compression over all the region.

maximum compression = −16296 kg/m

$$\text{compressive stress} = \frac{16296}{100\times 10} = 16.296 \text{ kg/sq cm}$$

No reinforcement is required except the nominal reinforcement of 0.18 percent spaced at not more than 5 times the thickness of the shell.

Area of nominal steel $= 0.0018 \times 10 \times 100$
$= 1.8$ sq cm/m

Use 10 mm mild steel bars at 40 cm apart.

(b) Shear reinforcement:
Maximum shear force $= 8414$ kg/m
Principal tension $= 8414$ kg/m

$$\text{Area of steel required} = \frac{8414}{1400} = 5.97 \text{ sq cm/m}$$

Use 10 mm mild steel bars at 12 cm apart at 45° to the axis of the shell near the edge beam. (1400 kg/sq cm is used as allowable stress in the steel).

Shear force decreases gradually towards the crown upto $\phi = 30°$ and then reduces considerably. So provide 10 mm bars at 12 cm for the first 5 m length along the curve then use 10 mm bars at 16 cm apart upto the crown. This spacing should be adopted upto L/8 from support.

The shear force decreases toward the centre of the shell as a cosine function. Tension reinforcement along the length due to diagonal tension has to be designed based on principal tension. N_ϕ and N_x are both compressive stresses which are zero at the support and maximum at the middle of the span. Complete reinforcement details are shown in fig. 11.9.5.

(c) Reinforcement due to hoop force N_ϕ:

N_ϕ is compressive force throughout the shell, so reinforcement is not required.

(d) Transverse bending reinforcement due to M_ϕ:

The maximum bending moment occurs at the middle of the span for $\phi = 20°$.

$M_{\phi\,max} = 104.0$ kgm/m

$\because$ Area of steel required $= 4$ sq cm/m

Use 10 mm mild steel bars at 20 cm apart at the bottom of the slab for the middle quarter span of the shell. Increase the spacing to 25 cm for the next L/8 span and then to 30 cm spacing for the L/8 span near the support.

(e) Beam reinforcement:

Prestressing force $= P_e = 536700$ kg

$$P_t = \frac{536700}{0.85} = 631300 \text{ kg}$$

$$\therefore A_s = \frac{631300}{0.7 \times 15000} = 60 \text{ sq cm}$$

Use 14 nos. of 12 no. 7 mm cables. Provide also nominal shear and torsional reinforcement. Use 10 mm shear stirrups at 25 cm apart with 4 nos. of 12 mm corner bars. The reinforcement details in the beam are shown in fig. 11.9.6.

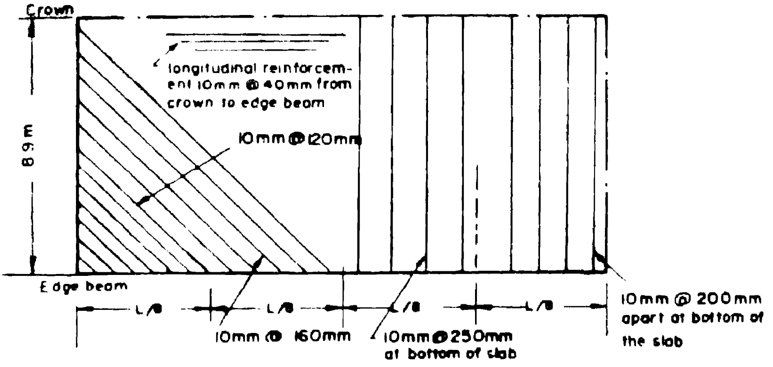
Crown
longitudinal reinforcement 10mm @ 40mm from crown to edge beam
10mm @ 120mm
8.9 m
Edge beam
L/8
L/8
L/8
L/8
10mm @ 160mm
10mm @ 250mm at bottom of slab
10mm @ 200mm apart at bottom of the slab

Fig. 11.9.5 : Shell reinforcement

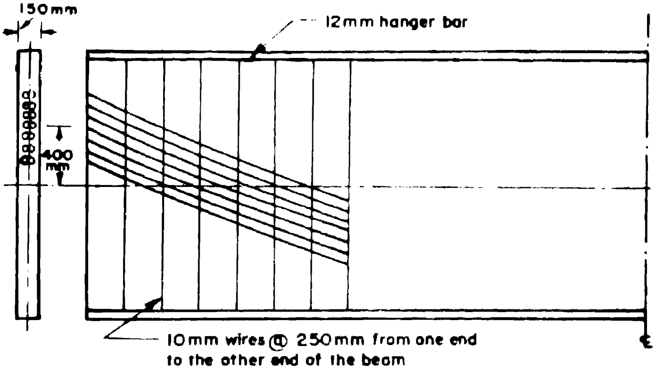
150mm
12mm hanger bar
400 mm
10mm wires @ 250mm from one end to the other end of the beam
℄

Fig. 11.9.6 : Edge beam reinforcement

Problems :

11.1 An area of 20 by 30 m is to be provided by a folded plate roof. The length of the folded plate be taken as 30 m and the folds as inverted V type of 5 m fold width. The rise of the fold should not exceed 2 m. Design the folded plate using $f'_c = 400$ kg/sq cm, and $f'_s = 15000$ kg/sq cm for a service load of 100 kg/sq m.

11.2 A circular tank is to be designed for storage of 650000 litres of water. Design the complete details of the water tank listed below using $f'_c = 450$ kg/sq cm, and $f'_s = 15000$ kg/sq cm.

(a) Vertical walls of the tank as prestressed with base hinged or fixed.

(b) Top ring beam as prestressed concrete beam.

(c) Top dome as ordinary reinforced concrete in the radial direction. Hoop prestressing steel if desirable.

11.3 Design a 30 m long and 10 m wide circular cylindrical shell for a service load of 120 kg/sq m. Provide an edge beam of depth not exceeding 100 cm. The shell is to be supported by end diaphrams resting on columns.

CHAPTER XII

BOND IN PRESTRESSED CONCRETE

12.1. INTRODUCTION : Bond between steel and concrete in prestressed concrete construction exists on two different basis. In pre-tensioning system, bond is used as a means of transferring the prestressing force of steel to the concrete section while in post-tensioning system, bond is found to be necessary for two different purposes :

(i) protection against corrosion ; and
(ii) increase in ultimate strength.

Importance of bond in pre-tensioned construction was recognised from the very beginning, whereas the need for bond in post-tensioned construction has come into light with the progress in the methods of constructions.

12.2. BOND IN PRE-TENSIONED CONSTRUCTION: Bond in pre-tensioned construction is furnished by two factors. When a prestressing cable is tensioned, it is accompanied by a reduction in area of cross section of steel. As the tendon is released, a part of the lateral strain is recovered, especially at the ends of the cable. Due to this increased cross sectional area, frictional bond is developed between steel and concrete. A second factor contributing to the bond is the adhesive property between the two materials as the concrete hardens. The bond of wires at the edges is of great importance since there is no special provision to transfer the prestressing force.

When a wire is released from the prestressing bed, it tends to regain its original length. The force at the very end of the cable has to be zero since it is free; therefore the original area of the cross section is restored at the face. Due to the increase in the cross section of the tendon, there will be a high restraining force between the tendon and concrete. This phenomenon of recovery of lateral contraction develops a wedge action at the end of the cable through which the prestressing force is transferred. This type of self anchoring property was discussed by Hoyer and is called "Hoyer effect". The Hoyer effect is illustrated in fig. 12.2.1. The bond length needed to transmit the complete prestressing force is called "transmission length" (l_t). The bond stress along the transmission length is maximum immediately after the free surface and slowly evens out to uniform at the end of transmission length. The bond and other stress distributions along the transmission length are shown in fig. 12.2.2.

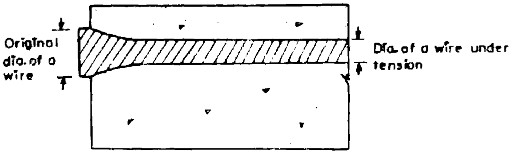

Fig. 12.2.1 : Illustration of Hoyer effect in pre-tensioned construction

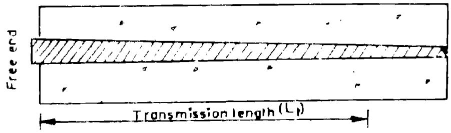

(a) variation of diameter of steel

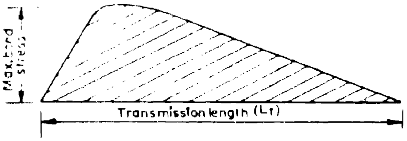

(b) Bond stress distribution

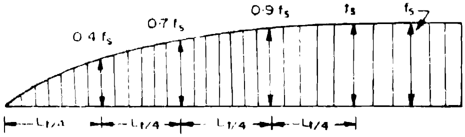

(c) Approximate variation in prestressing force (fs)

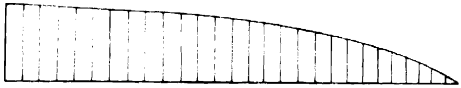

(d) Variation of stress in concrete

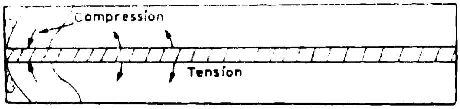

(e) Radial forces

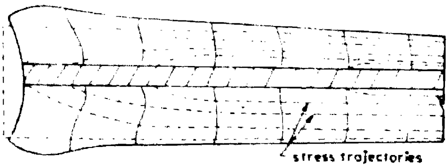

(f) Stress trajectories

Fig. 12.2.2 : Stress variations along the transmission length

It is seen from fig. 12.2.2 that compressive as well as tensile stresses exist in the transmission zone, so transverse reinforcement has to be provided to take the tensile force.

Bond length is generally equal to transfer or transmission length and is derived by Hoyer as

$$l_t = \frac{D}{2\mu}(1 + m_c)\left(\frac{n}{m_s} - \frac{f_{st}}{E_c}\right)\frac{f_{se}}{(2f_{st} - f_{se})} \quad .. \quad (12.2.1)$$

where

D = diameter of the wire

μ = coefficient of friction

m_c = Poisson's ratio for concrete

m_s = Poisson's ratio for steel

n = modular ratio

Let

$m_c = 0.1$, $m_s = 0.3$

$E_c = 3 \times 10^5$ kg/sqcm, $E_s = 2 \times 10^6$ kg/sqcm

$f_{se} = 0.6\, f'_s$, $f_{st} = 0.7\, f'_s$

$$\text{Then } l_t = \frac{D}{2\mu}(1.1)\left(\frac{20}{0.9} - \frac{f_{st}}{E_c}\right)\left(\frac{6}{8}\right)$$

$\frac{f_{st}}{E_c}$ is small as compared to $\frac{20}{0.9}$, so neglecting $\frac{f_{st}}{E_c}$

$$l_t = \frac{55}{6} \times \frac{D}{\mu} \simeq \frac{9D}{\mu} \quad .. \quad (12.2.2)$$

Eq. 12.2.2. gives an approximate idea of the bond length. For $\mu = 0.1$ or in that order, an approximate transfer length could be suggested as

l_t (approx.) = 90 D to 100 D

The initial transfer length will be disturbed due to creep and some times due to slip which forces the required transfer length to a value greater than given by eq. 12.2.1. The approximate experimental value of slip of the wire is shown in Fig 12.2.3. Any extra loading or disturbance in the transfer zone will cause more slip because of the stress concentrations existing at the end.

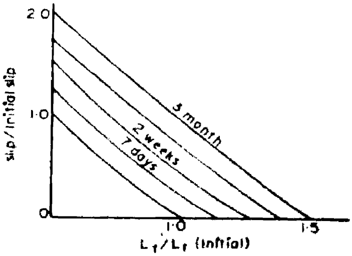

Fig 12.2.3 : Slip of steel with time

In addition to the transfer bond length, flexural bond length based on ultimate stress should also be checked in all designs. If l_b is the bond length, it is given by

$$A_s (f_{su}-f_{se}) = (\pi D l_b) \tau_b$$

$$l_b = (f_{su}-f_{se}) A_s/\pi D \tau_b \qquad .. \quad (12.2.3)$$

$$l_u = l_b \text{ or } t_t \text{ (maximum)} \qquad .. \quad (12.2.4)$$

where

τ_b = bond stress

l_u = total bond length at the end of the cable at ultimate load

Transfer length in general is an important factor in determining where the end support has to be placed. The centre of the supports should be beyond the transfer length. Following conclusions obtained on experimental data regarding transfer length should be observed while designing pre-tensioned beams (12.1 to 12.3) :

(i) if the transfer length is defined as $l_t = \alpha D$, then α is found to be a function of D which increases with D. In general α varies from 50 to 200 and for small wires it could be taken as 100 ;

(ii) deformed bars require less transfer length but these bars of small diameter may not be economical as the percentage of effective steel area will be small ;

(iii) every care should be taken to get good compaction at the ends ;

(iv) it is desirable to use high strength concrete at end zones ;

(v) transfer of prestress should be done gradually instead of cutting the wires suddenly ;

(vi) heavy concentration of wires should be avoided ;

(vii) sufficient transverse reinforcement should be provided to take care of the radial stresses ;

(viii) transfer length should be beyond the support point ; and

(ix) repeated loading increases the transfer length so additional allowance in transfer length should be given for creep as well as for repeated loads.

Example 12.2.1 : Check the bond length of example 3.10.1 consider- the beam as pre-tensioned concrete beam.

Given data :

Span = 50 m, A = 10,000 sq cm, A_s = 268 nos. of 7 mm wire,
coefficient of friction = 0.1, f'_c = 450 kg/sq cm,
f'_s = 15000 kg/sq cm,
$E_c = 3.82 \times 10^5$ kg/sq cm, $E_s = 2.1 \times 10^6$ kg/sq cm,
Poisson's ratio of concrete = m_c = 0.1, Poisson's ratio of steel = 0.3,
allowable bond stress = 10 kg/sq cm

Solution :

On substitution of the respective quantities as given in the data, the eq. 12.2.1 gives

$l_t = 53$ cm

Bond length at ultimate load is given by eq. 12.2.3 and works out to be $l_b = 272.7$ cm

Since the beam is simply supported of 50 m span, the stress in steel at the end of the beam is not equal to the ultimate stress of the steel. Hence the ultimate bond length be taken as 53 cm. There should be at least 55 cm of beam projection beyond the centre of the support.

12.3. BOND IN POST-TENSIONED CONSTRUCTION : Effect of bond in post-tensioned construction has two distinct purposes :

(i) protection against stress corrosion, and (ii) increase in ultimate strength. In an unbonded construction, if any moisture enters into the duct either through a crack or through some leak, the entrapped moisture will cause corrosion to the high tensile steel wires. As the diameter of the wires is small, any small amount of rusting of the wires reduces the effective area considerably. Corrosion once started will increase rapidly and develop cracks. Grouting of the ducts after anchoring of the prestressed wires reduces the corrosion considerably. The alkaline property of cement grout tends to prevent the development of any corrosion. The grouting has to be done as early as possible so that rusting of wires does not start at any time.

Effect of bond on ultimate strength is an interesting phenomenon. As soon as a crack is developed at maximum moment location, steel strain is increased considerably. In an unbonded construction, this increased steel strain is more or less evenly distributed along the length of the cable thus causing excessive deformation of the structure. Due to this large deformation, cracks open much wider reducing the compressive zone. Once the compressive area of concrete is reduced, ultimate strength is also reduced ; whereas in bonded construction, the initial crack at the critical section does not affect the steel strain at any other point and more cracks of small width area formed in maximum bending moment zone. Because of the large number of cracks, the deformation is evenly distributed thus keeping the propagation of the cracks as low as possible; and at any section, the compressive area is not reduced considerably. Thus ultimate strength of the bonded structures is greater than that of the unbonded one. General analytical calculation gives only one ultimate strength for either bonded or unbonded construction since it does not take into consideration the spacing of the cracks. Ultimate strength of unbonded construction in general is less than the computed value. It all depends upon the spacing and number of cracks ; fewer cracks, the less is the ultimate strength.

Ultimate strength of members without bond is about 10 to 20% less than those with bond. A typical crack formation in bonded and unbonded construction is shown in fig. 12.3.1.

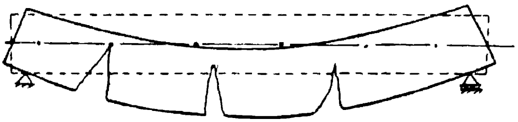

(a) Small number of large cracks in construction without bond

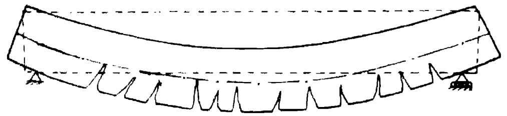

(b) Large number of small cracks in bonded construction

Fig. 12.3.1 : Crack formation in bonded and unbonded construction

Once a duct is grouted to establish a bond between steel and concrete, the differential force in the cable has to be controlled by bond. There are two layers of bonding media in post-tensioned construction :

(i) bond between the steel and the sheath or duct, and

(ii) bond between the sheath and the concrete.

Absolute bond is difficult to attain through grouting even though the method of grouting sounds fairly simple. Therefore allowable bond stress in such a bonded construction should be low. A certain amount of testing is desirable to test the effectiveness of the grouting material on any particular major job before assuming any allowable stresses. Bond stress is obtained in a similar way as is done in reinforced concrete construction (Fig. 12.3.2).

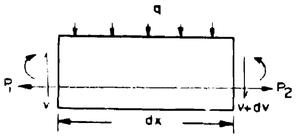

Fig. 12.3.2 : Element forces

$$(P_2a - P_1a) = V\ dx$$

$$(P_2 - P_1) = \frac{V\ dx}{a}$$

where

a = lever arm

Assuming a uniform bond stress

$$(P_2 - P_1) = \tau(\Sigma o)\ dx$$

where

(Σo) = total parameter of the steel

$$\tau = \left(\frac{V}{a\,\Sigma\, o}\right) \qquad \text{.. (12.3.1)}$$

Allowable bond stress in prestressed concrete will be less than that of the reinforced concrete construction as the bonding of tendons is less. Similarly, bond between the sheathing and the concrete is also different.

An allowable bond stress of about 10 kg/sq cm is generally permitted in static loading conditions. In bridges, where a repetition of load comes more often, the permissible bond stres is about 5 kg/sq cm.

Problems :

12.1 Determine the bond length of a pre-tensioned concrete beam of 100 by 60 cm in cross section, provided by 4 prestressing cables of 40000 kg each. Each cable consists of 12 numbers of 7 mm wires.

12.2 A cantilever beam of span 6 m is under 1000 kg/m uniformly distributed load. Design a pre-tensioned concrete beam with 450 kg/sq cm concrete. Also design the bond length based on prestress and ultimate strength bond criteria.

CHAPTER XIII

ANCHORAGE OF PRESTRESSING CABLES

13.1. POST-TENSIONED CONSTRUCTION: Transfer of prestressing force from the cable to the concrete section in post-tensioned construction is done at some selected areas such as end of the beam. As a consequence of the transfer of force, stress concentrations are developed at the transfer zone resulting in secondary stress which dominates the design criteria of the zone. Anchor plates are used as a medium of transfer of the prestressing force. The size of the plate and type of anchoring arrangements govern the stresses in concrete at the transfer zone. The prestressing force applied through the anchor plate propagates into the beam along the axis and after some distance, a linear stress distribution is developed. The zone in which the stress variation reaches a linear distribution over the cross section is called "transmission zone"; the length of this zone is called "transmission length". A typical representation of transmission of force is shown in fig. 13.1.1. Since the application of any concentrated load over a cross section generates a transmission zone before a linear distribution of the stress is achieved over the cross-section, the determination of stress distribution within the transmission zone is difficult even though it could be analysed by elastic and photoelastic theory. The stress distribution within the transmission zone is analysed with reasonable accuracy based upon elastic plate theory; the results are checked with photoelastic experiments. The material along the axis of the concentrated force is subjected to transverse tensile force which is called "bursting force" and the surface at end section just adjacent to the anchor plate is subjected to tensile force which is called "spalling force". Only the design aspects of the transmission zone with a qualitative study of the stresses are discussed in this chapter. A general discussion on the type of stress distribution for various cross sections and application of loads is not

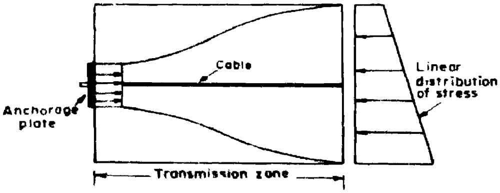

Fig. 13.1.1 : Transmission zone

possible, so some practical cases are presented. For further discussion the reader is referred to *Prestress Concrete* by Guyon (13.1).

13.2. PRESTRESSING CABLE AT THE CENTROIDAL AXIS :

The existence of transverse tensile force could easily be illustrated through fig. 13.2.1. Let the section AA be the end section at which the prestressing force is applied through an anchor plate and let BB be the end of transmission zone at which the stress distribution is linear over the entire section. Considering a free body diagram of an element of the transmission zone cut by a horizontal plane 'cc', it could be seen that there should be some tensile as well as shear stress in the horizontal plane to keep the body in equilibrium. Typical stress trajectories for concentrated force are shown in fig. 13.2.2.

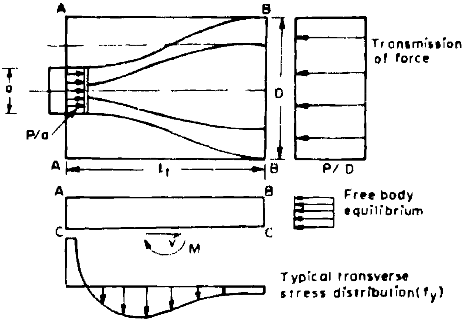

Fig. 13.2.1 : Transmission zone-stress distribution

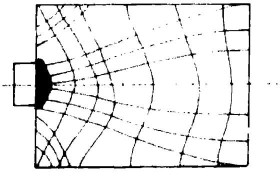

Fig. 13.2.2 : Principal stress trajectories

The transmission length and the stress distribution depends upon the depth of the anchor plate relative to that of the beam. The transmission length and the transverse tensile force (bursting force) are found to be inversely proportional to the ratio of depth of the anchor plate to depth of the beam. A typical representation of bursting force is approximated by a straight line (13.2) and expressed as

$$F_b = 0.3\,P\left(1 - \frac{a}{D}\right) \qquad .. \quad (13.2.1)$$

It is also important to find the position of zero and the maximum transverse tension to locate the reinforcement properly. Fig. 13.2.3 gives the location of zero and maximum tensile stresses along the axis of the tendon. Even though the transmission length varies with depth of the anchor plate, the maximum transmission length is found to be approximately equal to the depth of the beam.

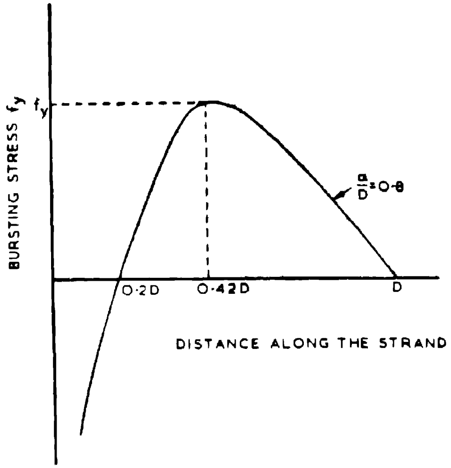

Fig. 13.2.3 : Approximate variation of bursting force

Example : 13.2.1 : Determination of bursting force, and the reinforcement requirement in a simply supported beam of rectangular cross section 80×30 cm subjected to an axial prestressing force of 240 T.

Solution :

Let the size of the anchor plate be 40×24 cm. It is assumed that there are several cables but all of them are going through the same duct with a common anchor plate having an over hang of 3 cm on all sides (fig. 13.2.4).

The intensity of reaction on the plates is

$$=\frac{240000}{40\times24}=250 \text{ kg/sq cm}$$

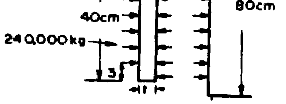

Fig. 13.2.4 : Forces on anchor plate

Design of anchor plate :

Max. B. M. on plate = $250\times3\times3/2=1125$ kg cm/cm

Let the allowable stress in the anchor plate $=1400$ kg/sq cm, then modulus of section required $=1125/1400=0.804$ sq cm

Thickness of plate, 't' $=\sqrt{6\times 0.804}=2.20$ cm

Use 2.5 cm thick anchor plate.

Design of reinforcement in the vertical plane :

Bursting force $=0.3\times 240000\ (1-40/80)=36000$ kg

Bursting force per unit length 'F_b' $=36000/24=1500$ kg/cm

The zero tension occurs at 0.21 D and maximum tension occurs at 0.42 D, for $a/D=0.5$. The approximate bursting force distribution is shown in fig. 13.2.5.

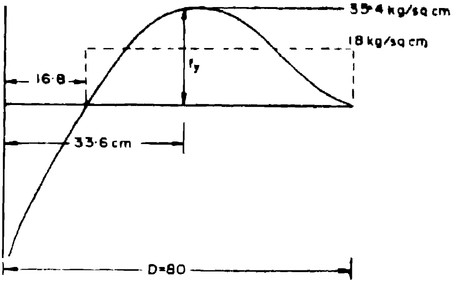

Fig. 13.2.5 : Bursting force distribution

For simplicity of the solution, the tensile stress is assumed to be of parabolic distribution over the tension zone. The maximum tension ordinate is then obtained by equating the area under the curve to the bursting force. If f_y (max), is the maximum tensile stress ordinate, then

$$\frac{2}{3}f_{y\,(max)}\ (80-16.8)=1500$$

$$f_{y\,(max)}=35.4 \text{ kg/sq cm}$$

Reinforcement has to be provided for tension zone where the tension exceeds the allowable concrete tensile stress. Approximate zone in which the tension exceeds the allowable limits is indicated in fig. 13.2.6.

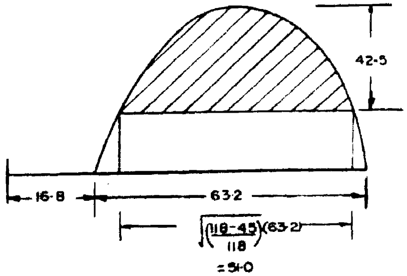

Fig. 13.2.6: Zone of tensile reinforcement

Let 18 kg/sq cm be the allowable tensile stress. Then total tensile force for which the reinforcement is to be provided

$$= \frac{2}{3} \times 51 \times (35.4 - 18) \times 24 = 14200 \text{ kg}$$

Area of reinforcement = 14200/1400 = 10.1 sq cm

Use 7 nos. of 1.5 cm rods over the middle 51 cm tensile zone and provide a nominal 1 cm rods at 6 cm spacing over the rest of the transmission zone.

Design of reinforcement in the horizontal plane :

Bursting force = 0.3 × 240000 (−24/30) = 14400 kg

Then bursting force per unit length, 'F_b' = 14400/72 = 200 kg/cm

The zero and maximum tensile stresses occur at 0.24 D and 0.48 D. The maximum tensile stress ordinate may be obtained as

$$\left(\frac{2}{3}\right) f_y \,(\textbf{max})\ (1 - 0.24)\ 80 = 200$$

$$f_y \,(\textbf{max}) = 5 \text{ kg/sq cm}$$

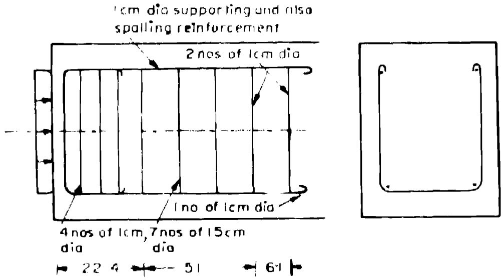

Fig. 13.2.7 : Reinforcement in the bursting zone

The tensile stress on the vertical plane is very small, so no horizontal reinforcement is required other than the nominal steel. The reinforcement provided in the vertical plane may be taken as 'U' stirrups in which case it also serves as nominal horizontal reinforcement.

13.3. SYMMETRIC MULTIPLE CABLES CAUSING AXIAL THRUST : When separate anchor plates distributed over the depth of the beam are used for different cables, the transmission zone and distribution of stress are altered considerably. The even distribution of the anchor plates reduces the transmission length and also the bursting forces. A typical behaviour of the multiple cable force is shown in fig. 13.3.1.

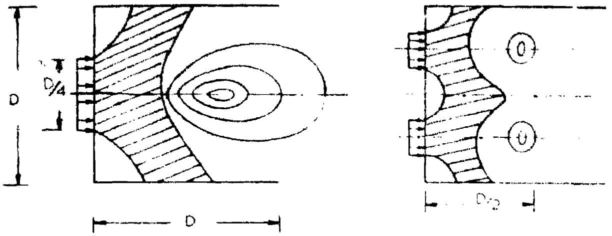

(a) Single anchor plate (b) Two cables with two plates

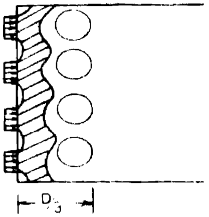

(c) Four cables with four plates

Fig. 13.3.1 : Approximate isobars for transverse tensile stress

The bursting force could be calculated by dividing the total depth into a number of equivalent prism depths. A simple example illustrating the procedure is given below :

Example 13.3.1 : A prestressed beam of 80 by 30 cm cross section is subjected to two symmetric cables each with 120000 kg transfer prestressing force. An anchor plate of 30 by 20 cm is provided for each cable. Determine the reinforcement in the transmission zone.

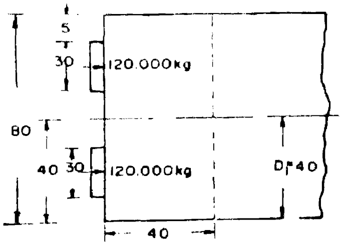

Fig. 13.3.2 : Transmission zone of example 13.3.1

Solution:

$$F_b = \frac{(0.3 \times 120000)}{20}\left(1 - \frac{30}{40}\right) = 450 \text{ kg/cm}$$

(dividing over the width of the anchor plate)

The zero and maximum bursting stress ordinates are at 0.24 D and 0.48 D and are marked in fig. 13.3.3.

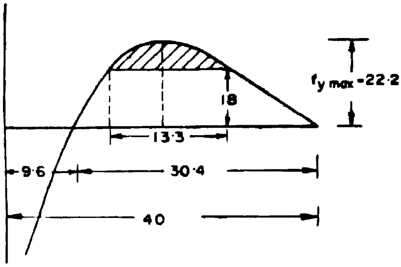

Fig. 13.3.3 : Bursting stress distribution

$f_y\ (\text{max}) = (3/2)\ (450/30.4) = 22.2$ kg/sq cm

Assuming parabolic distribution, the length over which the reinforcement is to be provided is

$= 30.4 \times \sqrt{4.2/22.2} = 13.3$ cm

Total tensile force for which reinforcement is to be provided

$= (2/3)\ (13.3 \times 4.2) \times 20 = 760$ kg

$$\text{Area of steel} = \frac{760}{1400} = 0.54 \text{ sq cm}$$

The area of steel required is relatively small so provide nominal stirrups of 1 cm diameter bars at 10 cm spacing. It is not necessary to check for the other transverse reinforcement because of the anticipated low stresses.

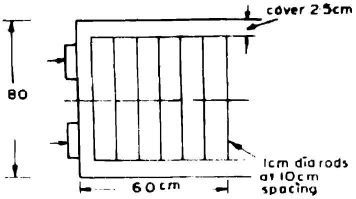

Fig. 13.3.4 : Transmission zone reinforcement

13.4. CABLE WITH ECCENTRICITY: Eccentrically acting prestressing force would cause reorientation in the principal stress trajectories and also in the magnitude of bursting force. A typical representation of isobars and lines of compression are shown in fig. 13.4.1 from which it may be observed that the bursting force is shifted towards the eccentricity. Guyon has suggested an "equivalent prism" method in which a prism is selected where the axis of the load is the axis of the bursting line and the depth of the prism is twice the smallest distance from the load axis to the edge of the concrete. The stress analysis is to be made based on the equivalent prism. This method is found to be satisfactory even though it has some disadvantages in limiting cases. The design of transmission zone is best shown through an illustrative example.

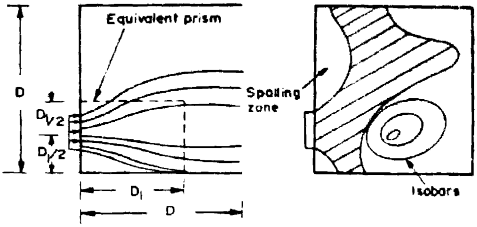

Fig. 13.4.1 : Equivalent prism and isobars for eccentrically acting force

Example 13.4.1 : A beam of cross section 80 by 30 cm is subjected to an eccentric prestressing force of 160000 kg with 10 cm eccentricity. Assuming an anchor plate of size 40 by 20 cm, determine the bursting stress and the necessary reinforcement.

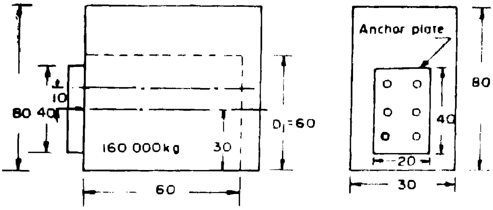

Fig. 13.4.2 : Section of example 13.4.1

Solution:

Vertical plane reinforcement:

Depth of equivalent prism $= D_1 = 60$ cm

$$\frac{a}{D} = \frac{40}{60} = 0.667$$

Procedure as adopted in the previous section is followed from here onwards taking only the width of the anchor plate as effective width.

$F_b = 0.3 \times 160000 \times (1 - 40/60)/20 = 800$ kg/cm

Zero tensile stress occurs at $0.22\ D_1 = 13.2$ cm

$f_y\ (_{max}) = (3 \times 800)/(2 \times 46.8) = 25.6$ kg/sq cm

Assuming 18 kg/sq cm as allowable tension, the length over which reinforcement is required

$= \sqrt{(7.5/25.6) \times (60 - 13.2)} = 25.3$ cm

Total tensile force for which reinforcement is to be provided is

$$= \frac{2}{3} \times (25.3 \times 7.5) \times 20 = 2530 \text{ kg}$$

Area of steel = 2530/1400 = 1.8 sq cm
Use 1 cm dia bars at 10 cm spacing.

13.5. INCLINED PRESTRESSING CABLE:

Most of the practical problems are associated with inclined cable at the end section. The effect of the inclination of the cable is to reorient the stress trajectories and the isobars so that the symmetric axis of the stress trajectories is along the inclined cable axis. The inclination of the cable is generally small, so the reorientation of the axis is not very appreciable. Typical stress trajectories for an inclined cable are shown in fig. 13.5.1. If the inclination is small, as is the case in many practical problems, the bursting force is not much altered; however the spalling forces are increased appreciably. The effect of the vertical component of the cable force will generate secondary splitting stresses which may be neglected for small inclinations of the cables. Design of transmission zone for small inclined cables may be done as adopted for horizontal forces. When the inclination of the cable is large, which might be the case when the cables are terminated in flanges at middle zone of the beam, additional spiral and hoop stirrups should be provided.

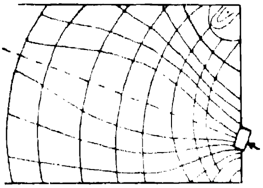

Fig. 13.5.1: Typical stress trajectories for an inclined cable

13.6. SPALLING STRESSES:

Spalling stresses are developed on the edge surfaces of the beam adjacent to the anchor plate. High bearing stresses cause higher lateral tensile strains which are probably the main reasons for spalling of the concrete. The spalling stresses are directly proportional to the bearing stresses imposed and inversely proportional to the interval of the bearing forces. In most cases, the spalling stresses are in the region of 0.3 to 0.4 of P/A and, if the intensity of bearing stress is very high, then the spalling stress could be very high. A typical variation of spalling stresses are shown in fig. 13.6.1. Since the spalling stress is only a localised character at the surfaces adjacent to the anchor plates, the total amount of reinforcement involved is not considerable. A high percentage of small diameter loop stirrup reinforcement should be provided against spalling.

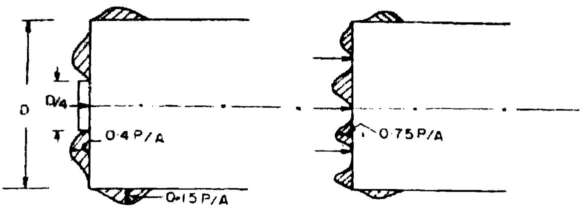

Fig. 13.6.1 : Typical spalling stresses

Problems :

13.1 A post-tensioned concrete beam having end section 100 by 160 cm is provided with 4 cables of 40000 kg each. The cables are spaced in a vertical line so that the centroid of the cables coincide with the centre of gravity of the section. Design anchor plates, vertical and horizontal bursting reinforcement and spalling reinforcement.

13.2 A post-tensioned concrete beam having end section of 60 by 100 cm is provided with two cables of 30000 kg each. The two cables are spaced at 20 cm on either side of the centroid of the beam with 4° inclination. Design the anchor plates, the bursting and spalling reinforcements.

APPENDIX A—TABLES

TABLE 1—VALUES OF Δ_o (FOR FULL STRESS CONDITION AS PER I. S. I.)

Post-tensioned

η	f'_c kg/cm²	c'_{tt}	c'_{ct}	c'_{ce}	c'_{te}	Δ_o
0.80	350	.0286	.5000	.4000	.0286	1.0135
	400	.0250	.4806	.3889	.0250	1.0014
	450	.0222	.4611	.3778	.0222	0.9888
	500	.0200	.4417	.3667	.0200	0.9756
	530	.0189	.4300	.3600	.0189	0.9674
0.85	350	.0286	.5000	.4000	.0286	1.0690
	400	.0250	.4806	.3889	.0250	1.0569
	450	.0222	.4611	.3778	.0222	1.0441
	500	.0200	.4417	.3667	.0200	1.0306
	530	.0189	.4300	.3600	.0189	1.0222

Pre-tensioned

η	f'_c kg/cm²	c'_{tt}	c'_{ct}	c'_{ce}	c'_{te}	Δ_o
0.80	420	.0238	.5000	.4000	.0238	1.0114
	500	.0200	.4741	.3852	.0200	0.9952
	550	.0182	.4579	.3759	.0182	0.9847
	600	.0167	.4417	.3667	.0167	0.9737
	630	.0157	.4300	.3600	.0157	0.9655
0.85	420	.0238	.5000	.4000	.0238	1.0680
	500	.0200	.4741	.3852	.0200	1.0517
	550	.0182	.4579	.3759	.0182	1.0409
	600	.0167	.4417	.3667	.0167	1.0295
	636	.0157	.4300	.3600	.0157	1.0210

TABLE 2—SECTIONAL PROPERTIES

c_t	c_b	c_a	c_l	c_{yb}	c_{yt}	ρ	Δ
	$c_f =$	.40		$c_w =$	.12		
.08	.08	.212	.027	.603	.396	.128	1.523
.08	.10	.218	.028	.590	.409	.132	1.442
.08	.12	.224	.030	.578	.421	.134	1.372
.10	.08	.230	.028	.627	.372	.125	1.682
.10	.10	.236	.030	.614	.385	.129	1.593
.10	.12	.241	.031	.602	.397	.131	1.517
.12	.08	.248	.030	.645	.354	.121	1.823
.12	.10	.253	.031	.633	.366	.125	1.728
.12	.12	.259	.033	.622	.377	.128	1.647
	$c_f =$	.40		$c_w =$	.16		
.08	.08	.246	.029	.589	.410	.120	1.436
.08	.10	.251	.030	.580	.419	.122	1.381
.08	.12	.256	.031	.571	.428	.124	1.332
.10	.08	.263	.031	.610	.389	.118	1.564
.10	.10	.268	.032	.600	.399	.121	1.504
.10	.12	.272	.033	.592	.407	.123	1.451
.12	.08	.280	.032	.626	.373	.116	1.679
.12	.10	.284	.033	.617	.382	.119	1.616
.12	.12	.289	.035	.609	.390	.121	1.560
	$c_f =$	.40		$c_w =$	.20		
.08	.08	.280	.031	.578	.421	.113	1.374
.08	.10	.284	.032	.571	.428	.115	1.336
.08	.12	.288	.033	.565	.434	.116	1.301
.10	.08	.296	.033	.596	.403	.113	1.479
.10	.10	.300	.034	.590	.410	.115	1.439
.10	.12	.304	.035	.583	.416	.116	1.402
.12	.08	.312	.034	.611	.388	.111	1.575
.12	.10	.316	.035	.605	.394	.113	1.532
.12	.12	.320	.036	.599	.401	.115	1.493

$c_f =$ .50 $c_w =$ .12

.08	.08	.220	.029	.583	.416	.135	1.399
.08	.10	.228	.031	.566	.433	.138	1.309
.08	.12	.236	.033	.552	.447	.140	1.233
.10	.08	.238	.031	.607	.392	.132	1.547
.10	.10	.246	.033	.591	.408	.136	1.447
.10	.12	.253	.035	.577	.422	.139	1.364
.12	.08	.256	.032	.626	.373	.128	1.680
.12	.10	.263	.035	.611	.388	.132	1.573
.12	.12	.271	.036	.597	.402	.136	1.483

$c_f =$ .50 $c_w =$ .16

.08	.08	.254	.032	.572	.427	.125	1.338
.08	.10	.261	.033	.559	.440	.128	1.271
.08	.12	.268	.034	.548	.451	.130	1.214
.10	.08	.271	.033	.593	.406	.124	1.458
.10	.10	.278	.035	.580	.419	.127	1.386
.10	.12	.284	.036	.569	.430	.129	1.323
.12	.08	.288	.035	.610	.389	.122	1.567
.12	.10	.294	.037	.598	.401	.125	1.490
.12	.12	.301	.038	.587	.412	.128	1.424

$c_f =$ .50 $c_w =$ .20

.08	.08	.288	.034	.563	.436	.118	1.292
.08	.10	.294	.035	.554	.445	.120	1.243
.08	.12	.300	.036	·545	.454	.122	1.199
.10	.08	.304	.035	.582	.417	.118	1.392
.10	.10	·310	.037	.572	.427	.120	1.339
.10	.12	.316	.038	.563	.436	.122	1.292
.12	.08	.320	.037	.597	.402	.116	1.484
.12	.10	.326	.038	.588	.411	.119	1.428
.12	.12	.332	.040	.579	.420	.121	1.378

$c_f =$ .60 $c_w =$ .12

.08	.08	.228	.032	.564	.435	.140	1.295
.08	.10	.238	.034	.545	.454	.143	1.198
.08	.12	.248	.035	.528	.471	.144	1.120
.10	.08	.246	.034	.589	.410	.138	1.433
.10	.10	.256	.036	.570	.429	.142	1.327
.10	.12	.265	.038	.553	.446	.144	1.240
.12	.08	.264	.035	.609	.390	.134	1.558
.12	.10	.273	.038	.590	.409	.139	1.444
.12	.12	.283	.040	.574	.425	.142	1.350

	$c_f=$	.60		$c_w=$	.16		
.08	.08	.262	.034	.556	.443	.130	1.252
.08	.10	.271	.036	.540	.459	.133	1.178
.08	.12	.280	.037	.527	.472	.134	1.116
.10	.08	.279	.036	.577	.422	.129	1.366
.10	.10	.288	.038	.562	.437	.132	1.285
.10	.12	.296	.039	.549	.450	.134	1.217
.12	.08	.296	.037	.595	.404	.127	1.469
.12	.10	.304	.039	.580	.419	.131	1.384
.12	.12	.313	.041	.567	.432	.133	1.311

	$c_f=$	.60		$c_w=$	.20		
.08	.08	.296	.036	.549	.450	.122	1.220
.08	.10	.304	.037	.537	.462	.124	1.162
.08	.12	.312	.039	.526	.473	.126	1.112
.10	.08	.312	.038	.568	.431	.122	1.315
.10	.10	.320	.040	.556	.443	.125	1.253
.10	.12	.328	.041	.545	.454	.126	1.199
.12	.08	.328	.039	.583	.416	.121	1.403
.12	.10	.336	.041	.572	.427	.124	1.337
.12	.12	.344	.043	.561	.438	.126	1.279

	$c_f=$	.70		$c_w=$	.12		
.08	.08	.236	.034	.546	.453	.144	1.205
.08	.10	.248	.036	.525	.474	.147	1.106
.08	.12	.260	.038	.506	.493	.148	1.027
.10	.08	.254	.036	.571	.428	.143	1.335
.10	.10	.266	.039	.550	.449	.146	1.225
.10	.12	.277	.041	.532	.467	.148	1.138
.12	.08	.272	.038	.592	.407	.140	1.453
.12	.10	.283	.044	.571	.428	.144	1.335
.12	.12	.295	.043	.553	.446	.146	1.240

	$c_f=$	.70		$c_w=$	.16		
.08	.08	.270	.036	.540	.459	.134	1.177
.08	.10	.281	.038	.523	.476	.136	1.098
.08	.12	.292	.040	.508	.491	.137	1.033
.10	.08	.287	.038	.562	.437	.133	1.285
.10	.10	.298	.040	.545	.454	.136	1.199
.10	.12	.308	.042	.530	.469	.138	1.128
.12	.08	.304	.040	.580	.419	.132	1.383
.12	.10	.314	.042	.563	.436	.135	1.291
.12	.12	.325	.044	.548	.451	.137	1.215

	$c_f =$	.70		$c_w =$	.20		
.08	.08	.304	.038	.536	.463	.126	1.156
.08	.10	.314	.040	.522	.477	.128	1.092
.08	.12	.324	.041	.509	.490	.129	1.038
.10	.08	.320	.040	.555	.445	.126	1.247
.10	.10	.330	.042	.540	.459	.128	1.178
.10	.12	.340	.044	.528	.471	.130	1.119
.12	.08	.336	.042	.570	.429	.125	1.330
.12	.10	.346	.044	.557	.442	.128	1.257
.12	.12	.356	.046	.544	.455	.130	1.195
	$c_f =$	.80		$c_w =$	.12		
.08	.08	.244	.036	.530	.469	.148	1.127
.08	.10	.258	.038	.506	.493	.149	1.028
.08	.12	.272	.040	.487	.512	.149	.949
.10	.08	.262	.038	.555	.444	.147	1.249
.10	.10	.276	.041	.523	.467	.150	1.139
.10	.12	.289	.043	.512	.487	.151	1.052
.12	.08	.280	.040	.576	.432	.144	1.361
.12	.12	.293	.043	.554	.445	.148	1.242
.12	.10	.307	.046	.534	.465	.150	1.147
	$c_f =$	.80		$c_w =$	.16		
.08	.08	.278	.038	.526	.473	.137	1.111
.08	.10	.291	.040	.507	.492	.139	1.029
.08	.12	.304	.042	.490	.509	.139	.962
.10	.08	.295	.040	.548	.451	.137	1.213
.10	.10	.308	.043	.529	.470	.140	1.124
.10	.12	.320	.045	.512	.487	.141	1.051
.12	.08	.312	.042	.566	.433	.136	1.307
.12	.10	.324	.045	.547	.452	.139	1.211
.12	.12	.337	.047	.531	.468	.140	1.133
	$c_f =$	.80		$c_w =$	.20		
.08	.08	.312	.040	.523	.476	.129	1.099
.08	.10	.324	.042	.507	.492	.130	1.030
.08	.12	.336	.044	.493	.506	.131	.973
.10	.08	.328	.042	.542	.457	.129	1.185
.10	.10	.340	.044	.526	.473	.132	1.111
.10	.12	.352	.046	.512	.487	.133	1.050
.12	.08	.344	.044	.558	.441	.128	1.265
.12	.10	.356	.046	.542	.457	.131	1.187
.12	.12	.368	.049	.528	.471	.133	1.121

	$c_f=$	.90		$c_w=$	.12		
.08	.08	.252	.038	.514	.485	.150	1.059
.08	.10	.268	.040	.489	.510	.151	.960
.08	.12	.284	.042	.469	.530	.151	.883
.10	.08	.270	.040	.540	.459	.150	1.175
.10	.10	.286	.043	.515	.484	.152	1.064
.10	.12	.301	.046	.494	.505	.152	.979
.12	.08	.288	.042	.561	.438	.148	1.281
.12	.10	.303	.046	.537	.462	.151	1.161
.12	.12	.319	.048	.516	.483	.152	1.068

	$c_f=$	.90		$c_w=$	.16		
.08	.08	.286	.040	.512	.487	.140	1.052
.08	.10	.301	.042	.492	.507	.141	.968
.08	.12	.316	.044	.474	.525	.141	.901
.10	.08	.303	.042	.534	.465	.140	1.149
.10	.10	.318	.045	.514	.485	.142	1.058
.10	.12	.332	.047	.496	.503	.143	.984
.12	.08	.320	.044	.553	.446	.139	1.239
.12	.10	.334	.047	.533	.466	.142	1.141
.12	.12	.349	.050	.515	.484	.143	1.062

	$c_f=$	.90		$c_w=$	.20		
.08	.08	.320	.042	.511	.488	.131	1.047
.08	.10	.334	.044	.493	.506	.133	.975
.08	.12	.348	.046	.478	.521	.133	.917
.10	.08	.336	.044	.530	.469	.132	1.129
.10	.10	.350	.047	.512	.487	.134	1.052
.10	.12	.364	.049	.497	.502	.135	.989
.12	.08	.352	.046	.546	.453	.132	1.206
.12	.10	.366	.049	.529	.470	.134	1.124
.12	.12	.380	.051	.513	.486	.135	1.057

	$c_f=$	1.00		$c_w=$	.12		
.08	.08	.260	.039	.500	.500	.152	1.000
.08	.10	.278	.042	.474	.525	.153	.901
.08	.12	.296	.044	.452	.547	.151	.826
.10	.08	.278	.042	.525	.474	.153	1.109
.10	.10	.296	.045	.500	.500	.154	1.000
.10	.12	.313	.048	.478	.521	.154	.916
.12	.08	.296	.044	.547	.452	.151	1.210
.12	.10	.313	.048	.521	.478	.154	1.091
.12	.12	.331	.051	.500	.500	.154	1.000

	$c_t =$	1.00		$c_w =$	.16		
.08	.08	.294	.041	.500	.500	.142	1.000
.08	.10	.311	.044	.477	.522	.143	.915
.08	.12	.328	.046	.459	.540	.142	.848
.10	.08	.311	.044	.522	.477	.143	1.092
.10	.10	.328	.047	.500	.500	.144	1.000
.10	.12	.344	.049	.480	.519	.144	.926
.12	.08	.328	.046	.540	.459	.142	1.178
.12	.10	.344	.049	.519	.480	.144	1.079
.12	.12	.361	.052	.500	.500	.145	1.000

	$c_t =$	1.00		$c_w =$	.20		
.08	.08	.328	.043	.500	.500	.133	1.000
.08	.10	.344	.046	.480	.519	.134	.926
.08	.12	.360	.048	.464	.535	.134	.867
.10	.08	.344	.046	.519	.480	.134	1.079
.10	.10	.360	.049	.500	.500	.136	1.000
.10	.12	.376	.051	.483	.516	.137	.935
.12	.08	.360	.048	.535	.464	.134	1.153
.12	.10	.376	.051	.516	.483	.137	1.068
.12	.12	.392	.054	.500	.509	.137	1.000

Table. 3. Fixed end moments due to prestressing force

Tendon profile	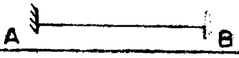
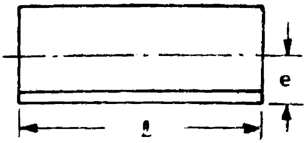	$M'_A=-Pe$ $M_A=0$ $M'_B=-Pe$ $M_B=0$
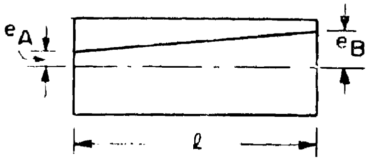	$M'_A=-Pe_A$ $M_A=0$ $M'_B=-Pe_B$ $M_B=0$
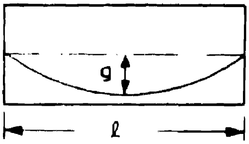	$\left.\begin{array}{l}M'_A\\M_A\\M'_B\\M_B\end{array}\right\}=-\frac{2}{3}Pg$
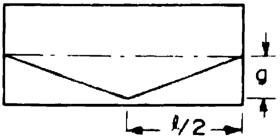	$\left.\begin{array}{l}M'_A\\M_A\\M'_B\\M_B\end{array}\right\}=-\frac{1}{2}Pg$
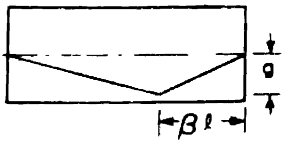	$\left.\begin{array}{l}M_A\\M_A\end{array}\right\}=-Pg\beta$ $\left.\begin{array}{l}M_B\\M_B\end{array}\right\}=-Pg(1-\beta)$
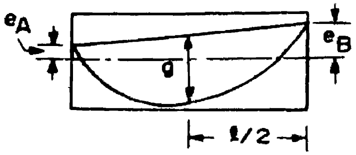	$M'_A=-\frac{P}{3}(2g+3e_A)$ $M_A=-\frac{2}{3}Pg$ $M_B'=-\frac{P}{3}(2g+3e_B)$ $M_B=-\frac{2}{3}Pg$

TABLE 4(a)—MEMBRANE FORCES AND DISPLACEMENTS IN SIMPLY SUPPORTED CYLINDRICAL SHELLS ; LOADS UNIFORMLY DISTRIBUTED ALONG THE LENGTH OF THE BARREL

(a) Uniform Transverse Load[a]

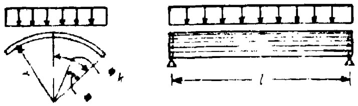

Longitudinal Force N_x—

$$qr\left(\frac{l}{r}\right)^2\times\frac{x}{l}\left(1-\frac{x}{l}\right)\times\text{Col. (1)}$$

Shearing Force $N_{x\phi}$—

$$qr\left(\frac{l}{r}\right)\times\left(1-\frac{2x}{l}\right)\times\text{Col. (2)}$$

Transverse Force N_ϕ—

$$qr\times\text{Col. (3)}$$

Vertical Displacement[b] w—

$$qr\times\frac{l^4}{r^3tE}\times\left\{2\left(\frac{r}{l}\right)^4+\left(\frac{x}{l}\right)^4-2\left(\frac{x}{l}\right)^3+\frac{x}{l}+6\left(\frac{r}{l}\right)^2\left[\frac{x}{l}-\left(\frac{x}{l}\right)^2\right]\right\}\times\text{Col. (4)}$$

Horizontal Displacement[c] v—

$$qr\ \frac{l^4}{r^3tE}\left\{\left(\frac{r}{l}\right)^4\times\text{Col. (5)}+\left[2\left(\frac{r}{l}\right)^4-2\left(\frac{x}{l}\right)^2+\left(\frac{x}{l}\right)^4+\frac{x}{l}+6\left(\frac{r}{l}\right)^2\left(\frac{x}{l}-(x/l)^2\right)\right]\times\text{Col. (6)}\right\}$$

---

[a]The use of column numbers in the formulas refers to the appropriate coefficient in the column cited. [b]Downward direction is positive. [c]Inward direction is positive.

TABLE 4(a)—MEMBRANE FORCES AND DISPLACEMENTS IN SIMPLY SUPPORTED CYLINDRICAL SHELLS ; LOADS UNIFORMLY DISTRIBUTED ALONG THE LENGTH OF THE BARREL (*Contd.*)

(*a*) *Uniform Transverse Load*

$\phi_K - \phi$	N_x	$N_{x\phi}$	N_ϕ	w	v	v
	(1)	(2)	(3)	(4)	(5)	(6)
0	−1.500	0	−1.0000	0.5000	0	0
5	−1.477	−0.1302	−0.9924	0.4944	0.0872	−0.0003
10	−1.409	−0.2565	−0.9698	0.4775	0.1736	−0.0026
15	−1.295	−0.3749	−0.9330	0.4506	0.2588	−0.0072
20	−1.150	−0.4820	−0.8830	0.4148	0.3420	−0.0200
25	−0.965	−0.5746	−0.8214	0.3722	0.4226	−0.0377
30	−0.750	−0.6503	−0.7500	0.3447	0.5000	−0.0625
35	−0.513	−0.7048	−0.6710	0.2748	0.5736	−0.0944
40	−0.261	−0.7385	−0.5868	0.2247	0.6428	−0.1328
45	0	−0.7500	−0.5000	0.1767	0.7071	−0.1768
50	0.261	−0.7385	−0.4132	0.1328	0.7660	−0.2247
55	0.513	−0.7048	−0.3290	0.0944	0.8191	−0.2749
60	0.750	−0.6503	−0.2500	0.0625	0.8660	−0.3248
65	0.965	−0.5746	−0.1786	0.0377	0.9063	−0.3722
70	1.150	−0.4820	−0.1170	0.0199	0.9397	−0.4149
75	1.295	−0.3749	−0.0669	0.0086	0.9659	−0.4506
80	1.409	−0.2565	−0.0301	0.0026	0.9848	−0.4776
85	1.477	−0.1302	−0.0076	0.0004	0.9962	−0.4943
90	1.500	0	0	0	1.0000	−0.5000

TABLE 4(b)—MEMBRANE FORCES AND DISPLACEMENTS IN SIMPLY SUPPORTED CYLINDRICAL SHELLS; LOADS UNIFORMLY DISTRIBUTED ALONG THE LENGTH OF THE BARREL

(b) Dead Weight Load[a]

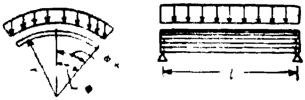

Longitudinal Force N_x—

$$q_g r \left(\frac{l}{r}\right)^2 \times \frac{x}{l}\left(1-\frac{x}{l}\right)\times \text{Col. } (7)$$

Shearing Force $N_{x\phi}$—

$$q_g r \left(\frac{l}{r}\right)\times\left(1-\frac{2x}{l}\right)\times \text{Col. } (8)$$

Transverse Force N_ϕ—

$$q_g r \times \text{Col. } (9)$$

Vertical Displacement[b] w—

$$q_g r \frac{l^4}{r^3 tE}\left\{-\frac{1}{6}\left(\frac{x}{l}\right)^3+\frac{1}{12}\left(\frac{x}{l}\right)^4+\frac{1}{12}\left(\frac{x}{l}\right)+2\left(\frac{r}{l}\right)^2\left[\frac{x}{l}-\left(\frac{x}{l}\right)^2\right]+\left(\frac{r}{l}\right)^4\times \text{Col. } (10)\right\}$$

Horizontal Displacement[c] v—

$$q_g r \frac{l^4}{r^3 tE}\left(\frac{r}{l}\right)^4\times \text{Col. } (11)$$

---

[a] The use of column numbers in the formulas refers to the appropriate coefficient in the column cited. [b] Downward direction is positive. [c] Inward direction is positive.

TABLE 4(b)—MEMBRANE FORCES AND DISPLACEMENTS IN SIMPLY SUPPORTED CYLINDRICAL SHELLS; LOADS UNIFORMLY DISTRIBUTED ALONG THE LENGTH OF THE BARREL (*Contd.*)

(*b*) *Dead Weight Load*

$\phi_K-\phi$	N_x (7)	$N_{x\phi}$ (8)	N_ϕ (9)	w (10)	v (11)
0	−1.0000	0	−1.0000	1.0000	0
5	−0.9962	−0.0871	−0.9962	0.9924	0.0868
10	−0.9848	−0.1736	−0.9848	0.9698	0.1710
15	−0.9659	−0.2589	−0.9659	0.9330	0.2500
20	−0.9397	−0.3421	−0.9397	0.8830	0.3214
25	−0.9063	−0.4225	−0.9063	0.8214	0.3830
30	−0.8660	−0.5000	−0.8660	0.7500	0.4330
35	−0.8191	−0.5737	−0.8191	0.6710	0.4698
40	−0.7660	−0.6428	−0.7660	0.5868	0.4924
45	−0.7071	−0.7071	−0.7071	0.5000	0.5000
50	−0.6428	−0.7661	−0.6428	0.4132	0.4924
55	−0.5736	−0.8192	−0.5736	0.3290	0.4698
60	−0.5000	−0.8660	−0.5000	0.2500	0.4330
65	−0.4226	−0.9062	−0.4226	0.1786	0.3830
70	−0.3420	−0·9397	−0.3420	0.1170	0.3214
75	−0.2588	−0.9659	−0.2588	0.0669	0.2500
80	−0.1736	−0.9847	−0.1736	0.0301	0.1710
85	−0.0872	−0.9962	−0.0872	0.0076	0.0868
90	0	−1.0000	0	0	0

TABLE 5(a)—MEMBRANE FORCES AND DISPLACEMENTS IN SIMPLY SUPPORTED CYLINDRICAL SHELLS ; LOADS VARYING FROM ZERO AT THE ENDS TO MAXIMUM AT THE MIDDLE

(a) Uniform Transverse Load

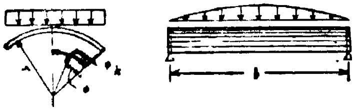

Longitudinal Force N_x—

$$qr\left[\left(\frac{l}{r}\right)^2 \times \text{Col. (1)}\right]\sin\frac{\pi x}{l}$$

Shearing Force $N_{x\phi}$—

$$qr\left[\left(\frac{l}{r}\right) \times \text{Col. (2)}\right]\cos\frac{\pi x}{l}$$

Transverse Force N_ϕ—

$$qr \times \text{Col. (3)} \times \sin\frac{\pi x}{l}$$

Vertical Displacement w—

$$qr\,\frac{l^4}{r^3 tE}\left[\left(1+\frac{1}{2}(\pi r/l)^2+\frac{1}{12}(\pi r/l)^4\right) \times \text{Col. (4)}\right]\sin\frac{\pi x}{l}$$

Horizontal Displacement v—

$$+\,qr\,\frac{l^4}{r^3 tE}\left\{\left(\frac{r}{l}\right)^4 \times \text{Col. (5)} + \left[1+\frac{1}{2}\left(\frac{\pi r}{l}\right)^2+\frac{1}{12}\left(\frac{\pi r}{l}\right)^4\right] \times \text{Col. (6)}\right\} \times \sin\frac{\pi x}{l}$$

TABLE 5(a)—MEMBRANE FORCES AND DISPLACEMENTS IN SIMPLY SUPPORTED CYLINDRICAL SHELLS; LOADS VARYING FROM ZERO AT THE ENDS TO MAXIMUM AT THE MIDDLE (*Contd.*)

(*a*) *Uniform Transverse Load*

$\phi_K-\phi$	N_ϕ	$N_{x\phi}$	N_ϕ	w	v	v
	(1)	(2)	(3)	(4)	(5)	(6)
0	−0.3040	0	−1.0000	0.12319	0	0
5	−0.2993	−0.0829	−0.9924	0.12180	0.0872	−0.00009
10	−0.2856	−0.1633	−0.9698	0.11766	0.1736	−0.00064
15	−0.2623	−0.2387	−0.9330	0.11102	0.2588	−0.00213
20	−0.2329	−0.3069	−0.8830	0.10222	0.3420	−0.00490
25	−0.1954	−0.3658	−0.8214	0.09170	0.4226	−0.00930
30	−0.1520	−0.4140	−0.7500	0.08001	0.5000	−0.01539
35	−0.1040	−0.4487	−0.6710	0.06771	0.5736	−0.02325
40	−0.0528	−0.4702	−0.5868	0.05537	0.6428	−0.03272
45	0	−0.4775	−0.5000	0.04355	0.7071	−0.04355
50	0.0528	−0.4702	−0.4132	0.03272	0.7660	−0.05537
55	0.1040	−0.4487	−0.3290	0.02325	0.8191	−0.06771
60	0.1520	−0.4140	−0.2500	0.01539	0.8660	−0.08001
65	0.1954	−0.3658	−0.1786	0.00930	0.9063	−0.09170
70	0.2329	−0.3069	−0.1170	0.00490	0.9397	−0.10222
75	0.2623	−0.2387	−0.0669	0.00213	0.9659	−0.11102
80	0.2856	−0.1633	−0.0301	0.00064	0.9848	−0.11766
85	0.2993	−0.0829	−0.0076	0.00009	0.9962	−0.12180
90	0.3040	0	0	0	1.0000	−0.12319

TABLE 5(b)—MEMBRANE FORCES AND DISPLACEMENTS IN SIMPLY SUPPORTED CYLINDRICAL SHELLS; LOADS VARYING FROM ZERO AT THE ENDS TO MAXIMUM AT THE MIDDLE

(b) Dead Weight Load

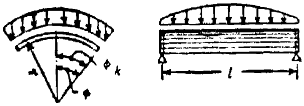

Longitudinal Force N_x

$$q_g\, r \left[\left(\frac{l}{r}\right)^2 \times \text{Col. (7)}\right] \sin\frac{\pi x}{l}$$

Shearing Force $N_{x\phi}$—

$$q_g\, r \left[\left(\frac{l}{r}\right) \times \text{Col. (8)}\right] \cos\frac{\pi x}{l}$$

Transverse Force N_ϕ—

$$q_g\, r \times \text{Col. (9)} \times \sin\frac{\pi x}{l}$$

Vertical Diplacement w—

$$q_g\, r\, \frac{l^4}{r^3 t E}\left[\left(\frac{2r}{\pi l}\right)^2 + \frac{2}{\pi^4} + \left(\frac{r}{l}\right)^4 \times \text{Col. (10)}\right] \sin\frac{\pi x}{l}$$

Horizontal Displacement v—

$$+q_g\, r\, \frac{l^4}{r^3 t E}\left[\left(\frac{r}{l}\right)^4 \times \text{Col. (11)}\right] \times \sin\frac{\pi x}{l}$$

TABLE 5(b)—MEMBRANE FORCES AND DISPLACEMENTS IN SIMPLY SUPPORTED CYLINDRICAL SHELLS ; LOADS VARYING FROM ZERO AT THE ENDS TO MAXIMUM AT THE MIDDLE (*Contd.*)

(*b*) *Dead Weight Load*

$\phi_K-\phi$	N_x	$N_{x\phi}$	N_ϕ	w	v
	(7)	(8)	(9)	(10)	(11)
0	−0.2026	0	−1.000	1.0000	0
5	−0.2019	−0.0555	−0.9962	0.9924	0.0868
10	−0.1996	−0.1105	−0.9848	0.9698	0.1710
15	−0.1957	−0.1648	−0.9659	0.9330	0.2500
20	−0.1904	−0.2178	−0.9397	0.8830	0.3214
25	−0.1837	−0.2690	−0.9063	0.8214	0.3830
30	−0.1754	−0.3183	−0.8660	0.7500	0.4330
35	−0.1660	−0.3652	−0.8191	0.6710	0.4698
40	−0.1552	−0.4092	−0.7660	0.5868	0.4924
45	−0.1433	−0.4502	−0.7071	0.5000	0.5000
50	−0.1302	−0.4877	−0.6428	0.4132	0.4924
55	−0.1162	−0.5215	−0.5736	0.3290	0.4698
60	−0.1013	−0.5513	−0.5000	0.2500	0.4330
65	−0.0856	−0.5769	−0.4226	0.1786	0.3830
70	−0.0693	−0.5982	−0.3420	0.1170	0.3214
75	−0.0524	−0.6149	−0.2588	0.0669	0.2500
80	−0.0351	−0.6269	−0.1736	0.0301	0.1710
85	−0.0177	−0.6342	−0.0872	0.0076	0.0868
90	0	−0.6366	0	0	0

TABLE 6(a)—MEMBRANE FORCES AND DISPLACEMENTS IN SIMPLY SUPPORTED CYLINDRICAL SHELLS ; LOADS VARYING FROM ZERO AT THE ENDS TO MAXIMUM NEGATIVE AT THE MIDDLE

(*a*) *Uniform Transverse Load*

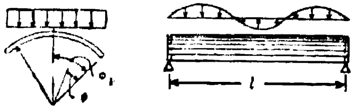

Longitudinal Force N_x—

$$qr\left(\frac{l}{r}\right)^2\times\text{Col. (1)}\times\sin\frac{3\pi x}{l}$$

Shearing Force $N_{x\phi}$—

$$qr\,\frac{l}{r}\times\text{Col. (2)}\times\cos\frac{3\pi x}{l}$$

Transverse Force N_ϕ—

$$qr\times\text{Col. (3)}\times\sin\frac{3\pi x}{l}$$

Vertical Displacement w—

$$qr\,\frac{l^4}{r^3tE}\left[1+\frac{9}{2}\left(\frac{\pi r}{l}\right)^2+\frac{81}{12}\left(\frac{\pi r}{l}\right)^4\right]\text{Col. (4)}\times\sin\frac{3\pi x}{l}$$

Horizontal Displacement v—

$$qr\,\frac{l^4}{r^3tE}\left\{\left(\frac{r}{l}\right)^4\times\text{Col. (5)}+\left[1+\frac{9}{2}\left(\frac{\pi r}{l}\right)^4+\frac{81}{12}\left(\frac{\pi r}{l}\right)^4\right]\text{Col. (6)}\right\}\sin\frac{3\pi x}{l}$$

TABLE 6(a)—MEMBRANE FORCES AND DISPLACEMENTS IN SIMPLY SUPPORTED CYLINDRICAL SHELLS; LOADS VARYING FROM ZERO AT THE ENDS TO MAXIMUM NEGATIVE AT THE MIDDLE (*Contd.*)

(*a*) *Uniform Transverse Load*

$\phi_K-\phi$	N_x	$N_{x\phi}$	N_ϕ	w	v	v
	(1)	(2)	(3)	(4)	(5)	(6)
0	−0.0338	0	−1.0000	0.00152	0	0
5	−0.0332	−0.0276	−0.9924	0.00150	0.0872	−0.00000
10	−0.0317	−0.0544	−0.9698	0.00145	0.1736	−0.00000
15	−0.0291	−0.0796	−0.9330	0.00137	0.2588	−0.00002
20	−0.0259	−0.1023	−0.8830	0.00126	0.3420	−0.00006
25	−0.0217	−0.1219	−0.8214	0.00113	0.4226	−0.00011
30	−0.0169	−0.1380	−0.7500	0.00099	0.5000	−0.00019
35	−0.0116	−0.1496	−0.6710	0.00084	0.5736	−0.00029
40	−0.0059	−0.1567	−0.5868	0.00068	0.6428	−0.00040
45	0	−0.1592	−0.5000	0.00054	0.7071	−0.00054
50	0.0059	−0.1567	−0.4132	0.00040	0.7660	−0.00068
55	0.0116	−0.1496	−0.3290	0.00029	0.8191	−0.00084
60	0.0169	−0.1380	−0.2500	0.00019	0.8660	−0.00099
65	0.0217	−0.1219	−0.1786	0.00011	0.9063	−0.00113
70	0.0259	−0.1023	−0.1170	0.00006	0.9397	−0.00126
75	0.0291	−0.0796	−0.0669	0.00002	0.9659	−0.00137
80	0.0317	−0.0544	−0.0301	0.00000	0.9848	−0.00145
85	0.0332	−0.0276	−0.0076	0.00000	0.9962	−0.00150
90	0.0338	0	0	0	1.0000	−0.00152

TABLE 6(b)—MEMBRANE FORCES AND DISPLACEMENTS IN SIMPLY SUPPORTED CYLINDRICAL SHELLS; LOADS VARYING FROM ZERO AT THE ENDS TO MAXIMUM NEGATIVE AT THE MIDDLE

(*b*) *Dead Weight Load*

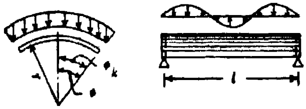

Longitudinal Force N_x—

$$q_g\, r \left(\frac{l}{r}\right)^2 \times \text{Col. (7)} \times \sin \frac{3\pi x}{l}$$

Shearing Force $N_{x\phi}$—

$$q_g\, r \left(\frac{l}{r}\right) \times \text{Col. (8)} \times \cos \frac{3\pi x}{l}$$

Transverse Force N_ϕ—

$$q_g\, r \times \text{Col. (9)} \times \sin \frac{3\pi r}{l}$$

Vertical Displacement w—

$$q_g\, r\, \frac{l^4}{r^3 t E}\left[\frac{2}{81(\pi)^4} + \frac{4}{9}\left(\frac{r}{\pi l}\right)^2 + \left(\frac{r}{l}\right)^4 \times \text{Col. (10)}\right] \sin \frac{3\pi x}{l}$$

Horizontal Displacement v—

$$q_g\, r\, \frac{l^4}{r^3 t E}\left(\frac{r}{l}\right)^4 \times \text{Col. (11)} \times \sin \frac{3\pi x}{l}$$

'able 6(b)—Membrane Forces and Displacements in Simply Supported Cylindrical Shells; Loads Varying from Zero at the Ends to Maximum Negative at the Middle (*Contd.*)

(*b*) *Dead Weight Load*

$\phi_K - \phi$	N_x	$N_{x\phi}$	N_ϕ	w	v
(1)	(7)	(8)	(9)	(10)	(11)
0	−0.0225	0	−1.0000	1.0000	0
5	−0.0224	−0.0185	−0.9962	0.9924	0.0868
10	−0.0222	−0.0368	−0.9848	0.9698	0.1710
15	−0.0219	−0.0549	−0.9659	0.9330	0.2500
20	−0.0212	−0.0726	−0.9397	0.8830	0.3214
25	−0.0204	−0.0897	−0.9063	0.8214	0.3830
30	−0.0195	−0.1061	−0.8660	0.7500	0.4330
35	−0.0184	−0.1217	−0.8191	0.6710	0.4698
40	−0.0172	−0.1364	−0.7660	0.5868	0.4924
45	−0.0159	−0.1501	−0.7071	0.5000	0.5000
50	−0.0145	−0.1626	−0.6428	0.4132	0.4924
55	−0.0129	−0.1738	−0.5736	0.3290	0.4698
60	−0.0113	−0.1838	−0.5000	0.2500	0.4330
65	−0.0095	−0.1923	−0.4226	0.1786	0.3830
70	−0.0077	−0.1994	−0.3420	0.1170	0.3214
75	−0.0058	−0.2050	−0.2588	0.0669	0.2500
80	−0.0040	−0.2090	−0.1736	0.0301	0.1710
85	−0.0019	−0.2114	−0.0872	0.0076	0.0868
90	0	−0.2122	0	0	0

TABLE 7(a)—SYMMETRICAL EDGE LOADS ON SIMPLY SUPPORTED CYLINDRICAL SHELLS

VERTICAL EDGE LOAD	HORIZONTAL EDGE LOAD
(a) Basic Formulas and Loading Diagrams	
Longitudinal Force N_x—	Longitudinal Force N_x—
$V_L\left[\left(\frac{l}{r}\right)^2\times\text{Col. (1)}\right]\sin\frac{\pi x}{l}$	$H_L\left[\left(\frac{l}{r}\right)^2\times\text{Col. (5)}\right]\sin\frac{\pi x}{l}$
Shearing Force $N_{x\phi}$—	Shearing Force $N_{x\phi}$—
$V_L\left[\frac{l}{r}\times\text{Col. (2)}\right]\cos\frac{\pi x}{l}$	$H_L\left[\frac{l}{r}\times\text{Col. (6)}\right]\cos\frac{\pi x}{l}$
Transverse Force N_ϕ—	Transverse Force N_ϕ—
$V_L\times\text{Col. (3)}\times\sin\frac{\pi x}{l}$	$H_L\times\text{Col. (7)}\times\sin\frac{\pi x}{l}$
Transverse Moment M_ϕ—	Transverse Moment M_ϕ—
$V_L\,[r\times\text{Col. (4)}]\sin\frac{\pi x}{l}$	$H_L\,[r\times\text{Col. (8)}]\sin\frac{\pi x}{l}$

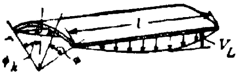

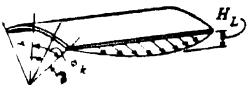

ϕ	N_x (1)	$N_{x\phi}$ (2)	N_ϕ (3)	M_ϕ (4)	N_x (5)	$N_{x\phi}$ (6)	N_ϕ (7)	M_ϕ (8)
(b) r/t=100 and r/l=0.1								
$\phi_K=30$:								
30	−5.382	0	−3.471	−0.3278	−0.0013	0	+0.9997	+0.1310
20	−3.575	−2.619	−2.656	−0.2779	+0.0017	−0.0001	+0.9848	+0.1162
10	+1.809	−3.265	−0.775	−0.1512	+0.0034	+0.0017	+0.9399	+0.0722
0	+10.69	0	+0.500	0	−0.0151	0	+0.8660	0
$\phi_K=35$:								
35	−3.430	0	−2.959	−0.3703	−0.0061	0	+0.9986	+0.1754
30	−3.220	−0.921	−2.820	−0.3594	−0.0043	−0.0068	+0.9951	+0.1717
20	−1.538	−2.302	−1.812	−0.2781	+0.0060	+0.0136	+0.9663	+0.1425
10	+1.822	−2.301	−0.330	−0.1444	+0.0080	+0.0041	+0.9071	+0.0848
0	+6.845	0	+0.574	0	−0.0316	0	+0.8192	0

TABLE 7(a) (*Contd.*)

(*b*) (Continued)

	VERTICAL EDGE LOAD				HORIZONTAL EDGE LOAD			
ϕ	N_x (1)	$N_{x\phi}$ (2)	N_ϕ (3)	M_ϕ (4)	N_x (5)	$N_{x\phi}$ (6)	N_ϕ (7)	M_ϕ (8)
$\phi_K=40$:								
40	− 2.210	0	−2.534	−0.4048	−0.0165	0	+0.9954	+0.2247
30	− 1.806	−1.138	−2.168	−0.3683	−0.0049	−0.0068	+0.9836	+0.2041
20	− 0.578	−1.830	−1.205	−0.2691	+0.0176	−0.0032	+0.9420	+0.1672
10	+ 1.516	−1.614	−0.045	−0.1352	+0.0156	+0.0081	+0.8685	+0.1047
0	+ 4.534	0	+0.643	0	−0.0631	0	+0.7660	0
$\phi_K=45$:								
45	− 1.602	0	−2.231	−0.4355	−0.0359	0	+0.9873	+2.2779
40	− 1.546	−0.434	−2.163	−0.4274	−0.0309	−0.0094	+0.9849	+0.2743
30	− 1.098	−1.180	−1.646	−0.3654	+0.0033	−0.0181	+0.9642	+0.2461
20	− 0.166	−1.550	−0.763	−0.2562	+0.0412	−0.0050	+0.9138	+0.1899
10	+ 1.310	−1.263	+0.179	−0.1255	+0.0260	+0.1175	+0.8251	+0.1072
0	+ 3.407	0	+0.707	0	−0.1185	0	+0.7071	0
$\phi_K=50$:								
50	− 1.051	0	−1.931	−0.4541	−0.0693	0	+0.9696	+0.3336
40	− 0.948	−0.558	−1.741	−0.4265	−0.0213	−0.0326	+0.9650	+0.3198
30	− 0.619	−0.999	−1.208	−0.3492	+0.0284	+0.0366	+0.9430	+0.2786
20	− 0.001	−1.184	−0.451	−0.2379	+0.0820	−0.0039	+0.8851	+0.2104
10	+ 0.998	−0.930	+0.317	−0.1141	+0.0374	+0.0357	+0.7738	+0.1167
0	+ 2.488	0	+0.766	0	−0.2047	0	+0.6428	0
(c) $r/t=100$ and $r/l=0.2$								
$\phi_K=30$:								
30	− 5.160	0	−3.420	−0.3028	−0.0742	0	+0.9815	+0.1219
20	− 3.440	−2.531	−2.632	−0.2565	−0.0123	−0.0292	+0.9757	+0.1084
10	− 1.763	−3.228	−0.787	−0.1395	+0.0700	−0.0087	+0.9427	+0.0678
0	+10.92	0	+0.500	0	−0.1140	0	+0.8660	0

TABLE 7(a) (*Contd.*)

(*c*) (Continued)

ϕ	VERTICAL EDGE LOAD				HORIZONTAL EDGE LOAD			
	N_x (1)	$N_{x\phi}$ (2)	N_ϕ (3)	M_ϕ (4)	N_x (5)	N_ϕ (6)	$N_{x\phi}$ (7)	M_ϕ (8)
$\phi_K=35$:								
35	− 3.087	0	−2.871	−0.3347	−0.1552	0	+0.9603	+0.1591
30	− 2.939	−0.833	−2.744	−0.3248	−0.1260	−0.0399	+0.9622	+0.1559
20	− 1.639	−2.156	−1.807	−0.2514	+0.0561	−0.0634	+0.9649	+0.1301
10	+ 1.501	−2.296	−0.365	−0.1302	+0.1526	+0.0074	+0.9224	+0.0781
0	+ 7.434	0	+0.574	0	−0.3244	0	+0.8192	0
$\phi_K=40$:								
40	− 1.764	0	−2.398	−0.3556	−0.3096	0	+0.9087	+0.1962
30	− 1.640	−0.947	−2.105	−0.3239	−0.1336	−0.1389	+0.9351	+0.1845
20	− 0.965	−1.697	−1.251	−0.2374	+0.2243	−0.1133	+0.9680	+0.1487
10	+ 1.111	−1.753	−0.109	−0.1188	+0.2753	+0.0557	+0.9101	+0.0870
0	+ 5.836	0	+0.643	0	−0.7210	0	+0.7660	0
$\phi_K=45$:								
45	− 0.775	0	−1.934	−0.3619	−0.5679	0	+0.7941	+0.2293
40	− 0.820	−0.217	−1.897	−0.3556	−0.4987	−0.1493	+0.8118	+0.2269
30	− 1.062	−0.731	−1.584	−0.3068	−0.0210	−0.3078	+0.9229	+0.2071
20	− 0.934	−1.317	−0.910	−0.2175	+0.5381	−0.1552	+1.008	+0.1641
10	+ 0.700	−1.478	+0.039	−0.1073	+0.4245	+0.1611	+0.9154	+0.0946
0	+ 5.344	0	+0.707	0	−1.392	0	+0.7071	0
$\phi_K=50$:								
50	+ 0.052	0	−1.437	−0.3493	−0.9469	0	+0.5813	+0.2514
40	− 0.291	−0.028	−1.413	−0.3315	−0.5827	−0.4585	+0.7040	+0.2452
30	− 1.016	−0.383	−1.246	−0.2786	+0.2885	−0.5526	+0.9656	+0.2228
20	− 1.244	−1.059	−0.745	−0.1953	+0.1015	−0.1620	+1.112	+0.1764
10	+ 0.381	−1.427	+0.110	−0.0943	+0.5624	+0.3610	+0.9471	+0.1015
0	+ 5.670	0	+0.766	0	−2.398	0	+0.6428	0

TABLE 7(a) (*Contd.*)

(*c*) (Conclude)

ϕ	VERTICAL EDGE LOAD				HORIZONTAL EDGE LOAD			
	N_x (1)	$N_{x\phi}$ (2)	N_ϕ (3)	M_ϕ (4)	N_x (5)	$N_{x\phi}$ (6)	N_ϕ (7)	M_ϕ (8)
(d) r/t=100 and r/l=0.3								
$\phi_K=30$:								
30	− 4.709	0	−3.362	−0.2769	− 0.2662	0	+0.9571	+0.1099
20	− 3.568	−2.381	−2.632	−0.2347	− 0.0094	−0.0961	+0.9752	+0.0982
10	+ 1.053	−3.290	−0.837	−0.1275	+ 0.2942	+0.0035	+0.9639	+0.0622
0	+12.43	0	+0.500	0	− 0.6606	0	+0.8660	0
$\phi_K=35$:								
35	− 2.156	0	−2.682	−0.2903	− 0.6039	0	+0.8706	+0.1362
30	− 2.203	−0.595	−2.591	−0.2821	− 0.4823	−0.1544	+0.8892	+0.1338
20	− 2.106	−1.817	−1.850	−0.2201	+ 0.2698	−0.2300	+0.9859	+0.1137
10	+ 0.513	−2.456	−0.482	−0.1148	+ 0.6242	+0.0755	+0.9800	+0.0698
0	+10.03	0	+0.574	0	− 1.543	0	+0.8192	0
$\phi_K=40$:								
40	− 0.216	0	−1.977	−0.2853	− 1.176	0	+0.6733	+0.1553
30	− 1.020	−0.275	−1.892	−0.2631	− 0.4865	−0.5149	+0.8208	+0.1488
20	− 2.210	−1.203	−1.430	−0.1982	+ 0.9141	−0.3958	+1.069	+0.1252
10	− 0.295	−2.141	−0.338	−0.1018	+ 1.073	+0.2676	+1.040	+0.0762
0	+10.01	0	+0.643	0	− 3.068	0	+0.7660	0
$\phi_K=45$:								
45	+ 1.400	0	−1.178	−0.2565	− 1.970	0	+0.3055	+0.1591
40	+ 1.083	+0.354	−1.224	−0.2537	− 1.728	−0.5178	+0.3766	+0.1589
30	− 1.040	+0.432	−1.454	−0.2296	− 0.0472	−1.061	+0.8385	+0.1550
20	− 3.110	−0.788	−1.326	−0.1743	+ 1.941	−0.5051	+1.279	+0.1338
10	− 0.946	−2.214	−0.330	−0.0899	+ 1.513	+0.6328	+1.158	+0.0821
0	+11.24	0	+0.707	0	− 5.257	0	+0.7071	0

TABLE 7(a) (*Contd.*)

(*d*) (Continued)

	VERTICAL EDGE LOAD				HORIZONTAL EDGE LOAD			
ϕ	N_x (1)	$N_{x\phi}$ (2)	N_ϕ (3)	M_ϕ (4)	N_x (5)	$N_{x\phi}$ (6)	N_ϕ (7)	M_ϕ (8)
$\phi_K=50$:								
50	+ 2.605	0	−0.326	−0.2300	− 2.821	0	−0.2407	+0.1409
40	+ 1.276	+1.180	−0.676	−0.2032	− 1.744	−1.346	+0.1577	+0.1474
30	− 1.837	+1.062	−1.342	−0.1926	+ 0.8732	−1.624	+1.033	+0.1561
20	− 4.099	−0.690	−1.432	−0.1527	+ 3.129	−0.4486	+1.623	+0.1422
10	− 1.187	−2.497	−0.379	−0.0801	+ 1.766	+1.155	+1.315	+0.0885
0	+12.66	0	+0.766	0	− 7.773	0	+0.6428	0

(e) r/t=100 and r/l=0.4

$\phi_K=30$:								
30	− 3.508	0	−3.175	−0.2404	− 0.736	0	+0.881	+0.0947
20	− 3.500	−1.942	−2.592	−0.2048	− 0.038	−0.2682	+0.958	+0.0856
10	− 0.244	−3.281	−0.947	−0.1121	+ 0.804	−0.0008	+1.008	+0.0544
0	+15.23	0	+0.500	0	− 1.772	0	+0.866	0
$\phi_K=35$:								
35	− 0.217	0	−2.261	−0.2351	− 1.518	0	+0.670	+0.1091
30	− 0.656	−0.102	−2.241	−0.2293	− 1.214	−0.3878	+0.723	+0.1078
20	− 2.982	−1.086	−1.911	−0.1833	+ 0.680	−0.5777	+1.014	+0.0952
10	− 1.512	−2.715	−0.712	−0.0982	+ 1.596	+0.1982	+1.092	+0.0612
0	+15.11	0	+0.574	0	− 3.990	0	+0.819	0
$\phi_K=40$:								
40	+ 2.485	0	−1.221	−0.2044	− 2.664	0	+0.250	+0.1088
30	+ 0.117	+0.913	−1.512	−0.1948	− 1.123	−1.171	+0.606	+0.1093
20	− 4.296	−0.278	−1.730	−0.1580	+ 2.058	−0.9139	+1.236	+0.1013
10	− 2.814	−2.749	−0.749	−0.0862	+ 2.495	+0.6036	+1.272	+0.0665
0	+17.20	0	+0.643	0	− 7.122	0	+0.766	0

TABLE 7(a) (*Contd.*)

(*e*) (Continued)

ϕ	VERTICAL EDGE LOAD				HORIZONTAL EDGE LOAD			
	N_x	$N_{x\phi}$	N_ϕ	M_ϕ	N_ϕ	$N_{x\phi}$	N_ϕ	M_ϕ
	(1)	(2)	(3)	(4)	(5)	(6)	(7)	(8)
$\phi_K=45$:								
45	+4.329	0	−0.119	−0.1513	−3.817	0	−0.372	+0.0899
40	+3.663	+1.126	−0.277	−0.1526	−3.381	−1.005	−0.230	+0.0923
30	−0.918	+2.029	−1.249	−0.1564	−0.150	−2.079	+0.703	+0.1060
20	−6.034	−0.008	−1.889	−0.1377	+3.796	−1.015	+1.638	+0.1083
10	−3.355	−3.194	−0.854	−0.0780	+3.104	+1.260	+1.497	+0.0731
0	+19.64	0	+0.707	0	−10.78	0	+0.707	0
$\phi_K=50$:								
50	+4.973	0	+0.784	−0.0881	−4.477	0	−1.043	+0.0545
40	+2.829	+2.328	+0.079	+0.1028	−2.858	−2.155	−0.394	+0.0716
30	−2.433	+2.516	−1.399	−0.1279	+1.235	−2.673	+1.065	+0.1057
20	−6.881	−0.213	−2.118	−0.1244	+5.125	−0.8202	+2.120	+0.1184
10	−3.049	−3.540	−0.904	−0.0724	+3.212	+1.909	+1.707	+0.0810
0	+20.35	0	+0.766	0	−13.59	0	+0.643	0

(f) $r/t=100$ and $r/l=0.5$

$\phi_K=30$:								
30	−1.757	0	−2.879	−0.2019	−1.420	0	+0.767	+0.0789
20	−3.508	−1.323	−2.524	−0.1738	−0.037	−0.5108	+0.932	+0.0727
10	−2.292	−3.378	−1.108	−0.0969	+1.616	+0.0381	+1.071	+0.0489
0	+20.22	0	+0.500	0	−3.767	0	+0.866	0
$\phi_K=35$:								
35	+2.471	0	−1.677	−0.1788	−2.776	0	+0.395	+0.0816
30	+1.493	+0.587	−1.758	−0.1758	−2.223	−0.7101	+0.495	+0.0816
20	−4.209	−0.060	−2.002	−0.1480	+1.246	−1.062	+1.056	+0.0775
10	−4.426	−3.090	−1.055	−0.0837	+2.986	+0.3737	+1.252	+0.0535
0	+22.54	0	+0.574	0	−7.555	0	+0.819	0

TABLE 7(a) (*Contd.*)

(*f*) (Continued)

	VERTICAL EDGE LOAD				HORIZONTAL EDGE LOAD			
ϕ	N_x (1)	$N_{x\phi}$ (2)	N_ϕ (3)	M_ϕ (4)	N_x (5)	$N_{x\phi}$ (6)	N_ϕ (7)	M_ϕ (8)
$\phi_K=40$:								
40	+ 5.472	0	−0.358	−0.1324	− 4.282	0	−0.220	+0.0682
30	+ 1.404	+2.232	−1.069	−0.1354	− 1.839	−1.889	+0.363	+0.0754
20	− 6.661	+0.757	−2.062	−0.1254	+ 3.336	−1.488	+1.415	+0.0819
10	− 5.826	−3.503	−1.214	−0.0751	+ 4.196	+1.017	+1.528	+0.0593
0	+26.12	0	+0.643	0	−12.17	0	+0.766	0
$\phi_K=45$:								
45	+ 6.655	0	+0.771	−0.0750	− 4.823	0	−0.923	+0.0405
40	+ 5.749	+1.741	+0.524	−0.0793	− 4.625	−1.375	−0.727	+0.0448
30	− 0.652	+3.364	−1.053	−0.1039	− 0.365	−2.902	+0.573	+0.0709
20	− 8.443	+0.730	−2.362	−0.1125	+ 5.266	−1.497	+1.929	+0.0901
10	− 5.758	−4.033	−1.326	−0·0708	+ 4.705	+1.781	+1.798	+0.0670
0	+27.76	0	+0.707	0	−16.12	0	+0.707	0
$\phi_K=50$:								
50	+ 6.074	0	+1.416	−0.0253	− 5.122	0	−1.462	+0.0088
40	+ 3.738	+2.900	+0.542	−0.0469	− 3.478	−2.507	−0.713	+0.0302
30	− 2.427	+3.394	−1.371	−0.0900	+ 1.103	−3.275	+1.025	+0 0759
20	− 8.536	+0.212	−2.512	−0.1065	+ 6.245	−1.164	+2.385	+0.1024
10	− 4.760	−4.221	−1.261	−0.0672	+ 4.596	+2.387	+1.966	+0.0752
0	+ 26.68	0	+0.766	0	− 18.51	0	+0.643	0
(g) r/t=100 and r/l=0.6								
$\phi_K=30$:								
30	+ 0.690	0	−2.477	−0.1646	− 2.375	0	+0.609	+0.0636
20	− 3.149	−0.438	−2.432	−0.1447	− 0.079	−0.8580	+0.895	+0.0605
10	− 5.088	−3.429	−1.334	−0.0837	+ 2.720	+0.0560	+1.160	+0.0431
0	+26.76	0	+0.500	0	− 6.379	0	+0.866	0

TABLE 7(a) (*Contd.*)

(g) (Conclude)

	VERTICAL EDGE LOAD				HORIZONTAL EDGE LOAD			
ϕ	N_x (1)	$N_{x\phi}$ (2)	N_ϕ (3)	M_ϕ (4)	N_x (5)	N_ϕ (6)	N_ϕ (7)	M_ϕ (8)
$\phi_K=35$:								
35	+ 5.530	0	+0.999	−0.1294	− 4.187	0	+0.085	+0.0577
30	+ 3.964	+1.371	−1.194	−0.1291	− 3.368	−1.072	+0.231	+0.0589
20	− 5.521	+1.142	−2.096	−0.1187	+ 1.835	−1.625	+1.098	+0.0628
10	− 7.862	−3.492	−1.452	−0.0731	+ 4.617	+0.5579	+1.438	+0.0477
0	+31.29	0	+0.574	0	−11.74	0	+0.891	0
$\phi_K=40$:								
40	+ 8.029	0	+0.412	−0.0781	− 5.611	0	+0.632	+0.0378
30	+ 2.640	+3.389	−0.660	−0.0907	− 2.518	−2.498	+0.140	+0.0500
20	− 8.598	+1.754	−2.347	−0.1015	+ 4.328	−2.036	+1.563	+0.0673
10	− 8.783	−4.118	−1.651	−0.0674	+ 5.859	+1.341	+1.421	+0.0538
0	+34.71	0	+0.643	0	−17.02	0	+0.766	0
$\phi_K=45$:								
45	+ 7.904	0	+1.346	−0.0293	− 5.855	0	−1.258	+0.0115
40	+ 6.935	+2.078	+1.051	−0.0352	− 5.259	−1.550	−1.038	+0.0166
30	− 0.196	+4.195	−0.884	−0.0712	− 0.727	−3.373	+0.459	+0.0490
20	− 9.841	+1.352	−2.657	−0.0959	+ 6.025	−1.905	+2.094	+0.0775
10	− 7.893	−4.563	−1.682	−0.0659	+ 6.150	+2.089	+2.020	+0.0623
0	+34.56	0	+0.707	0	−20.64	0	+0.707	0
$\phi_K=50$:								
50	+ 6.029	0	+1.647	+0.0038	− 4.847	0	−1.571	−0.0114
40	+ 4.096	+2.955	+0.283	−0.0192	− 3.656	−2.446	−0.851	+0.0100
30	− 1.803	+3.754	−1.264	−0.0627	+ 0.458	−3.469	+0.919	+0.0574
20	− 9.145	+0.659	−2.736	−0.0932	+ 6.530	−1.539	+2.469	+0.0897
10	− 6.445	−4.528	−1.501	−0.0624	+ 6.010	+2.570	+2.141	+0.0696
0	+31.83	0	+0.766	0	−22.64	0	+0.643	0

TABLE 7(a) (*Contd.*)

	VERTICAL EDGE LOAD				HORIZONTAL EDGE LOAD			
ϕ	N_x (1)	$N_{x\phi}$ (2)	N_ϕ (3)	M_ϕ (4)	N_x (5)	$N_{x\phi}$ (6)	N_ϕ (7)	M_ϕ (8)
(h) r/t=200 and r/l=0.1								
$\phi_K=30$:								
30	− 5.388	0	−3.482	−0.3278	− 0.0129	0	+0.9979	+0.1310
20	− 3.600	−2.628	−2.666	−0.2779	+ 0.0014	−0.0043	+0.9845	+0.1162
10	+ 1.787	−3.290	−0.781	−0.1511	+ 0.0164	+0.0020	+0.9410	+0.0722
0	+10.83	0	+0.500	0	− 0.0447	0	+0.8660	0
$\phi_K=35$:								
35	− 3.373	0	−2.947	−0.3692	− 0.0349	0	+0.9926	+0.1751
30	− 3.175	−0.907	−2.810	−0.3584	− 0.0272	−0.0089	+0.9901	+0.1715
20	− 1.566	−2.282	−1.814	−0.2774	+ 0.0192	−0.0121	+0.9675	+0.1424
10	+ 1.763	−2.310	−0.337	−0.1441	+ 0.0378	+0.0075	+0.9107	+0.0832
0	+ 6.999	0	+0.574	0	− 0.1053	0	+0.8192	0
$\phi_K=40$:								
40	− 2.193	0	−2.526	−0.4041	− 0.0791	0	+0.9782	+0.2237
30	− 1.834	−1.137	−2.168	−0.3677	− 0.0303	−0.0341	+0.9742	+0.2095
20	− 0.678	−1.866	−1.220	−0.2690	+ 0.0667	−0.0239	+0.9491	+0.1669
10	+ 1.483	−1.699	−0.048	−0.1354	+ 0.0718	+0.0226	+0.8777	+0.0965
0	+ 4.960	0	+0.643	0	− 0.2243	0	+0.7660	0
$\phi_K=45$:								
45	− 1.415	0	−2.167	−0.4305	− 0.1591	0	+0.9446	+0.2747
40	− 1.384	−0.385	−2.106	−0.4226	− 0.1386	−0.0418	+0.9469	+0.2713
30	− 1.097	−1.081	−1.635	−0.3622	+ 0.0019	−0.0838	+0.9561	+0.2441
20	− 0.350	−1.505	−0.798	−0.2550	+ 0.1623	−0.0353	+0.9371	+0.1892
10	+ 1.175	−1.323	+0.148	−0.1254	+ 0.1167	+0.0570	+0.8460	+0.1071
0	+ 3.887	0	+0.707	0	− 0.4371	0	+0.7071	0

TABLE 7(a) (*Contd.*)

(*h*) (Continued)

	VERTICAL EDGE LOADS				HORIZONTAL EDGE LOAD			
ϕ	N_x (1)	$N_{x\phi}$ (2)	N_ϕ (3)	M_ϕ (4)	N_x (5)	$N_{x\phi}$ (6)	N_ϕ (7)	M_ϕ (8)
$\phi_K=50$:								
50	− 0.838	0	−1.831	−0.4457	− 0.2911	0	+0.8743	+0.3250
40	− 0.842	−0.461	−1.678	−0.4195	− 0.1746	−0.1378	+0.9021	+0.3125
30	− 0.759	−0.908	−1.225	−0.3455	+ 0.1012	−0.1615	+0.9516	+0.2745
20	− 0.314	−1.227	−0.517	−0.2369	+ 0.3240	−0.0358	+0.9439	+0.2092
10	+ 0.907	−1.111	+0.281	−0.1142	+ 0.1645	+0.1245	+0.8204	+0.1167
0	+ 3.402	0	+0.766	0	− 0.7874	0	+0.6428	0

(**i**) **r/t=200 and r/l=0.2**

$\phi_K=30$:								
30	− 4.804	0	−3.394	−0.3054	− 0.2444	0	+0.9630	+0.1216
20	− 3.563	−2.414	−2.649	−0.2592	− 0.0144	−0.0894	+0.9776	+0.1084
10	+ 1.170	−3.280	−0.836	−0.1412	+ 0.2619	−0.0028	+0.9629	+0.0679
0	+12.12	0	+0.500	0	− 0.5594	0	+0.8660	0
$\phi_K=35$:								
35	− 2.269	0	−2.720	−0.3304	− 0.5645	0	+0.8832	+0.1560
30	− 2.290	−0.624	−2.624	−0.3211	− 0.4523	−0.1446	+0.9000	+0.1531
20	− 2.035	−1.854	−1.855	−0.2507	+ 0.2416	−0.2183	+0.9868	+0.1291
10	+ 0.648	−2.423	−0.474	−0.1313	+ 0.5770	+0.0604	+0.9767	+0.0783
0	+ 9.620	0	+0.574	0	− 1.373	0	+0.8191	0
$\phi_K=40$:								
40	− 0.324	0	−2.021	−0.3363	− 1.133	0	+0.6921	+0.1847
30	− 1.057	−0.319	−1.919	−0.3098	− 0.4724	−0.4965	+0.8324	+0.1760
20	− 2.100	−1.229	−1.425	−0.2331	+ 0.8653	−0.3869	+1.067	+0.1458
10	− 0.178	−2.090	−0.327	−0.1202	+ 1.021	+0.2424	+1.036	+0.0873
0	+ 9.537	0	+0.643	0	− 2.851	0	+0.7660	0

TABLE 7(a) (*Contd.*)

(*i*) (Continued)

ϕ	VERTICAL EDGE LOAD				HORIZONTAL EDGE LOAD			
	N_x (1)	$N_{x\phi}$ (2)	N_ϕ (3)	M_ϕ (4)	N_x (5)	$N_{x\phi}$ (6)	N_ϕ (7)	M_ϕ (8)
$\phi_K=45$:								
45	+ 1.358	0	−1.210	−0.3140	− 1.967	0	+0.3169	+0.1973
40	+ 1.046	+0.344	−1.254	−0.3103	− 1.725	−0.5171	+0.3877	+0.1967
30	− 1.033	−0.270	−1.469	−0.2789	− 0.050	−0.6113	+0.8459	+0.1884
20	− 3.035	−0.788	−1.324	−0.2104	+ 1.916	−0.5110	+1.281	+0.1588
10	− 0.885	−2.169	−0.327	−0.1087	+ 1.486	+0.6094	+1.159	+0.0955
0	+10.91	0	+0.707	0	− 5.085	0	+0.7071	0
$\phi_K=50$:								
50	+ 2.686	0	−0.312	−0.2588	− 2.918	0	−0.2665	+0.1807
40	+ 1.320	+1.218	−0.671	−0.2562	− 1.798	−1.391	+0.1445	+0.1856
30	− 1.860	+1.105	−1.355	−0.2385	+ 0.904	−1.675	+1.046	+0.1889
20	− 4.145	−0.669	−1.455	−0.1867	+ 3.198	−0.4671	+1.649	+0.1655
10	− 1.190	−2.490	−0.395	−0.0979	− 1.779	+1.160	+1.332	+0.0992
0	+12.58	0	+0.766	0	− 7.777	0	+0.6428	0
(j) r/t=200 and r/l=0.3								
$\phi_K=30$:								
30	− 2.875	0	−3.097	−0.2688	− 1.018	0	+0.8433	+0.1065
20	− 3.544	−1.727	−2.595	−0.2300	− 0.025	−0.3675	+0.9558	+0.0961
10	− 1.006	−3.351	−1.021	−0.1270	+ 1.142	+0.0251	+1.038	+0.0619
0	+17.18	0	+0.500	0	− 2.618	0	+0.8660	0
$\phi_K=35$:								
35	+ 1.157	0	−2.003	−0.2639	− 3.540	0	+0.5377	+0.1233
30	+ 0.434	+0.250	−2.034	−0.2580	− 1.763	−0.5643	+0.6157	+0.1220
20	− 3.630	−0.571	−1.989	−0.2098	+ 1.001	−0.8379	+1.051	+0.1087
10	− 2.937	−2.907	−0.903	−0.1149	+ 2.318	+0.2927	+1.184	+0.0698
0	+18.66	0	+0.574	0	− 5.780	0	+0.8192	0

TABLE 7(a) (*Contd.*)

(*j*) (Continued)

	VERTICAL EDGE LOAD				HORIZONTAL EDGE LOAD			
ϕ	N_x (1)	$N_{x\phi}$ (2)	N_ϕ (3)	M_ϕ (4)	N_x (5)	$N_{x\phi}$ (6)	N_ϕ (7)	M_ϕ (8)
$\phi_K=40$:								
40	+ 4.491	0	−0.695	−0.2230	− 4.689	0	−0.0553	+0.1198
30	+ 0.927	+1.787	−1.263	−0.2170	− 1.599	−1.680	+0.4612	+0.1225
20	− 5.904	+0.374	−1.979	−0.1836	+ 2.992	−1.296	+1.378	+0.1168
10	− 4.643	−3.248	−1.057	−0.1038	+ 3.576	+0.8937	+1.451	+0.0774
0	+22.55	0	+0.643	0	−10.29	0	+0.7660	0
$\phi_K=45$:								
45	+ 6.463	0	+0.608	−0.1511	− 5.443	0	−0.8614	+0.0899
40	+ 5.541	+1.688	+0.369	−0.1543	− 4.617	−1.379	−0.6652	+0.0937
30	− 0.843	+3.190	−1.138	−0.1700	− 0.203	−2.859	+0.6257	+0.1158
20	− 8.160	+0.555	−2.324	−0.1610	+ 5.220	−1.401	+1.929	+0.1250
10	− 5.055	−3.891	−1.245	−0.0955	+ 4.276	+1.728	+1.762	+0.0858
0	+25.47	0	+0.707	0	−14.77	0	+0.7071	0
$\phi_K=50$:								
50	+ 6.626	0	+1.510	−0.0742	− 5.740	0	−1.603	+0.0441
40	+ 3.900	+3.127	+0.564	−0.0969	− 3.696	−2.769	−0.7707	+0.0676
30	− 2.878	+3.516	−1.463	−0.1393	+ 1.552	−3.453	+1.111	+0.1158
20	− 8.823	+0.094	−2.598	+0.1467	+ 6.637	−1.072	+2.491	+0.1375
10	− 4.273	−4.274	−1.262	−0.0891	+ 4.214	+2.483	+1.987	+0.0953
0	+25.53	0	+0.766	0	−17.75	0	+0.6428	0

(k) $r/t=200$ and $r/l=0.4$

$\phi_K=30$:								
30	+ 1.124	0	−2.479	−0.2211	− 2.625	0	+0.5943	+0.0868
20	− 3.463	−0.295	−2.481	−0.1937	− 0.066	−0.9430	+0.9092	+0.0810
10	− 5.528	−3.468	−1.407	−0.1117	+ 2.974	+0.0700	+1.194	+0.0553
0	+27.68	0	+0.500	0	− 6.899	0	+0.8660	0

TABLE 7(a) (*Contd.*)

(*k*) (Conclude)

	VERTICAL EDGE LOAD				HORIZONTAL EDGE LOAD			
ϕ	N_x (1)	$N_{x\phi}$ (2)	N_ϕ (3)	M_ϕ (4)	N_x (5)	$N_{x\phi}$ (6)	N_ϕ (7)	M_ϕ (8)
$\phi_K = 35$:								
35	+ 6.873	0	−0.795	−0.1830	− 4.932	0	−0.0417	+0.0837
30	+ 5.012	+1.712	−1.039	−0.1820	− 3.951	−1.261	+0.1374	+0.0848
20	− 6.203	+1.614	−2.206	−0.1647	+ 2.208	−1.889	+1.153	+0.0862
10	− 9.087	−3.682	−1.633	−0.1001	+ 5.303	+0.6597	+1.536	+0.0621
0	+34.19	0	+0.574	0	−13.36	0	+0·8192	0
$\phi_K = 40$:								
40	+11.34	0	+0.768	−0.1216	− 7.637	0	−0.8602	+0.0620
30	+ 3.392	+4.247	−0.465	−0.1293	− 2.992	−3.037	+0.0122	+0.0723
20	−10.20	+2.361	−2.620	−0.1409	+ 5.333	−2.419	+1.731	+0.0915
10	−10.34	−4.580	−1.955	−0.0931	+ 6.841	+1.629	+1.957	+0.0704
0	+39.09	0	+0.643	0	−19.78	0	+0.7660	0
$\phi_K = 45$:								
45	+ 9.787	0	+1.934	−0.0436	− 7.229	0	−1.692	+0.0199
40	+ 8.573	+2.572	+1.567	−0.0513	− 6.456	−1.911	−1.419	+0.0264
30	− 0.227	+5.188	−0.825	−0.0982	− 0.709	−4.101	+0.4128	+0.0678
20	−11.70	+1.769	−3.045	−0.1296	+ 7.382	−2.215	+2.378	+0.1027
10	− 9.060	−5.153	−2.000	−0.0887	+ 7.017	+2.520	+2.255	+0.0800
0	+38.68	0	+0.707	0	−23.69	0	+0.7071	0
$\phi_K = 50$:								
50	+ 7.414	0	+2.207	+0.0042	− 6.022	0	−2.055	−0.0134
40	+ 4.947	+3.616	+1.124	−0.0267	− 4.389	−3.008	−1.161	+0.0151
30	− 2.266	+4.540	−1.356	−0.0910	+ 0.8355	−4.146	+0.9927	+0.0776
20	−10.69	+0.849	−3.073	−0.1245	+ 7.857	−1.711	+2.811	+0.1179
10	− 7.142	−5.081	−1.774	−0.0835	+ 6.637	+3.045	+2.378	+0.0892
0	+35.00	0	+0.766	0	−25.44	0	+0.6428	0

TABLE 7(a) (*Contd.*)

	VERTICAL EDGE LOAD				HORIZONTAL EDGE LOAD			
ϕ	N_x (1)	$N_{x\phi}$ (2)	N_ϕ (3)	M_ϕ (4)	N_x (5)	$N_{x\phi}$ (6)	N_ϕ (7)	M_ϕ (8)
				(l) r/t=200 and r/l=0.5				
$\phi_K=30$:								
30	+ 6.908	0	−1.578	−0.1695	− 4.932	0	+0.2325	+0.0656
20	− 3.091	+1.791	−2.323	−0.1564	− 2.320	−1.780	+0.8452	+0.0654
10	−12.18	−3.626	−1.972	−0.0957	+ 5.663	+0.128	+1.422	+0.0492
0	+43.35	0	+0.500	0	−13.29	0	+0.8660	0
$\phi_K=35$:								
35	+12.92	0	+0.520	−0.1106	− 7.760	0	−0.6687	+0.0486
30	+10.14	+3.193	+0.037	−0.1151	− 6.371	−1.952	−0.3803	+0.0518
20	− 8.763	+4.022	−2.425	−0.1266	+ 3.367	−3.036	−1.253	+0.0670
10	−16.09	−4.484	−2.447	−0.0897	+ 8.692	+1.030	+1.926	+0.0564
0	+52.21	0	+0.574	0	−22.16	0	−0.8192	0
$\phi_K=40$:								
40	+13.93	0	+1.963	−0.0443	− 8.898	0	−1.529	+0.0185
30	+ 5.361	+5.888	+0.146	−0.0720	− 4.097	−3.897	−0.3259	+0.0398
20	−12.79	+3.938	−3.042	−0.1129	+ 6.622	−3.303	+1.951	+0.0737
10	−15.31	−5.476	−2.659	−0.0866	+ 9.721	+2.099	+2.350	+0.0645
0	+53.53	0	+0.643	0	−28.17	0	+0.7660	0
$\phi_K=45$:								
45	+10.22	0	+2.435	+0.0045	− 7.196	0	−1.959	−0.0106
40	+ 9.385	+2.771	+2.035	−0.0052	− 6.757	−1.967	−1.675	−0.0034
30	+ 0.957	+5.868	−0.565	−0.0616	− 1.640	−4.438	+0.2286	+0.0431
20	−12.61	+2.686	−3.298	−0.1102	+ 7.723	−2.850	+2.505	+0.0881
10	−12.52	−5.653	−2.457	−0.0832	+ 9.498	+2.791	+2.554	+0.0750
0	+48.96	0	+0.707	0	−30.94	0	+0.7071	0

TABLE 7(a)—(*Contd.*)

(*l*) (Continued)

	VERTICAL EDGE LOAD				HORIZONTAL EDGE LOAD			
ϕ	N_x (1)	$N_{x\phi}$ (2)	N_ϕ (3)	M_ϕ (4)	N_x (5)	$N_{x\phi}$ (6)	N_ϕ (7)	M_ϕ (8)
$\phi_K=50$:								
50	+ 5.720	0	+2.151	+0.0279	− 4.333	0	−1.931	−0.0295
40	+ 5.105	+3.070	+1.265	−0.0015	− 4.431	−2.438	−1.238	−0.0037
30	− 0.025	+4.652	−1.014	−0.0656	− 1.252	−4.161	+0.6846	+0.0569
20	−10.40	+1.897	−3.112	−0.1093	+ 7.442	−2.639	+2.813	+0.1043
10	−12.65	−5.039	−2.643	−0.0852	+11.50	+3.115	+3.155	+0.0913
0	+42.10	0	+0.766	0	−31.89	0	+0.6428	0
(m) r/t=200 and r/l=0.6								
$\phi_K=30$:								
30	+13.41	0	−0.550	−0.1215	− 7.494	0	−0.177	+0.0459
20	− 2.95	+4.174	−2.106	−0.1221	− 0.317	−2.725	+0.756	+0.0512
10	−19.88	−3.751	−2.624	−0.0867	+ 8.756	+0.171	+1.682	+0.0443
0	+61.86	0	+0.500	0	−20.84	0	+0.866	0
$\phi_K=35$:								
35	+17.48	0	+1.581	−0.0576	− 9.794	0	−1.155	+0.0231
30	+13.76	+4.442	+0.942	−0.0648	− 8.004	−2.520	−0.794	+0.0279
20	−10.37	+6.000	−2.570	−0.0989	+ 4.010	−3.973	+1.313	+0.0531
10	−22.33	−5.090	−3.136	−0.0827	+11.70	+1.270	+2.252	+0.0523
0	+68.85	0	+0.574	0	−30.32	0	+0.819	0
$\phi_K=40$:								
40	+14.46	0	+2.530	−0.0052	− 8.900	0	−1.788	−0.0029
30	+ 6.70	+6.504	+0.519	−0.0397	− 4.840	−4.143	−0.527	+0.0213
20	−13.24	+4.992	−3.187	−0.0946	+ 6.608	−3.889	+2.003	+0.0630
10	−19.32	−5.810	−3.114	−0.0812	+12.10	+2.231	+2.601	+0.0616
0	+65.23	0	+0.643	0	−35.15	0	+0.766	0

TABLE 7(a)—(*Concld.*)

(*m*) (Conclude)

	VERTICAL EDGE LOAD				HORIZONTAL EDGE LOAD			
ϕ	N_x (1)	$N_{x\phi}$ (2)	N_ϕ (3)	M_ϕ (4)	N_x (5)	$N_{x\phi}$ (6)	N_ϕ (7)	M_ϕ (8)
$\phi_K=45$:								
45	+8.60	0	+2.397	+0.0217	−5.729	0	−1.858	−0.0205
40	+8.15	+2.319	+2.068	+0.0133	−5.622	−1.562	−1.636	−0.0140
30	+2.68	+5.666	−0.311	−0.0418	−2.980	−4.165	+0.041	+0.0293
20	−11.68	+3.500	−3.237	−0.0948	+6.764	−3.438	+2.416	+0.0759
10	−16.02	−5.641	−2.752	−0.0772	+12.12	+2.709	+2.752	+0.0695
0	+58.53	0	+0.707	0	−38.04	0	+0.707	0
$\phi_K=50$:								
50	+3.09	0	+1.709	+0.0284	−1.816	0	−1.467	−0.0273
40	+4.42	+1.981	+1.179	+0.0063	−3.693	−1.374	−1.120	−0.0084
30	+2.57	+4.287	−0.638	−0.0476	−3.650	−3.722	+0.325	+0.0406
20	−9.53	+2.775	−2.920	−0.0908	+6.372	−3.425	+2.581	+0.0862
10	−14.34	−5.142	−2.383	−0.0706	+13.11	+2.955	+2.877	+0.0757
0	+53.46	0	+0.766	0	−41.80	0	+0.643	0

TABLE 7(b)—SYMMETRICAL EDGE LOAD ON SIMPLY SUPPORTED CYLINDRICAL SHELLS

SHEAR EDGE LOAD	EDGE MOMENT LOAD
(a) Basic Formulas and Loading Diagrams	
Longitudinal Force N_x—	Longitudinal Force N_x—
$S_L \left[\left(\frac{l}{r}\right)^2 \times \text{Col. (9)}\right] \sin\frac{\pi x}{l}$	$\frac{M_L}{r}\left[\left(\frac{l}{r}\right)^2 \times \text{Col. (13)}\right] \sin\frac{\pi x}{l}$
Shearing Force $N_{x\phi}$—	Shearing Force $N_{x\phi}$—
$S_L \left[\frac{l}{r} \times \text{Col. (10)}\right] \cos\frac{\pi x}{l}$	$\frac{M_L}{r}\left[\frac{l}{r} \times \text{Col. (14)}\right] \cos\frac{\pi x}{l}$
Transverse Force N_ϕ—	Transverse Force N_ϕ—
$S_L \times \text{Col. (11)} \times \sin\frac{\pi x}{l}$	$\frac{M_L}{r} \times \text{Col. (15)} \times \sin\frac{\pi x}{l}$
Transverse Moment M_ϕ—	Transverse Moment M_ϕ—
$S_L\ [r \times \text{Col. (12)} \sin\frac{\pi x}{l}$	$M_L \times \text{Col. (16)} \times \sin\frac{\pi x}{l}$

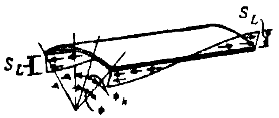

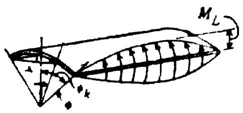

ϕ	N_x (9)	$N_{x\phi}$ (10)	N_ϕ (11)	M_ϕ (12)	N_x (13)	$N_{x\phi}$ (14)	N_ϕ (15)	M_ϕ (16)
(b) r/t = 100 and r/l = 0.1								
$\phi_K = 30$:								
30	−0.0904	0	−0.0207	−0.0010	−0.0038	0	+0.0008	+0.9738
20	−0.0396	−0.0403	−0.0081	−0.0007	+0.0172	+0.0021	+0.0022	+0.9767
10	+0.1118	−0.0250	+0.0142	+0.0002	+0.0264	+0.0173	+0.0014	+0.9854
0	+0.3600	+0.1000	0	0	−0.1370	0	0	+1.000
$\phi_K = 35$:								
35	−0.0774	0	−0.0243	−0.0015	−0.0310	0	−0.0051	+0.9642
30	−0.0694	−0.0205	−0.0213	−0.0014	−0.0211	−0.0076	−0.0037	+0.9650
20	−0.0054	−0.0439	−0.0015	−0.0008	+0.0373	−0.0043	+0.0040	+0.9710
10	+0.1212	−0.0149	+0.0185	−0.0002	+0.0469	+0.0251	+0.0045	+0.9825
0	+0.3076	+0.1000	0	0	−0.2051	0	0	+1.000

TABLE 7(b)—(*Contd.*)

(*b*) (Continued)

	SHEAR EDGE LOAD				EDGE MOMENT LOAD			
ϕ	N_x (9)	$N_{x\phi}$ (10)	N_ϕ (11)	M_ϕ (12)	N_x (13)	$N_{x\phi}$ (14)	N_ϕ (15)	M_ϕ (16)
$\phi_K=40$:								
40	−0.0675	0	−0.0279	−0.0022	−0.0712	0	−0.0184	+0.9530
30	−0.0461	−0.0331	−0.0179	−0.0018	−0.0196	−0.0293	−0.0074	+0.9570
20	+0.0181	−0.0423	+0.0054	−0.0009	+0.0815	−0.0118	+0.0112	+0.9653
10	+0.1236	−0.0057	+0.0221	−0.0002	+0.0724	+0.0998	+0.0106	+0.9798
0	+0.2682	+0.1000	0	0	−0.3099	0	0	+1.000
$\phi_K=45$:								
45	−0.0596	0	−0.0315	−0.0031	−0.1280	0	−0.0437	0.9392
40	−0.0559	−0.0160	−0.0292	−0.0030	−0.1102	−0.0325	−0.0385	+0.9402
30	−0.0258	−0.0398	−0.0123	−0.0022	+0.0128	−0.0642	−0.0047	−0.9469
20	+0.0338	−0.0389	+0.0120	−0.0010	+0.1523	−0.0158	+0.0277	+0.9595
10	+0.1222	+0.0025	+0.0250	−0.0002	+0.0981	+0.0680	+0.0212	+0.9771
0	+0.2378	+0.1000	0	0	−0.4613	0	0	+1.000
$\phi_K=50$:								
50	−0.0531	0	−0.0350	−0.0042	−0.2048	0	−0.0885	+0.9218
40	−0.0423	−0.0271	−0.0268	−0.0037	−0.1192	−0.0964	−0.0573	+0.9258
30	−0.0098	−0.0424	−0.0057	−0.0025	+0.0849	−0.1086	+0.0111	+0.9371
20	+0.0440	−0.0340	+0.0181	−0.0010	+0.2503	−0.0099	+0.0576	+0.9537
10	+0.1188	+0.0077	+0.0275	−0.0002	+0.1176	+0.1119	+0.0373	+0.9745
0	+0.2138	+0.1000	0	0	−0.6695	0	0	+1.000

(c) $r/t=100$ and $r/l=0.2$

$\phi_K=30$:								
30	−0.1946	0	−0.0414	−0.0005	−0.549	0	−0.0813	+0.9009
20	−0.0755	−0.0776	−0.0145	0	−0.073	−0.2142	−0.0153	+0.9124
10	+0.2208	−0.0469	+0.0287	+0.0009	+0.557	−0.0429	+0.0568	+0.9456
0	+0.7119	+0.2000	0	0	−1.067	0	0	+1.000

TABLE 7(b)—(*Contd.*)

(*c*) (Conclude)

ϕ	Shear Edge Load N_x (9)	 $N_{x\phi}$ (10)	 N_ϕ (11)	 M_ϕ (12)	Edge Moment Load N_x (13)	 $N_{x\phi}$ (14)	 N_ϕ (15)	 M_ϕ (16)
$\phi_K=35$:								
35	−0.1487	0	−0.0458	−0.0024	−0.912	0	−0.1914	+0.8637
30	−0.1334	−0.0394	−0.0401	−0.0022	−0.742	−0.2343	−0.1585	+0.8669
20	−0.0106	−0.0845	−0.0018	−0.0012	+0.327	−0.3747	−0.0315	+0.8914
10	+0.2378	−0.0280	+0.0369	−0.0001	+0.928	+0.0486	+0.1212	+0.9362
0	+0.6159	+0.2000	0	0	−2.045	0	0	+1.000
$\phi_K=40$:								
40	−0.1273	0	−0.0525	−0.0035	−1.421	0	−0.3885	+0.1856
30	−0.0880	−0.0626	−0.0335	−0.0029	−0.631	−0.6461	−0.2007	+0.8306
20	+0.0323	−0.0817	+0.0109	−0.0013	+1.015	−0.5396	+0.1574	+0.8707
10	+0.2408	−0.0111	+0.0434	−0.0007	+1.316	+0.2523	+0.2259	+0.9271
0	+0.5460	+0.2000	0	0	−3.452	0	0	+1.000
$\phi_K=45$:								
45	−0.1067	0	−0.0577	−0.0050	−2.074	0	−0.7365	+0.7509
40	−0.0988	−0.0287	−0.0535	−0.0048	−1.828	−0.5460	−0.6582	+0.7558
30	−0.0506	−0.0726	−0.0228	−0.0034	−0.116	−1.138	−0.1410	+0.7920
20	+0.0570	−0.0737	+0.0224	−0.0014	+1.958	−0.5987	+0.3956	+0.8510
10	+0.2353	+0.0028	+0.0482	0	+1.641	+0.5811	+0.3778	+0.9196
0	+0.4995	+0.2000	0	0	−5.299	0	0	+1.000
$\phi_K=50$:								
50	−0.0848	0	−0.0601	−0.0065	−2.814	0	−1.245	+0.6613
40	−0.0714	−0.0439	−0.0468	−0.0056	−1.762	−1.381	−0.8336	+0.6869
30	−0.0258	−0.0723	−0.0113	−0.0035	+0.797	−1.690	+0.0859	+0.7523
20	+0.0664	−0.0639	+0.0312	−0.0013	+3.038	−0.536	+0.7607	+0.8338
10	+0.2257	+0.0125	+0.0513	0	+1.811	+1.083	−0.5718	−0.9154
0	+0.4748	+0.2000	0	0	−7.473	0	0	+1.000

TABLE 7(b)—(*Contd.*)

ϕ	SHEAR EDGE LOAD				EDGE MOMENT LOAD			
	N_x (9)	$N_{x\phi}$ (10)	N_ϕ (11)	M_ϕ (12)	N_x (13)	$N_{x\phi}$ (14)	N_ϕ (15)	M_ϕ (16)
	(d) r/t=100 and r/t=0.3							
$\phi_K=30$:								
30	−0.2618	0	−0.0596	−0.0024	− 2.101	0	−0.3444	+0.7859
20	−0.1182	−0.1174	−0.0231	−0.0016	− 0.108	−0.7669	−0.0802	+0.8119
10	+0.3251	−0.0750	+0.0421	−0.0003	+ 2.372	+0.0141	+0.1945	+0.8845
0	+1.102	+0.3000	0	0	− 5.456	0	0	+1.000
$\phi_K=35$:								
35	−0.2140	0	−0.0685	−0.0036	− 3.493	0	−0.7613	+0.7084
30	−0.1937	−0.0568	−0.0603	−0.0033	− 2.808	−0.8945	−0.6139	+0.7161
20	−0.0244	−0.1248	−0.0046	−0.0018	+ 1.506	−1.358	+0.1098	+0.7726
10	+0.3456	−0.0471	+0.0535	−0.0002	+ 3.764	+0.4236	+0.4372	+0.8689
0	+0.9676	+0.3000	0	0	− 9.403	0	0	+1.000
$\phi_K=40$:								
40	−0.1668	0	−0.0736	−0.0048	− 5.193	0	−1.469	+0.6071
30	−0.1238	−0.0837	−0.0485	−0.0039	− 2.222	−2.288	−0.7475	+0.6444
20	+0.0263	−0.1164	+0.0125	−0.0018	+ 3.993	−1.809	+0.5716	+0.7382
10	+0.3397	−0.0252	+0.0611	−0.0001	+ 5.004	+1.180	+0.7966	+0.8572
0	+0.8934	+0.3000	0	0	−14.38	0	0	+1.000
$\phi_K=45$:								
45	−0.1142	0	+0.0719	−0.0059	− 6.844	0	−2.463	+0.4746
40	−0.1112	−0.0310	−0.0674	−0.0056	− 6.032	−1.802	−2.202	+0.4871
30	−0.0776	−0.0851	−0.0328	−0.0040	− 0.316	−3.743	−0.4779	+0.5768
20	+0.0382	−0.1013	+0.0241	−0.0016	+ 6.770	−1.867	+1.312	+0.7124
10	+0.3209	−0.0128	+0.0645	−0.0001	+ 5.696	+2.230	+1.229	+0.8510
0	+0.8743	+0.3000	0	0	−19.61	0	0	+1.000

TABLE 7(b)—(*Contd.*)

(*d*) (Continued)

	SHEAR EDGE LOAD				EDGE MOMENT LOAD			
ϕ	N_x (9)	$N_{x\phi}$ (10)	N_ϕ (11)	M_ϕ (12)	N_x (13)	$N_{x\phi}$ (14)	N_ϕ (15)	M_ϕ (16)
$\phi_K=50$:								
50	−0.0565	0	−0.0611	−0.0063	− 7.871	0	−3.553	+0.3153
40	−0.0651	−0.0327	−0.0514	−0.0056	− 4.994	−3.782	−2.394	+0.3754
30	−0.0643	−0.0700	−0.0208	−0.0036	+ 2.207	−4.666	+0.2204	+0.5257
20	+0.0214	−0.0879	+0.0276	−0.0013	+ 8.917	−1.422	+2.171	+0.6995
10	+0.3005	−0.0113	+0.0639	+0.0002	+ 5.588	+3.317	+1.625	+0.8508
0	+0.8992	+0.3000	0	0	−23.76	0	0	+1.000
(e) **r/t=100 and r/t=0.4**								
$\phi_K=30$:								
30	−0.3318	0	−0.0772	−0.0028	− 5.33	0	−0.879	+0.6558
20	−0.1568	−0.1503	−0.0304	−0.0019	− 0.14	−1.920	−0.196	+0.6995
10	+0.4153	−0.0998	+0.0545	−0.0003	+ 6.27	+0.187	+0.502	+0.8169
0	+1.508	+0.4000	0	0	−15.27	0	0	+1.000
$\phi_K=35$:								
35	−0.2518	0	−0.0842	−0.0040	− 8.48	0	−1.890	+0.5364
30	−0.2316	−0.0672	−0.0746	−0.0037	− 6.82	−2.173	−1.574	+0.5500
20	−0.0480	−0.1540	−0.0073	−0.0019	+ 3.69	−3.300	+0.248	+0.6463
10	+0.4268	−0.0671	+0.0673	−0.0001	+ 9.37	+1.106	+1.064	+0.8000
0	+1.373	+0.4000	0	0	−23.99	0	0	+1.000
$\phi_K=40$:								
40	−0.1542	0	−0.0818	−0.0049	−11.15	0	−3.211	+0.3896
30	−0.1315	−0.0851	−0.0567	−0.0039	− 4.83	−4.928	−0.164	+0.4541
20	+0.0023	−0.1351	+0.0099	−0.0017	+ 8.71	−3.904	+1.250	+0.6098
10	+0.4228	−0.0471	+0.0728	0	+11.30	+2.733	+1.764	+0.7918
0	+1.368	+0.4000	0	0	−33.39	0	0	+1.000

TABLE 7(b)—(*Contd.*)

(*e*) (Continued)

	SHEAR EDGE LOAD				EDGE MOMENT LOAD			
ϕ	N_x (9)	$N_{x\phi}$ (10)	N_ϕ (11)	M_ϕ (12)	N_x (13)	$N_{x\phi}$ (14)	N_ϕ (15)	M_ϕ (16)
$\phi_K=45$:								
45	−0.0653	0	−0.0657	−0.0051	−12.50	0	−4.647	+0.2210
40	−0.0723	−0.0186	−0.0630	−0.0049	−11.09	−3.299	−4.168	+0.2412
30	−0.1030	−0.0673	−0.0384	−0.0035	− 0.92	−6.970	−0.971	+0.3846
20	−0.0344	−0.1142	+0.0158	−0.0013	+12.56	−3.637	+2.441	+0.5941
10	+0.3651	−0.0449	+0.0716	+0.0003	+11.51	+4.262	+2.363	+0.7936
0	+1.388	+0.4000	0	0	−39.59	0	0	+1.000
$\phi_K=50$:								
50	+0.0216	0	−0.0395	−0.0045	−11.45	0	−5.493	+0.0676
40	−0.0276	+0.0025	−0.0408	−0.0041	− 7.65	−4.182	−3.773	+0.1539
30	−0.1165	−0.0382	−0.0313	−0.0029	+ 2.61	−3.745	+0.216	+0.3594
20	−0.0779	−0.1025	+0.0109	−0.0010	+13.82	−1.157	+3.391	+0.5981
10	+0.3428	−0.0541	+0.0667	+0.0003	+10.19	+5.359	+2.668	+0.7998
0	+1.459	+0.4000	0	0	−41.80	0	0	+1.000
(**f**) **r/t=100 and r/l=0.5**								
$\phi_K=30$:								
30	−0.3849	0	−0.0912	−0.0030	−10.64	0	−1.779	+0.5185
20	−0.1963	−0.1773	−0.0368	−0.0020	− 0.48	−3.877	−0.421	+0.5825
10	+0.4854	−0.1263	+0.0654	−0.0002	+12.53	+0.236	+0.998	+0.7480
0	+1.964	+0.5000	0	0	−30.35	0	0	+1.000
$\phi_K=35$:								
35	−0.2558	0	−0.0962	−0.0039	−14.99	0	−3.345	+0.3692
30	−0.2428	−0.0837	−0.0875	−0.0037	−12.12	−4.668	−2.786	+0.3888
20	−0.0879	−0.1706	−0.0227	−0.0018	+ 6.40	−5.907	+0.453	+0.5266
10	+0.4733	−0.0921	+0.0629	+0.0000	+17.12	+1.978	+1.931	+0.7345
0	+1.867	+0.5000	0	0	−44.56	0	0	+1.000

TABLE 7(b)—(*Contd.*)

(*f*) (Continued)

	SHEAR EDGE LOAD				EDGE MOMENT LOAD			
ϕ	N_x (9)	$N_{x\phi}$ (10)	N_ϕ (11)	M_ϕ (12)	N_x (13)	$N_{x\phi}$ (14)	N_ϕ (15)	M_ϕ (16)
$\phi_K=40$:								
40	−0.1143	0	−0.0775	−0.0034	−17.17	0	−5.060	+0.2033
30	−0.1408	−0.0683	−0.0585	−0.0034	− 7.86	−7.678	−2.645	+0.2912
20	−0.0853	−0.1408	+0.0027	−0.0014	+13.14	−6.372	+1.904	+0.5001
10	+0.4218	−0.0802	+0.0780	+0.0003	+18.72	+4.129	+2.821	+0.7347
0	+1.908	+0.5000	0	0	−54.72	0	0	+1.000
$\phi_K=45$:								
45	+0.0153	0	−0.0477	−0.0038	−15.73	0	−6.128	+0.0523
40	−0.0054	+0.0023	−0.0480	−0.0037	−14.17	−4.167	−5.525	+0.0765
30	−0.1266	−0.0318	−0.0417	−0.0028	− 2.11	−9.122	−1.418	+0.2487
20	−0.1395	−0.1180	+0.0012	−0.0011	+16.12	−5.253	+3.200	+0.5015
10	+0.3807	−0.0882	+0.0726	+0.0003	+17.30	+5.658	+3.294	+0.7426
0	+2.002	+0.5000	0	0	−58.57	0	0	+1.000
$\phi_K=50$:								
50	+0.1028	0	−0.0139	−0.0027	−11.38	0	−6.094	−0.0520
40	+0.0147	+0.0398	−0.0269	−0.0027	− 8.59	−5.742	−4.363	+0.0339
30	−0.1664	−0.0015	−0.0410	−0.0022	+ 0.92	−8.235	−0.093	+0.2533
20	−0.1868	−0.1144	−0.0079	−0.0010	+15.24	−3.756	+3.776	+0.5154
10	+0.3719	−0.1018	+0.0671	+0.0003	+14.96	+6.079	+3.305	+0.7497
0	+2.065	+0.5000	0	0	−56.51	0	0	+1.000
(g) $r/t=100$ and $r/l=0.6$								
$\phi_K=30$:								
30	−0.4130	0	−0.1015	−0.0031	−17.24	0	−2.909	+0.3912
20	−0.2349	−0.1448	−0.0424	−0.0010	− 0.99	−6.327	−0.707	+0.4746
10	+0.5284	−0.1530	+0.0739	−0.0001	+16.89	+0.297	+1.631	+0.6844
0	+2.481	+0.6000	0	0	−50.48	0	0	+1.000

TABLE 7(b)—(*Contd.*)

(*g*) (Conclude)

ϕ	SHEAR EDGE LOAD				EDGE MOMENT LOAD			
	N_ϕ (9)	$N_{x\phi}$ (10)	N_ϕ (11)	M_ϕ (12)	N_x (13)	$N_{x\phi}$ (14)	N_ϕ (15)	M_ϕ (16)
$\phi_K=35$:								
35	−0.2245	0	−0.0937	−0.0036	−21.54	0	−4.900	+0.2286
30	−0.2258	−0.0617	−0.0849	−0.0034	−17.56	−5.539	−4.097	+0.2534
20	−0.1434	−0.1738	−0.0163	−0.0014	+ 8.78	−8.709	+0.609	+0.4257
10	+0.4825	−0.1215	+0.0821	+0.0005	+25.70	+2.778	+2.864	+0.6789
0	+2.453	+0.6000	0	0	−67.87	0	0	+1.000
$\phi_K=40$:								
40	−0.0378	0	−0.0653	−0.0034	−20.91	0	−6.413	+0.0741
30	−0.1275	−0.0385	−0.0561	−0.0020	−10.34	−9.508	−3.449	+0.1748
20	−0.1799	−0.1354	−0.0078	−0.0012	+16.02	−8.383	+2.316	+0.4147
10	+0.4136	−0.1192	+0.0787	+0.0004	+25.53	+5.071	+3.686	+0.6842
0	+2.558	+0.6000	0	0	−75.81	0	0	+1.000
$\phi_K=45$:								
45	+0.1009	0	−0.0267	−0.0026	−15.56	0	−6.655	−0.0364
40	+0.0669	+0.0245	−0.0302	−0.0025	−14.36	−4.156	−6.057	−0.0122
30	−0.1460	+0.0082	−0.0439	−0.0022	− 3.96	−9.685	−1.817	+0.1633
20	−0.2510	−0.1174	−0.0148	−0.0010	+16.43	−6.537	+3.383	+0.4285
10	+0.3813	−0.1339	+0.0714	+0.0004	+22.53	+6.087	+3.873	+0.6947
0	+2.659	+0.6000	0	0	−74.68	0	0	+1.000
$\phi_K=50$:								
50	+0.1678	0	+0.0073	−0.0015	− 8.26	0	−5.666	−0.0950
40	+0.0523	+0.0699	−0.0151	−0.0017	− 8.00	−4.483	−4.344	−0.0164
30	−0.2030	+0.0305	−0.0491	−0.0018	− 1.93	−7.812	−0.623	+0.1835
20	−0.2862	−0.1225	−0.0245	−0.0010	+13.86	−5.044	+3.549	+0.4425
10	+0.3899	−0.1463	+0.0675	+0.0003	+20.05	+5.942	+3.658	+0.6986
0	+2.688	+0.6000	0	0	−70.37	0	0	+1.000

TABLE 7(b)—(*Contd.*)

	SHEAR EDGE LOAD				EDGE MOMENT LOAD			
ϕ	N_x (9)	$N_{x\phi}$ (10)	N_ϕ (11)	M_ϕ (12)	N_x (13)	$N_{x\phi}$ (14)	N_ϕ (15)	M_ϕ (16)
				(h) r/t=200 and r/l=0.1				
$\phi_K=30$:								
30	−0.0905	0	−0.0207	−0.0009	− 0.1005	0	−0.0164	+0.9730
20	−0.0397	−0.0403	−0.0080	−0.0006	+ 0.0123	−0.0332	−0.0024	+0.9761
10	+0.1117	−0.0251	+0.0142	−0.0002	+ 0.1340	+0.0177	+0.0099	+0.9852
0	+0.3604	+0.1000	0	0	− 0.3807	0	0	+1.000
$\phi_K=35$:								
35	−0.0773	0	−0.0243	−0.0015	−0.2044	0	−0.0435	+0.9623
30	−0.0693	−0.0205	−0.0212	−0.0014	−0.1601	−0.0520	−0.0356	+0.9632
20	−0.0055	−0.0439	−0.0015	−0.0008	+0.1134	−0.0710	+0.0090	+0.9700
10	+0.1211	−0.0150	+0.0185	−0.0002	+0.2305	+0.0464	+0.0256	+0.9823
0	+0.3082	+0.1000	0	0	−0.6605	0	0	+1.000
$\phi_K=40$:								
40	−0.0670	0	−0.0278	−0.0022	−0.3607	0	−0.1000	+0.9476
30	−0.0458	−0.0329	−0.0178	−0.0018	−0.1407	−0.1563	−0.0487	+0.9521
20	+0.0177	−0.0425	+0.0054	−0.0009	+0.3060	−0.1102	+0.0428	+0.9635
10	+0.1231	−0.0058	+0.0220	−0.0002	+0.3419	+0.1068	+0.0540	+0.9795
0	+0.2696	+0.1000	0	0	−1.083	0	0	+1.000
$\phi_K=45$:								
45	−0.0585	0	−0.0311	−0.0031	−0.5815	0	−0.2039	+0.9270
40	−0.0549	−0.0127	−0.0288	−0.0030	−0.5076	−0.1526	−0.1817	+0.9284
30	−0.0259	−0.0392	−0.0122	−0.0021	+0.0014	−0.3085	−0.0344	+0.9392
20	+0.0326	−0.0387	+0.0118	−0.0010	+0.5987	−0.1323	+0.1135	+0.9566
10	+0.1213	+0.0021	+0.0248	−0.0002	+0.4491	+0.2141	+0.0996	+0.9768
0	+0.2407	+0.1000	0	0	−1.684	0	0	+1.000

TABLE 7(b)—(*Contd.*)

(*h*) (Continued)

	SHEAR EDGE LOAD				EDGE MOMENT LOAD			
ϕ	N_x (9)	$N_{x\phi}$ (10)	N_ϕ (11)	M_ϕ (12)	N_x (13)	$N_{x\phi}$ (14)	N_ϕ (15)	M_ϕ (16)
$\phi_K=50$:								
50	−0.0506	0	+0.0340	−0.0041	−0.8725	0	−0.3803	+0.8948
40	−0.0408	−0.0260	−0.0262	−0.0036	−0.5294	−0.4145	−0.2512	+0.9030
30	−0.0107	−0.0411	−0.0176	−0.0024	+0.2947	−0.4901	+0.0344	+0.9238
20	+0.0369	−0.0337	+0.0174	−0.0010	+0.9856	−0.1131	+0.2362	+0.9497
10	+0.1175	+0.0087	+0.0271	−0.0001	+0.5268	+0.3830	+0.1664	+0.9741
0	+0.2199	+0.1000	0	0	−2.487	0	0	+1.000

(i) **r/t=200 and r/l=0.2**

$\phi_K=30$:								
30	−0.1770	0	−0.0407	−0.0017	−1.972	0	−0.3043	+0.8904
20	−0.0792	−0.0792	−0.0160	−0.0012	−0.154	−0.7298	−0.0618	+0.9051
10	+0.2192	−0.0502	+0.0279	−0.0003	+2.142	+0.0427	+0.1925	+0.9435
0	+0.7297	+0.2000	0	0	−4.639	0	0	+1.000
$\phi_K=35$:								
35	−0.1455	0	−0.0466	−0.0027	− 3.344	0	−0.7035	+0.8373
30	−0.1313	−0.0386	−0.0410	−0.0025	− 2.696	−0.8582	−0.5812	+0.8425
20	−0.0150	−0.0842	−0.0033	−0.0014	+ 1.373	−1.319	+0.1200	+0.8787
10	+0.2331	−0.0309	+0.0358	−0.0002	+ 3.519	+0.3350	+0.4303	+0.9335
0	+0.6376	+0.2000	0	0	− 8.444	0	0	+1.000
$\phi_K=40$:								
40	−0.1144	0	−0.0503	−0.0037	− 5.147	0	−1.422	+0.7549
30	−0.0838	−0.0572	−0.0331	−0.0030	− 2.213	−2.270	−0.7127	+0.7838
20	+0.0202	−0.0785	+0.0084	−0.0015	+ 3.880	−1.816	+0.5816	+0.8519
10	+0.2295	−0.0158	+0.0411	−0.0002	+ 4.849	+1.085	+0.8003	+0.9255
0	+0.5858	+0.2000	0	0	− 13.55	0	0	+1.000

TABLE 7(b)—(*Contd.*)

(*i*) (Continued)

	SHEAR EDGE LOAD				EDGE MOMENT LOAD			
ϕ	N_x (9)	$N_{x\phi}$ (10)	N_ϕ (11)	M_ϕ (12)	N_x (13)	$N_{x\phi}$ (14)	N_ϕ (15)	M_ϕ (16)
$\phi_K=45$:								
45	−0.0793	0	−0.0494	−0.0047	− 7.076	0	−2.500	+0.6266
40	−0.0769	−0 0215	−0.0462	−0.0045	− 6.231	−1.862	−2.231	+0.6378
30	−0.0516	−0.0642	−0.0223	−0.0032	− 0.316	−2.536	−0.5827	+0.7167
20	+0.0289	−0.0681	+0.0165	−0.0014	+ 6.897	−1.941	+1.367	+0.8267
10	+0.2164	−0.0071	+0.0436	−0.0001	+ 5.708	+2.201	+1.273	+0.9200
0	+0.5724	+0.2000	0	0	−19.32	0	0	+1.000
$\phi_K=50$:								
50	−0.0395	0	−0.0419	−0.0052	− 8.502	0	−3.770	+0.4461
40	−0.0445	−0.0226	−0.0351	−0.0046	− 5.350	−4.060	−2.523	+0.5106
30	−0.0420	−0.0476	−0.0140	−0.0031	+ 2.433	−4.983	+0 2750	+0.6671
20	+0.0168	−0.0585	+0.0187	−0.0013	+ 9.459	−1.527	+2.336	+0.8314
10	+0.2016	−0.0062	+0.0428	−0.0001	+ 5.734	+3.392	+1.737	+0.9393
0	+0.5914	+0.2000	0	0	−24.30	0	0	+1.000
				(j) r/t=200 and r/l=0.3				
$\phi_K=30$:								
30	−0.2481	0	−0.0585	−0.0023	− 8.01	0	−1.251	+0.7583
20	−0.1187	−0.0759	−0.0236	−0.0916	− 0.32	−2.906	−0.242	+0.7953
10	+0.3098	−0.1126	+0.0402	−0.0003	+ 9.20	+0.158	+0.787	+0.8828
0	+1.138	+0.3000	0	0	−21.66	0	0	+1.000
$\phi_K=35$:								
35	−0.1777	0	−0.0616	−0.0033	−12.73	0	+ 2.708	+0.6320
30	−0.1650	−0.0475	−0·0548	−0.0031	−10.23	−3.260	− 2.236	+0.6464
20	−0.0418	−0.1115	−0.0066	−0.0017	+ 5.57	−4.934	+ 0.474	+0.7427
10	+0.3091	−0.0522	+0.0487	−0.0002	+13.92	+1.650	+ 1.650	+0.8689
0	+1.058	+0.3000	0	0	−35.32	0	0	+1.000

TABLE 7(b)—(*Contd.*)

(*j*) (Continued)

ϕ	SHEAR EDGE LOAD				EDGE MOMENT LOAD			
	N_x (9)	$N_{x\phi}$ (10)	N_ϕ (11)	M_ϕ (12)	N_x (13)	$N_{x\phi}$ (14)	N_ϕ (15)	M_ϕ (16)
$\phi_K=40$:								
40	−0.0958	0	−0.0550	−0.0039	−16.80	0	−4.723	+0.4470
30	−0.0958	−0.0529	−0.0397	−0.0032	−7.30	−7.430	−2.380	+0.5253
20	−0.0298	−0.0936	+0.0040	−0.0016	+12.97	−5.929	+1.932	+0.6997
10	+0.2786	−0.0416	+0.0506	−0.0001	+16.75	+3.932	+2.673	+0.8621
0	+1.069	+0.3000	0	0	−48.57	0	0	+1.000
$\phi_K=45$:								
45	−0.0114	0	−0.0370	−0.0038	−17.92	0	−6.551	+0.2280
40	−0.0214	−0.0039	−0.0364	−0.0037	−15.90	−4.718	−5.866	+0.2542
30	−0.0772	−0.0304	−0.0273	−0.0028	−1.34	−9.994	−1.292	+0.4354
20	−0.0627	−0.0765	+0.0042	−0.0013	+17.97	−5.233	+3.575	+0.6795
10	+0.2474	−0.0456	+0.0471	−0.0000	+16.41	+6.050	+3.437	+0.8640
0	+1.134	+0.3000	0	0	−56.01	0	0	+1.000
$\phi_K=50$:								
50	+0.0544	0	−0.0135	−0.0031	−15.39	0	−7.343	+0.0368
40	+0.0026	+0.0201	−0.0201	−0.0029	−10.44	−7.529	−5.048	+0.1442
30	−0.1000	−0.0070	−0.0254	−0.0023	+3.25	−9.817	+0.304	+0.4060
20	−0.1008	−0.0715	−0.0025	−0.0011	+18.60	−3.576	+4.612	+0.6832
10	+0.2354	−0.0563	+0.0424	−0.0000	+14.04	+7.094	+3.666	+0.8700
0	+1.193	+0.3000	0	0	−56.30	0	0	+1.000
(k) $r/t=200$ and $r/l=0.4$								
$\phi_K=30$:								
30	−0.2847	0	−0.0710	−0.0026	−20.19	0	−3.173	+0.5913
20	−0.1583	−0.1339	−0.0302	−0.0018	−0.87	−7.343	−0.619	+0.6619
10	+0.3622	−0.1029	+0.0493	−0.0003	+23.57	+0.435	+1.999	+0.8155
0	+1.634	+0.4000	0	0	−56.52	0	0	+1.000

TABLE 7(b)—(*Contd.*)

(*k*) (Conclude)

	SHEAR EDGE LOAD				EDGE MOMENT LOAD			
ϕ	N_x (9)	$N_{x\phi}$ (10)	N_ϕ (11)	M_ϕ (12)	N_x (13)	$N_{x\phi}$ (14)	N_ϕ (15)	M_ϕ (16)
$\phi_K=35$:								
35	−0.1462	0	−0.0635	−0.0032	− 27.50	0	− 5.935	+0.3911
30	−0.1482	−0.0403	−0.0577	−0.0030	− 22.24	− 7.055	− 4.913	+0.4179
20	−0.0986	−0.1152	−0.0124	−0.0017	+ 11.73	−10.85	+ 1.001	+0.5937
10	+0.3204	−0.0822	+0.0539	−0.0001	+ 31.27	+ 3.583	+ 3.651	+0.8049
0	+1.639	+0.4000	0	0	− 80.78	0	0	+1.000
$\phi_K=40$:								
40	+0.0319	0	−0.0448	−0.0032	− 32.54	0	− 8.301	+0.2027
30	−0.0781	−0.0171	−0.0365	−0.0026	− 13.32	−12.80	− 4.292	+0.2888
20	−0.1367	−0.0848	−0.0086	−0.0014	+ 21.73	−10.76	+ 3.315	+0.5642
10	+0.2620	−0.0845	+0.0492	−0.0000	+ 31.74	+ 6.881	+ 4.858	+0.8083
0	+1.744	+0.4000	0	0	− 92.98	0	0	+1.000
$\phi_K=45$:								
45	+0.0957	0	−0.0099	−0.0065	− 22.45	0	− 8.938	−0.0169
40	+0.0691	+0.0238	−0.0133	−0.0043	− 20.42	− 5.970	− 8.074	+0.0165
30	−0.0987	+0.0199	−0.0292	−0.0020	− 4.08	−13.43	− 2.116	+0.2506
20	−0.1953	−0.0728	−0.0161	−0.0012	+ 23.35	− 8.260	+ 4.819	+0.5714
10	+0.2396	−0.0981	+0.0429	−0.0000	+ 27.40	+ 8.293	+ 5.115	+0.8168
0	+1.826	+0.4000	0	0	− 91.16	0	0	+1.000
$\phi_K=50$:								
50	+0.1395	0	+0.0147	−0.0013	− 13.14	0	− 7.852	−0.1157
40	+0.0505	+0.0598	−0.0042	−0.0015	− 11.30	− 6.932	− 5.801	−0.0061
30	−0.1446	+0.0347	−0.0352	−0.0017	− 1.18	−10.95	− 0.390	+0.2725
20	−0.2195	−0.0793	−0.0240	−0.0011	+ 19.84	− 6.154	+ 5.079	+0.5892
10	+0.2513	−0.1076	+0.0402	+0.0001	+ 23.56	+ 7.944	+ 4.801	+0.8219
0	+1.840	+0.4000	0	0	− 84.42	0	0	+1.000

TABLE 7(b)—(*Contd.*)

	SHEAR EDGE LOAD				EDGE MOMENT LOAD			
ϕ	N_x (9)	$N_{x\phi}$ (10)	N_ϕ (11)	M_ϕ (12)	N_x (13)	$N_{x\phi}$ (14)	N_ϕ (15)	M_ϕ (16)
				(1) r/t=200 and r/l=0.5				
$\phi_K=30$:								
30	−0.2715	0	−0.0759	−0.0026	− 36.86	0	− 5.858	+0.4164
20	−0.1974	−0.1375	−0.0355	−0.0018	− 2.00	−13.49	− 1.174	+0.5258
10	+0.3600	−0.1314	+0.05366	−0.0002	+ 43.95	+ 0.71	+ 3.711	+0.7505
0	+2.253	+0.5000	0	0	−107.5	0	0	+1.000
$\phi_K=35$:								
35	+0.0566	0	−0.0528	−0.0027	− 41.17	0	− 9.181	+0.1851
30	−0.0847	−0.0181	−0.0505	−0.0025	− 33.79	−10.62	− 7.611	+0.2222
20	−0.1818	−0.0966	−0.0204	−0.0015	+ 16.53	−16.90	+ 1.429	+0.4668
10	+0.2700	−0.1200	+0.0516	−0.0001	+ 50.25	+ 5.26	+ 5.747	+0.7504
0	+2.374	+0.5000	0	0	−132.8	0	0	+1.000
$\phi_K=40$:								
40	+0.1093	0	−0.0175	−0.0020	− 32.96	0	−10.30	−0.0072
30	−0.0475	+0.0298	−0.0294	−0.0019	− 17.70	−15.29	− 5.586	+0.1389
20	−0.2613	−0.0652	−0.0242	−0.0012	+ 24.15	−14.33	+ 3.905	+0.4653
10	+0.2136	−0.1319	+0.0433	−0.0000	+ 44.95	+ 8.13	+ 6.422	+0.7611
0	+2.509	+0.5000	0	0	−133.2	0	0	+1.000
$\phi_K=45$:								
45	+0.1830	0	+0.0132	−0.0011	− 18.31	0	− 8.981	−0.1089
40	+0.1446	+0.0466	+0.0066	−0.0012	− 17.78	− 4.98	− 8.263	−0.0771
30	−0.1100	+0.0637	−0.0303	−0.0014	− 8.90	−13.02	− 2.879	+0.1523
20	−0.3155	−0.0676	−0.0341	−0.0011	+ 20.73	−10.69	+ 4.696	+0.4876
10	+0.2211	−0.1467	+0.0389	−0.0001	+ 38.31	+ 8.33	+ 6.068	+0.7681
0	+2.539	+0.5000	0	0	−123.1	0	0	+1.000

TABLE 7(b)—(*Contd.*)

(*l*) (Continued)

ϕ	SHEAR EDGE LOAD				EDGE MOMENT LOAD			
	N_x (9)	$N_{x\phi}$ (10)	N_ϕ (11)	M_ϕ (12)	N_x (13)	$N_{x\phi}$ (14)	N_ϕ (15)	M_ϕ (16)
$\phi_K=50$:								
50	+0.1739	0	+0.0295	+0.0002	− 4.66	0	− 6.575	−0.1404
40	+0.0786	+0.0777	+0.0054	−0.0007	− 9.77	− 3.60	− 5.629	−0.0518
30	−0.1578	+0.0593	−0.0387	−0.0013	− 10.31	− 9.96	− 1.682	+0.1945
20	−0.2949	−0.0794	−0.0364	−0.0011	+ 16.18	− 9.65	+ 4.675	+0.5157
10	+0.2141	−0.1221	+0.0366	−0 0000	+ 41.78	+ 9.30	+ 7.575	+0.8127
0	+2.441	+0.5000	0	0	−116.1	0	0	+1.000
(m) r/t=200 and r/l=0.6								
$\phi_K=30$:								
30	−0.2086	0	−0.0732	−0.0024	− 53.95	0	− 8.721	+0.2589
20	−0.2355	−0.1233	−0.0394	−0.0016	− 4.01	−20.04	− 1.828	+0.4042
10	+0.3019	−0.1613	+0.0532	−0.0001	+ 66.27	+ 0.71	+ 5.559	+0.6931
0	+3.003	+0.6000	0	0	−166.4	0	0	+1.000
$\phi_K=35$:								
35	+0.0614	0	−0.0363	−0.0020	− 48.68	0	−11.31	+0.0433
30	+0.0019	+0.0113	−0.0381	−0.0020	− 40.77	−12.62	− 9.488	+0.0867
20	−0.2759	−0.0663	−0.0294	−0.0012	+ 17.11	−21.22	+ 1.522	+0.3710
10	+0.1839	−0.1613	+0.0454	−0.0000	+ 66.22	+ 5.83	+ 7.338	+0.7029
0	+3.204	+0.6000	0	0	−180.9	0	0	+1.000
$\phi_K=40$:								
40	+0.2096	0	+0.0030	−0.0012	− 29.22	0	−10.53	−0.0850
30	−0.0157	+0.0719	−0.0224	−0.0013	− 20.21	−14.50	− 6.191	+0.0578
20	−0.3733	−0.0458	−0.0384	−0.0010	+ 19.37	−16.37	+ 3.594	+0.3909
10	+0.1569	−0.1797	+0.0373	−0.0001	+ 56.09	+ 7.56	+ 7.285	+0.7139
0	+3.297	+0.6000	0	0	−169.2	0	0	+1.000

TABLE 7(b)—(*Concld.*)

(*m*) (Conclude)

ϕ	SHEAR EDGE LOAD N_x (9)	 $N_{x\phi}$ (10)	 N_ϕ (11)	 M_ϕ (12)	EDGE MOMENT LOAD N_x (13)	 $N_{x\phi}$ (14)	 N_ϕ (15)	 M_ϕ (16)
$\phi_K=45$:								
45	+0.2347	0	+0.0286	−0.0004	− 8.38	0	− 7.554	−0.1241
40	+0.1924	+0.0605	+0.0199	−0.0005	− 10.38	− 2.49	− 7.198	−0.0988
30	−0.1065	+0.0944	−0.0306	−0.0011	− 15.36	−10.11	− 3.686	+0.0939
20	−0.4030	−0.0596	−0.0476	−0.0011	+ 12.42	−13.03	+ 3.667	+0.4113
10	−0.1906	−0.1895	+0.0361	−0.0001	+ 50.54	+ 6.80	+ 6.668	+0.7160
0	+3.268	+0.6000	0	0	−158.3	0	0	+1.000
$\phi_K=50$:								
50	+0.1854	0	+0.0382	+0.0002	+ 7.18	0	− 3.972	−0.1088
40	+0.1051	+0.0872	+0.0118	−0.0003	− 5.77	+ 1.40	− 4.634	−0.0572
30	−0.1481	+0.0826	−0.0419	−0.0012	− 20.51	− 6.83	− 3.347	+0.1206
20	−0.3819	−0.0757	−0.0497	−0.0012	+ 7.78	−12.83	+ 3.041	+0.4149
10	+0.2199	−0.1883	+0.0384	−0.0001	+ 51.00	+ 5.85	+ 6.371	+0.7134
0	+3.218	+0.6000	0	0	−156.6	0	0	+1.000

TABLE 8(a)—SYMMETRICAL EDGE LOADS ON SIMPLY SUPPORTED CYLINDRICAL SHELLS (DISPLACEMENT OF EDGE AT $\phi=0$)

VERTICAL EDGE LOAD	HORIZONTAL EDGE LOAD
Vertical Displacement w (Downward Positive)	
$V_L \frac{l^4}{r^3 t E} \times$ Col. (1) $\times \sin \frac{\pi x}{l}$	$H_L \frac{l^4}{r^3 t E} \times$ Col. (4) $\times \sin \frac{\pi x}{l}$
Horizontal Displacement v (Inward Positive)	
$V_L \frac{l^4}{r^3 t E} \times$ Col. (2) $\times \sin \frac{\pi x}{l}$	$H_L \frac{l^4}{r^3 t E} \times$ Col. (5) $\times \sin \frac{\pi x}{l}$
Rotation θ—	Rotation θ—
$V_L \frac{r^2}{E I} \times$ Col. (3) $\times \sin \frac{\pi x}{l}$	$H_L \frac{r^2}{E I} \times$ Col. (6) $\times \sin \frac{\pi x}{l}$

ϕ_K	w (1)	v (2)	θ (3)	w (4)	v (5)	θ (6)
			(a) r/t=100			
$r/l=0.1$:						
30	12.53	0.1445	0.1108	− 0.1445	− 0.0585	−0.04556
35	6.265	0.2508	0.1420	− 0.2508	− 0.1231	−0.07108
40	3.611	0.4009	0.1752	− 0.4009	− 0.2325	−0.1039
45	2.591	0.5987	0.2088	− 0.5981	− 0.4040	−0.1444
50	2.043	0.8434	0.2410	− 0.8434	− 0.6558	−0.1925
$r/l=0.2$:						
30	17.38	2.031	0.0982	− 2.031	− 0.8742	−0.04288
35	12.87	3.538	0.1259	− 3.538	− 1.794	−0.06530
40	12.51	5.544	0.1524	− 5.544	− 3.282	−0.09256
45	13.47	7.956	0.1748	− 7.956	− 5.447	−0.1233
50	14.54	10.50	0.1899	−10.50	− 8.270	−0.1546
$r/l=0.3$:						
30	35.24	9.474	0.0891	− 9.474	− 4.010	−0.03866
35	37.31	15.65	0.1092	−15.65	− 7.890	−0.05606
40	42.38	22.99	0.1245	−22.99	−13.59	−0.07595
45	46.06	30.12	0.1317	−30.12	−20.69	−0.09384
50	45.75	35.11	0.1285	−35.11	−27.93	−0.1070

TABLE 8(a)—(*Contd.*)

(*a*) (Continued)

	VERTICAL EDGE LOAD			HORIZONTAL EDGE LOAD		
ϕ_K	w (1)	v (2)	θ (3)	w (4)	v (5)	θ (6)
$r/l=0.4$:						
30	75.06	26.10	0.07760	–26.10	–11.06	–0.03483
35	87.57	40.75	0.09046	–40.75	–20.25	–0.04716
40	96.68	55.00	0.09596	–55.00	–32.68	–0.05921
45	96.10	64.69	0.09256	–64.69	–44.95	–0.06746
50	85.15	67.32	0.08360	–67.32	–54.74	–0.07216
$r/l=0.5$:						
30	142.2	54.14	0.06634	–54.14	–22.98	–0.02900
35	163.2	78.77	0.07239	–78.77	–39.97	–0.03811
40	167.7	97.43	0.07124	–97.43	–58.47	–0.04484
45	152.4	104.9	0.06505	–104.9	–74.31	–0.04883
50	127.5	103.9	0.05747	–103.9	–87.21	–0.05166
$r/l=0\ 6$:						
30	238.5	88.47	0.05559	–88.47	–39.78	–0.02434
35	257.7	126.7	0.05714	–126.7	–64.74	–0.03049
40	245.4	144.9	0.05366	–144.9	–88.10	–0.03396
45	212.3	149.5	0.04873	–149.5	–108.3	–0.03700
50	175.8	143.7	0.04304	–147.9	–127.9	–0.03967
			(b) $r/t=200$			
$r/l=0.1$:						
30	13.59	0.5598	0.10563	–0.5598	–0.3112	–0.04555
35	7.732	0.9838	0.13813	–0.9838	–0.4916	–0.07100
40	5.711	1.576	0.1719	–1.576	–0.9269	–0.1036
45	5.186	2.354	0.2050	–2.354	–1.462	–0.1434
50	5.265	3.292	0.2352	–3.292	–2.576	–0.1895

TABLE 8(a)—(*Contd.*)

(*b*) (Continued)

	Vertical Edge Load			Horizontal Edge Load		
ϕ_K	w (1)	v (2)	θ (3)	w (4)	v (5)	θ (6)
$r/l=0.2$:						
30	32.02	8.267	0.0986	−8.267	−3.492	−0.04257
35	33.96	14.07	0.1245	−14.07	−7.090	−0.06423
40	39.51	21.38	0.1468	−21.38	−12.62	−0.08898
45	44.27	28.96	0.1600	−28.96	−19.84	−0.1132
50	45.16	34.63	0.1600	−34.63	−27.44	−0.1321
$r/l=0.3$:						
30	110.9	37.12	0.08756	−37.12	−15.70	−0.03796
35	123.0	58.70	0.10342	−58.70	−29.63	−0.05150
40	136.4	78.62	0.10899	−78.62	−46.73	−0.06707
45	131.1	89.18	0.10274	−89.18	−62.16	−0.07481
50	111.5	89.27	0.09013	−89.27	−73.18	−0.07807
$r/l=0.4$:						
30	247.6	98.82	0.07423	−98.82	−41.89	−0.03237
35	283.3	139.7	0.07945	−139.7	−70.98	−0.04180
40	273.8	161.7	0.07471	−161.7	−97.64	−0.04717
45	232.0	163.1	0.06551	−163.1	−117.2	−0.04975
50	187.9	157.7	0.05768	−157.7	−135.5	−0.05270
$r/l=0.5$:						
30	473.4	194.4	0.06058	−194.4	−82.77	−0.02666
35	486.4	244.3	0.05905	−244.3	−125.5	−0.03167
40	424.2	256.6	0.05240	−256.6	−158.6	−0.03414
45	349.1	254.2	0.04653	−254.2	−189.1	−0.03671
50	295.1	260.4	0.04398	−260.4	−234.5	−0.04173

TABLE 8(a)—(*Concld.*)

(*b*) (Conclude)

	VERTICAL EDGE LOAD			HORIZONTAL EDGE LOAD		
ϕ_K	w (1)	v (2)	θ (3)	w (4)	v (5)	θ (6)
$r/l=0.6$:						
30	756.0	315.3	0.04838	−315.3	−135.1	−0.02155
35	706.1	360.6	0.04430	−360.6	−188.1	−0.02429
40	591.7	367.3	0.03930	−367.3	−232.8	−0.02637
45	498.8	374.8	0.03615	−374.8	−287.2	−0.02931
50	431.9	389.3	0.03392	−389.3	−357.3	−0.03284

TABLE 8(b)—SYMMETRICAL EDGE LOADS ON SIMPLY SUPPORTED CYLINDRICAL SHELLS (DISPLACEMENT OF EDGE AT $\phi=0$)

SHEAR EDGE LOAD	MOMENT EDGE LOAD
Vertical Displacement w (Downward Positive)	
$S_L \dfrac{l^4}{r^3\,t\,E} \times$ Col. (7) $\times \sin\dfrac{\pi x}{l}$	$M_L \times \dfrac{l^4}{r^4\,t\,E} \times$ Col. (10) $\times \sin\dfrac{\pi x}{l}$
Horizontal Displacement v (Inward Positive)	
$S_L \dfrac{l^4}{r^3\,t\,E} \times$ Col. (8) $\times \sin\dfrac{\pi x}{l}$	$M_L \times \dfrac{l^4}{r^4\,t\,E} \times$ Col. (11) $\times \sin\dfrac{\pi x}{l}$
Rotation θ—	Rotation θ—
$S_L \dfrac{r^2}{E\,I} \times$ Col. (9) $\times \sin\dfrac{\pi x}{l}$	$M_L \times \dfrac{r}{E\,I} \times$ Col. (12) $\times \sin\dfrac{\pi x}{l}$

ϕ_K	w (7)	v (8)	θ (9)	w (10)	v (11)	θ (12)
(a) r/t=100						
$r/l=0.1$:						
30	0.3401	0.000480	0.000363	− 1.330	− 0.5469	−0.5144
35	0.2178	0.001006	0.000544	− 1.704	− 0.8531	−0.5964
40	0.1443	0.002009	0.000822	− 2.102	− 1.247	−0.6749
45	0.1084	0.003771	0.001223	− 2.505	− 1.734	−0.7542
50	0.0792	0.006516	0.001776	− 2.892	− 2.312	−0.8290
$r/l=0.2$:						
30	0.6950	0.00726	0.000353	− 18.86	− 8.233	−0.4893
35	0.4733	0.02065	0.000678	− 24.18	− 12.54	−0.5564
40	0.3715	0.04590	0.001145	− 29.25	− 17.77	−0.6159
45	0.3402	0.08862	0.001757	− 33.56	− 23.67	−0.6651
50	0.3610	0.1526	0.002478	− 36.46	− 29.70	−0.6986
$r/l=0.3$:						
30	1.187	0.06357	0.000536	− 86.64	− 37.58	−0.4499
35	0.9583	0.1474	0.000923	−106.2	− 54.50	−0.4965
40	0.9561	0.2931	0.001413	−121.0	− 73.83	−0.5288
45	1.073	0.5020	0.001927	−127.9	− 91.21	−0.5434
50	1.209	0.7422	0.002334	−124.9	−104.0	−0.5402

TABLE 8(b)—(*Contd.*)

(*a*) (Continued)

	SHEAR EDGE LOAD			MOMENT EDGE LOAD		
ϕ_K	w (7)	v (8)	θ (9)	w (10)	v (11)	θ (12)
$r/l=0.4$:						
30	1.940	0.2256	0.000632	−239.2	−104.0	−0.4049
35	1.924	0.5080	0.000994	−277.7	−145.2	−0.4320
40	2.189	0.9067	0.001384	−293.8	−181.4	−0.4417
45	2.500	1.372	0.001641	−284.1	−207.1	−0.4348
50	2.591	1.731	0.001732	−255.7	−220.8	−0.4228
$r/l=0.5$:						
30	3.218	0.5995	0.000644	−497.6	−216.6	−0.3602
35	3.588	1.202	0.000945	−542.9	−285.9	−0.3706
40	4.141	1.938	0.001160	−535.2	−335.5	−0.3668
45	4.418	2.566	0.001242	−487.9	−366.2	−0.3568
50	4.246	2.945	0.001199	−431.0	−387.5	−0.3493
$r/l=0.6$:						
30	5.112	1.218	0.000620	−864.6	−378.6	−0.3247
35	5.976	2.242	0.000834	−888.7	−474.2	−0.3185
40	6.629	3.250	0.000932	−834.6	−528.2	−0.3171
45	6.601	3.942	0.000918	−743.9	−575.4	−0.3042
50	6.678	4.324	0.000865	−669.4	−618.7	−0.3086

(b) $r/t=200$

$r/l=0.1$:						
30	0.3446	0.001423	0.000252	− 5.070	− 2.186	−0.5143
35	0.2228	0.003352	0.000438	− 6.630	− 3.408	−0.5958
40	0.1579	0.007139	0.000718	− 8.250	− 4.974	−0.6749
45	0.1237	0.01391	0.001117	− 9.842	− 6.883	−0.7503
50	0.1083	0.02506	0.001649	−11.29	− 9.097	−0.8195

TABLE 8(b)—(*Contd.*)

(*b*) (Continued)

	SHEAR EDGE LOAD			MOMENT EDGE LOAD		
ϕ_K	w (7)	v (8)	θ (9)	w (10)	v (11)	θ (12)
$r/l=0.2$:						
30	0.7716	0.03561	0.000385	−75.70	−32.70	−0.4866
35	0.6124	0.08739	0.000700	−95.68	−49.33	−0.5497
40	0.6071	0.1815	0.001123	−112.7	−68.34	−0.5990
45	0.6944	0.3237	0.001601	−122.9	−86.91	−0.6273
50	0.8010	0.4950	0.002014	−122.8	−101.0	−0.6299
$r/l=0.3$:						
30	1.641	0.2500	0.000532	−340.4	−147.6	−0.4443
35	1.782	0.5520	0.000868	−402.2	−200.2	−0.4792
40	2.154	0.9824	0.001193	−423.7	−260.8	−0.4884
45	2.432	1.410	0.001376	−399.4	−290.9	−0.4749
50	2.437	1.695	0.001382	−350.4	−303.5	−0.4550
$r/l=0.4$:						
30	3.525	0.9471	0.000586	−912.9	−397.8	−0.3936
35	4.354	1.701	0.000837	−976.3	−513.6	−0.4011
40	4.977	2.518	0.000964	−918.0	−579.7	−0.3884
45	4.925	3.016	0.000945	−805.0	−611.3	−0.3732
50	4.456	3.239	0.000875	−708.8	−647.5	−0.3670
$r/l=0.5$:						
30	6.899	2.116	0.000570	−1817.	−800.0	−0.3421
35	8.309	3.527	0.000704	−1772.	−950.2	−0.3343
40	8.519	4.483	0.000707	−1572.	−1024.	−0.3210
45	7.792	4.924	0.000653	−1396.	−1101.	−0.3156
50	6.701	5.075	0.000616	−1319.	−1252.	−0.3226

TABLE 8(b)—(*Concld.*)

(*b*) (Conclude)

	SHEAR EDGE LOAD			MOMENT EDGE LOAD		
ϕ_K	w (7)	v (8)	θ (9)	w (10)	v (11)	θ (12)
$r/l=0.6$:						
30	11.82	3.979	0.000510	−3009.	−1341.	−0.2961
35	13.15	5.790	0.000555	−2756.	−1511.	−0.2847
40	12.46	6.714	0.000519	−2445.	−1640.	−0.2778
45	11.18	7.265	0.000486	−2249.	−1823.	−0.2782
50	10.21	7.983	0.000481	−2110.	−2043.	−0.2807

TABLE 9(a)—EDGE LOADS ON SIMPLY SUPPORTED CYLINDRICAL SHELL

TANGENTIAL EDGE LOAD	RADIAL EDGE LOAD

(*a*) **Basic Formulas for n=1; for n=3 Substitute $\frac{3\pi x}{l}$ Instead of $\frac{\pi x}{l}$**

TANGENTIAL EDGE LOAD	RADIAL EDGE LOAD
Longitudinal Force N_x—	Longitudinal Force N_x—
$T_L \times$ Col. (1) $\times \sin\frac{\pi x}{l}$	$R_L \times \frac{l}{t} \times$ Col. (5) $\times \sin\frac{\pi x}{l}$
Shearing Force $N_{x\phi}$—	Shearing Force $N_{x\phi}$—
$T_L \times$ Col. (2) $\times \cos\frac{\pi x}{l}$	$R_L \times \frac{l}{t} \times$ Col. (6) $\times \cos\frac{\pi x}{l}$
Transverse Force N_ϕ—	Transverse Force N_ϕ—
$T_L \times$ Col. (3) $\times \sin\frac{\pi x}{l}$	$R_L \times \frac{l}{t} \times$ Col. (7) $\times \sin\frac{\pi x}{l}$
Transverse Moment M_ϕ—	Transverse Moment M_ϕ—
$T_L \times t \times$ Col. (4) $\times \sin\frac{\pi x}{l}$	$R_L \times l \times$ Col. (8) $\times \sin\frac{\pi x}{l}$

(*b*) **n=1**

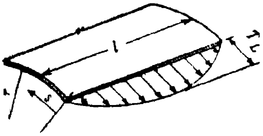

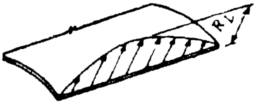

$\frac{s}{\sqrt[4]{rtl^2}}$	N_x (1)	$N_{x\phi}$ (2)	N_ϕ (3)	M_ϕ (4)	N_x (5)	$N_{x\phi}$ (6)	N_ϕ (7)	M_ϕ (8)
$\frac{rt}{l^2}=0.002$:								
3.2	− 0.595	−0.337	+ 0.032	+0.3010	+0.0209	+0.00594	+0.00026	−0.0039
1.6	+ 0.635	+1.303	−0.188	−1.8271	−0.0633	−0.02668	−0.00011	+0.0313
0.8	−10.323	−1.441	−0.434	−2.1133	+0.1676	−0.00575	+0.01432	+0.0766
0.4	− 2.658	−3.637	+0.283	−0.5169	+0.1185	+0.04052	+0.00946	+0.0512
0.2	+11.837	−3.132	+0.754	+0.0620	−0.1123	+0.04313	+0.00356	+0.0270
0.1	+23.039	−1.990	+0.929	+0.1309	−0.3127	+0.02938	+0.00108	+0.01362
0.0	+37.430	0	+1.000	0	−0.5848	0	0	0

TABLE 9(a)—(*Contd.*)

(*b*) (Continued)

	TANGENTIAL EDGE LOAD				RADIAL EDGE LOAD			
$\frac{s}{\sqrt[4]{rt\,l^2}}$	N_x (1)	$N_{x\phi}$ (2)	N_ϕ (3)	M_ϕ (4)	N_x (5)	$N_{x\phi}$ (6)	N_ϕ (7)	M_ϕ (8)
$\frac{rt}{l^2}=0.003$:								
3.2	− 0.393	−0.288	+0.038	+0.2387	+0.0203	+0.00695	+0.00015	−0.00432
1.6	+ 0.316	+1.115	−0.204	−1.4220	−0.0629	−0.03104	+0.00041	+0.03275
0.8	− 8.063	−1.331	−0.405	−1.5481	+0.1741	−0.00573	+0.01853	+0·07812
0.4	− 1.920	−3.205	+0.305	−0.3150	+0.1214	+0.04716	+0.01212	+0.05225
0.2	+ 9.454	−2.742	+0.762	+0.1030	−0.1185	+0.04990	+0.00455	+0.02758
0.1	+18.230	−1.739	+0.931	+0.1323	−0.3269	+0.03395	+0.00138	+0.01394
0.0	+29.509	0	+1.000	0	−0.6104	0	0	0
$\frac{rt}{l^2}=0.004$:								
3.2	− 0.278	−0.254	+0.042	+0.2008	+0.0196	+0.00771	+0.00000	−0.00459
1.6	+ 0.142	+0.991	−0.215	−1.1832	−0.0618	−0.03434	+0.00103	+0.03355
0.8	− 6.733	−1.259	−0.381	−1.2254	+0 1776	−0.00550	+0.02214	+0.07856
0.4	− 1.500	−2.923	+0.321	−0.2052	+0.1226	+0.05223	+0.01437	+0.05255
0.2	+ 8.039	−2.488	+0.769	+0.1217	−0.1224	+0.05501	+0.00539	+0.02779
0.1	+15.393	−1.575	+0.933	+0.1301	−0.3353	+0.03740	+0.00163	+0.01407
0.0	+24.846	0	+1.000	0	−0.6254	0	0	0
$\frac{rt}{l^2}=0.006$:								
3.2	− 0.153	−0.209	+0.047	+0.1550	+0.0179	+0.00877	−0.00034	−0.00493
1.6	− 0.103	+0.827	−0.230	−0.9042	−0.0591	−0.03918	+0.00239	+0.03457
0.8	− 5.182	−1.161	−0.344	−0.8634	+0.1807	−0.00480	+0.02822	+0.07956
0.4	− 1.030	−2.556	+0.347	−0.0900	+0.1227	+0 .05977	+0.01810	+0.05372
0.2	+ 6.371	−2.158	+0.778	+0.1355	−0.1270	+0.06253	+0.00677	+0.02870
0.1	+12.071	−1.363	+0.936	+0.1232	−0.3444	+0.04246	+0.00205	+0.01463
0.0	+19.407	0	+1.000	0	−0.6412	0	0	0

TABLE 9(a)—(*Contd.*)

(*b*) (Continued)

	TANGENTIAL EDGE LOAD				RADIAL EDGE LOAD			
$\frac{s}{\sqrt[4]{rt\,l^2}}$	N_x (1)	$N_{x\phi}$ (2)	N_ϕ (3)	M_ϕ (4)	N_x (5)	$N_{x\phi}$ (6)	N_ϕ (7)	M_ϕ (8)
$\frac{rt}{l^2}=0.008$:								
3.2	−0.086	−0.178	+0.050	+0.1271	+0.0163	+0.00949	−0.00072	−0.00511
1.6	−0.131	+0.719	−0.240	−0.7409	−0.0562	−0.04265	+0.00383	+0.03459
0.8	−4.278	−1.094	−0.313	−0.6617	+0.1813	−0.00397	+0.03329	+0.07719
0.4	−0.770	−2.316	+0.367	−0.0315	+0.1217	+0.06531	+0.02116	+0.05188
0.2	+5.382	−1.945	+0.785	+0.1383	−0.1293	+0.06797	+0.00791	+0.02768
0.1	+10.120	−1.226	+0.938	+0.1163	−0.3483	+0.04611	+0.00239	+0.01411
0.0	+16.225	0	+1.000	0	−0.6479	0	0	0
$\frac{rt}{l^2}=0.010$:								
3.2	−0.045	−0.155	+0.052	+0.1079	+0.0148	+0.00997	−0.00111	−0.00521
1.6	−0.183	+0.640	−0.246	−0.6312	−0.0534	−0.04527	+0.00527	+0.03458
0.8	−3.671	−1.043	−0.288	−0.5322	+0.1807	−0.00313	+0.03767	+0.07597
0.4	−0.604	−2.141	+0.384	+0.0026	+0.1202	+0.06960	+0.02378	+0.05126
0.2	+4.712	−1.789	+0.791	+0.1370	−0.1305	+0.07215	+0.00887	+0.02748
0.1	+8.807	−1.127	+0.940	+0.1100	−0.3496	+0.04892	+0.00268	+0.01406
0.0	+14.089	0	+1.000	0	−0.6501	0	0	0
$\frac{rt}{l^2}=0.015$:								
3.2	+0.011	−0.115	+0.055	+0.0775	+0.0117	+0.01060	−0.00205	−0.00527
1.6	−0.243	+0.504	−0.255	−0.4648	−0.0474	−0.04966	+0.00882	+0.03405
0.8	−2.753	−0.952	−0.236	−0.3476	+0.1769	−0.00114	+0.04659	+0.07280
0.4	−0.371	−1.845	+0.416	+0.0440	+0.1159	+0.07720	+0.02902	+0.04970
0.2	+3.678	−1.529	+0.803	+0.1287	−0.1309	+0.07946	+0.01080	+0.02699
0.1	+6.801	−0.961	+0.943	+0.0969	−0.3472	+0.05383	+0.00326	+0.01393
0.0	+10.843	0	+1.000	0	−0.6465	0	0	0

TABLE 9(a)—(*Contd.*)

(*b*) (Continued)

	TANGENTIAL EDGE LOAD				RADIAL EDGE LOAD			
$\dfrac{s}{\sqrt[4]{rt\,l^2}}$	N_x (1)	$N_{x\phi}$ (2)	N_ϕ (3)	M_ϕ (4)	N_x (5)	$N_{x\phi}$ (6)	N_ϕ (7)	M_ϕ (8)
$\frac{rt}{l^2}=0.020$:								
3.2	+ 0.033	−0.088	+0.054	+0.0594	+0.0091	+0.01073	−0.00290	−0.00518
1.6	− 0.263	+0.415	−0.258	−0.3689	−0.0424	−0.05224	+0.01217	+0.03322
0.8	− 2.225	−0.888	−0.195	−0.2500	+0.1720	+0.00061	+0.05358	+0.06986
0.4	− 0.250	−1.652	+0.440	+0.0601	+0.1117	+0.08214	+0.03306	+0.04833
0.2	+ 3.068	−1.361	+0.812	+0.1192	−0.1296	+0.08417	+0.01230	+0.02659
0.1	+ 5.634	−0.854	+0.946	+0.0868	−0.3426	+0.05700	+0.00371	+0.01384
0.0	+ 8.964	0	+1.000	0	−0.6374	0	0	0
$\frac{rt}{l^2}=0.025$:								
3.2	+ 0.044	−0.069	+0.053	+0.0472	+0.0071	+0.01060	−0.00364	−0.00502
1.6	− 0.268	+0.351	−0.257	−0.3054	−0.0382	−0.05380	+0.01529	+0.03229
0.8	− 1.875	−0.839	−0.161	−0.1901	+0.1667	+0.00212	+0.05928	+0.06722
0.4	− 0.177	−1.512	+0.460	+0.0668	+0.1078	+0.08554	+0.03631	+0.04747
0.2	+ 2.656	−1.240	+0.819	+0.1104	−0.1275	+0.08738	+0.01350	+0.02630
0.1	+ 4.853	−0.777	+0.948	+0.0787	−0.3362	+0.05918	+0.00407	+0.01380
0.0	+ 7.714	0	+1.000	0	−0.6263	0	0	0
$\frac{rt}{l^2}=0.030$:								
3.2	+ 0.050	−0.054	+0.051	+0.0383	+0.0054	+0.01031	−0.00428	−0.00482
1.6	− 0.265	+0.301	−0.254	−0.2599	−0.0346	−0.05470	+0.01818	+0.03133
0.8	− 1.625	−0.798	−0.131	−0.1497	+0.1616	+0.00344	+0.06403	+0.06485
0.4	− 0.129	−1.403	+0.477	+0.0693	+0.1043	+0.08796	+0.03900	+0.04617
0.2	+ 2.355	−1.147	+0.825	+0.1028	−0.1249	+0.08966	+0.01449	+0.02607
0.1	+ 4.287	−0.719	+0.949	+0.0722	−0.3292	+0.06074	+0.00437	+0.01379
0.0	+ 6.811	0	+1.000	0	−0.6144	0	0	0

TABLE 9(a)—(*Contd.*)

(*b*) (Continued)

	TANGENTIAL EDGE LOAD				RADIAL EDGE LOAD			
$\frac{s}{\sqrt[4]{r t l^2}}$	N_x (1)	$N_{x\phi}$ (2)	N_ϕ (3)	M_ϕ (4)	N_x (5)	$N_{x\phi}$ (6)	N_ϕ (7)	M_ϕ (8)
$\frac{r t}{l^2}=0.040$:								
3.2	+ 0.053	−0.033	+0.045	+0.0263	+0.0028	+0.00947	−0.00526	−0.00439
1.6	− 0.253	+0.227	−0.246	−0.1986	−0.0289	−0.05524	+0.02329	+0.02949
0.8	− 1.286	−0.735	−0.081	−0.1002	+0.1516	+0.00551	+0.07145	+0.06091
0.4	− 0.072	−1.241	+0.505	+0.0682	+0.0980	+0.09076	+0.04319	+0.04469
0.2	+ 1.938	−1.010	+0.834	+0.0895	−0.1195	+0.09230	+0.01605	+0.02586
0.1	+ 3.512	−0.632	+0.952	+0.0618	−0.3152	+0.06258	+0.00485	+0.01389
0.0	+ 5.579	0	+1.000	0	−0.5904	0	0	0
$\frac{r t}{l^2}=0.060$:								
3.2	+ 0.047	−0.009	+0.034	+0.0135	−0.0003	+0.00747	−0.00631	−0.00356
1.6	− 0.222	+0.137	−0.222	−0.1313	−0.0213	−0.05387	+0.03126	+0.02620
0.8	− 0.910	−0.645	−0.005	−0.0531	+0.1343	+0.00814	+0.08098	+0.05495
0.4	− 0.023	−1.035	+0.545	+0.0605	+0.0881	+0.09213	+0.04853	+0.04274
0.2	+ 1.456	−0.838	+0.848	+0.0708	−0.1084	+0.09368	+0.01807	+0.02586
0.1	+ 2.629	−0.524	+0.956	+0.0480	−0.2886	+0.06370	+0.00547	+0.01425
0.0	+ 4.187	0	+1.000	0	−0.5452	0	0	0
$\frac{r t}{l^2}=0.080$:								
3.2	+ 0.039	+0.002	+0.023	+0.0072	−0.0018	+0.00559	−0.00651	−0.00285
1.6	− 0.195	+0.083	−0.196	−0.0951	−0.0166	−0.05117	+0.03683	+0.02346
0.8	− 0.705	−0.581	+0.052	−0.0320	+0.1199	+0.00946	+0.08620	+0.05066
0.4	− 0.005	−0.904	+0.574	+0.0523	+0.0801	+0.09073	+0.05150	+0.04162
0.2	+ 1.179	−0.730	+0.857	+0.0582	−0.0980	+0.09256	+0.01923	+0.02615
0.1	+ 2.130	−0.458	+0.959	+0.0391	−0.2648	+0.06315	+0.00583	+0.01471
0.0	+ 3.407	0	+1.000	0	−0.5051	0	0	0

TABLE 9(a)—(*Concld.*)

(*b*) (Conclude)

$\frac{s}{\sqrt[4]{r t l^2}}$	TANGENTIAL EDGE LOAD N_x (1)	$N_{x\phi}$ (2)	N_ϕ (3)	M_ϕ (4)	RADIAL EDGE LOAD N_x (5)	$N_{x\phi}$ (6)	N_ϕ (7)	M_ϕ (8)
$\frac{r\,t}{l^2}=0.100$:								
3.2	+ 0.032	+0.008	+0.015	+0.0038	−0.0026	+0.00400	−0.00620	−0.00229
1.6	− 0.171	+0.048	−0.171	−0.0728	−0.0135	−0.04807	+0.04061	+0.02117
0.8	− 0.576	−0.533	+0.097	−0.0210	+0.1078	+0.00995	+0.08883	+0.04740
0.4	+ 0.002	−0.811	+0.595	-0.0454	+0.0747	+0.08805	+0 05308	+0.04093
0.2	+ 0.997	−0.655	+0.865	+0.0490	−0.0886	+0.09028	+0.01989	+0.02656
0.1	+ 1.807	−0.411	+0.961	+0.0328	−0.2437	+0.06183	+0.00605	+0.01520
0.0	+ 2.903	0	+1.000	0	−0.4697	0	0	0

TABLE 9(b)

	TANGENTIAL EDGE LOAD				RADIAL EDGE LOAD			
				(*c*) n=3				
Ratio	N_x (1)	$N_{x\phi}$ (2)	N_ϕ (3)	M_ϕ (4)	N_x (5)	$N_{x\phi}$ (6)	N_ϕ (7)	M_ϕ (8)
$\frac{rt}{l^2}=0.002$:								
1.6	+0.285	−0.025	+0.090	+0.0576	−0.0034	+0.00384	−0.00282	−0.00287
0.8	−0.902	+0.307	−0.353	−0.4678	−0.0010	−0.01922	+0.00817	+0.01637
0.4	−2.287	−1.204	−0.080	−0.1920	+0.0635	+0.00753	+0.01653	+0.02281
0.2	+0.448	−1.717	+0.538	+0.0868	+0.0227	+0.02868	+0.00880	+0.01449
0.1	+3.947	−1.310	+0.851	+0.1194	−0.0602	+0.02591	+0.00309	+0.00779
0.0	+9.616	0	+1.000	0	−0.2138	0	0	0
$\frac{rt}{l^2}=0.003$:								
1.6	+0.221	+0.009	+0.071	+0.0296	−0.0042	+0.00318	−0.00328	−0.00243
0.8	−0.730	+0.195	−0.331	−0.3235	+0.0006	−0.01981	+0.01074	+0.01530
0.4	−1.664	−1.058	−0.020	−0.1060	+0.0600	+0.00878	+0.01978	+0.02138
0.2	+0.399	−1.458	−0.567	+0.0889	+0.0211	+0.03082	+0.01044	+0.01395
0.1	+3.028	−1.106	+0.861	+0.1027	−0.0583	+0.02775	+0.00366	+0.00767
0.0	+7.321	0	+1.000	0	−0.2072	0	0	0
$\frac{rt}{l^2}=0.004$:								
1.6	+0.177	+0.026	+0.055	+0.0155	−0.0046	+0.00252	−0.00351	−0.00206
0.8	−0.619	+0.126	−0.308	−0.2442	+0.0016	−0.01982	+0.01281	+0.01433
0.4	−1.314	−0.959	+0.026	−0.0647	+0.0566	+0.00958	+0.02211	+0.02024
0.2	+0.358	−1.290	+0.590	+0.0843	+0.0198	+0.03193	+0.01162	+0.01357
0.1	+2.492	−0.975	+0.868	+0.0899	−0.0561	+0.02872	+0.00408	+0.00762
0.0	+6.005	0	+1.000	0	−0.2000	0	0	0

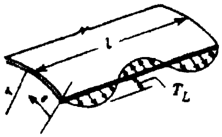

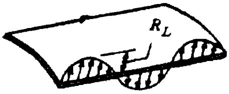

TABLE 9(b)—(*Contd.*)

(*c*) (Continued)

Ratio	TANGENTIAL EDGE LOAD				RADIAL EDGE LOAD			
	N_x (1)	$N_{x\phi}$ (2)	N_ϕ (3)	M_ϕ (4)	N_x (5)	$N_{x\phi}$ (6)	N_ϕ (7)	M_ϕ (8)
$\frac{r\,t}{l^2}=0.006$:								
1.6	+0.122	+0.041	+0.031	+0.0025	−0.0047	+0.00138	−0.00353	−0.00150
0.8	−0.478	+0.045	−0.265	−0.1588	+0.0026	−0.00913	+0.01586	+0.01271
0.4	−0.929	−0.825	+0.096	−0.0271	+0.0507	+0.01044	−0.02518	+0.01853
0.2	+0.296	−1.076	+0.622	+0.0726	+0.0180	+0.03269	−0.01317	+0.01309
0.1	+1.875	−0.810	+0.879	+0.0716	−0.0515	+0.02942	+0.00463	+0.00763
0.0	+4.514	0	+1.000	0	−0.1861	0	0	0
$\frac{r\,t}{l^2}=0.008$:								
1.6	+0.088	+0.044	+0.014	−0.0028	−0.0045	+0.00050	−0.00324	−0.00111
0.8	−0.390	−0.001	−0.226	−0.1141	+0.0030	−0.01811	+0.01791	+0.01142
0.4	−0.719	−0.736	+0.148	−0.0116	+0.0458	+0.01070	+0.02698	+0.01731
0.2	+0.252	−0.940	+0.646	+0.0623	+0.0167	+0.03247	+0.01409	+0.01284
0.1	+1.520	−0.707	+0.886	+0.0591	−0.0473	+0.02930	+0.00496	+0.00773
0.0	+3.674	0	+1.000	0	−0.1735	0	0	0
$\frac{r\,t}{l^2}=0.010$:								
1.6	+0.066	+0.044	+0.002	−0.0050	−0.0042	−0.00015	−0.00282	−0.00083
0.8	−0.329	−0.030	−0.191	−0.0869	+0.0030	−0.01702	+0.01925	+0.01037
0.4	−0.588	−0.669	+0.189	−0.0042	+0.0416	+0.01064	+0.02798	+0.01639
0.2	+0.218	−0.844	+0.663	+0.0539	+0.0157	+0.03177	+0.01463	+0.01271
0.1	+1.288	−0.635	+0.892	+0.0501	−0.0434	+0.02880	+0.00516	+0.00786
0.0	+3.131	0	+1.000	0	−0.1623	0	0	0

TABLE 9(b)—(*Contd.*)

(*c*) (Continued)

Ratio	TANGENTIAL EDGE LOAD				RADIAL EDGE LOAD			
	N_x (1)	$N_{x\phi}$ (2)	N_ϕ (3)	M_ϕ (4)	N_x (5)	$N_{x\phi}$ (6)	N_ϕ (7)	M_ϕ (8)
$\frac{rt}{l^2}=0.015$:								
1.6	+0.034	+0.035	−0.014	−0.0060	−0.0034	−0.00107	−0.00166	−0.00040
0.8	−0.236	−0.067	−0.121	−0.0512	+0.0026	−0.01450	+0.02065	+0.00844
0.4	−0.409	−0.558	+0.261	+0.0022	+0.0337	+0.00979	+0.02859	+0.01481
0.2	+0.160	−0.692	+0.694	+0.0393	+0.0141	+0.02924	+0.01506	+0.01262
0.1	+0.948	−0.523	+0.901	+0.0358	−0.0354	+0.02686	+0.00536	+0.00824
0.0	+2.351	0	+1.000	0	−0.1390	0	0	0
$\frac{rt}{l^2}=0.020$:								
1.6	+0.019	+0.026	−0.018	−0.0053	−0.0027	−0.00140	−0.00071	−0.00019
0.8	−0.183	−0.081	−0.070	−0.0346	+0.0019	−0.01244	+0.02045	+0.00713
0.4	−0.320	−0.489	+0.306	+0.0033	+0.0280	+0.00858	+0.02783	+0.01380
0.2	+0.123	−0.604	+0.711	+0.0302	+0.0130	+0.02646	+0.01483	+0.01265
0.1	+0.763	−0.459	+0.906	+0.0274	−0.0291	+0.02469	+0.00533	+0.00860
0.0	+1.939	0	+1.000	0	−0.1209	0	0	0
$\frac{rt}{l^2}=0.025$:								
1.6	+0.011	+0.019	−0.018	−0.0044	−0.0021	−0.00146	−0.00006	−0.00008
0.8	−0.150	−0.086	−0.033	−0.0254	+0.0013	−0.01080	+0.01948	+0.00619
0.4	−0.269	−0.441	+0.336	+0.0031	+0.0237	+0.00736	+0.02650	+0.01307
0.2	+0.096	−0.547	+0.722	+0.0241	+0.0122	+0.02384	+0.01433	+0.01273
0.1	+0.649	−0.419	+0.909	+0.0221	−0.0243	+0.02262	+0.00520	+0.00892
0.0	+1.690	0	+1.000	0	−0.1065	0	0	0

TABLE 9(b)—(*Contd.*)

(*c*) (Continued)

Ratio	TANGENTIAL EDGE LOAD				RADIAL EDGE LOAD			
	N_x (1)	$N_{x\phi}$ (2)	N_ϕ (3)	M_ϕ (4)	N_x (5)	$N_{x\phi}$ (6)	N_ϕ (7)	M_ϕ (8)
$\frac{r\,t}{l^2}=0.030$:								
1.6	+0.007	+0.014	−0.016	−0.0037	−0.0017	−0.00139	+0.00035	−0.00002
0.8	−0.127	−0.086	−0.006	−0.0197	+0.0009	−0.00949	+0.01820	+0.00548
0.4	−0.236	−0.406	+0.354	+0.0025	+0.0203	+0.00624	+0.02497	+0.01251
0.2	+0.076	−0.508	+0.728	+0.0199	+0.0115	+0.02149	+0.01370	+0.01280
0.1	+0.571	−0.392	+0.911	+0.0184	−0.0204	+0.02074	+0.00502	+0.00920
0.0	+1.527	0	+1.000	0	−0.0948	0	0	0
$\frac{r\,t}{l^2}=0.040$:								
1.6	+0.002	+0.008	−0.011	−0.0025	−0.0011	−0.00114	+0.00069	+0.00003
0.8	−0.099	−0.084	+0.027	−0.0134	+0.0001	−0.00756	+0.01547	+0.00448
0.4	−0.198	−0.361	+0.373	+0.0013	+0.0155	+0.00439	+0.02195	+0.01167
0.2	+0.053	−0.461	+0.732	+0.0142	+0.0104	+0.01764	+0.01241	+0.01292
0.1	+0.483	−0.362	+0.911	+0.0135	−0.0148	+0.01761	+0.00462	+0.00965
0.0	+1.351	0	+1.000	0	−0.0771	0	0	0
$\frac{r\,t}{l^2}=0.060$:								
1.6	−0.000	+0.002	−0.005	−0.0013	−0.0006	−0.00069	+0.00066	+0.00005
0.8	−0.071	−0.072	+0.052	−0.0079	−0.0005	−0.00521	+0.01099	+0.00330
0.4	−0.168	−0.309	+0.375	+0.0001	+0.0100	+0.00207	+0.01705	+0.01054
0.2	+0.012	−0.415	+0.725	+0.0091	+0.0086	+0.01245	+0.01024	+0.01303
0.1	+0.375	−0.337	+0.907	+0.0092	−0.0085	+0.01326	+0.00394	+0.01027
0.0	+1.165	0	+1.000	0	−0.0554	0	0	0

TABLE 9(b)—(*Concld.*)

(*c*) (Conclude)

Ratio	TANGENTIAL EDGE LOAD				RADIAL EDGE LOAD			
	N_x (1)	$N_{x\phi}$ (2)	N_ϕ (3)	M_ϕ (4)	N_x (5)	$N_{x\phi}$ (6)	N_x (7)	M_ϕ (8)
$\frac{rt}{l^2}=0.080$:								
1.6	−0.001	+0.001	−0.002	−0.0008	−0.0003	−0.00043	+0.00047	+0.00004
0.8	−0.056	−0.062	+0.056	−0.0055	−0.0007	−0.00387	+0.00803	+0.00263
0.4	−0.155	−0.280	+0.362	−0.0005	+0.0070	+0.00084	+0.01368	+0.00975
0.2	−0.012	−0.396	+0.712	+0.0065	+0.0073	+0.00933	+0.00865	+0.01305
0.1	+0.323	−0.331	+0.901	+0.0069	−0.0052	+0.01054	+0.00342	+0.01069
0.0	+1.097	0	+1.000	0	−0.0428	0	0	0
$\frac{rt}{l^2}=0.100$:								
1.6	−0.001	−0.000	−0.000	−0.0005	−0.0002	−0.00028	+0.00033	+0.00003
0.8	−0.047	−0.054	+0.053	−0.0042	−0.0007	−0.00300	+0.00609	+0.00219
0.4	−0.146	−0.260	+0.346	−0.0009	+0.0052	+0.00017	+0.01131	+0.00913
0.2	−0.029	−0.385	+0.698	+0.0050	+0.0063	+0.00730	+0.00750	+0.01302
0.1	+0.289	−0.330	+0.895	+0.0056	−0.0033	+0.00870	+0.00303	+0.01100
0.0	+1.064	0	+1.000	0	−0.0348	0	0	0

TABLE 9(c)—EDGE LOADS ON SIMPLY SUPPORTED CYLINDRICAL SHELL

(*a*) **Basic Formulas for n=1; for n=3 Substitute $\frac{3\pi x}{l}$ Instead of $\frac{\pi x}{l}$**

SHEAR EDGE LOAD	MOMENT EDGE LOAD
Longitudinal Force N_x—	Longitudinal Force N_x—
$S_L \times$ Col. (9) $\times \sin\frac{\pi x}{l}$	$M_L \times \frac{l}{t} \times$ Col. (13) $\times \sin\frac{\pi x}{l}$
Shearing Force $N_{x\phi}$—	Shearing Force $N_{x\phi}$—
$S_L \times$ Col. (10) $\times \cos\frac{\pi x}{l}$	$M_L \times \frac{l}{t} \times$ Col. (14) $\times \cos\frac{\pi x}{l}$
Transverse Force N_ϕ—	Transverse Force N_ϕ—
$S_L \times$ Col. (11) $\times \sin\frac{\pi x}{l}$	$M_L \times \frac{l}{t} \times$ Col. (15) $\times \sin\frac{\pi x}{l}$
Transverse Moment M_ϕ—	Transverse Moment M_ϕ—
$S_L \times t \times$ Col. (12) $\times \sin\frac{\pi x}{l}$	$M_L \times$ Col. (16) $\times \sin\frac{\pi x}{l}$

(*b*) **n=1**

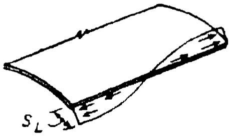

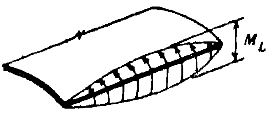

$\frac{s}{\sqrt[4]{rtl}}$	N_x (9)	$N_{x\phi}$ (10)	N_ϕ (11)	M_ϕ (12)	N_x (13)	$N_{x\phi}$ (14)	N_ϕ (15)	M_ϕ (16)
$\frac{rt}{l^2}=0.002$:								
3.2	−0.012	−0.039	+0.0084	+0.0419	+0.1022	+0.0127	+0.00503	−0.001
1.6	−0.204	+0.123	−0.0368	−0.2418	−0.3372	−0.0526	−0.02517	+0.075
0.8	−0.788	−0.260	−0.0180	−0.1408	+0.4747	−0.0790	+0.02973	+0.534
0.4	+1.580	−0.230	−0.0607	+0.0162	+0.6238	+0.0956	+0.02863	+0.761
0.2	+4.371	+0.150	+0.0701	+0.0348	−0.1552	+0.1370	+0.01205	+0.872
0.1	+6.321	+0.503	+0.0491	+0.0222	−0.9661	+0.1017	+0.00382	+0.932
0.0	+8.706	+1.000	0	0	−2.1686	0	0	+1.000

TABLE 9(c)—(*Contd.*)

(*b*) (Continued)

	SHEAR EDGE LOAD				MOMENT EDGE LOAD			
$\frac{s}{\sqrt[4]{rtl^2}}$	N_x (9)	$N_{x\phi}$ (10)	N_ϕ (11)	M_ϕ (12)	N_x (13)	$N_{x\phi}$ (14)	N_ϕ (15)	M_ϕ (16)
$\frac{rt}{l^2}=0.003$:								
3.2	+0.000	−0.036	+0.0098	+0.0360	+0.0904	+0.0132	+0.00529	−0.002
1.6	−0.205	+0.113	−0.0421	−0.2075	−0.3010	−0.0517	−0.02790	+0.066
0.8	−0.665	−0.261	−0.0160	−0.1067	+0.4217	−0.0796	+0.03239	+0.493
0.4	+1.451	−0.219	+0.0697	+0.0260	+0.5681	+0.0942	+0.03157	+0.728
0.2	+3.919	+0.161	+0.0785	+0.0369	−0.1315	+0.1367	+0.01334	+0.852
0.1	+5.642	+0.510	+0.0546	+0.0227	−0.8691	+0.1019	+0.00424	+0.922
0.0	+7.750	+1.000	0	0	−1.9706	0	0	+1.000
$\frac{rt}{l^2}=0.004$:								
3.2	+0.008	−0.033	+0.0108	+0.0320	+0.0817	+0.0134	+0.00539	−0.002
1.6	−0.205	+0.106	−0.0461	−0.1849	−0.2743	−0.0502	−0.02974	+0.060
0.8	−0.585	−0.262	−0.0136	−0.0851	+0.3819	−0.0794	+0.03386	+0.462
0.4	+1.366	−0.208	+0.0771	+0.0318	+0.5264	+0.0918	+0.03339	+0.702
0.2	+3.624	+0.169	+0.0851	+0.0378	−0.1135	+0.1348	+0.01418	+0.837
0.1	+5.200	+0.515	+0.0589	+0.0227	−0.7959	+0.1008	+0.00452	+0.913
0.0	+7.129	+1.000	0	0	−1.8212	0	0	+1.000
$\frac{rt}{l^2}=0.006$:								
3.2	+0.017	−0.029	+0.0122	+0.0265	+0.0692	+0.0134	+0.00536	−0.002
1.6	−0.202	+0.094	−0.0522	−0.1554	−0.2359	−0.0467	−0.03216	+0.050
0.8	−0.481	−0.263	−0.0089	−0.0585	+0.3234	−0.0780	+0.03503	+0.417
0.4	+1.253	−0.197	+0.0890	+0.0380	+0.4651	+0.0860	+0.03538	+0.664
0.2	+3.240	+0.182	+0.0955	+0.0382	−0.0872	+0.1294	+0.01514	+0.814
0.1	+4.628	+0.523	+0.0655	+0.0224	−0.6882	+0.0975	+0.00484	+0.901
0.0	+6.328	+1.000	0	0	−1.6010	0	0	+1.000

TABLE 9(c)—(*Contd.*)

(*b*) (Continued)

	SHEAR EDGE LOAD				MOMENT EDGE LOAD			
$\frac{s}{\sqrt[4]{r t\, l^2}}$	N_x (9)	$N_{x\phi}$ (10)	N_ϕ (11)	M_ϕ (12)	N_x (13)	$N_{x\phi}$ (14)	N_ϕ (15)	M_ϕ (16)
$\frac{r\,t}{l^2}=0.008$:								
3.2	+0.022	−0.025	+0.0132	+0.0227	+0.0605	+0.0132	+0.00522	−0.002
1.6	−0.199	+0.084	−0.0567	−0.1360	−0.2087	−0.0432	−0.03372	+0.043
0.8	−0.414	−0.263	−0.0042	−0.0422	+0.2814	−0.0763	+0.03497	+0.385
0.4	+1.177	−0.187	+0.0988	+0.0410	+0.4211	+0.0803	+0.03618	+0.637
0.2	+2.990	+0.191	+0.1036	+0.0379	−0.0676	+0.1235	+0.01561	+0.796
0.1	+4.256	+0.530	+0.0707	+0.0218	−0.6093	+0.0937	+0.00501	+0.892
0.0	+5.810	+1.000	0	0	−1.4397	0	0	+1.000
$\frac{r\,t}{l^2}=0.010$:								
3.2	+0.026	−0.022	+0.0138	+0.0199	+0.0539	+0.0128	+0.00503	−0.002
1.6	−0.196	+0.076	−0.0601	−0.1218	−0.1880	−0.0399	−0.03485	+0.038
0.8	−0.365	−0.262	+0.0004	−0.0312	+0.2487	−0.0746	+0.03426	+0.359
0.4	+1.121	−0.178	+0.1071	+0.0425	+0.3866	+0.0748	+0.03637	+0.614
0.2	+2.807	+0.199	+0.1105	+0.0372	−0.0524	+0.1178	+0.01581	+0.783
0.1	+3.986	+0.534	+0.0750	+0.0212	−0.5477	+0.0899	+0.00509	+0.884
0.0	+5.435	+1.000	0	0	−1.3134	0	0	+1.000
$\frac{r\,t}{l^2}=0.015$:								
3.2	+0.030	−0.016	+0.0146	+0.0149	+0.0425	+0.0119	+0.00455	−0.002
1.6	−0.187	+0.059	−0.0657	−0.0980	−0.1518	−0.0325	−0.03674	+0.028
0.8	−0.284	−0.260	+0.0112	−0.0145	+0.1904	−0.0708	+0.03121	+0.313
0.4	+1.023	−0.160	+0.1242	+0.0435	+0.3249	+0.0626	+0.03557	+0.573
0.2	+2.498	+0.214	+0.1242	+0.0352	−0.0252	+0.1047	+0.01574	+0.757
0.1	+3.533	+0.544	+0.0836	+0.0197	−0.4365	+0.0811	+0.00511	+0.869
0.0	+4.811	+1.000	0	0	−1.0849	0	0	+1.000

TABLE 9(c)—(*Contd.*)

(*b*) (Continued)

	SHEAR EDGE LOAD				MOMENT EDGE LOAD			
$\frac{s}{\sqrt[4]{rt\,l^2}}$	N_x (9)	$N_{x\phi}$ (10)	N_ϕ (11)	M_ϕ (12)	N_x (13)	$N_{x\phi}$ (14)	N_ϕ (15)	M_ϕ (16)
$\frac{r\,t}{l^2}=0.020$:								
3.2	+0.031	−0.011	+0.0147	+0.0116	+0.0352	+0.0111	+0.00412	−0.002
1.6	−0.178	+0.047	−0.0689	−0.0825	−0.1279	−0.0264	−0.03805	+0.022
0.8	−0.233	−0.257	+0.0212	−0.0052	+0.1510	−0.0676	+0.02741	+0.281
0.4	+0.957	−0.146	+0.1381	+0.0428	+0.2824	+0.0523	+0.03381	+0.544
0.2	+2.297	+0.225	+0.1350	+0.0331	−0.0068	+0.0934	+0.01527	+0.738
0.1	+3.241	+0.550	+0.0902	+0.0183	−0.3599	+0.0735	+0.00500	+0.859
0.0	+4.410	+1.000	0	0	−0.9265	0	0	+1.000
$\frac{r\,t}{l^2}=0.025$:								
3.2	+0.031	−0.008	+0.0143	+0.0092	+0.0301	+0.0103	+0.00376	−0.001
1.6	−0.170	+0.036	−0.0705	−0.0715	−0.1107	−0.0213	−0.03912	+0.017
0.8	−0.197	−0.253	+0.0305	+0.0005	+0.1221	−0.0649	+0.02345	+0.257
0.4	+0.906	−0.135	+0.1499	+0.0416	+0.2507	+0.0436	+0.03181	+0.521
0.2	+2.150	+0.234	−0.1440	+0.0312	+0.0067	+0.0838	+0.01466	+0.723
0.1	+3.029	+0.556	+0.0958	+0.0170	−0.3028	+0.0670	+0.00484	+0.850
0.0	+4.123	+1.000	0	0	−0.8076	0	0	+1.000
$\frac{r\,t}{l^2}=0.030$:								
3.2	+0.030	−0.005	+0.0137	+0.0073	+0.0263	+0.0096	+0.00345	−0.001
1.6	−0.163	+0.028	−0.0712	−0.0630	−0.0976	−0.0170	−0.04002	+0.013
0.8	−0.169	−0.250	+0.0392	+0.0044	+0.0998	−0.0627	+0.01962	+0.237
0.4	+0.866	−0.125	+0.1604	+0.0402	+0.2259	+0.0360	+0.02977	+0.502
0.2	+2.035	+0.242	+0.1518	+0.0294	+0.0171	+0.0754	+0.01401	+0.710
0.1	+2.866	+0.560	+0.1005	+0.0159	−0.2581	+0.0613	+0.00467	+0.843
0.0	+3.902	+1.000	0	0	−0.7141	0	0	+1.000

TABLE 9(c)—(*Contd.*)

(*b*) (Continued)

	SHEAR EDGE LOAD				MOMENT EDGE LOAD			
$\frac{s}{\sqrt[4]{rt\,l^2}}$	N_x (9)	$N_{x\phi}$ (10)	N_ϕ (11)	M_ϕ (12)	N_x (13)	$N_{x\phi}$ (14)	N_ϕ (15)	M_ϕ (16)
$\frac{rt}{l^2}=0.040$:								
3.2	+0.028	+0.000	+0.0120	+0.0047	+0.0210	+0.0085	+0.00297	−0.000
1.6	−0.150	+0.014	−0.0704	−0.0507	−0.0787	−0.0100	−0.04169	+0.008
0.8	−0.131	−0.242	+0.0550	+0.0088	+0.0678	−0.0589	+0.01218	+0.208
0.4	+0.804	−0.109	+0.1781	+0.0372	+0.1887	+0.0238	+0.02556	+0.473
0.2	+1.866	+0.253	+0.1648	+0.0263	+0.0315	+0.0615	+0.01258	+0.690
0.1	+2.625	+0.567	+0.1085	+0.0140	−0.1925	+0.0517	+0.00426	+0.831
0.0	+3.580	+1.000	0	0	−0.5749	0	0	+1.000
$\frac{rt}{l^2}=0.060$:								
3.2	+0.023	+0.005	+0.0081	+0.0017	+0.0151	+0.0070	+0.00225	−0.001
1.6	−0.130	−0.005	−0.0646	−0.0359	−0.0563	−0.0007	−0.04437	+0.001
0.8	−0.085	−0.230	+0.0822	+0.0122	+0.0302	−0.0533	−0.00023	+0.170
0.4	+0.718	−0.086	+0.2059	+0.0319	+0.1416	+0.0065	+0.01821	+0.431
0.2	+1.647	+0.269	+0.1850	+0.0216	+0.0474	+0.0415	+0.01001	+0.661
0.1	+2.321	+0.575	+0.1207	+0.0112	−0.1122	+0.0378	+0.00352	+0.814
0.0	+3.179	+1.000	0	0	−0.4003	0	0	+1.000
$\frac{rt}{l^2}=0.080$:								
3.2	+0.018	+0.008	+0.0044	+0.0002	+0.0118	+0.0061	+0.00166	−0.000
1.6	−0.114	−0.018	−0.0564	−0.0271	−0.0433	+0.0050	−0.04634	−0.002
0.8	−0.060	−0.218	+0.1045	+0.0128	+0.0100	−0.0491	−0.00982	+0.146
0.4	+0.659	−0.071	+0.2273	+0.0277	+0.1128	−0.0047	+0.01226	+0.402
0.2	+1.506	+0.278	+0.2004	+0.0182	+0.0549	+0.0280	+0.00787	+0.639
0.1	+2.130	+0.580	+0.1301	+0.0093	−0.0654	+0.0283	+0.00289	+0.801
0.0	+2.931	+1.000	0	0	−0.2949	0	0	+1.000

TABLE 9(c)—(*Concld.*)

(*b*) (Conclude)

	SHEAR EDGE LOAD				MOMENT EDGE LOAD			
$\frac{s}{\sqrt[4]{rtl^2}}$	N_x (9)	$N_{x\phi}$ (10)	N_ϕ (11)	M_ϕ (12)	N_x (13)	$N_{x\phi}$ (14)	N_ϕ (15)	M_ϕ (16)
$\frac{rt}{l^2}=0.100$:								
3.2	+0.015	+0.009	+0.0014	−0.0006	+0.0097	+0.0056	+0.00110	−0.000
1.6	−0.102	−0.026	−0.0474	−0.0214	−0.0347	+0.0086	−0.04764	−0.004
0.8	−0.045	−0.209	+0.1231	+0.0126	−0.0027	−0.0456	−0.01715	+0.128
0.4	+0.614	−0.059	+0.2446	+0.0243	+0.0922	−0.0123	+0.00751	+0.380
0.2	+1.406	+0.285	+0.2129	+0.0156	+0.0578	+0.0183	+0.00611	+0.622
0.1	+1.995	+0.583	+0.1378	+0.0078	−0.0360	+0.0213	+0.00237	+0.790
0.0	+2.760	+1.000	0	0	−0.2250	0	0	+1.000

TABLE 9(d)

(*c*) **n=3**

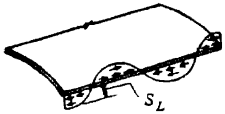

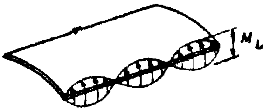

	SHEAR EDGE LOAD				MOMENT EDGE LOAD			
Ratio	N_x (9)	$N_{x\phi}$ (10)	N_ϕ (11)	M_ϕ (12)	N_x (13)	$N_{x\phi}$ (14)	N_ϕ (15)	M_ϕ (16)
$\frac{rt}{l^2}=0.002$:								
1.6	+0.082	+0.015	+0.0153	+0.0020	+0.0364	+0.0312	−0.00623	−0.014
0.8	−0.309	−0.009	−0.0737	−0.0861	−0.1255	−0.0620	−0.02633	+0.069
0.4	−0.069	−0.278	+0.0506	+0.0107	+0.2392	−0.0438	+0.03600	+0.352
0.2	+1.288	−0.082	+0.1401	+0.0436	+0.2567	+0.0734	+0.03054	+0.601
0.1	+2.610	+0.298	+0.1229	+0.0304	−0.0956	+0.0961	+0.01249	+0.775
0.0	+4.553	+1.000	0	0	−0.9839	0	0	+1.000
$\frac{rt}{l^2}=0.003$:								
1.6	+0.066	+0.020	+0.0111	−0.0019	+0.0287	+0.0267	−0.00637	−0.011
0.8	−0.267	−0.027	−0.0723	−0.0638	−0.1024	−0.0486	−0.03020	+0.05
0.4	−0.024	−0.267	+0.0697	+0.0174	+0.1734	−0.0444	+0.02937	+0.306
0.2	+1.157	−0.061	+0.1609	+0.0406	+0.2128	+0.0560	+0.02767	+0.562
0.1	+2.312	+0.313	+0.1378	+0.0272	−0.0527	+0.0796	+0.01165	+0.750
0.0	+4.028	+1.000	0	0	−0.7678	0	0	+1.000
$\frac{rt}{l^2}=0.004$:								
1.6	+0.054	+0.023	+0.0071	−0.0039	+0.0242	+0.0236	−0.00633	+0.008
0.8	−0.237	−0.039	−0.0686	−0.0503	−0.0878	−0.0386	−0.03359	+0.039
0.4	+0.002	−0.256	+0.0860	+0.0199	+0.1311	−0.0449	+0.02933	+0.274
0.2	+1.069	−0.046	+0.1774	+0.0376	+0.1835	+0.0425	+0.02458	+0.534
0.1	+2.119	+0.323	+0.1494	+0.0244	−0.0253	+0.0667	+0.02008	+0.732
0.0	+3.694	+1.000	0	0	−0.6246	0	0	+1.000

TABLE 9(d)—(*Contd.*)

(*c*) (Continued)

Ratio	SHEAR EDGE LOAD				MOMENT EDGE LOAD			
	N_x (9)	$N_{x\phi}$ (10)	N_ϕ (11)	M_ϕ (12)	N_x (13)	$N_{x\phi}$ (14)	N_ϕ (15)	M_ϕ (16)
$\frac{rt}{l^2}=0.006$:								
1.6	+0.038	+0.025	+0.0003	−0.0055	+0.0190	+0.0195	+0.00617	−0.006
0.8	−0.196	−0.055	−0.0583	−0.0344	−0.0695	+0.0247	+0.03921	+0.025
0.4	+0.030	−0.239	+0.1132	+0.0210	+0.0798	+0.0452	+0.01138	+0.232
0.2	+0.950	−0.024	+0.2032	+0.0322	+0.1453	+0.0231	+0.01888	+0.495
0.1	+1.871	+0.337	+0.1674	+0.0202	+0.0074	+0.0477	+0.00882	+0.706
0.0	+3.277	+1.000	0	0	−0.4429	0	0	+1.000
$\frac{rt}{l^2}=0.008$:								
1.6	+0.027	+0.024	−0.0048	−0.0059	+0.0160	+0.0170	−0.00614	−0.005
0.8	−0.168	−0.064	−0.0468	−0.0253	−0.0581	−0.0158	−0.04352	+0.016
0.4	+0.043	−0.226	+0.1354	+0.0203	+0.0499	−0.0450	+0.00214	+0.205
0.2	+0.871	−0.009	+0.2231	+0.0280	+0.1208	+0.0099	+0.01408	+0.467
0.1	+1.713	+0.346	+0.1811	+0.0171	+0.0253	+0.0345	+0.00720	+0.686
0.0	+3.018	+1.000	0	0	−0.3316	0	0	+1.000
$\frac{rt}{l^2}=0.010$:								
1.6	+0.020	+0.023	−0.0084	−0.0058	+0.0139	+0.0152	−0.00623	−0.004
0.8	−0.147	−0.070	−0.0353	−0.0196	−0.0500	−0.0096	−0.04672	+0.011
0.4	+0.050	−0.214	+0.1539	+0.0190	+0.0308	−0.0443	−0.00521	+0.184
0.2	+0.812	+0.002	+0.2394	+0.0247	+0.1032	+0.0006	+0.01013	+0.445
0.1	+1.599	+0.352	+0.1924	+0.0147	+0.0359	+0.0249	+0.00584	+0.671
0.0	+2.838	+1.000	0	0	−0.2567	0	0	+1.000

TABLE 9(d)—(*Contd.*)

(*c*) (Continued)

Ratio	SHEAR EDGE LOAD				MOMENT EDGE LOAD			
	N_x (9)	$N_{x\phi}$ (10)	N_ϕ (11)	M_ϕ (12)	N_x (13)	$N_{x\phi}$ (14)	N_ϕ (15)	M_ϕ (16)
$\frac{rt}{l^2}=0.015$:								
1.6	+0.009	+0.017	−0.0127	−0.0049	+0.0104	+0.0124	−0.00668	−0.003
0.8	−0.114	−0.076	−0.0097	−0.0118	−0.0366	−0.0007	−0.05099	+0.003
0.4	+0.055	−0.193	+0.1888	+0.0157	+0.0054	−0.0415	−0.01754	+0.150
0.2	+0.710	+0.019	+0.2698	+0.0187	+0.0749	−0.0130	+0.00308	+0.406
0.1	+1.415	+0.359	+0.2138	+0.0107	+0.0469	+0.0098	+0.00336	+0.642
0.0	+2.560	+1.000	0	0	−0.1481	0	0	+1.000
$\frac{rt}{l^2}=0.020$:								
1.6	+0.004	+0.012	−0.0131	−0.0039	+0.0081	+0.0104	−0.00702	−0.002
0.8	−0.094	−0.077	+0.0103	−0.0081	−0.0282	+0.0036	−0.05168	−0.001
0.4	+0.051	−0.179	+0.2123	+0.0130	−0.0060	−0.0379	−0.02428	+0.127
0.2	+0.642	+0.026	+0.2910	+0.0150	+0.0575	−0.0192	−0.00126	+0.377
0.1	+1.301	+0.360	+0.2295	+0.0083	+0.0486	+0.0018	+0.00176	+0.620
0.1	+2.401	+1.000	0	0	−0.0928	0	0	+1.000
$\frac{rt}{l^2}=0.025$:								
1.6	+0.002	+0.009	−0.0118	−0.0031	+0.0065	+0.0088	−0.00706	−0.002
0.8	−0.080	−0.076	+0.0252	−0.0061	−0.0223	+0.0059	−0.05036	−0.003
0.4	+0.045	−0.170	+0.2284	+0.0109	−0.0114	−0.0342	−0.02778	+0.111
0.2	+0.592	+0.028	+0.3066	+0.0124	+0.0457	−0.0220	−0.00395	+0.356
0.1	+1.223	+0.357	+0.2418	+0.0067	+0.0470	−0.0028	+0.00071	+0.603
0.0	+2.301	+1.000	0	0	−0.0614	0	0	+1.000

TABLE 9(d)—(*Contd.*)

(*c*) (Continued)

Ratio	SHEAR EDGE LOAD				MOMENT EDGE LOAD			
	N_x (9)	$N_{x\phi}$ (10)	N_ϕ (11)	M_ϕ (12)	N_x (13)	$N_{x\phi}$ (14)	N_ϕ (15)	M_ϕ (16)
$\frac{rt}{l^2}=0.030$:								
1.6	+0.000	+0.006	−0.0099	−0.0025	+0.0053	+0.0076	−0.00683	−0.001
0.8	−0.071	−0.073	+0.0358	−0.0049	−0.0179	+0.0071	−0.04799	−0.004
0.4	+0.039	−0.163	+0.2392	+0.0092	−0.0140	−0.0307	−0.02938	+0.099
0.2	+0.533	+0.027	+0.3183	+0.0106	+0.0372	−0.0229	−0.00563	+0.338
0.1	+1.165	+0.353	+0.2516	+0.0057	+0.0443	−0.0054	+0.00002	+0.588
0.0	+2.233	+1.000	0	0	−0.0424	0	0	+1.000
$\frac{rt}{l^2}=0.040$:								
1.6	−0.001	+0.003	−0.0065	−0.0017	+0.0037	+0.0056	−0.00595	−0.001
0.8	−0.058	−0.068	+0.0483	−0.0036	−0.0119	+0.0080	−0.04220	−0.006
0.4	+0.026	−0.154	+0.2511	+0.0069	−0.0156	−0.0248	−0.02964	+0.081
0.2	+0.494	+0.021	+0.3343	+0.0082	+0.0258	−0.0224	−0.00724	+0.310
0.1	+1.083	+0.340	+0.2668	+0.0043	+0.0381	−0.0078	−0.00072	+0.565
0.0	+2.150	+1.000	0	0	−0.0223	0	0	+1.000
$\frac{rt}{l^2}=0.060$:								
1.6	−0.001	+0.000	−0.0023	−0.0009	+0.0021	+0.0031	−0.00397	−0.001
0.8	−0.046	−0.058	+0.0549	−0.0025	−0.0057	+0.0077	−0.03157	−0.006
0.4	+0.005	−0.146	+0.2546	+0.0043	−0.0142	−0.0165	−0.02659	+0.058
0.2	+0.415	+0.003	+0.3503	+0.0057	+0.0141	−0.0189	−0.00797	+0.271
0.1	+0.983	+0.314	+0.2867	+0.0030	+0.0282	−0.0084	−0.00133	+0.530
0.0	+2.076	+1.000	0	0	−0.0081	0	0	+1.000

TABLE 9(d)—(*Concld.*)

(*c*) (Conclude)

Ratio	SHEAR EDGE LOAD				MOMENT EDGE LOAD			
	N_x (9)	$N_{x\phi}$ (10)	N_ϕ (11)	M_ϕ (12)	N_x (13)	$N_{x\phi}$ (14)	N_ϕ (15)	M_ϕ (16)
$\frac{rt}{l^2}=0.080$:								
1.6	−0.001	−0.000	−0.0007	−0.0005	+0.0013	+0.0020	−0.00259	−0.000
0.8	−0.038	−0.050	+0.0527	−0.0020	−0.0029	+0.0068	−0.02401	−0.006
0.4	−0.010	−0.141	+0.2485	+0.0029	−0.0121	−0.0115	−0.02306	+0.044
0.2	+0.362	−0.015	+0.3569	+0.0044	+0.0084	−0.0158	−0.00764	+0.244
0.1	+0.919	+0.289	+0.2997	+0.0024	+0.0218	−0.0078	−0.00145	+0.505
0.0	+2.045	+1.000	0	0	−0.0037	0	0	+1.000
$\frac{rt}{l^2}=0.100$:								
1.6	−0.001	−0.000	−0.0001	−0.0003	+0.0008	+0.0013	−0.00173	−0.000
0.8	−0.033	−0.043	+0.0484	−0.0016	−0.0015	+0.0059	−0.01878	−0.006
0.4	−0.020	−0.138	+0.2398	+0.0021	−0.0104	−0.0084	−0.02088	+0.035
0.2	+0.323	−0.030	+0.3594	+0.0036	+0.0051	−0.0135	−0.00706	+0.224
0.1	+0.872	+0.268	+0.3091	+0.0020	+0.0174	−0.0072	−0.00135	+0.485
0.0	+2.020	+1.000	0	0	−0.0020	0	0	+1.000

Note : Tables 4 to 9 are reproduced from ASCE Manual 31 with the permission of the American Society of Civil Engineers.

APPENDIX B—REFERENCES

1.1 Lin, T. Y., "Load Balancing for Design and Analysis of Prestressed Concrete Structures", *Jr. of the ACI*, Vol. 60, No. 6, June 1963, pp. 719-42.

1.2 Desai, P. and Krishnan, S., "Equation for Stress Strain Curve of Concrete", *Jr. of the ACI*, Vol. 61, No. 3, March 1964.

1.3 Evans, R.H. and Kong, F.K., "Estimation of Shrinkage of Concrete in Reinforced and Prestressed Concrete Design", *Jr. of Civil Engineering and Public Works Review*, Vol. 62, No. 5, May 1967, pp. 563-75.

2.1 Abeles, P. W. and Czuprynski, L., "Partial Prestressing; Its history, research, application and future development", *Annales Travanx Publics de Belgigue*, (Brussells), No. 2, April 1966, pp. 131-39.

2.2 Abeles, P. W., "Saving Reinforcement by Prestressing," *Concrete and Constructional Engineering*, V. 35, 1944, pp. 328-332.

2.3 Abeles, P. W., "Static and Fatigue Tests on Partially Prestressed Concrete Construction," *Jr. of the ACI*, Vol. 26, No. 4, 1954, pp. 361-376.

2.4 Abeles, P. W., "The Condition of Partially Prestressed Concrete Structures after 3-7 years use," *IABSE, Sixth Congress, Final Report*, Lisbon, 1956, pp. 625-630.

2.5 "Practical Recommendations for the Design and Construction of Prestressed Concrete Structures," *FIP-CEB Joint Committee Report*, Provisional Edition June 1966, Cement and Concrete Association, London.

2.6 Abeles, P. W., "Design of Partially Prestressed Concrete Beams," *Jr. of the ACI*, October 1967, V. 64, No. 10, pp. 669-677.

2.7 Thurlimann, B., "Partially Prestressed Members," *IABSE, Eighth Congress 1968*, New York.

2.8 Abeles, P. W., "The Practical Application of Partial Prestressing Research on Cracking and Deflection under Static, Sustained and Fatigue Loading," *IABSE, 8th Congress 1968*.

2.9 Abeles, P. W., and Gill, V. L., "The behaviour of Partially Prestressed Beams Containing Bonded, Nontensioned Strands and Curved, Nontensioned Tendons," *IABSE, 8th Congress 1968*, New York.

2.10 Visvesvaraya, H. C. and Raghavendra, N., "Partial Prestressing in Concrete Structures," *Proceedings of The Seminar on Problems of Prestressing, ING IABSE*, Madras, January-February 1970, pp. II-1 II-20.

3.1 Khachaturian, N., "Service Load Design of Prestressed Concrete Beams—Part I, Non-Composite Simple Beams", *Bulletin of the Engineering Experimentation Station*, University of Illinois.

3.2 Dayaratnam, P., "Minimum Weight Design of Simply Supported Prestressed Concrete Beams, *Cement and Concrete*", Vol. 9, No. 2, July-September 1968.

4.1 Khachaturian, N., "Service Load Design of Prestressed Concrete Beams—Part II, Composite Simple Beams", *Bulletin of the Engineering Experimentation Station*, University of Illinois.

4.2 Lu-Ln Wang, "A Direct Method for Designing Composite Sections in Prestressed Concrete", *Jr. of PCI*, Vol. 10, No. 5, October 1965.

5.1 Leonhard, F., *Prestressed Concrete Design and Construction*, Wilhelm Ernst and Sohn, Berlin, 1964, pp. 364-5.

5.2 Bailey, D. M. and Ferguson, M. Phil., "Fixed End Moment Equations for Continuous Prestressed Concrete Beams", *Jr. of PCI*, Vol. 11, No. 1, February 1966, pp 76-94.

5.3 **Burns, N.H.**, "Development of Continuity Between Precast Prestressed Concrete Beams", *Jr. of PCI*, Vol. 11, No. 3, June 1966, pp. 23-36.

5.4 Libby, J. R., *Prestressed Concrete Design and Construction*, The Ronald Press Co., New York, 1961.

6.1 Hoppe, "Mass Production of Prestressed Concrete Auxiliary Members", *Jr. of PCI*, Vol. 8, No. 5, October 1963.

6.2 Elliston Jr., W.J., "Connections Between Precast Beam and Column Members", *Jr. of PCI*, Vol. 8, No. 4, August 1963.

6.3 LaFrangh, R. W. and Magura, D. D., "Connections in Precast Concrete Structures—Column Base Plates", *Jr. of PCI*, Vol. 11. No. 6, December 1966, pp. 18-39.

6.4 Gerwick Jr., B. C., "Long Span Prestressed Concrete Bridges Utilising Precast Elements", *Jr. of PCI*, Vol. 9, No. 1, February 1964.

6.5 Sauter, F., "Post-Tensioned Multi-story Rigid Frames for the New Banco Central in Costa Rica", *Jr. of PCI*, Vol. 8, No. 3, June 1963.

6.6 Riley, W.E., "Post-Tensioned Cast-in-place Multi-story Building Frame", *Jr. of the ACI*, Vol. 63, No. 3, March 1966.

6.7 Report of PCI Committee, "Recommended Practice for Driving Prestressed Concrete Piling", *Jr. of PCI*, Vol. 11, No. 4, August 1966, pp. 18-27.

6.8 Weller, N. H. E., "Prestressed Concrete Piles", *Jr. of PCI*, Vol. 7, No. 5, October 1962.

6.9 Sauter, S., "Tall Precast Towers", *Jr. of PCI*, Vol. 6, No. 3, September 1961, pp. 72-74.

6.10 Swanson, H. V., "Design of Prestressed Concrete Pressure Pipe", *Jr. of PCI*, Vol. 10, No. 4, August 1965, pp. 69-82.

6.11 Renz, C. F. and Melville, P. L., "Experience With Prestressed Concrete Airfield Pavement in the United States", *Jr. of PCI*, Vol. 6. No. 1, March 1961, pp. 75-92.

6.12 Vandepitte, D., "Prestressed Concrete Pavements—A Review of European Practice", *Jr. of PCI*, Vol. 6, No. 1, March 1961, pp. 60-74.

6.13 McIntyre, J. P., "Prestressed Concrete Airport Pavement", *Jr. of PCI*, Vol. 5, No. 2, June 1960, pp. 69-72.

6.14 Young, L. E., "A Sliding Joint Prestressed Concrete Pavement," *Jr. of PCI*, Vol. 6, No. 3, September 1961, pp. 92-99.

6.15 Zetlin, L., "A Novel Concept of Prestressed Concrete Pavement", *Jr. of PCI*, Vol. 6, No. 1, March 1961, pp. 93-102.

7.1 Scordelies, A. C., Branson, D. E. and Sozen, M. A., "Deflection of Prestressed Concrete Members," *Jr. af the ACI*, Vol. 60, No. 12, December 1963, pp. 1697-1728.

8.1 Gurfinkel, G. and Khachaturian, N., "Ultimate Design of Prestressed Concrete Beams", *Research Bulletin*, No. 478, Engineering Experimentation Station, University of Illinois.

8.2 Burr Bennet Jr., W., Limit Design With Prestressed Concrete", *Jr. of PCI*, Vol. 8, No. 2, April 1963.

8.3 Bennett, E. W., Cook, N., and Naughton, L. P., "Deformation of Continuous Prestressed Concrete Beams and Its Effect on Ultimate Load", *Proce. Inst. of Civil Engineers (Lond.)*, Vol. 37, May 1967, pp. 57-74.

8.4 **Raina, V. K.**, "Ultimate Load Carrying Capacity of Continuous Prestressed Concrete Beams", *The Construction Engineer*, Vol. 31, No. 7, July 1967, pp. 77-86.

9.1 Dayaratnam, P. and Rao, C. V. S. K., "Theory of Failure of Concrete by Distortion Energy", *Research report CE 1-67,* April 1967, Indian Institute of Technology, Kanpur.

9.2 Baikov, V. N., *Reinforced Concrete Constructions,* Rajkamal Prakashan, Delhi, 1963, p. 12.

9.3 Pattanayak, U. C. and Dayaratnam, P., "Shear Flexure Capacity of Prestressed Concrete Beams, *Proce. of the International Conference on Shear, Bond and Torsion of Reinforced and Prestressed Concrete,* Coimbatore, January 1969.

9.4 Sheikh, M. A., de Paiva, H. A. R. and Neville, A. M., "Calculation of Flexure Shear Strength of Prestressed Concrete Beam", *Jr. of PCI,* Vol. 13, No. 1, February 1968, pp. 68-85.

9.5 Sozen, M. A., "Research on Shear Srength of Prestressed Beams", *Jr. of PCI,* Vol. 5, No. 2, June 1960, pp. 40-49.

9.6 McGregor, J. F., Sozen, M. A. and Siess, C. P., "Effect of Draped Reinforcement on Behaviour of Prestressed Concrete Beams", *Jr. of the ACI,* Vol. 57, No. 6, December 1960.

10.1 Dayaratnam, P., "Design of Two-way Slab as an Orthotropic Plate", *Indian Concrete Journal,* Vol. 38, No. 3, March 1964 p. 89.

10.2 Timoshenko, S. and Woinowsky—Krieger, S., *Theory of Plates and Shells,* McGraw-Hill, 1959, p. 120.

10.3 Zielinski, Z. A., "Prestressed Slabs and Shell made of Prefabricated Components", *Jr. of PCI,* Vol. 9, No. 4, August 1964, pp. 69-80.

10.4 Felix, Adler, "Precast Plate Units for Roof Construction," *Proce. of Inst. of Civil Engineers (Lond).* Vol. 23, November 1962, pp. 321-326.

10.5 Chen-Hwa Wang, "Direct Design Method for Prestressed Concrete Slab", *Jr. of PCI,* Vol. 13, No. 3, June 1968, pp. 62-72.

10.6 Omsted, H., "Notes on Post-Tensioned Lift Slab", *Jr. of PCI,* Vol. 10, No. 6, December 1965, pp. 84-90.

10.7 Rozvany, G. I. N. and Hampson, A. J. K., "Optimum Design of Prestressed Plates", *Jr. of the ACI,* Vol. 60, No. 8, August 1963, pp. 1065-82.

10.8 Timoshenko, S. and Woinowsky—Krieger, S., *Theory of Plates and Shells,* McGraw-Hill, 1959, pp. 245-58.

11.1 Flugge, W., *Stresses in Shells,* Springer-Verlog, Berlin, 1962.

11.2 Ramaswamy, G. S., *Design and construction of concrete shell roofs,* McGraw-Hill, New York, 1968.

11.3 Billington, D. P., *Thin shell concrete structures,* McGraw-Hill, New York, 1965.

11.4 Gibson, J. E., *The design of cylindrical shell roofs,* Van Nostrand, Princeton, 1961.

11.5 Novozhiloy V. V., *Thin shell theory,* P. Noordhoff Ltd., Groningen, The Netherlands, 1964.

11.6 Hass, A. M., *Design of Thin Concrete Shells,* John Wiley & Sons, Inc., New York, 1962.

11.7 Powell, G. H., "Comparison of Simplified Theories for Folded Plates", *Jr. of Struct. Div. of ASCE,* Vol. 91, No. ST 6, December 1965, pp. 1-33.

11.8 Brough J. C. and Stephens, B. H., "Long Span Prestressed Concrete Folded Plate Roofs", *Jr. of Struct. Div. of ASCE,* October 1960, paper No. 2630.

11.9 Power, J. O., "Folded Plate Concrete Roof in Post-Tensioned in Place," *Jr. of PCI,* Vol. 5, No. 1, February 1963, pp. 29-34.

11.10 Ramaswamy, G. S., Tamahankar, M. G. and Naithani, K. C., "Precast Pretensioned Folded Plate Roof", *Indian Concrete Journal*, January 1966, pp. 6-12.

11.11 Edwards, H. H., "Facts on Precast Prestressed Folded Plate Slabs", *Modern Concrete*, Vol. 24, No. 2, June 1960, pp. 42-46.

11.12 Edwards, H. H., "Precast Prestressed Folded Plate Slabs", *Jr. of the ACI.*, Vol. 57, April 1956, pp. 1313-22.

11.13 Timoshenko, S. and Woinowsky—Krieger, S., *Theory of Plates and Shells*, McGraw-Hill, 1959, pp. 471-87.

11.14 Timoshenko, S. and Woinowsky—Krieger, S., *Theory of Plates and Shells*, McGraw-Hill, 1959, p. 436.

11.15 *ASCE Manual* on Design of Cylindrical Concrete Shell Roofs, Manual 31, ASCE, New York.

11.16 Lin, T. Y. and Kulka, F., "Concrete Shells Prestressed for Load Balancing", *Proce. of World Conference on Shell Structures*, San Fransisco, 1962, pp. 423-30.

12.1 Marshall, W. T., "A Theory for End Zone Stresses in Pretensioned Concrete Beams", *Jr. of PCI*, Vol. 11, No. 2, April 1966, pp. 45-51.

12.2 Jenney, J. R., "Report of Stress Transfer Length Studies on 270k Prestressing Strand", *Jr. of PCI*, Vol. 8, No. 1, February 1963.

12.3 Linger, D. A. and Bhonsle, S. R., "An Investigation of Transfer Length in Pretensioned Concrete Using Photo-elasticity", *Jr. of PCI*, Vol. 8, No. 4, August 1963.

12.4 Nawy, E. G. and Salek, F., "Moment-Rotation Relationships of Non Bonded Post-Tensioned I and T Beams", *Jr. of PCI*, Vol. 13, No. 4, August 1968, pp. 40-55.

13.1 Guyon, Y., *Prestressed Concrete*, Vol. I, Jhon Wiley and Sons, New York, 1953.

13.2 Leonhard, F., *Prestressed Concrete Design and Construction*, Wilhelm Ernst and Sohn Berlin, 1964, p. 271.

INDEX

Abeles, P. W.—320
anchor—225, 228-30, 234
anchorage—19-22, 26, 32, 47, 57
ASCE Manual—323

Baikov, V. N.—322
Bailey, D. M.—320
balancing Force—9
beam Column—115
Bennett, E. W.—321
Bhonsle, S. R.—323
Billington, D. P.—322
bond—19, 25, 26
bond length—221, 223-25
Branson, D. E.—321

Brough, J. C.—322
buckling
  lateral—120
  torsional—120
Burns, N. H.—321
Burr Bennet Jr., W.—321
bursting force—228, 232, 226

Camber—117, 118
Chen—Hwa Wang—322
Compatibility—173, 190, 192, 196, 203, 205, 214
Composite—67, 74, 76
Concordant—80, 84, 86, 88, 92
Cook, N.—321
Cracks—119, 132, 135-36, 138, 142, 144, 184, 225-26
Creep—11, 13, 16, 23, 25, 30, 32, 33, 52, 223, 224
Czuprynski, L.—320

Dayaratnam, P.—320, 322
deflection
  beam—114
  creep—118
  slab—156
de Paiva, H. A.R.—322
depth factor—39, 40, 74
Desai, P.—320

Edward, H. H.—323
efficiency factor—39, 40, 57, 74, 76
Elliston Jr., W. J.—321
Euler's buckling load—115
Evans, R. H.—320

factor of safety—119, 147
failure
  anchorage—120
  brittle—120
  buckling—120
  bursting—228-32, 236
  crushing—120
  ductile—120
  flexural—120, 145
  limit—143
  section—142
  shear—135, 142-43, 145
  spalling—228, 236
Felix, Adler—322
Ferguson, M. Phil—320
friction—26, 27, 28, 32
Freyssinet—21, 22

Gerwick, Jr., B. C.—321
Gifford—Udall—21
Gill, V. L.—320
Gurfinkel, G.—321
Guyon—229, 234

Hampson, A. J. K.—322
Hass, A. M.—322
Hobling—21
Hognestad—15
Hoppe—321
Hoyer effect—221-23

I. S. code—131

Jenney, J. R.—323

Khachaturian—39, 71 , 320
Kong, F. K.—320
Krishnan, S.—320
Kulka, F.—323

La Frangh, R. W.—321
Lee McCall—21
Leonhardt—21, 329, 324
Libby, J. R.—321
limit design—143
Lin, T. Y.—245, 320, 324
Linger, D. A.—323
load balancing—8, 9, 17, 61, 62, 65, 66, 88, 94, 96, 114
load balancing method—114, 149, 151, 159, 162, 175, 181, 184, 206
load factors—119
looping—21
Lu, Ln Wang—320
Magnel—21
Magura, D. D.—321
Marshall, W. T.—323
McGregor—144
McIntyre, J. P.—321
Melville, P. L.—321
membrane—187, 189, 202, 211-12
modulus of elasticity—12, 14, 15, 75

Naithani, K. C.—323
Naughton, L. P.—321
Nawy, E. G.—323
Neville, A. M.—322
Novozhiloy, V. V.—322

Omsted, H.—322
orthotropic plate theory—152

Pattanayak, U. C.—322
PCI Committee—321
Poisson's ratio—15
Post-tensioned—13, 19, 20, 24, 25, 28, 49, 76, 96, 221, 225, 226, 228
Powell, G. H.—322
Power, J. O.—322
prestressing
  circular—19
  definition—1,2
  effective—10, 11, 31
  external—18
  force—4, 5
  internal—18
  loss—11
  partial—20
  profile—3-5, 17, 29, 33, 47, 80, 81, 96
  tendon—1, 7, 19, 25,26, 80, 138-39
pre-tensioned—13, 19, 20, 24, 28-30, 221, 224
proportional limit—12

Raina, V. K.—321
Ramaswamy, G. S.—322, 323
Renz, C. F.—321
Riley. W. E.—321
ring beam—192, 196
Rozvany, G. I. N.—322
Ryerson BBRV—21

Salek, F.—323
Sauter, F.—321
Scordelics, A. C.—321
Shape factor—39, 40, 74
Shear connections—67, 68
Sheikh, M. A.—322
Shrinkage—10, 11, 15, 16, 22, 24, 30, 32, 33, 52, 74, 75, 196
Siess—144
slabs
  one way—147-49
  two way—147, 152
  flat—147, 157
  lift—157
Sozen—144
spalling force—228, 236
statically indeterminate structures—18
Stephens, B. H.—322
stirrups—133, 134, 138, 145, 236
strand—11
Stress
  bearing—236
  bending—137
  bond—221, 224, 226-27
  compressive—3, 37, 41, 44, 136, 223
  cuble—136
  normal—133
  permissible—37, 44, 45
  plane—133
  principal—133-34, 138, 142

  prism—136-37
  shear—132, 202, 209, 229
  tensile—3, 135-37, 145, 223, 229, 232
  thermal—187
stress corrosion—225
Swanson, H. V.—321

Tamahankar, M. G.—323
Thurlimann, B.—320
Timoshenko—156-57, 185-86
transfer prestress—10
transmission
  zone—228-29, 235
  length—221, 223, 228-30

Ultimate load—104, 108, 119-20, 124, 128-30
Ultimate load design—127-29
Ultimate moment capacity
  flexure—121-22, 124, 126, 131, 224-27
  shear flexure—132, 138-140, 143
Ultimate strain—14

Vandepitte, D.—321
Vertical prestress—145

Water cement ratio—13, 14, 16
Weller, N. H. E.—321
Woinowsky Krieger, S.—322
Working load—2

Yield line—156
Yield limit—10, 11, 12
Young, L. E.—321

Zetlin, L.—321
Zielinski, Z. A.—322